EFFECT OF REDUCING AGENTS AND NUTRIENT DEPRIVATION ON HYDROGEN PRODUCTION BY THE HALOTOLERANT UNICELLULAR CYANOBACTERIUM *Aphanothece halophytica*

NATTANON CHINCHUSAK

A THESIS SUMMITTED IN PARTIAL FULFILLMENT OF THE REQUIREMENT FOR
THE DEGREE OF DOCTOR OF PHILOSOPHY IN BIOTECHNOLOGY
DEPARTMENT OF BIOLOGY SCHOOL OF SCIENCE
KING MONGKUT'S INSTITUTE OF TECNOLOGY LADKRABANG
2024

KMITL-2024-SC-D-020-002

Thesis Title	Effect of reducing agents and nutrient deprivation on hydrogen production by the halotolerant unicellular cyanobacterium *Aphanothece halophytica*
Student	Nattanon Chinchusak
Student ID	59605009
Degree	Doctor of Philosophy (Biotechnology)
Program	Biology
Year	2024
Thesis Advisor	Assoc.Prof.Dr. Saranya Phunpruch
Thesis Co-advisor	Prof.Dr. Aran Incharoensakdi

ABSTRACT

The unicellular halotolerant cyanobacterium *Aphanothece halophytica* is known as one of potential H_2 cyanobacterial producers. This study aimed to investigate the enhancement of H_2 production under dark anaerobic conditions by treatment with various kinds of reducing sugars and reducing agents. The result showed that by supplementation of reducing sugars, the highest H_2 production rate of 55.80 ± 0.50 μmol H_2 g dry weight^{-1} h^{-1} was found in *A. halophytica* cells incubated in $BG11_0$ containing 0.189 mmol C-atom L^{-1} glucose under dark anaerobic conditions. It was 1.5 folds higher than that without any supplementations. Among ten reducing agents, β-mercaptoethanol, dithiothreitol, L-cysteine and sodium sulfide showed potential as effective reducing agents to promote H_2 production by *A. halophytica* The highest H_2 production rate of 971.09 ± 64.42 μmol H_2 g dry weight^{-1} h^{-1} and H_2 accumulation of 4,815.59 ± 194.78 μmol H_2 g dry weight^{-1} after dark anaerobic incubation for 2h and 24 h, respectively, were found in *A. halophytica* cells incubated in $BG11_0$ treated with 50 mM sodium sulfide. The H_2 accumulation was approximately 20 folds higher than that without treatment. The increase in H_2 production was ascribed to an increase in hydrogenase activity and a decrease in O_2 production rate. Sodium sulfide at 50 mM showed non-toxicity to *A. halophytica* cells since the IC_{50} of sodium sulfide was higher than 100 mM. The reduced ferredoxin at 1.5 μM-1.5 mM, NADH and NADPH at 0.15-1.5 mM supported *in vitro* [NiFe]-H_2ase activity, showing the ability of

these redox partners to direct electrons towards [NiFe]-H_2ase in *A. halophytica*. Another way to promote H_2 production by *A. halophytica* is incubation cells under deprivation of nutrients such as nitrogen (N), phosphorus (P), potassium (K), and sulfur (S). The result showed that N- and K-deprivation induced H_2 production by *A. halophytica* by stimulation of H_2ase activity whereas no differences of H_2 production were found in cells incubated under S- and P-deprivation. The effect of adaptation time under N- and K-deprivation on H_2 production was investigated. The highest H_2 accumulation of 1,261.96 ± 96.99 μmol H_2 g dry wt^{-1} and maximum H_2ase activity of 179.39 ± 8.18 μmol H_2 g dry wt^{-1} min^{-1} were obtained in *A. halophytica* cells adapted in the N- and K-deprived BG11 supplemented with Turk Island salt solution ($BG11_0$-K) for 48 h. An increase in H_2ase activity was attributed to the decreased O_2 concentration in the system, due to a reduction of photosynthetic O_2 evolution rate and a promotion of dark respiration rate. Moreover, N- and K-deprivation stimulated glycogen accumulation and decreased specific activity of pyruvate kinase. Transcriptome analysis of genes involved in H_2 metabolism using RNA-seq confirmed the above results. Several genes involved in glycogen biosynthesis (*glgA*, *glgB*, *glgP*) were upregulated under both N- and K-deprivation, but genes regulating enzymes in the glycolytic pathway were downregulated, especially *pyk* encoding pyruvate kinase. Interestingly, genes involved in the oxidative pentose phosphate pathway (OPP) were upregulated. Thus, OPP became the favored pathway for glycogen catabolism and the generation of reduced nicotinamide adenine dinucleotide phosphate (NADPH), which resulted in an increase in H_2 production under dark anaerobic conditions in both N- and K-deprived cells.

Keywords: *Aphanothecce halophytica*, Hydrogen production, Gene expression, Potassium deprivation, Nitrogen deprivation, Cyanobacteria, Reducing agents, Redox partner

ACKNOWLEDGEMENTS

This research was financially supported by School of Science, King Mongkut's Institute of Technology Ladkrabang, Bangkok, Thailand. I would like to thank all these people who have always supported me for seven years until my thesis was completed.

First, I'm deeply grateful to my advisor, Associate Professor Dr. Saranya Phunpruch for accepting me to be her advisee as Ph. D. student. I appreciate her effort, time and vigor, great understanding, terrific counseling, to help me finish my research and publish my paper. Many thanks to my co-advisor, Professor Dr. Aran Incharoensakdi for his helpful advice and exceptional discussion on my whole thesis and critical review of the manuscript.

I am very thankful to Professor Dr. Duangrat Inthorn, Associate Professor Dr. Chokchai Kittiwongwattana, Associate Professor Dr. Cherdsak Maneeruttanarungroj, and Assistant Professor Dr. Tipachai Vatanavicharn, for serving as thesis committee, for their precious comments and valuable suggestion.

I also truly appreciate to all members and friends in 407 Molecular Biology Room, Department of Biology, School of Science, King's Mongkut Institute of Technology Ladkrabang (KMITL) for seven-year precious time we've spent together, for sharing both good and bad moments together, for assisting me whenever I needed help. Thank you everyone.

Last but not least, thank you my family for always besides and supporting me. They always give me the opportunities to learn and study, that is very important. I also would like to thank everyone who I do not mention here and who are very important for my success in this thesis.

Nattanon Chinchusak

CONTENTS

Page

ABSTRACT....II
ACKNOWLEDGEMENTS....III
CONTENTS....IV
LIST OF TABLES....IX
LIST OF FIGURES....XI
CHAPTER 1 INTRODUCTION....1
1.1 Statement and significance of the problems....1
1.2 Objectives of the study....4
1.3 Scope of the Study....4
1.4 Benefits of the research project....4
CHAPTER 2 THEORY AND LITERATURE REVIEWS....6
2.1 Hydrogen (H_2)....6
2.2 H_2 production....10
2.2.1 Thermal methods....10
2.2.1.1 Steam reforming....10
2.2.1.2 Autothermal reforming....10
2.2.1.3 Gasification....11
2.2.1.4 Thermochemical water splitting....11
2.2.2 Photocatalytic Methods....11
2.2.3 Electrical Methods....12
2.2.4 Biological process....12
2.2.4.1 Dark-fermentation....12
2.2.4.2 Photofermentation....13
2.2.4.3 CO Gas-Fermentation....14
2.2.4.4 Bio-photolysis....14
2.3 Hydrogen production by cyanobacteria....15

CONTENTS (CONTINUED)

Page

2.4 Enzymes involving in H_2 metabolism of cyanobacteria....18
2.4.1 Nitrogenase....18
2.4.2 Hydrogenase....19
2.5 Cyanobacteria....22
2.5.1 Cell structure of cyanobacteria....22
2.5.2 Reproduction of cyanobacteria....23
2.5.3 Photosynthetic pigments in cyanobacteria....24
2.6 *Aphanothece halophytica*....24
2.7 Reducing agents affecting H_2 production in cyanobacteria....25
2.7.1 Reducing sugars....25
2.7.2 β-mercaptoethanol....26
2.7.3 DL-dithiothreitol....27
2.7.4 Formic acid....27
2.7.5 L-ascorbic acid....28
2.7.6 L-cysteine....28
2.7.7 Oxalic acid....28
2.7.8 Potassium hexacyanoferrate (II) trihydrate....29
2.7.9 Sodium hydrosulfite....29
2.7.10 Sodium sulfide nonahydrate....30
2.8 Effect of nutrient starvation on H_2 production by cyanobacteria....30
2.8.1 Nitrogen deprivation....30
2.8.2 Phosphorus deprivation....31
2.8.3 Potassium deprivation....32
2.8.4 Sulfur deprivation....32
2.9 Literature reviews....33

CONTENTS (CONTINUED)

Page

CHAPTER 3 RESEARCH METHODOLOGY.....40
3.1 Cyanobacteria.....40
3.2 Chemical reagents.....40
3.2.1 Culture media.....40
3.2.2 Enzymes.....40
3.2.3 Chemicals for cultivation.....40
3.2.4 Chemicals and gases for quantitative analyses.....41
3.2.5 Chemicals for genetic studies.....42
3.2.6 Reducing substances.....42
3.3 Instruments.....43
3.4 Cyanobacterial cultivation.....44
3.5 Analytical methods.....44
3.5.1 Optical density measurement.....44
3.5.2 Dry cell weight determination.....44
3.5.3 Cell concentration measurement by hemocytometer.....45
3.5.4 Chlorophyll *a* measurement.....45
3.5.5 H_2 and O_2 production measurement.....45
3.5.6 *In vivo* Hydrogenase activity measurement.....46
3.5.7 Glycogen determination.....47
3.5.8 Phenol sulfuric assay.....47
3.5.9 Protein determination by Bradford assay.....48
3.5.10 Pyruvate kinase activity determination.....48
3.6 Molecular analysis methods.....49
3.6.1 Total RNA isolation.....49
3.6.2 Determination of total nucleic acid.....49
3.6.2.1 Quantitative measurement of total nucleic acid.....
concentration by Nanodrop 2000/2000c.....
Spectrophotometer.....49

CONTENTS (CONTINUED)

Page

3.6.2.2 Nucleic acid analysis by agarose gel electrophoresis.....49
3.6.3 mRNA sequencing by Illumina HiSeq/Novaseq or MGI2000.....50
3.7 Screening of reducing substance types affecting H_2 production.....50
3.7.1 Screening of reducing sugars.....50
3.7.2 Screening of reducing agents.....51
3.7.3 Cell toxicity assay in cells incubated with selective reducing agents.....51
3.7.4 Analysis of redox partners for H_2ase by *in vitro* H_2ase activity measurement.....52
3.8 Cyanobacterial adaptation conditions under nutrient deprivation.....52
3.8.1 Screening of nutrient deprivation for H_2 production.....52
3.8.2 Effect of the limited nutrient concentration on H_2 production under selected nutrient deprivation.....53
3.8.3 Time course of H_2ase activity, H_2 production, O_2 production, glycogen content and specific activity of pyruvate kinase under selected nutrient deprivation.....53
3.8.4 mRNA sequencing by Illumina HiSeq/Novaseq or MGI2000 of the selective nutrient deprivation.....54
3.9 Statistical Analysis.....54
CHAPTER 4 RESULTS.....55
4.1 Effect of reducing substances on H_2 production by *A. halophytica*.....55
4.1.1 Effect of reducing sugars on H_2 production by *A. halophytica* 55
4.1.2 Screening of effective reducing agents for H_2 production by *A. halophytica*.....58
4.1.3 Long-term H_2 production by *A. halophytica* treated with reducing agents.....66
4.1.4 Effect of selective reducing agents on cell toxicity.....69

CONTENTS (CONTINUED)

Page

4.2 Effect of ferredoxin, NADH and NADPH on *in vitro* hydrogenase activity.....73
4.3 Effect of nutrient deprivation on H_2 production and H_2 metabolism.....
of *A. halophytica*.....75
4.3.1 Screening of nutrient deprivation on H_2 production.....75
4.3.2 Effect of nutrient deprivation on H_2 production.....76
4.3.2.1 Effect of nitrogen concentration under potassium.....
deprivation and effect of potassium concentration.....
under nitrogen deprivation on H_2 production and.....
H_2ase activity.....76
4.3.2.2 Effect of adaptation time on H_2 production, H_2ase activity,.....
O_2 production, glycogen accumulation and pyruvate.....
kinase activity.....78
4.3.3 RNA-seq based transcriptome analysis of genes involved in H_2.....
metabolism under N and K deprivation.....84
CHAPTER 5 DISCUSSION.....97
5.1 Effect of reducing substances on H_2 production by *A. halophytica*.....97
5.1.1 Effect of reducing sugars on H_2 production.....97
5.1.2 Effect of reducing agents on H_2 production.....98
5.2 Redox partners for [NiFe]-H_2ase enzyme.....100
5.3 Nutrient deprivation on H_2 production and H_2 metabolism in.....
A. halophytica.....102
5.3.1 N- and K- deprivation for H_2 production by *A. halophytica*.....103
CHAPTER 6 CONCLUSIONS.....110
REFERENCES.....113
APPENDIX.....129
AUTHOR'S BIOGRAPHY.....134

LIST OF TABLES

Table **Page**

2.1 H_2 properties and specifications.....7

3.1 Gas chromatograph conditions used for measurement of H_2 production.....36

4.1 H_2 production rate (μmol H_2 g cell dry wt^{-1} h^{-1}) at 2 h and H_2 accumulation.....
(μmol H_2 g cell dry wt^{-1}) at 24 h of *A. halophytica* incubated in $BG11_0$.....
under dark anaerobic conditions with and without reducing sugars.....57

4.2 H_2 production rate and H_2 accumulation of *A. halophytica* cells in $BG11_0$.....
containing various kinds of reducing agents at concentrations of 0, 0.1,.....
1.0and 10.0 mM after dark anaerobic incubations for 2 and 24 h,.....
respectively.....63

4.3 Cell concentration and culture pH of *A. halophytica* cells in $BG11_0$ containing.....
various kinds of reducing agents at 0, 0.1, 1.0 and 10.0 mM after dark.....
anaerobic incubation for 24 h.....65

4.4 H_2 production, *in vivo* H_2ase activity and O_2 generation rate by *A. halophytica*.....
after incubation in $BG11_0$ containing 10 mM β-mercaptoethanol, 50 mM.....
dithiothreitol, 50 mM L-cysteine and 50 mM sodium sulfide under.....
dark anaerobic conditions for 24 h.....69

4.5 *In vitro* H_2ase activity from cell homogenate of *A. halophytica* in the presence.....
of different types of electron donors; sodium dithionite, ferredoxin, NADH.....
and NADPH.....74

4.6 H_2 production and H_2ase activity by *A. halophytica* cells incubated in various.....
types of media; BG11, potassium-deprived BG11 containing various.....
concentrations of $NaNO_3$, nitrogen-deprived BG11 containing.....
various concentrations of KCl, potassium- and nitrogen-.....
deprived BG11 for 1 day.....78

4.7 Gene expression as log_2FC in oxidative phosphorylation pathway in cells.....
adapted in $BG11_0$, BG11-K and $BG11_0$-K compared to those in BG11.....86

4.8 Gene expression as log_2FC in glycolysis and gluconeogenesis pathways in cells.....
adapted in $BG11_0$, BG11-K and $BG11_0$-K compared to those in BG11.....88

LIST OF TABLES (CONTINUED)

Table **Page**

4.9 Gene expression as log_2FC in pentose phosphate pathway in cells adapted in..... $BG11_0$, BG11-K and $BG11_0$-K compared to those in BG11.....89

4.10 Gene expression as log_2FC in nitrogen metabolism in cells adapted in $BG11_0$,..... BG11-K and $BG11_0$-K compared to those in BG11.....90

4.11 Gene expression as log_2FC in photosynthetic pathway in cells adapted in..... $BG11_0$, BG11-K and $BG11_0$-K compared to those in BG11.....91

4.12 Gene expression in carbon fixation in photosynthetic pathway between..... $BG11_0$, BG11-K and $BG11_0$-K treatment compared to BG11 sample in log_2FC.....94

A Bradford reagent.....133

LIST OF FIGURES

Figure **Page**

2.1 Three of H_2-producing bacteria 13
2.2 Direct and indirect bio-photolysis process of photosynthetic microorganisms.....15
2.3 The electron flows for H_2 production in cyanobacteria.....17
2.4 Cyanobacterial enzymes involving H_2 metabolism.....20
2.5 Cyanobacterial morphology.....23
2.6 Cell morphology of halotolerant unicellular cyanobacterium *Aphanothece* ..... *halophytica* observed under light microscope.....25
2.7 Chemical structure of glucose, mannose and fructose.....25
2.8 Disaccharides structure, sucrose (glucose+fructose), Lactose..... (Galactose+glucose) and maltose (glucose+glucose).....26
2.9 Structure of β-mercaptoethanol.....27
2.10 Structure of DL-dithiothreitol.....27
2.11 Structure of Formic acid.....27
2.12 Structure of L-ascorbic acid.....28
2.13 Structure of L-cysteine.....28
2.14 Structure of oxalic acid.....29
2.15 Structure of potassium hexacyanoferrate (II) trihydrate.....29
2.16 Structure of sodium hydrosulfite.....29
2.17 Structure of sodium sulfide nonahydrate.....30
4.1 H_2 production rate by *A. halophytica* after incubation in $BG11_0$ containing..... Various concentrations of 0, 0.189, 1.89, 18.9 and 189 mmol C atom L^{-1}..... of glucose, fructose, maltose and lactose, after 2 h of dark anaerobic..... conditions.....56
4.2 H_2 production rate of *A. halophytica* cells in $BG11_0$ treated with different..... types of reducing agents at 0, 0.1, 1.0 and 10.0 mM under dark anaerobic..... conditions for 2 h.....61

LIST OF FIGURES (CONTINUED)

Figure **Page**

4.3 H_2 accumulation of *A. halophytica* cells in $BG11_0$ treated with different types..... of reducing agents at 0, 0.1, 1.0 and 10.0 mM under dark anaerobic conditions..... for 24 h.....62

4.4 Long-term H_2 production by *A. halophytica* treated with different..... concentrations (0 mM (O), 10 mM (◊), 20mM (Δ), 50mM (□) and..... 100 mM (■) of β-mercaptoethanol, dithiothreitol, L-cysteine..... and Sodium sulfide for various times under dark anaerobic..... conditions.....67

4.5 Cell concentration of *A. halophytica* cells after incubation with various..... concentrations of β-mercaptoethanol (a), dithiothreitol (b), L-cysteine..... (c), and sodium sulfide (d) under dark anaerobic conditions for 24 h.....71

4.6 Chlorophyll *a* concentration of *A. halophytica* cells after incubation with..... various concentrations of β-mercaptoethanol (a), dithiothreitol (b),..... L-cysteine (c), and sodium sulfide (d) under dark anaerobic conditions for 24 h.....72

4.7 H_2 production by *A. halophytica* cells incubated in BG11 (●), $BG11_0$ (▲),..... BG11-K (■), BG11-P (+) and BG11-S (✳) under dark anaerobic conditions.....76

4.8 H_2 production by *A. halophytica* cells adapted in BG11 (●), $BG11_0$ (▲),..... BG11-K (■) and $BG11_0$-K (♦) under light aerobic conditions for 5 days.....79

4.9 H_2ase activity of A. halophytica cells adapted in BG11 (●), $BG11_0$ (▲),.....80 BG11-K (■) and $BG11_0$-K (♦) under light aerobic conditions for 5 days.....80

4.10 O_2 evolution rate by *A. halophytica* adapted in BG11 (●), $BG11_0$ (▲),..... BG11-K (■) and $BG11_0$-K (♦) under light aerobic conditions for 5 days.....81

4.11 Specific activity of pyruvate kinase of *A. halophytica* cells adapted in BG11 (●),.... $BG11_0$ (▲), BG11-K (■) and $BG11_0$-K (♦) under light aerobic conditions for..... 5 days..... 82

LIST OF FIGURES (CONTINUED)

Figure **Page**

4.12 Glycogen accumulation of *A. halophytica* cells adapted in BG11 (●),..... $BG11_0$ (▲), BG11-K (■) and $BG11_0$-K (♦) under light aerobic..... conditions for 5 days.....83

4.13 Number of up- and down-regulated genes between treatment samples;..... *A. halophytica* adapted in BG11, $BG11_0$, BG11-K and $BG11_0$-K ($BG11_0$-K).....85

5.1 Transcriptional level of genes involving in photosynthetic pathway, carbon..... assimilation such as Calvin-Benson cycle, glycolysis, oxidative pentose..... phosphate pathway, and nitrate assimilation in *A. halophytica*.....108

5.2 Proposed schematic mechanism of H_2 production by *A. halophytica* based..... on the RNA-seq after adaptation in nitrogen and/or potassium deprivation..... for 2 days.....109

A Line drawing of ruling of Neubauer type hemocytometer chamber. Chamber..... units are 1 mm with a depth of 0.1 mm. (Absher, 1973).....131

B Standard calibration curve of glycogen.....132

C Standard calibration curve of bovine serum albumin.....133

CHAPTER 1
INTRODUCTION

1.1 Statement and significance of the problems

Nowadays, energy is very important for living organisms. Humans use energy for daily activities in many ways such as in the household, in agriculture and in industry. The main source of energy comes from fossil fuel that is a limited supply and a non-renewable resource. Fossil fuel is going to run out soon due to an increase in energy consumption. In addition, the main disadvantage of fossil fuel combustion is the release of CO_2 and greenhouse gases in the atmosphere, resulting in environmental problems and global warming. Therefore, environmental-friendly renewable fuels are expected to be used instead of fossil fuel.

Hydrogen (H_2) is one of the promising sustainable alternative renewable energy carriers that is not a primary energy source like coal, gas, or oil. Rather, its role is considered as a secondary energy source or 'energy carrier', which must be produced by using energy from other sources and then transported to end-use applications. H_2 can be stored as fuel and used in transportation and in many applications. The combustion of H_2 provides a high heating value of 141.6 MJ kg^{-1} (Perry, 1963). No greenhouse gases are obtained from H_2 combustion (Gupta and Parkhey, 2017). When H_2 is burned with O_2, water is the only by-product. H_2 can be produced from both renewable (wind, hydro, solar, wave, biomass and geothermal) and non-renewable (natural gas, nuclear and coal) resources.

H_2 can also be produced by various kinds of microorganisms such as anaerobic bacteria, fermentative bacteria, green algae, and cyanobacteria, etc. H_2 produced by microorganisms is called "Biohydrogen". Biohydrogen production is dependent on the type of microorganisms and their metabolic pathways. Biohydrogen can be produced by many processes including direct biophotolysis, indirect biophotolysis photofermentation and dark fermentation. Cyanobacteria or blue-green algae are photosynthetic prokaryotes that show high potential in H_2 production (Bothe et al., 2010). Cyanobacterial characteristics are different depending on types of organisms, and physiological conditions.

Three enzymes are involved in H_2 metabolism in cyanobacteria, that are nitrogenase, uptake hydrogenase and reversible hydrogenase. Nitrogenase catalyzes nitrogen fixation to produce ammonia as a main product and provide H_2 as a by-product. Nitrogenase is usually located in heterocyst cells of N_2-fixing cyanobacteria. However, nitrogenase can also be found in non-heterocystous unicellular cyanobacteria such as *Synechococcus* sp., *Gloeothece* sp. and *Cyanothece* sp. (Reddy et al., 1993; Chow and Tabita, 1994; Compaoré and Stal, 2010). Uptake or unidirectional hydrogenase occurs in N_2-fixing species. It oxidizes H_2 produced by nitrogenase activity. Reversible or bidirectional hydrogenase can both oxidize and generate H_2. It is found in all kinds of cyanobacteria including heterocystous, filamentous, and non-heterocystous unicellular cyanobacteria (Taikhao et al., 2013; Sjoholm et al., 2007; Gutekunst et al., 2014; Kentemich et al., 1989; Serebryakova et al., 1998).

To increase H_2 production by microorganisms, it is required to enhance efficiency of hydrogenase and to overcome obstacles of hydrogenase limitation. One obstacle is the inhibition of hydrogenase and nitrogenase activities by O_2. In photosynthetic organisms, O_2 is evolved by photosystem II in oxygenic photosynthesis. Therefore, H_2 production is induced under anaerobic conditions. In addition, to sustain and enhance H_2 production by preventing inactivity of enzymes by O_2, the two-stage H_2 production process has been proposed (Ananyev et al., 2012). In the first stage, cyanobacterial cells grow in abundant media to accumulate biomass. After that, In the second stage, cells are incubated under stress conditions and produce H_2 under dark anaerobic conditions.

Aphanothece halophytica is the unicellular halotolerant cyanobacterium that shows a potential for H_2 production (Taikhao et al., 2013; Taikhao et al., 2015). *A. halophytica* is a model organism for studying the salt tolerance mechanism in cyanobacteria. In the photosystem I-driven reaction for CO_2 assimilation, H_2 can be used as an electron donor (Belkin and Padan, 1978). In *A. halophytica*, only *hox* operon encoding bidirectional [NiFe]-hydrogenase has been identified (Phunpruch et al., 2016). Under dark anaerobic conditions, H_2 can be produced by electrons obtained from a glycogen degradation of carbohydrate catabolism (Taikhao et al., 2015). The effects of many factors on H_2 production in *A. halophytica,* such as nutrient deprivation, concentration of carbon sources and NaCl, pH, light intensity and incubation temperature

have been investigated (Taikhao et al., 2015). Furthermore, H_2 production by *A. halophytica* is stimulated by cell immobilization (Pansook et al., 2019a) and by photosystem II inhibitor treatment (Pansook et al., 2019b; Pansook et al., 2022).

Reducing agent, one of external factors, can be used as excessive electron sources to increase H_2 production by cyanobacteria (Sadvakasova, 2020). Electrons from reducing agents can be provided to bidirectional [NiFe]-hydrogenase for balancing redox reactions, thus generating H_2 (Gutekunst et al., 2014). Previous studies showed that some reducing agents stimulated H_2 production in various cyanobacteria (Luo and Mitsui, 1996; Taikhao and Phunpruch, 2017; Baebprasert et al., 2010). However, the effect of reducing agents on cell toxicity has been less investigated.

Deprivation of nutrients in media can also induce H_2 production that is an effective way to sustain H_2 production in cyanobacteria (Srirangan et al., 2011). Under dark anaerobic conditions, N-deprived cells of *A. halophytica* showed high H_2 production (Taikhao et al., 2013; Taikhao et al., 2015). Nitrogen deprivation also enhanced H_2 evolution by *Calothrix membranacea* and *Oscillatoria brevis* (Lambert and Smith, 1977) and *Anabaena siamensis* TISIR 8012 (Taikhao and Phunpruch, 2017). The accumulation of glycogen is carried out via photoautotrophic conditions under nitrogen deprivation. The accumulated glycogen is catalyzed into glucose-6-phosphate and reduced nicotinamide adenine dinucleotide (NADH) and reduced nicotinamide adenine dinucleotide phosphate (NADPH), the electron donor of [NiFe]-hydrogenase, and H_2 is produced thereafter under dark anaerobic conditions (Ananyev et al., 2008). In N-deprived cells of *A. halophytica*, bidirectional [NiFe]-hydrogenase activity was significantly induced and expression of *narB* encoding ferredoxin-nitrate reductase was downregulated during dark anaerobic incubation (Phunpruch et al., 2016). Consequently, NADH was enhanced and then H_2 was produced increasingly (Phunpruch et al., 2016). In addition, sulfur deprivation increased H_2 production by *Gloeocapsa alpicola* (Antal and Lindblad, 2005) and *Microcystis aeruginosa* (Rashid et al., 2009). Potassium deprivation increased H_2 production by *Synechocystis* sp. PCC6803 (Ueda et al., 2016).

In this study, the effect of reducing sugar and reducing agent on dark fermentative H_2 production by N-deprived cells of *A. halophytica* was investigated. This work also

focused on H_2 production by *A. halophytica* under nutrient-deprived conditions and investigation on the H_2 metabolism under these conditions. H_2ase activity, glycogen content and pyruvate kinase activity were also determined. Transcriptional analysis of genes involving photosynthesis and carbon and nitrogen assimilation pathways in nitrogen- and potassium-deprived cells was performed by RNA sequencing.

1.2 Objectives of the study

The objectives of this study are:

1.2.1 To study the effect of reducing sugar and reducing agents on H_2 production by *A. halophytica*.

1.2.2 To investigate the effect of nutrient deprivation on H_2 production by *A. halophytica* and the transcriptional analysis of genes involved in H_2 production under nutrient-deprived conditions.

1.3 Scope of the study

The scope of this study is divided into three parts. Firstly, the effect of reducing agent on H_2ase activity, cell toxicity and H_2 production by *A. halophytica* was investigated. Secondly, the effect of nutrient deprivation on H_2 production was investigated. In addition, the effect of nitrogen and potassium deprivation on H_2ase activity, pyruvate kinase activity and glycogen metabolism, was studied. Finally, gene expression involved in H_2-related metabolisms such as photosynthetic pathway, glycogen metabolism, glycolytic pathway, oxidative pentose phosphate pathway and nitrate pathway under nitrogen and potassium deprivation was investigated.

1.4 Benefits of the research project

The expected benefits of this study are:

1.4.1 To improve H_2 production efficiency of *A. halophytica* by using reducing agents.

1.4.2 To investigate the effect of nutrient deprivations on H_2 production by *A. halophytica* and understand H_2 metabolism and related metabolisms in *A. halophytica* under nutrient-deprived conditions.

1.4.3 Knowledges obtained by this study can be used for enhancing H_2 production by *A. halophytica* that is able to grow in natural seawater for use in industrial scales.

CHAPTER 2
THEORY AND LITERATURE REVIEWS

2.1 Hydrogen (H_2)

The energy demand has been increased greatly due to the growth of global population and economy, including accelerated urbanization (Alanne and Cao, 2019; Zhang, 2018; Racliffe, 2018). Typical energy supply depends on limited fossil fuels depending on the geographical allocation (Tian, 2018; Dicks and Rand, 2018). As people have utilized fossil fuels as the main source of energy, especially in industry scale, an enormous increase in the levels of CO_2 and greenhouse gases in the atmosphere has been found, leading to the global warming (Dicks and Rand, 2018; Das, 2018; Boudellal, 2018; Sankir and Sankir, 2017). Thus, alternative sustainable and renewable energy sources are considered to use for decarbonization and are necessary for sustainability of future energy (Radcliffe, 2018; Boudellal, 2018; Council and Bulletin, 2018; Yuan, 2017; Silveira, 2017). Hydrogen (H_2) can be the solution for this idea because it can act as energy carrier (Boudellal, 2018; Sankir and Sankir, 2017) which is storable, transportable, and utilizable (Boudellal, 2018; Blanco and Faaij, 2018).

Hydrogen atom (H) is the most plentiful element in the universe. It is found in water and organic compounds on our earth planet (Gielen et al., 2019; Kotter et al., 2016). It is the simplest element consisting of only one electron and one proton (Gielen et al., 2019). H_2 is colorless, odorless, and flammable gas (Rivkin and Buttner, 2015). The atomic weight of H is 1.00794 g mol^{-1}. At higher energy value, H_2 energy content is 141.8 MJ kg^{-1} at 298 K and heating value of H_2 is 120 MJ kg^{-1} at lower heating value at 298 K, which is higher than that of most fuels (Vincent and Bessarabov, 2018; Liu et al., 2017). H_2 is lighter than air and it is a non-toxic gas. In case of leak, H_2 is dissolved and spread rapidly which makes it moderately safer than other fuels (Labs, 2019). However, H_2 is a flammable gas which may create a large portion of risk correlated with its usage (Rivkin and Buttner, 2015). The overview of H_2 properties is shown in Table 2.1.

Table 2.1 H_2 properties and specifications

Properties	SI Units	References
Discovery date / by / Chemical formula isotopes	1766 / Henry Cavendish / H_2 ^1H (99.98%), ^2H, ^3H, (^4H-^7H Unstable)	Blumenthal, 2013
Equivalence; Hydrogen solid, liquid and gas at pressure = 981 mbar and temperature = 20 °C	1 kg = 14,104 L = 12,126 m^3	Blumenthal, 2013
Molecular weight	1.00794	Huertas and Llompart, 2017
Vapor pressure at -252.8 °C	101.283 kPa	Dick and Rand, 2018; Rivkin and Buttner, 2015
Density of the gas at boiling point and 1 atm	1.331 kg m^{-3}	Dick and Rand, 2018; Rivkin and Buttner, 2015
Specific gravity of the gas at 0 °C and 1 atm (air = 1)	0.0696	Dick and Rand, 2018; Rivkin and Buttner, 2015; Halm et al., 2017
Specific volume of the gas at 21.1 °C and 1 atm	11.99 m^3 kg^{-1}	Dick and Rand, 2018; Rivkin and Buttner, 2015
Specific gravity of the liquid at boiling point and 1 atm	0.0710	Rivkin and Buttner, 2015
Density of the liquid at boiling point and 1 atm	67.76 kg m^{-3}	Rivkin and Buttner, 2015
Boiling point at 101.283 kPa	-252.8 °C	Rivkin and Buttner, 2015
Freezing/Melting point at 101.283 kPa	-259.2 °C	Dick and Rand, 2018; Rivkin and Buttner, 2015

Table 2.1 H_2 properties and specifications (continued)

Properties	SI Units	References
Critical temperature	-239.9 °C	Rivkin and Buttner, 2015
Critical pressure	1296.212 kPa, abs	Rivkin and Buttner, 2015
Critical density	30.12 kg m^{-3}	Rivkin and Buttner, 2015
Triple point	-259.3 °C at 7.042 kPa, abs	Dick and Rand, 2018; Rivkin and Buttner, 2015
Latent heat of fusion at the triple point	58.09 kJ kg^{-1}	Rivkin and Buttner, 2015
Latent heat of vaporization at boiling point	445.6 kJ kg^{-1}	Rivkin and Buttner, 2015
Solubility in water vol vol^{-1} at 15.6 °C	0.019	Rivkin and Buttner, 2015
Dilute gas viscosity at 26 °C (299 K)	9×10^{-6} Pa s	Tabkhi et al., 2008
Molecular diffusively in air	6.1×10^{-5} m^2 s^{-1}	Tabkhi et al., 2008
Cp	14.34 kJ kg^{-1} $°C^{-1}$	Liu et al. 2017; Rivkin and Buttner, 2015
Cv	10.12 kJ kg^{-1} $°C^{-1}$	Rivkin and Buttner, 2015
Ratio of specific heats (Cp/Cv)	1.42	Rivkin and Buttner, 2015; Tabkhi et al., 2008
Lower heating value, weight basis	120 MJ kg^{-1}	Tabkhi et al., 2008
Higher heating value, weight basis	141.8 MJ kg^{-1}	Tabkhi et al., 2008

Table 2.1 H_2 properties and specifications (continued)

Properties	SI Units	References
Lower heating value, volume basis at 1 atm	11 MJ m^{-3}	Tabkhi et al., 2008
Higher heating value, volume basis at 1 atm	13 MJ m^{-3}	Tabkhi et al., 2008
Stoichiometric air-to-fuel ratio at 27 °C and 1 atm	34.2 kg kg^{-1}	Liu et al., 2017
Flammable limits in air	4% - 75%	Tabkhi et al., 2008; Rivkin and Buttner, 2015
Explosive (detonability) limits	18.2 to 58.9 vol% in air	Tabkhi et al., 2008
Maximum combustion rate in air	2.7/3.46 (m s^{-1})	Dick and Rand, 2018; Huertas and Llompart, 2017
Maximum flame temperature	1526.85 °C	Tabkhi et al., 2008
Autoignition temperature / in air	400 °C / 571 °C	Rivkin and Buttner, 2015; Dick and Rand, 2018; Tabkhi et al., 2008

2.2 H_2 production

The major H_2 production processes are divided into 4 processes.

2.2.1 Thermal methods

Presently, most H_2 is produced by thermal processes as well as reforming, gasification, and thermochemical processes.

2.2.1.1 Steam reforming

In this process, H_2 is obtained via a catalysis reaction of a hydrocarbon and steam as shown in equation 2.1.

$$C_nH_m + nH_2O \leftrightarrow nCO + (n+1/2m)\ H_2 \quad (2.1)$$

There are many kinds of steam reforming processes depending on the type of substrates. Among these reforming processes, methane steam reforming (MSR) is the most practicable path to transform methane into H_2 (Shen et al., 2020). Methane is the simplest hydrocarbon molecule that has an energy value of 55.5 MJ kg^{-1}. In the reforming process, methane is reacted with steam at 700 to 1000 °C under pressure of 3 to 25 bar (Chen et al., 2020). In the gas steam outlet, CO, H_2, unreacted methane and CO_2 are present. Consequently, treatment and purification steps are necessary for providing pure H_2. One of the main challenges in MSR process is to control the high reaction temperatures reaching 700 to 800 °C at the center of the catalytic bed and 1200 °C on the external reactor partition. In addition, the substrate methane used in MSR is mainly from fossils. Therefore, the biomethane produced by the anaerobic digestion of sewage sludge can also be an alternative way (Grasham et al., 2020).

2.2.1.2 Autothermal reforming

Autothermal reforming (ATR) uses the heat of an exothermic reaction or partial oxidation to maintain the endothermic steam reforming reaction by feeding air, steam, and the reaction feedstock such as methane, and thus abundant H_2 steam is generated. The main advantage of ATR is the requirement of low energy. There is no external heat required by selecting the proper oxygen: fuel ratio. Ni-based catalysts are

the most practical in methane autothermal reaction due to the low cost. The catalyst preparation method is one of the features that can increase the catalytic performance by improving the catalyst physicochemical properties. These methods modify the metal-support interaction, thus changing the kinetics of the catalyst, resulting in enhancing productivity, reducing cost, and optimizing energy requirements (Osazuwa et al., 2021).

2.2.1.3 Gasification

Gasification is a process where carbonaceous materials are transformed to syngas at high temperature in the presence of an oxidizing agent. Several types of biomasses can be used as probable feedstocks for H_2 production in this process including algae, food waste and lignocellulosic biomass (Cao et al., 2020). H_2 yield is mainly dependent on the process conditions of the biomass gasification, temperature of steam flow and the type of raw materials (Singh et al., 2020). The optimization of biomass blending can be an effective way to overcome the problem of massive feedstock variability (Alnouss et al., 2020). One of the most problems of conventional gasification is an unfeasibility of using biomass with a high moisture content. Gasification in supercritical water cannot directly use the biomass with drying process because the reaction occurs in water phase.

2.2.1.4 Thermochemical water splitting

Water splitting is the reaction where water is split into H_2 and O_2 as equation: $2H_2O$ + heat $\longrightarrow$ H_2 + O_2. A single step of decomposition can be occurred only at high temperatures above 2,000 °C, while thermochemical cycles and lower operating temperatures can provide the required heat (Mehrpooya and Habibi, 2020).

2.2.2 Photocatalytic methods

This method generates H_2 by water splitting using solar energy. H_2 is produced via the production of electron-hole pairs by semiconductor and photons (Lim et al., 2020). Photoexcited electron-hole pairs can be divided by sacrificial agents. These agents provide the recombination of reduced electron-hole pair which allows the formation of H_2. To

overcome the challenges of low photon conversion efficiency by using visible light, the addition of different metals to titanium dioxide causes an increase in H_2 production.

2.2.3 Electrical methods

This process refers to water electrolysis, where hydrogen and oxygen are produced from molecules of water as the equation 2.2.

$$2H_2O \longrightarrow 2H_2 + O_2 \quad (2.2)$$

A significant amount of energy, ΔH^0 = 285.8 kJ mol^{-1} and ΔG^0 = 237.2 kJ mol^{-1} is required for water separation under standard conditions. In addition, for water separation, cell voltage with 1.23 V is required under standard conditions (Lamy and Millet, 2020). However, the limitation of this process is the slow kinetics. The requirement of cell voltages of 1.8 – 2.0 V for reaching the significant H_2 production rate increases the costs and decreases the efficiency of the process (Lamy and Millet, 2020).

2.2.4 Biological process

Biological processes produce H_2 from renewable resources such as biomass and solar energy. Biological H_2 production can be divided into four processes (Akhlaghi and Najafpour, 2020).

2.2.4.1 Dark-fermentation

In this process, anaerobic organisms can utilize organic substrates such as sugars, amino acids, waste materials and wastewater to produce H_2 without light (Christopher et al., 2021). Due to low production costs, this method is considered as a promising alternative way to produce H_2 (Dahiya et al., 2021). H_2-producing bacteria can be divided into 3 groups: facultative bacteria, non-sporulating anaerobes bacteria and spore-forming obligatory anaerobic bacteria (Fig. 2.1) (Castello and Nunes, 2020). The bacterium *Clostridium*, belonging to the spore-forming obligate anaerobic organism, is the most effective bacterium for H_2 production in both acetate-type fermentation (equation 2.3) and butyrate-type fermentation (equation 2.4) (Castello and Nunes, 2020).

$$C_6H_{12}O_6 + 2H_2O \longrightarrow 2CH_3COOH + 4H_2 + 2CO_2,\ \Delta G^0 = -206\ kJ\ mol^{-1} \quad (2.3)$$

$$C_6H_{12}O_6 \longrightarrow CH_3CH_2CH_2COOH + 2H_2 + 2CO_2,\ \Delta G^0 = 255\ kJ\ mol^{-1} \quad (2.4)$$

The yield of H_2 production depends on various factors such as pH, temperature, pressure hydraulic retention time (García et al., 2021), composition of the substrate, etc. However, the main limitation of this process is homoacetogenesis (equation 2.5) (Castello and Nunes, 2020).

$$4H_2 + 2CO_2 \longrightarrow CH_3COOH + 2H_2O,\ \Delta G^0 = -104\ kJ\ mol^{-1} \quad (2.5)$$

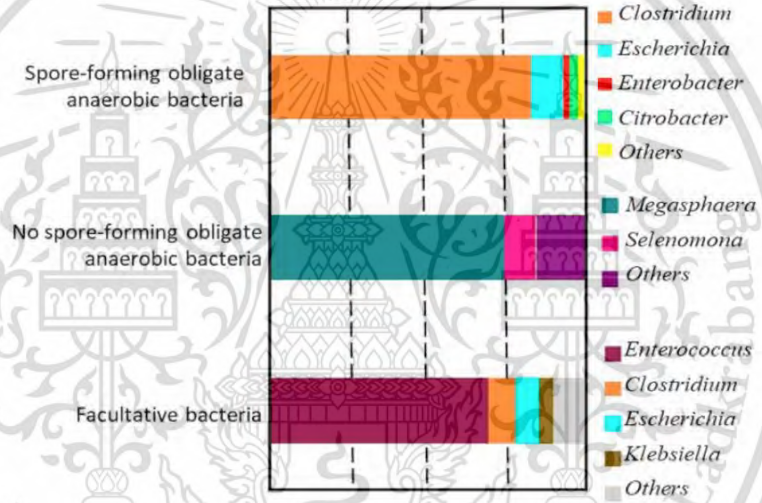

Fig. 2.1 Three groups of H_2-producing bacteria (Castello and Nunes, 2020)

2.2.4.2 Photofermentation

In this process, H_2 is produced from organic compounds via a nitrogenase-catalyzed reaction, under the presence of light energy, by photosynthetic or anaerobic bacteria, such as *Rhodobacter*, *Rhodobium*, *Rhodospirillum* and *Rhodopseudomonas* (Hitam and Jalil, 2020). Photofermentation requires specific substrates i.e., small fatty acids, acetate, propionate, and butyrate (equation 2.6) (Baeyens et al., 2020).

$$CH_3COOH + 2H_2O + Light \longrightarrow 4H_2 + CO_2,\ \Delta G^0 = +104\ kJ\ mol^{-1} \quad (2.6)$$

2.2.4.3 CO Gas-Fermentation

In the presence of photosynthetic bacteria, carbon monoxide and water are used to produce H_2 under anaerobic conditions (equation 2.7) (Akhlaghi and Najafpour, 2020).

$$CO + H_2O \longrightarrow CO_2 + H_2,\ \Delta G^0 = -201\ kJ\ mol^{-1} \quad (2.7)$$

Although this process is considered as promising for alternative H_2 production, H_2 consumption by homoacetogenesis is still the main limitation.

2.2.4.4 Bio-photolysis

Bio-photolysis or photonic-driven H_2 production process is the method to produce H_2 via water splitting in cyanobacteria and blue-green algae (Hitam and Jalil, 2020). This process can be divided into direct bio-photolysis and indirect bio-photolysis (Fig. 2.2). The direct process is H_2 production by a photosynthetic reaction in microalgae in the presence of solar energy (equation 2.8) (Kumar et al. 2020).

$$2H_2O + \text{Light energy} \longrightarrow O_2 + 2H_2 \quad (2.8)$$

Meanwhile, indirect bio-photolysis is a two-step process. The first step is the photosynthetic process (equation 2.9) and the second step is the generation of H_2 and CO_2 (equation 2.10) (Kumar et al., 2020). H_2 is produced by hydrogenase and nitrogenase activities.

$$12H_2O + 6CO_2 + \text{Solar energy} \longrightarrow 6O_2 + C_6H_{12}O_6 \quad (2.9)$$

$$C_6H_{12}O_6 + 12H_2O + \text{Solar energy} \longrightarrow 6CO_2 + 12H_2 \quad (2.10)$$

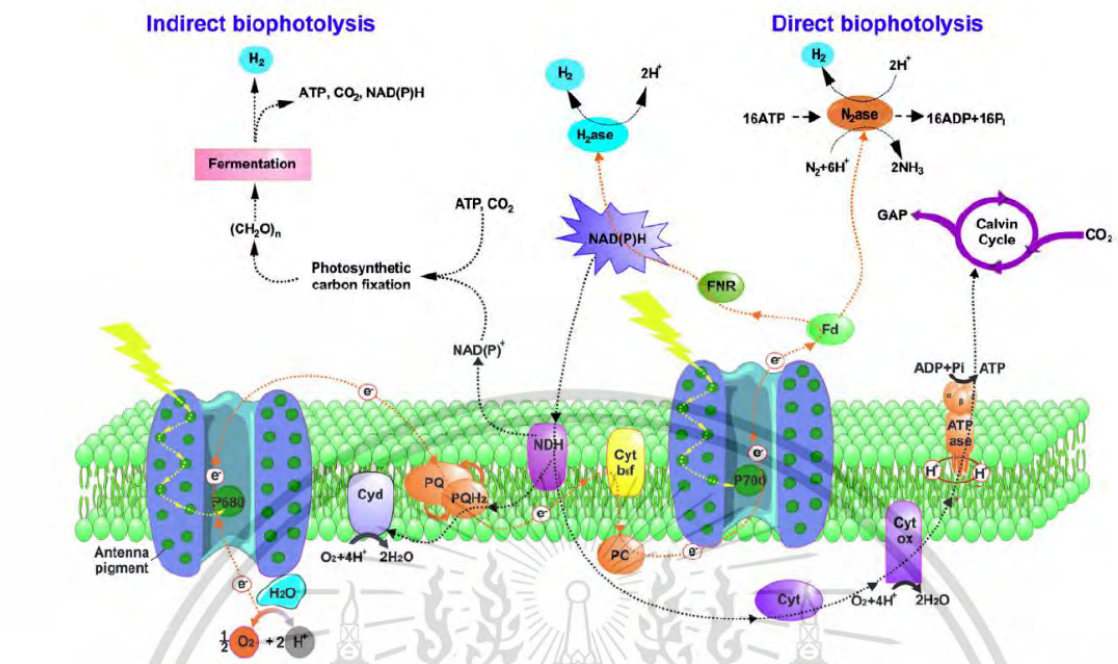

Fig. 2.2 Direct and indirect bio-photolysis process of photosynthetic microorganisms. Abbreviation: Cyd, quinol oxidase; PQH_2/PQ, plastoquinol/plastoquinone; ATPase, ATP synthase; Cyt b_6f, cytochrome b_6f complex; Fd, ferredoxin; FNR, ferredoxin NAD(P) reductase; H_2ase, hydrogenase; NDH, NAD(P)H dehydrogenase; PC, plastocyanin; PQ, plastoquinones; P680, Photosystem II; P700, Photosystem I; N_2ase, nitrogenase; H_2, hydrogen (Kossalbayev et al., 2020).

2.3 Hydrogen production by cyanobacteria

Hydrogen as a by-product of biochemical production in the metabolism of microorganisms is considerately a promising renewable energy source for the future. The bio-photolysis process performed by cyanobacteria has been studied over the past 35 years (Weare and Benemann, 1973). In water bio-photolysis systems, electron transport chain of photosynthesis and water splitting system occur, resulting in H_2 production. There are two processes of bio-photolysis system, direct and indirect bio-photolysis (Bolakhan et al., 2019). The process of direct bio-photolysis is involved in absorption of light energy by the photosynthesis apparatus for water splitting with the formation of O_2 and to produce low-potential reducing agents, resulting in the reduction of protons and the production of H_2 (Fig. 2.3). Throughout the direct bio-photolysis, reducing agents,

ferredoxin, or NADPH, produced by photosynthesis directly reduces hydrogenase. Meanwhile in indirect bio-photolysis, the products of water splitting in photosynthesis and the reduction of ferredoxin are used in the carbon dioxide fixation. The obtained carbon compounds can be used for accelerating H_2 production (Fig. 2.3). In direct bio-photolysis, cyanobacteria can generate protons and electrons in the process of water splitting. H_2 production resulted from the direct absorption of light and electron transfer via hydrogenases and nitrogenases (Manis and Banerjee, 2008). In anaerobic conditions or when the energy excess is available, photosynthetic microorganisms might release excessive electrons with the assistance of the hydrogenase to transform H^+ into H_2.

Cyanobacteria are one of the photosynthetic microorganisms that are suitable for photobiological H_2 production (Bolatkhan et al., 2019, Nagarajab et al., 2017). They can absorb CO_2 in the atmosphere as carbon source so that they can grow on simple nutrient media. Many cyanobacterial strains can reduce N_2 from the atmosphere to produce ammonia. There are various unique characteristics including their ability for survival under extreme conditions, photosynthesis involving in participation of unusual pigments, nitrogen fixation, the releasing of several compounds into cultural media (Akkerman et al., 2002).

There are two enzymes involved in H_2 metabolism, hydrogenase and nitrogenase (Fig. 2.3). Nitrogenase catalyzes the reduction of nitrogen to ammonia simultaneously with the production of H_2. Hydrogenase catalyzes the reduction of H_2 from protons and electrons. Both enzymes play a key role for biological production of H_2 in cyanobacteria. Hydrogenase and nitrogenase enzymes vary between species of cyanobacteria. Moreover, these enzymes can be either inducible or constitutive. Genes related in H_2 metabolism can be induced leading to the activation of enzyme synthesis under physiological conditions (Carrieri et al., 2011).

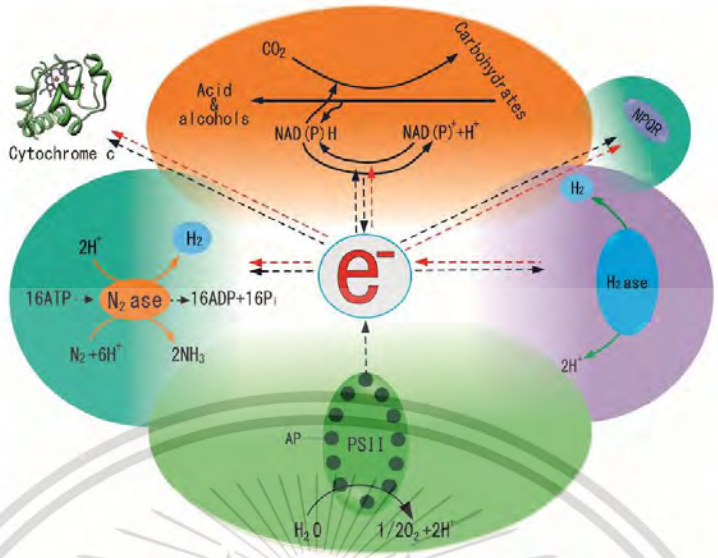

Fig. 2.3 The electron flows for H_2 production in cyanobacteria. Red arrows show the electrons flow and chemical reaction involving H_2 consumption. Black arrows show the electrons flow involving carbohydrate metabolism and photosynthesis. This figure is modified from the previous study (Srirangan et al., 2011).

H_2 can be produced via bidirectional [NiFe]-hydrogenase and nitrogenase in cyanobacteria. Electron transport in cyanobacteria is the essential process for H_2 production. Either electrons associated with photosynthesis or electrons from carbohydrate catabolism are important for H_2 production. The acquired electrons are transported to ferredoxin and donated to PQ, and FNR carries the electrons to nitrogenase. The energy for H_2 production in nitrogen fixation can be regenerated by H_2 consumption by [NiFe]-hydrogenase. The required electrons from H_2 consumption are recycled to photosynthetic electron transport chain through PQ pool and it can be used either by cytochrome c oxidase for the reduction of O_2 to water or transferred back to nitrogenase via PSI and ferredoxin located in heterocyst (Fig. 2.3) (Srirangan et al., 2011).

2.4 Enzymes involving in H_2 metabolism of cyanobacteria

2.4.1 Nitrogenase

Nitrogenase is a complex enzyme which plays a key role in nitrogen fixation. It is normally found in prokaryotes. Nitrogenase catalyzes N_2 fixation and provides the conversion of about 60% of fixed nitrogen from N_2 of the biogeochemical nitrogen cycle in planet earth. As shown in equation 2.11, nitrogenase catalyzes the reaction of nitrogen fixation using magnesium adenosine triphosphate (MgATP) and electrons to reduce substrates and protons.

$$N_2 + 8H^+ + 8e^- + 16ATP \longrightarrow 2NH_3 + H_2 + 16ADP + 16P_i \quad (2.11)$$

According to this equation, nitrogen fixation requires 8 electrons and 16 ATP molecules to generate one H_2 molecule per one nitrogen molecule. H_2 production is catalyzed by nitrogenase at the rate of one third of the rate of nitrogen fixation. However, nitrogenase is highly sensitive to oxygen. Nitrogen fixation needs several protective mechanisms to neutralize nitrogenase such as spatial separation in heterocyst cells. Nitrogenase can be divided into three types depending on the metal type in the active site of enzyme: 1) Mo-nitrogenase, 2) V-nitrogenase, and 3) Fe-nitrogenase.

Mo-nitrogenase is found in both vegetative and heterocyst cells (Ferreira et al., 2017). Its activity is regulated by the level of ATP/ADP in cells and the size of the endogenous pool of the reducing agents (Baebprasert et al., 2011; Suzuki et al., 1995). There is $\alpha 2\beta 2$ heterotetramer in dinitrogenase with a molecular weight of 220-240 kDa. It breaks down nitrogen atoms. Dinitrogenase reductase plays a key role as a mediator in the electron transfer from external electron donors (ferredoxin or flavodoxin) to dinitrogenase. Its molecular weight of 60-70 kDa.

Cyanobacterial V-nitrogenase was first demonstrated in *Anabaena variabilis* cells (Kentemich et al., 1988). In molybdenum depletion of cells and in the presence of vanadium in the medium, cells reduce acetylene to ethylene and produce H_2. V-nitrogenase was found in *Anabaena* sp. CH1 and *Anabaena azotica* (Boison et al., 2006), in two *Anabaena* strains and one *Nostoc* strain (Masukawa et al., 2012). Nevertheless, the

structural genes of V-nitrogenase were obtained and demonstrated in *A. variabilis*, *Nostoc punctiforme* (Thiel et al., 1997).

Fe-nitrogenase has the lowest ratio of N_2 reduction relative to H_2 production yield compared with the three forms of nitrogenase (Mo-nitrogenase, V-nitrogenase and Fe-nitrogenase). It is mainly found in some species of azotobacter and purple bacteria. In cyanobacteria, Fe-nitrogenase was found only in *A. variabilis* (Tsygankov, 2007).

In bacteria, nitrogenase complex has been well studied. H_2 production by Fe-nitrogenase is obviously higher than that by Mo-nitrogenase. However, the rate of H_2 production in *A. variabilis* associated with Fe-nitrogenase activity is lower than that with molybdenum or vanadium nitrogenase activities (Tsygankov, 2007). Different nitrogenases may take advantages from the conditions applied for H_2 production.

2.4.2 Hydrogenase

Hydrogenase is an enzyme participating in H_2 metabolism. It is a heterogeneous enzyme that can be characterized by a wide variety of properties, structures, and functions. This enzyme reversibly catalyzes the simplest chemical reaction, the formation of H_2 from protons and electrons as shown in equation 2.12.

$$2H^+ + 2e^- \leftrightarrow H_2 \qquad (2.12)$$

Hydrogenase is divided into three classes based on their active sites (Vignais, 2008): 1) nickel iron hydrogenase (NiFe-hydrogenase), 2) iron-iron containing hydrogenase (FeFe-hydrogenase), 3) iron-only hydrogenase (Fe-hydrogenase).

In photosynthetic microorganisms including cyanobacteria, there are two groups of hydrogenases. Uptake hydrogenase or Hup catalyzes the consumption of H_2 produced by nitrogen fixation, and reversible hydrogenase or Hox catalyzes both production and consumption of H_2 (Ghirardi and Mohanty, 2010). Based on the structure of active center structure, they belong to the NiFe-hydrogenase group.

Bidirectional Hox-hydrogenase belongs to NiFe hydrogenase. It consists of HoxE, HoxF, HoxE, HoxU, HoxY and HoxH proteins. A catalytic center catalyzing the oxidation of

H_2 occurs in HoxYH complexes (Fig. 2.4). A Fe_4S_4 cluster is found in HoxY, which assists the transfer of electrons to the catalytic center and *vice versa*.

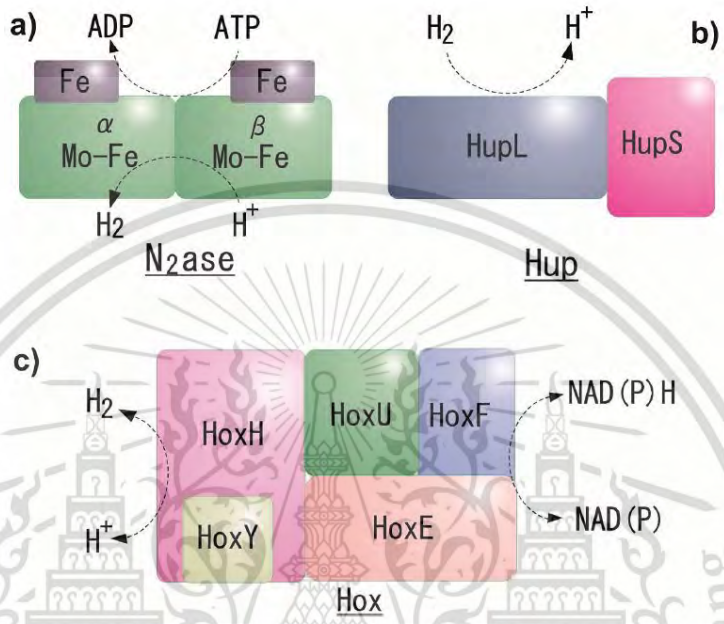

Fig. 2.4 Cyanobacterial enzymes involving H_2 metabolism. (a) Nitrogenase consists of two specific protein compounds: Mo-Fe protein, the $\alpha 2\beta 2$ complex, which comprises two P-clusters and Fe-MoCo clusters where the substrates are reduced, and Fe protein, a specific reductase for Mo-Fe protein. H_2 production is only found in the absence of nitrogen, which requires the hydrolysis of ATP synthesized by nitrogenase. (b) Uptake hydrogenase (Hup) is characterized as nickel-iron hydrogenase that plays a key role in hydrogen oxidation. (c) Reversible hydrogenase (Hox) is also nickel-iron hydrogenase. It interacts with pyridine dinucleotides (NAD, NADPH) and catalyzes both proton reduction and hydrogen oxidation relying on the metabolism in cells (Hallenbeck, 2011; Ferreira et al., 2017).

In active site, electrons are released by HoxH through HoxY subunit and then transferred to HoxEFU iron-sulfur clusters (Smith et al., 1992). Hydrogenase cooperates with NAD(P) directly. Hydrogenase reduces NAD(P) in the presence of H_2 or generating H_2 in the presence of reduced pyridine nucleotides. Regardless of morphology and nitrogen fixation capability, Hox hydrogenase was discovered in most cyanobacteria. However,

hydrogenase is highly sensitive to oxygen and needs anaerobic conditions for its action, as the evidence shown in the absence of Hox-hydrogenase in marine cyanobacterial strains (Houchins, 1984).

Uptake hydrogenase or HupSL consists of two subunits, HupL and HupS subunits. HupL is a large subunit of uptake hydrogenase with 60 kDa containing the active site of enzyme and is indicated as the bimetallic NiFe center. HupS is a small subunit of uptake hydrogenase containing iron-sulfur clusters that provides electrons from the active site to the electron acceptor. HupSL is found in nitrogen-fixing cyanobacterial cells under nitrogen starvation and is related to nitrogenase activity (Tamagnini et al., 2002; Schmitz et al., 2002). HupSL plays a key role in uptake of H_2 from both H_2 generated by nitrogen fixation and exogenous N_2. It is synthesized by heterocysts that do not generate H_2 into the air even under nitrogen fixing conditions. The presence of uptake hydrogenase has been shown to have a close relation with nitrogenase in *Nostoc punctiforme*. As shown in the previous report, uptake hydrogenase of *A. variabilis* ATCC29413 contributes in H_2 production associated with the uptake of oxygen (Happe et al., 2000). In heterocyst, this reaction reduces the partial pressure of oxygen, which inhibits nitrogenase activity and can supply electrons to nitrogenase (Tsygankov, 2007).

FeFe-hydrogenase is dimer and may have different numbers of subunits. There are one, two, three and four subunits of the enzymes (Tamagnini et al., 2002). The enzymes are involved in the H_2 producing process. They also show high oxygen sensitivity and high catalytic activity. This group of hydrogenases is found in algae. Due to the activity of FeFe-hydrogenase, it is demonstrated that green unicellular microalga *Chlamydomonas reinhardtii* is capable of light-dependent H_2 production after initial dark adaptation.

Fe-hydrogenase is homodimer containing only iron atom in active site (Tatsuhiko and Higuchi, 2013). It is a cytoplasmic enzyme found only in the archaea domain, in which it is synthesized only under nickel depletion conditions (Vignais, 2008). The role of Fe-hydrogenase is involved in one of the stages of reducing carbon dioxide to methane.

Since cyanobacteria obtain different nitrogenases and hydrogenases, the metabolic pathways participate in H_2 production are different depending on species. H_2

production via nitrogenase in heterocysts is considered as the most promising pathway. There are various mechanisms to protect the enzymes from oxygen inhibition. Heterocysts are microbial cells of cyanobacteria that deliver a quasi-anaerobic microenvironment for oxygen-sensitive nitrogenase and there is no photosystem II, so that, there is no oxygen emitted during water cleavage. Cyanobacteria contain respiratory systems located in membrane, which can consume a small amount of oxygen before it moves to nitrogenase in the cytoplasm. In the first stage, oxygen synthesized by photosynthesis is used to fix and store carbon in the form of reduced carbon compounds. In the second stage, the reduced carbon compounds can subsequently be used as the substrates for H_2 production under anaerobic conditions.

2.5 Cyanobacteria

Cyanobacteria or blue-green algae are classified in prokaryotes that are identified in the Kingdom of Monera, Division Eubacteria, Class Cyanobacteria. Until now, there are approximately 150 genera and 2,000 species of cyanobacteria. Cyanobacteria are ancient diverse microorganisms found over 3,500 million years (Schopf, 1993). Due to the scope of evolution, it can exist in a wide range of environments including fresh and marine water. Some cyanobacteria can grow in extreme habitats such as in frozen lakes, hot springs, and saline water (Whitton, 1992).

2.5.1 Cell structure of cyanobacteria

Cyanobacterial cells are larger than bacterial cells. Cell structure of cyanobacteria comprises one envelope in cell walls with peptidoglycan, naked DNA, and ribosome but does not contain membrane bound structures such as endoplasmic reticulum, mitochondria, plastids, golgi bodies, sap vacuoles, and lysosome. Some cyanobacteria occur solitary unicells. In most species, cells stick to each other to form a pair of cells such as *Synechococcus* (Fig. 2.5a). Some species hold groups of cells together to form colonies such as *Myxosarcina* (Fig. 2.5b). Commonly, cyanobacterial cells grow and form filaments (trichomes) where the cells are adhered end to end through steady divisions into one plane (Fig. 2.5c-g). Moreover, these filaments can be joint into bundles

or branched; true-branched and false branched shown in Fig. 2.5b and Fig. 2.5d, respectively. Several filamentous cyanobacteria produce exclusive cells known as heterocyst (Fig. 2.5d and g) functioning in nitrogen fixation. Such cyanobacteria are generally capable of producing akinete, specialized cells for dormancy, under unfavorable conditions.

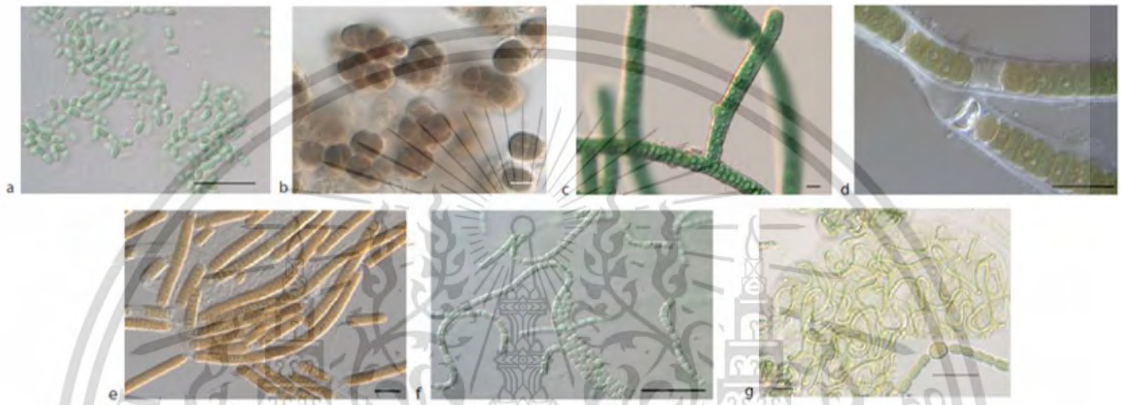

Fig. 2.5 Cyanobacterial morphology. a) unicellular *Synechococcus* sp., b) *Myxosarcina* sp., c) filamentous, true-branched *Stigonema* sp., d) filamentous, false-branched *Tolypothrix* sp., e) thick unbranched filamentous of *Lyngbya* sp. forming homogonia, f) thin unbranched filamentous *Pseudanabaena* sp. g) filamentous *Nostoc* sp. forming gelatinous colonies (Mohr et al., 2011).

2.5.2 Reproduction of cyanobacteria

There is no sexual reproduction in cyanobacteria. However, gene exchange might be comprehended through a viral transduction by specialized cyanophages (Coleman et al., 2006). The reproduction by cell division (binary fission) and fragmentation in colony occurs in cyanobacteria. In unicellular cyanobacteria, the division of the cytoplasm forms baeocytes (endospores) many times and in different planes whereas the size of the mother does not increase. In filamentous cyanobacteria, hormogonia (Fig. 2.5e) are short filaments, breaking up of a longer filament, encouraged by the controlling of death, or collapse of certain cells. Hormogonia displays gliding motility for several hours.

2.5.3 Photosynthetic pigments in cyanobacteria

Cyanobacteria obtain thylakoids located in photosynthetic membranes. Thylakoid in cyanobacteria normally contain chlorophyll *a* and *d*, but in some cyanobacteria, chlorophyll b can be also found. In addition, carotenoids and phycobilins are accessory pigments for capturing light energy and delivering it to the photosynthetic reaction centers located in thylakoid membranes. Phycobilins are red or blue water-soluble pigments bound to proteins forming hemispherical phycobilisomes which occur on the outer of thylakoid surfaces.

2.6 *Aphanothece halophytica*

The halotolerant unicellular cyanobacterium *Aphanothece halophytica* is originally isolated from Solar Lake, Israel and obtained from Dr. Tetsuko Takabe (Nagoya Universiry). *A. halophytica* is considered as a model organism for studying the high salt tolerance in cyanobacteria. Its shape is ovoid or cylindrical and its size is between 2 to 10 μm (Fig. 2.6). The higher salinity increases the cell size (Berland et al., 1989; Dor and Homoff, 1985; Kao et al., 1973; Yopp et al., 1978). The optimal salinity for growth of *A. halophytica* is usually 0.5 to 1.0 M NaCl. Moreover, it can grow extremely in media containing 3.0 M NaCl (Takabe et al., 1988). The doubling time of *A. halophytica* was 14.5, 18 and 30 h measured in the presence of various NaCl concentrations of 2, 3 and 4 M, respectively, with optimal pH of 7.0-7.8 (Tindall et al., 1978).

A. halophytica is one of the efficient cyanobacteria for H_2 production (Taikhao et al., 2013; Taikhao et al., 2015). *A. halophytica* utilizes H_2 as electron donor for CO_2 assimilation in photosystem I-driven reaction (Belkin and Padan, 1978). Only bidirectional [NiFe]-hydrogenase encoded by *hox* operon has been found in *A. halophytica.* It shows the highest similarity to that of *Halothece* sp. PCC 7418 (Phunpruch et al., 2016). Bidirectional hydrogenase in *A. halophytica* catalyzes H_2 production by electrons obtained from a glycogen catabolism under dark anaerobic conditions (Taikhao et al., 2015). Previous study showed that H_2 production is enhanced in immobilized *A. halophytica* cells (Pansook et al., 2019a). H_2 is also stimulated in the treatment of inhibitors of photosystem II, CCCP

(Carbonyl cyanide 3-chlorophenylhydrazone) and DCMU (3-(3,4-dichlorophenyl)-1,1-dimethylurea) (Pansook et al., 2019b).

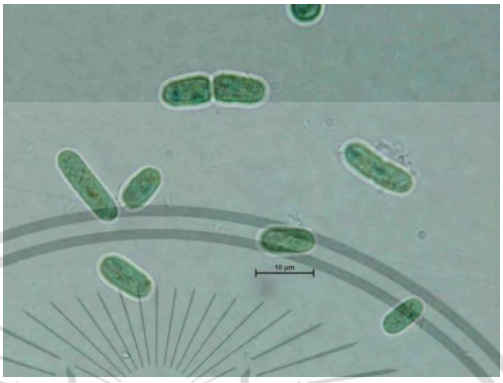

Fig. 2.6 Cell morphology of the halotolerant unicellular cyanobacterium *Aphanothece halophytica* observed under light microscope.

2.7 Reducing agents affecting H_2 production in cyanobacteria

2.7.1 Reducing sugars

Reducing agents are chemical compounds that can donate electrons to other molecules. Reducing sugar is one type of reducing agent that is a source of electron donors. Reducing sugar serves as a reducing agent such as glucose, fructose, lactose, glyceraldehyde, maltose, and arabinose (Fig. 2.7). All monosaccharides are reducing sugars, which can be categorized into two groups: 1) aldose containing free aldehyde group and 2) ketose containing ketone group. However, ketose must tautomerize to aldose before acting as reducing agents (Rizzo, 2011).

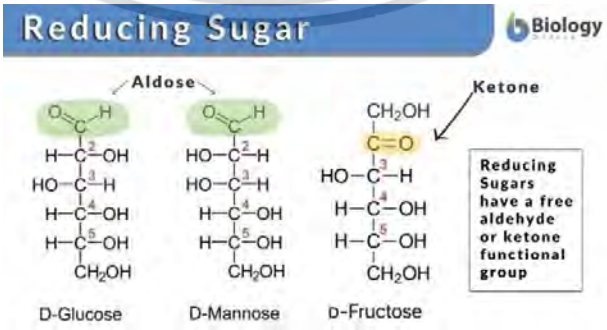

Fig. 2.7 Chemical structure of glucose, mannose, and fructose (BiologyOnline.com).

For monosaccharides, fructose is ketose whereas glucose and galactose are aldose. Disaccharides are formed by two monosaccharides and classified as either reducing or nonreducing sugars. Reducing disaccharides are lactose and maltose which contains only one of their two anomeric carbons involved in the glycosidic bond whereas the others can convert to an open-chain form with an aldehyde group (Fig. 2.8). For nonreducing disaccharides such as sucrose, they cannot convert to an open-chain form with an aldehyde group because they comprise glycosidic bond between their anomeric carbons, thus they are stuck in the cyclic form (Fig. 2.8).

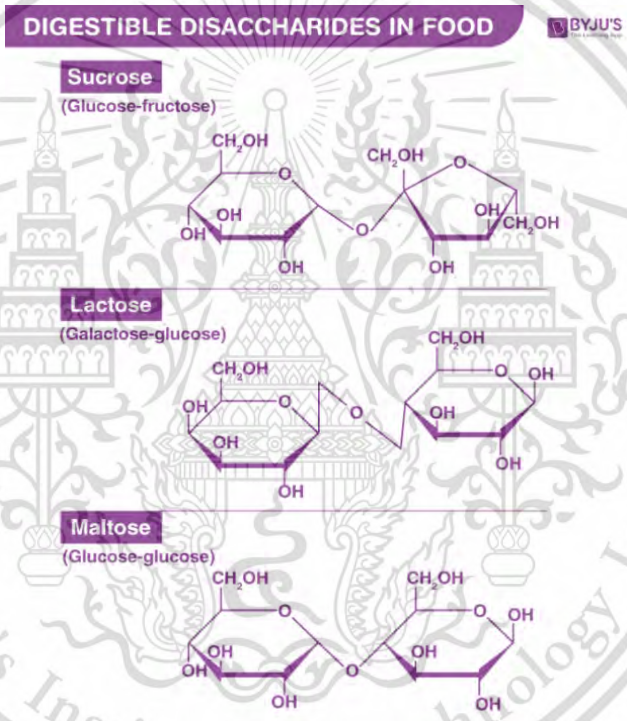

Fig. 2.8 Structure of disaccharides, sucrose (glucose+fructose), lactose (galactose+glucose) and maltose (glucose+glucose) (https://byjus.com/chemistry/disaccharides/)

2.7.2 β-mercaptoethanol (C_2H_6OS)

β-mercaptoethanol (also known as 2-mercaptoethanol, BME, 2-ME or β-met) has a chemical formula as C_2H_6OS (Fig. 2.9) and molecular weight of 78.13 g mol^{-1}. Its redox potential (at pH 7) is -0.26 V (Aitken et al., 2008). β-mercaptoethanol can act as a biological antioxidant and used to reduce disulfide bonds.

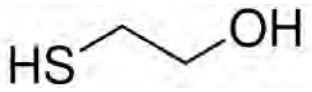

Fig. 2.9 Structure of β-mercaptoethanol
(https://www.sigmaaldrich.com/TH/en/product/aldrich/m6250)

2.7.3 DL-dithiothreitol ($C_4H_{10}O_2S_2$)

DL-dithiothreitol (DTT) is a reducing agent which forms a stable six-membered ring with an internal disulfide bond when it is oxidized. Its formula is $CH(OH)CH_2SH)_2$ (Fig. 2.10) and has a molecular weight of 154.25 g mol^{-1}. DTT has a redox potential (at pH 7) of -0.33 V (Aitken et al., 2008). It is classified as a dithiol.

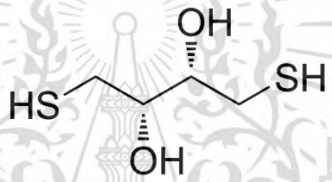

Fig. 2.10 Structure of DL-dithiothreitol
(https://en.wikipedia.org/wiki/Dithiothreitol)

2.7.4 Formic acid (CH_2O_2)

Formic acid (systematically called methanoic acid) is the simplest carboxylic acid containing a single carbon (Fig. 2.11). It has a molecular weight of 46.025 g mol^{-1} with a density of 10.2 lb gal^{-1}. The redox potential of formic acid is -0.25 V (Fang and Chen, 2021).

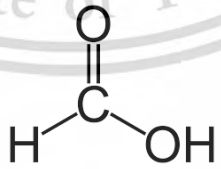

Fig. 2.11 Structure of formic acid
(https://www.acs.org/molecule-of-the-week/archive/f/formic-acid.html)

2.7.5 L-ascorbic acid ($C_6H_8O_6$)

L-ascorbic acid or vitamin C is a six-carbon compound related to glucose (Fig. 2.12). It is found naturally in citrus fruits and many vegetables. Vitamin C has a biologically active form functioning as a reducing agent and coenzyme in several metabolic pathways. It has a molecular weight of 176.12 g mol^{-1} and has a redox potential of -0.081 V (Fruton, 1934).

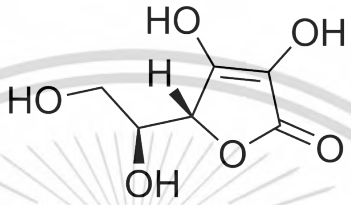

Fig. 2.12 Structure of L-ascorbic acid
(https://www.medchemexpress.com/L-Ascorbic-acid.html)

2.7.6 L-cysteine ($C_3H_7NO_2S$)

L-cysteine is an optically active form of cysteine (Fig. 2.13). It obtains L-configuration and has a molecular weight of 121.16 g mol^{-1}. The redox potential of cysteine is -80 mV (Iyer et al., 2009).

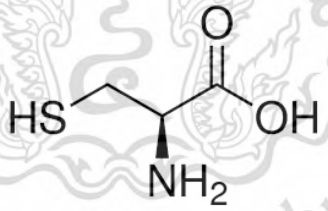

Fig. 2.13 Structure of L-cysteine
(https://www.sigmaaldrich.co.th/th_en/30089-25g-l-cysteine-bioultra-98)

2.7.7 Oxalic acid ($C_2H_2O_4$)

Oxalic acid is an alpha, omega-dicarboxylic acid that is ethane substituted by carboxyl groups at positions 1 and 2 (Fig. 2.14). It has a role as a human metabolite, a plant metabolite, and an algal metabolite. It has a molecular weight of 90.03 g mol^{-1}. The redox potential of oxalic acid is -0.25 V (Ferreira et al., 2012).

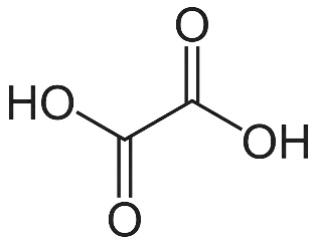

Fig. 2.14 Structure of oxalic acid

(https://en.wikipedia.org/wiki/Oxalic_acid)

2.7.8 Potassium hexacyanoferrate (II) trihydrate ($K_4[Fe(CN)_6]•3H_2O$)

Potassium hexacyanoferrate (II) is an inorganic compound with a chemical formula as $K_4[Fe(CN)_6]$ (Fig. 2.15). Industrially, it is produced from ferrous chloride, calcium hydroxide and hydrogen cyanide. It is important in organic chemistry as a reducing agent. Nowadays, potassium hexacyanoferrate is used in many niche applications in industries.

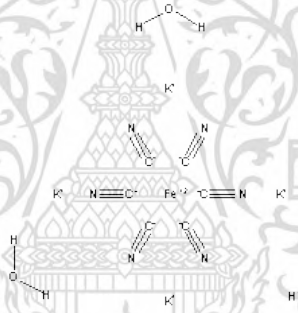

Fig. 2.15 Structure of potassium hexacyanoferrate (II) trihydrate

(https://www.chemnet.com/China/Offer-to-Sell/Potassium-hexacyanoferrate-4175806.html)

2.7.9 Sodium hydrosulfite ($Na_2O_4S_2$)

Sodium hydrosulfite or sodium dithionite is a white crystalline powder with a sulfurous odor (Fig. 2.16). It has a molecular weight of 174.107 g mol^{-1}.

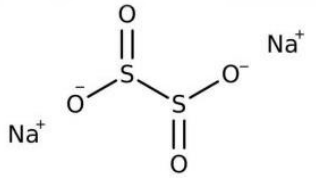

Fig. 2.16 Structure of sodium hydrosulfite

(https://shanghaichemex.com/product/sodium-hydrosulfite/)

2.7.10 Sodium sulfide nonahydrate ($Na_2S•9H_2O$)

Sodium sulfide is a chemical compound with the formula of Na_2S (Fig. 2.17). It is commonly found as $Na_2S·9H_2O$. It is a water-soluble compound which provides a strong alkaline solution.

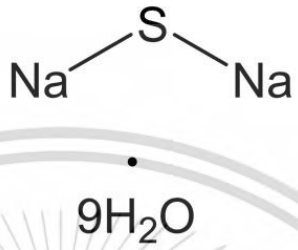

Fig. 2.17 Structure of sodium sulfide nonahydrate (https://www.pharmaffiliates.com/en/1313-84-4-sodium-sulfide-nonahydrate-pa270022593.html

2.8 Effect of nutrient starvation on H_2 production by cyanobacteria

The process of adaptation cells in a depletion of some nutrients in media is one of the effective ways to induce and maintain sustainable H_2 production in cyanobacteria, (Srirangan et al., 2011).

2.8.1 Nitrogen deprivation

Nitrogen is a fundamental element that is important for growth and reproduction in cyanobacteria. It is found in many important biomolecules such as amino acids, proteins, and nucleic acids. Commonly, nitrogen can be found in gas form (N_2), generating by a chemical bond of two nitrogen atoms. Some cyanobacteria show the capability to assimilate atmospheric nitrogen that is known as nitrogen fixation. Some strains can also assimilate some amino acids. In the assimilation, nitrate reduction provides ammonium through the two subsequent reactions of nitrate reductase and nitrite reductase that require two electrons and six electrons (Flores et al., 2005). However, nitrogen reduction and hydrogen production are competitive. Nitrate reduction is a preferred electron sink to

hydrogenase (Ananyev et al., 2008). Therefore, nitrogen sources in the cultivation medium would limit the production of hydrogen.

Previous study showed that nitrate assimilation was disrupted in the deprivation of nitrate in cyanobacterium *Synechocystis* sp. PCC 6803 (Baebprasert et al., 2011). Also, genes involved in glycogen synthesis were upregulated under nitrate starvation by *Synechocystis* sp. PCC 6803 (Osanai et al., 2006). This glycogen is the main electron source for H_2 production under dark anaerobic conditions. In respiratory electron transport, the expression of *coxA*, *ndhB* in *Synechocystis* sp. PCC 6803 were increased (Krasikov et al., 2010). This provided elimination of O_2 remaining in the cells, which could protect enzymes involved in H_2 production from O_2 inhibition.

A. halophytica provides high H_2 production under nitrogen depletion and dark anaerobic conditions (Taikhao et al., 2013; Taikhao et al., 2015). Furthermore, an increase in H_2 production by nitrogen depletion is also found in *Oscillatoria brevis*, *Calothrix membranacea* (Lambert and Smith, 1977), and *Anabaena siamensis* TISIR 8012 (Khetkorn et al., 2010; Taikhao and Punpruch, 2017). Under nitrogen deprivation, accumulated glycogen is enhanced via photoautotrophic processes. The accumulated glycogen is broken down into glucose-6-phosphate with the production of reduced nicotinamide adenine dinucleotide phosphate (NADPH), that is the electron donor of [NiFe]-hydrogenase, and then H_2 is produced under dark anaerobic conditions (Ananyev et al., 2008). Previously, the bidirectional hydrogenase activity in *A. halophytica* was clearly induced under nitrogen depletion and dark anaerobic conditions, and the gene expression of *narB* encoding ferredoxin-nitrate reductase was downregulated, resulting in an increase in H_2 production (Phunpruch et al., 2016).

2.8.2 Phosphorus deprivation

Phosphorus is an important element for growth of cyanobacteria. It has a key role in nutrient central to store and exchange information and energy in the cells (Rao et al., 2009; Dyhrman, 2016). Phosphorus deprivation was reported to inhibit O_2 evolution in algae (Wykoff et al., 1998). Therefore, it might prevent hydrogenase inhibition from O_2 in *Aphanothece halophytica*.

2.8.3 Potassium deprivation

Potassium is an important macronutrient for cyanobacteria. It is the most essential and abundant cation to cyanobacterial cells. Potassium plays a key role in electrical neutralization of anionic charges, protein synthesis, pH homeostasis, regulation of osmotic pressure and control of polarization (Epstein, 2003; Chérel et al., 2014). Potassium is also fundamental for metabolic enzyme and molecular chaperon activation (Page and Cera, 2006). During the binding of phosphate backbone of nucleic acid, potassium is involved in phosphoryl transfer reactions (Page and Cera, 2006). Across thylakoid membranes, the regulation of potassium essentially contributes to the maintenance of photosynthesis and respiratory electron transport chain in cyanobacteria, especially under photomixotrophic conditions (Checchetto et al., 2012).

Hydrogenase activity may be increased under potassium starvation. The previous study showed that organic acid biosynthesis has negative correlation with H_2 production, metabolite levels of downstream of sugar metabolism and anionic metabolites increased in the presence of potassium under dark anaerobic conditions (Ueda et al., 2016). In glycolysis, pyruvate kinase is known to be activated by potassium (Oria-Hernández et al., 2005). Thus, potassium might correspond in the regulation of metabolic enzymes in sugar metabolism in cyanobacteria.

2.8.4 Sulfur deprivation

Sulfur is an important element of sulfurous amino acids, cysteine, and methionine. In sulfur depletion, H_2 production was increased in *Gloeocapsa alpicola* (Antal and Lindblad, 2005) and *Microcystis aeruginosa* (Rashid et al., 2009). Under sulfur deprivation, D1 protein, a pivotal protein located in the PSII reaction center, was found to be impaired because of the chloroplast's inability to synthesize appropriate amounts of sulfurous amino acid (Wykiff et al., 1998). Thus, PSII activity declines and O_2 concentration decreases. H_2 could be reactivated under sulfur deprivation.

2.9 Literature reviews

Baebprasert et al. (2010) investigated the effects of external factors on both H_2 production and Hox-H_2ase activity in the non-N_2-fixing cyanobacterium *Synechocystis* sp. PCC6803. Glucose at 0.4% enhanced H_2 production by *Synechocystis* sp. PCC6803. Either DTT or β-mercaptoethanol at 100 μM caused an increase in H_2 production by *Synechocystis* sp. PCC6803. Moreover, nitrogen- and sulfur-deprived cells treated with β-mercaptoethanol enhanced H_2 production significantly. The highest Hox-H_2ase activity with 14.32 μmol H_2 mg chl a^{-1} min^{-1} was obtained in cells incubated in $BG11_0$-S-deprived supplemented with 750 μM β-mercaptoethanol at 70 °C. Furthermore, H_2ase activity of intact cells was stimulated by addition of NADH and ferredoxin.

Belkin and Padan (1978) demonstrated the capability of H_2 metabolism involved in CO_2 assimilation in *A. halophytica*. The unicellular halotolerant cyanobacterium *A. halophytica* could grow in the presence of Na_2S for 4-5 days under anaerobic conditions. After that, cells were washed twice and resuspended in the same medium without Na_2S. The photoreduction of CO_2 was detected at 300 nmol CO_2 photo-assimilated mg^{-1} protein h^{-1} after 30 h. In the reaction of light dependent and the presence of the photosystem II inhibitor DCMU, H_2 was an electron donor in a photosystem I driven reaction in *A. halophytica*.

Chen et al. (2008) showed that *Anabaena* sp. CH3 was able to use sugars as substrate for H_2 production under anaerobic conditions. H_2 production depended on growth phases. The result showed that cells at sub-stage of late-log phase showed higher ability to produce H_2 than those at log phase. In this case, O_2 level was too low to inhibit H_2 production. Among different kinds of sugar, fructose and glucose showed the best sugar source for producing H_2. H_2 accumulated to 0.6 mmol (in 40 ml head space) in 100 h from 1,000 ppm fructose. An Increase in light intensities from 65 to 130 μmol photons m^{-2} s^{-1} would enhance H_2 production to 0.8 mmol. Under illumination of 130 μmol photons m^{-2} s^{-1} and 2,000 ppm fructose, 1.7 mmol of H_2 could be accumulated. However, when fructose content was higher than 2,000 ppm, cells could not produce higher H_2 concentration.

Cournac et al. (2004) studied the *in vivo* activity of the bidirectional [NiFe]hydrogenase [H_2: NAD(P) oxidoreductase], encoded by the *hoxEFUYH* genes of *Synechocystis* sp. PCC6803 by measuring independently using the proton-deuterium (H-D) exchange reaction in the presence of D_2. This technique provided that the hydrogenase was insensitive to light, but was reversibly inactivated by O_2, and could be quickly reactivated by NADH or NADPH (+H_2). A sustained rate of photoevolution of H_2 corresponding to 6 μmol H_2 mg chlorophyll^{-1} h^{-1} or 2 ml L^{-1} h^{-1} was observed over a longer period in the presence of glucose and was slightly enhanced by an addition of the O_2 scavenger glucose oxidase.

Gutekunst et al. (2014) showed that flavodoxin and ferredoxin directly reduced the bidirectional NiFe-H_2ase of *Synechocystis* sp. PCC6803 *in vitro*. H_2ase was suggested to receive its electrons via pyruvate: flavodoxin/ferredoxin oxidoreductase (PFOR)-flavodoxin/ferredoxin under fermentative conditions, allowing cells to gain ATP. This convincingly supported that the bidirectional NiFe-H_2ase in cyanobacteria functioned as electron sinks for low potential electrons from photosystem I and as a redox balancing device under fermentative conditions.

Khetkorn et al. (2020) demonstrated that fructose supported N_2-fixing and H_2 metabolism in ΔHupL strain of *Anabaena* sp. PCC7120. Under light-fructose mixotrophic conditions, cells showed an increase in growth rate, pigment content, and the formation of mature heterocyst within 6 h after cultivation. Upon supplementation of optimum concentration of 60 mM fructose, 24-h old cells showed a 3.1-fold increase of N_2ase activity in combination with an increase in *nifD* expression, with the increase in electron flow from catabolism of fructose through the oxidative pentose phosphate pathway. N_2ase was likely responsible for increasing H_2 production mediated by fructose. The maximum H_2 production rate of ΔHupL strain under fructose mixotrophic growth was 101.33 μmol H_2 mg^{-1}chl *a* h^{-1}, comprising a 4.7-fold increase compared to wild type under the same conditions. It indicated that fructose supplementation increased N_2-fixation causing an enhanced H_2-production by *Anabaena* sp. PCC7120 strain ΔHupL.

Luo and Mitsui (1994) demonstrated the effect of forty kinds of organic compounds on H_2 photoproduction by *Synechococcus* sp. The results showed that glucose, fructose, maltose, and sucrose were effective electron donors. The maximum rates of H_2 photoproduction from a 6-day-old batch culture with 25 mmol of pyruvate, glucose, maltose, sucrose, fructose, and glycerol were 1.11, 0.62, 0.50, 0.47, 0.30, and 0.39 μmol H_2 mg^{-1} cell dry wt h^{-1}, respectively. Therefore, *Synechococcus* sp. might be capable of removing organic materials from wastewater and simultaneously transforming them to H_2 gas, a pollution-free energy. The activity of nitrogenase completely disappeared when intracellular glucose (glycogen) was used up; however, it could be restored by the addition of organic substrates such as glucose and pyruvate.

Luo and Mitsui (1996) showed that *Synechococcus* sp. Miami BG 043511 can utilize sulfide as electron source for H_2 photoproduction. Sulfide can either inhibit or stimulate H_2 production by *Synechococcus* sp. Miami BG 043511, depending on growth conditions, age, and sulfide concentration in the medium. In 3-day-old cells, the concentration of sodium sulfide higher than 5 mM inhibited H_2 production. The inhibition was slightly found in 7-day-old cells, whereas an encouraging effect was found in 15-day-old cells at stationary growth phase. At the latter stage, the limited light intensity and the deficiency in nutrients represent extreme stress conditions for the cyanobacterium. The encouraging effect of sulfide under these stress conditions could be stimulated by increasing sulfide concentrations. The stimulating effect of sulfide on H_2 production was further confirmed by gradually increasing sulfide concentrations. *Synechococcus* sp. strain Miami BG 043511 can use sulfide as electron donor for H_2 photoproduction, especially under stress conditions.

Pansook et al. (2016) reported that the immobilized cells of unicellular halotolerant cyanobacterium *A. halophytica* in alginate could produce higher H_2 than free cells. The highest H_2 production was found in immobilized cells in 4.5% (w/v) sodium alginate in 100 mM calcium chloride under nitrogen deprivation. H_2 production yield of 50 immobilized cell beads per 20 mL glass vial was higher than that of 100 and 150 immobilized cell beads.

Pansook et al. (2019b) investigated the effects of the photosystem II inhibitors carbonyl cyanide m-chlorophenyl hydrazone (CCCP) and 3-(3,4-dichlorophenyl)-1,1-dimethylurea (DCMU) on H_2 production by *A. halophytica* under light and dark conditions and on photosynthetic and respiratory activities. The results showed that *A. halophytica* treated with CCCP and DCMU produced 3-5 folds higher H_2 than cells without treatment in the presence of light. The highest H_2 photoproduction rates of 2.26 ± 0.24 and 3.63 ± 0.26 μmol H_2 g^{-1} dry weight h^{-1}, were found in cells treated with 0.5 μM CCCP and 50 μM DCMU, respectively. Under light conditions, CCCP and DCMU inhibited chlorophyll fluorescence, resulting in a low level of O_2, which encouraged bidirectional H_2ase activity in *A. halophytica* cells. Moreover, only CCCP increased the respiration rate, further reducing the O_2 level. On the contrary, DCMU decreased the respiration rate in *A. halophytica.*

Pansook et al. (2022) found that simazine efficiently enhanced H_2 production by *A. halophytica* under dark conditions. However, high concentration of simazine and long-term incubation caused a decrease in cells and chlorophyll concentrations. The optimal concentration of simazine for H_2 production by *A. halophytica* was 25 μM. Simazine inhibited photosynthetic O_2 evolution but enhanced dark respiration. Consequently, O_2 was decreased. Therefore, the bidirectional H_2ase activity and H_2 production were increased. *A. halophytica* provided the highest H_2 production rate and H_2 accumulation of 58.88 ± 0.22 μmol H_2 g^{-1} dry wt h^{-1} and 356.21 ± 6.04 μmol H_2 g^{-1} dry wt after treatment with 25 μM simazine under dark anaerobic conditions for 2 and 24 h, respectively.

Phunpruch et al. (2016) demonstrated that cyanobacterium *A. halophytica* produced H_2 via catabolism of glycogen under dark anerobic conditions. Amongst the H_2ase enzymes, only bidirectional [NiFe] H_2ase encoded by *hox* operon was found in *A. halophytica*. In *A. halophytica*, there are five structural genes of *hox* genes, *hoxE*, *hoxF*, *hoxU*, *hoxY*, and *hoxH*, without an insertion of other open reading frames (ORFs). The conserved cysteine motifs of iron-sulfur clusters involved in an electron transfer were found in all Hox subunits. The result of nucleotide sequencing showed that *hox* genes in *A. halophytica* provided the highest identity and similarity of those of *Halothece* sp. PCC 7418. As the result of reverse transcription polymerase chain reaction (RT-PCR) analysis,

hox genes were co-transcribed as a single operon in *A. halophytica*. Under nitrogen deprivation, the transcripts of *hoxH*, *glgB*, *coxA*, *psaA* and *ndhB* were upregulated. On the contrary, those of *glgP* and *narB* were downregulated. Consequently, H_2 production, H_2ase activity, glycogen content, and dark respiration rate were increased.

Reddy et al. (1996) demonstrated that *A. variabilis* dissimilated fructose to H_2 and CO_2 under argon atmosphere and light conditions. The net H_2 yield increased when fructose concentration increased up to 10 mM in the medium. The average apparent conversion efficiency of fructose to H_2 (net H_2 produced/fructose removed from the medium) was about 10. The higher conversion efficiencies of 15 to 17 could be provided during shorter periods and at optimum fructose concentrations. The rate of H_2 production by *A. variabilis* SA1 with 46 mL h^{-1} g^{-1} dry wt. was maintained for over 15 days.

Serebryakova et al. (2006) studied the main catalytic properties of the Hox type H_2ase isolated from *Gloeocapsa alpicola*. The enzyme effectively catalyzed reactions of oxidation and evolution of H_2 in the presence of methyl viologen (MV) and benzyl viologen (BV). The enzyme cooperated with $NADP^+$ and NADPH but is more specific to NAD^+ and NADH. To show the catalytic activity, the enzyme needed reductive activation, which occurred in the presence of H_2, and NADH accelerates this process. The final H_2ase activity depended on the redox potential of the activation medium (E_h). At pH 7.0, the enzyme activity in the MV-dependent oxidation of H_2 increased with a decrease in E_h from −350 mV and reached the maximum at E_h of about −390 mV. However, the rate of H_2 oxidation in the presence of NAD^+ in the E_h range under study was effectively constant and equal to 7–8% of the maximal rate of H_2 oxidation in the presence of MV.

Sukrachan and Incharoensakdi (2020) showed that agar bead–immobilized cells of *Nostoc* sp. CU2561 incubated in medium supplemented with 0.5% (w/v) increased H_2 production rate approximately 1.7-fold. Whereas the reducing agent β-mercaptoethanol increased H_2 production rate by about 8.2-fold. The highest H_2 production rate was found in agar bead–immobilized cells of *Nostoc* sp. CU2561 incubated in BG11-N-S containing 5 mM β-mercaptoethanol with 18.78 ± 1.44 μmol H_2 mg^{-1} chl *a* h^{-1}. In addition, agar

bead–immobilized cells continuously produced H_2 for 3 cycles. The immobilized cells could provide long-term H_2 production up to 120 h during the first cycle.

Taikhao et al. (2013) studied the effects of various physiological parameters on H_2 production by the unicellular halotolerant cyanobacterium *A. halophytica*. Under nitrogen deprivation, H_2 production rate was stimulated four-fold compared to that in abundant medium. Glucose, as the sugar source, was suggested to be preference for H_2 production by *A. halophytica*. The suitable conditions for H_2 production by *A. halophytica* were incubation cells in the presence of 0.75 M NaCl, or 0.4 μM Fe^{3+}, or 1 μM Ni^{2+}. The optimal light intensity and temperature were 30 μmol photons m^{-2} s^{-1} and 35 °C, respectively.

Taikhao et al. (2015) showed that *A. halophytica* was able to produce H_2 in cells incubated in seawater. The highest H_2 production of 82.79 ± 3.47 nmol H_2 mg^{-1} dry wt h^{-1} was found in *A. halophytica* cells incubated in seawater supplemented with 378 mmol C L^{-1} glucose, 0.25 M NaCl, and 0.4 μM Fe^{3+} at 35 °C, pH 6. The long-term H_2 accumulation of 1,864 ± 81 nmol H_2 mg^{-1} dry wt was found after 8 days under dark anaerobic conditions, which sustained for more than 17 days. Under dark fermentation, bidirectional [NiFe] H_2ase used electrons obtained from a glycogen catabolism.

Ueda et al. (2016) demonstrated that K^+ widely changed the primary carbon metabolism of *Synechocystis* sp. PCC 6803. Under dark anaerobic conditions, succinate and lactate emission from cells enhanced in the presence of K^+, while H_2 production was suppressed. The addition of K^+ and the genetic manipulation of acetate kinase AckA and an RNA polymerase sigma factor SigE additively increased succinate and lactate production to 141.0 and 217.6 mg L^{-1}, which were 11 and 46 times, compared to the wild-type strain without K^+, respectively. Intracellular levels of 2-oxoglutarate, succinate, fumarate and malate increased by K^+ under dark anaerobic conditions. This study provided evidence of the significant effect of K^+ on the biosynthesis of anionic metabolites in a unicellular cyanobacterium.

Wykoff et al. (1998) found that green alga *Chlamydomonas reinhardtii* incubated in phosphorus- and sulfur-deprived conditions provided declination of photosynthetic O_2 evolution by approximately 75% after 4 and 1 d, respectively. By quantitation of the partial

reactions of photosynthetic electron transport, it was suggested that the light-saturated rate of PSI activity was unaffected by phosphorus or sulfur limitation, whereas light-saturated PSII activity was reduced by higher than 50%.

Yuan et al. (2008) found that L-cysteine at 0.1-1 mM enhanced H_2 production with increasing substrate degradation efficiency in bacterium *Clostidium butyricum* under anaerobic conditions. Moreover, the maximum H_2 production rates were increased to 1.5–2.9 times compared with that without L-cysteine. In particular, the maximum H_2 yields were 3.10 mol H_2 mol^{-1} sucrose with addition of 0.6 mM L-cysteine at 35 ℃ and 3.28 mol H_2 mol^{-1} sucrose with addition of 0.1 mM L-cysteine at 30 ℃, which were 15.2% and 70% higher than those of the corresponding cells without L-cysteine, respectively. The results showed that L-cysteine was low-cost and highly efficient bioactive agent to increase dark fermentative H_2 production.

CHAPTER 3
RESEARCH METHODOLOGY

3.1 Cyanobacteria

The unicellular halotolerant cyanobacterium *A. halophytica* originally isolated from Solar Lake, Israel, was obtained from the laboratory of Cyanobacterial Biotechnology, Department of Biochemistry, Faculty of Science, Chulalongkorn University, Thailand.

3.2 Chemical reagents

3.2.1 Culture media

Blue Green (BG11) medium (Rippka et al., 1979) (Appendix A) supplemented with Turk Island salt solution (Garlick et al., 1977) (Appendix A)

3.2.2 Enzymes

3.2.2.1 α-amylase from *Aspergillus oryzae* (Sigma, Switzerland)

3.2.2.2 Amyloglucosidase from *Aspergillus niger* (Sigma, USA)

3.2.2.3 Catalase from *Micrococcus lysodeikticus* (Sigma, Japan)

3.2.2.4 Glucose oxidase from *Aspergillus niger* (Sigma, UK)

3.2.2.5 L-lactate dehydrogenase (Roche, Germany)

3.2.3 Chemicals for cultivation

3.2.3.1 Boric acid (H_3BO_3) (Merck, Germany)

3.2.3.2 Calcium chloride dihydrate ($CaCl_2 \cdot 2H_2O$) (Carlo Erba, Italy)

3.2.3.3 Citric acid ($C_6H_8O_7$) (Analar, England)

3.2.3.4 Cobalt chloride hexahydrate ($CoCl_2 \cdot 6H_2O$) (Fluka, Switzerland)

3.2.3.5 Cobalt nitrate hexahydrate ($Co(NO_3)_2 \cdot 6H_2O$) (Ajax, Australia)

3.2.3.6 Copper sulfate pentahydrate ($CuSO_4 \cdot 5H_2O$) (Carlo Erba, Italy)

3.2.3.7 Cupric chloride dihydrate ($CuCl_2 \cdot 2H_2O$) (Mallinckrodt Baker, USA)

3.2.3.8 Diaminoethylene tetraacetic acid disodium salt (Na_2EDTA) (Promega,USA)

3.2.3.9 Dipotassium hydrogen phosphate (K_2HPO_4) (Ajax, Australia)

3.2.3.10 Disodium hydrogen phosphate (Na_2HPO_4) (Sigma, USA)

3.2.3.11 Ferric ammonium citrate ($FeNH_4$ citrate) (British Drug Houses, England)

3.2.3.12 Manganese chloride tetrahydrate ($MnCl_2 \cdot 4H_2O$) (Ajax, Australia)

3.2.3.13 Magnesium sulfate heptahydrate ($MgSO_4 \cdot 7H_2O$) (Carlo Erba, Italy)

3.2.3.14 Sodium carbonate (Na_2CO_3) (Carlo Erba, Italy)

3.2.3.15 Sodium chloride (NaCl) (Ajax, Australia)

3.2.3.16 Sodium dihydrogen phosphate (NaH_2PO_4) (Sigma, USA)

3.2.3.17 Sodium hydroxide (NaOH) (Carlo Erba, Italy)

3.2.3.18 Sodium nitrate ($NaNO_3$) (Carlo Erba, Italy)

3.2.3.19 Potassium chloride (KCl) (Ajax, Australia)

3.2.3.20 Zinc chloride ($ZnCl_2$) (Fluka, Switzerland)

3.2.3.21 Zinc sulfate heptahydrate ($ZnSO_4 \cdot 7H_2O$) (Fluka, Switzerland)

3.2.4 Chemicals and gases for quantitative analyses

3.2.4.1 Acetic acid ($C_2H_4O_2$) (Sigma, Germany)

3.2.4.2 Adenosine 5'-diphosphate sodium salt (ADP) (Sigma, USA)

3.2.4.3 Argon (Ar) (99.999%) (TIG, Thailand)

3.2.4.4 Bovine serum albumin (BSA) (Thermo Scientific, Lituania)

3.2.4.5 Coomassie brilliant blue G250 ($C_{47}H_{48}N_3NaO_7S_2$) (Thermofisher Scientific, USA)

3.2.4.6 Ethanol (C_2H_5OH) (Fischer, USA)

3.2.4.7 Glycogen from bovine liver (Sigma, USA)

3.2.4.8 HEPES (2-[4-(2-hydroxyethyl) piperazine-1-yl] ethanesulfonic acid) buffer (Sigma, USA)

3.2.4.9 Hydrogen (H_2) (4%) (TIG, Thailand)

3.2.4.10 Magnesium Chloride ($MgCl_2$) (Merck, Germany)

3.2.4.11 Methyl viologen dichloride hydrate ($C_{12}H_{14}Cl_{12}N_2 \cdot H_2O$) (Sigma, USA)

3.2.4.12 Methanol (CH_3OH) (Scharlau, Spain)

3.2.4.13 Phenol (Merck, Germany)

3.2.4.14 Phosphoenolpyruvic acid monopotassium salt (PEP) (Sigma, Switzerland)

3.2.4.15 Potassium chloride (KCl) (Merck, Germany)

3.2.4.16 Potassium hydroxide (KOH) (Carlo Erba, Italy)

3.2.4.17 Reduced β-nicotinamide adenine dinucleotide (NADH) (Sigma, USA)

3.2.4.18 Sodium acetate (CH_3COONa) (Scharlau, Spain)

3.2.4.19 Sodium hydrosulfite ($Na_2O_4S_2$) (Sigma, Germany)

3.2.4.20 Sulfuric acid (Merck, Germany)

3.2.5 Chemicals for genetic studies

3.2.5.1 Agarose (Bio Whittaker Molecular Applications, USA)

3.2.5.2 Chloroform ($CHCl_3$) (Sigma, USA)

3.2.5.3 Deoxynucleotide triphosphates (dNTPs) (Promega, USA)

3.2.5.4 Diethyl pyrocarbonate (DEPC) ($C_6H_{10}O_5$) (Sigma, USA)

3.2.5.5 Ethanol (C_2H_5OH) (Fischer, USA)

3.2.5.6 GelStar® nucleic acid gel stain (BioWhittaker Molecular Applications, USA)

3.2.5.7 Isoamyl alcohol ($(CH_3)_2CHCH_2CH_2OH$) (Sigma, USA)

3.2.5.8 λDNA/*Hin*dIII fragments (Invitrogen, USA)

3.2.5.9 QIAzol®Lysis reagent (Qiagen, USA)

3.2.5.10 Tris (hydroxymethyl) aminomethane hydrochloride (Tris-HCl) (Scharlau, Spain)

3.2.6 Reducing substances

3.2.6.1 β-mercaptoethanol (C_2H_6OS) (Plusine, Sweden)

3.2.6.2 DL-dithiothreitol ($C_4H_{10}O_2S_2$) (Sigma, Canada)

3.2.6.3 Ferredoxin (Fd) from spinach (Sigma, USA)

3.2.6.4 Formic acid (CH_2O_2) (Carlo Erba, Italy)

3.2.6.5 Fructose ($C_6H_{12}O_6$) (Carlo Erba, Italy)

3.2.6.6 Glucose ($C_6H_{12}O_6$) (Carlo Erba, Italy)

3.2.6.7 Maltose monohydrate ($C_{12}H_{22}O_{11}•H_2O$) (Merck, Germany)

3.2.6.8 Lactose monohydrate ($C_{12}H_{22}O_{11}•H_2O$) (Sigma, USA)

3.2.6.9 L-ascorbic acid ($C_6H_8O_6$) (Vetec, China)

3.2.6.10 L-cysteine ($C_3H_7NO_2S$) (Sigma, China)

3.2.6.11 Oxalic acid ($C_2H_2O_4$) (Sigma, USA)

3.2.6.12 Potassium hexacyanoferrate (II) trihydrate ($K_4[Fe(CN)_6] \bullet 3H_2O$ (Sigma, Japan)

3.2.6.13 Reduced β-nicotinamide adenine dinucleotide 2' phosphate (NADPH) (Sigma, USA)

3.2.6.14 Reduced β-nicotinamide adenine dinucleotide (NADH) (Sigma, USA)

3.2.6.15 Sodium hydrosulfite ($Na_2O_4S_2$) (Sigma, Germany)

3.2.6.16 Sodium sulfide nanohydrate ($Na_2S \bullet 9H_2O$) (Carlo Erba, Italy)

3.3 Instruments

3.3.1 Autoclave (Tomy, autoclave-325, Japan)

3.3.2 Desiccator (Duran, Germany)

3.3.3 Gel Documentation (Syngene, MDI 1019, Japan)

3.3.4 Glass-mocrofiber filter GF/C (1.2 µm) (Whatman, UK)

3.3.5 Electrophoresis equipment (Advance, Mupid®exu, Japan)

3.3.6 Gas Chromatograph (Hewlett-Packard HP5890A, Japan)

3.3.7 Glasswares (Pyrex, USA)

3.3.8 Headspace crimp-top vial (National Scientific, C4020-210, USA)

3.3.9 Hemocytometer (Boeco, Germany)

3.3.10 Hot air oven (Contherm, Thermotec 2000, Thailand)

3.3.11 Incubator shaker (Gallenkamp, T490188, UK)

3.3.12 Laminar air flow cabinet (International Scientific Supply, HS123, Thailand)

3.3.13 Light incubator shaker (Vision Scientific, Green Seriker II, Korea)

3.3.14 Light microscope (Olympus, CH30, Japan)

3.3.15 Microcentrifuge (Labnet, Spectrafuge 16M, USA)

3.3.16 pH meter (Cyberscan, 2000^{pH}, Singapore)

3.3.17 Nanodrop 2000/2000c spectrophotometer (Thermo Fisher Scientific, USA)

3.3.18 Refrigerated centrifuge (Hermle Labortech, Z383K, Germany)

3.3.19 Semimicro cuvette rectangular 10 mm (Hellma, USA)

3.3.20 Suction pump (Gast manufacturing, 0523-101Q-G588DX, UK)

3.3.21 Ultrasonicate (Sonics and Materials, VC 505, USA)

3.3.22 UV-VIS spectrophotometer (Shimadzu, UV-1601, Japan)

3.3.23 Vortex (Scientific Industries, Genies2, USA)

3.3.24 Water bath (Heto-Holten, CBN 28-30, Denmark)

3.4 Cyanobacterial cultivation

The unicellular halotolerant cyanobacterium *Aphanothece halophytica* was grown in a 250-mL Erlenmeyer flask containing 100 mL of BG11 medium (pH 7.4) (Rippka et al., 1979) supplemented with Turk Island salt solution (Garlick et al., 1977) (Appendix A). In BG11, $NaNO_3$ at 17.6 mM is used as a nitrogen source. Turk Island salt solution contains high mineral concentrations including 0.5 M NaCl, 49 mM $MgCl_2 \cdot 6H_2O$, 30 mM $MgSO_4 \cdot 7H_2O$, and 8.9 mM KCl. Cell concentration was initially adjusted to an optical density at wavelength 730 nm at about 0.1. Cells were subsequently shaken at 120 rpm on a rotary shaker at 30°C under a white-light intensity of 30 µmol photons m^{-2} s^{-1} with a light (18 h/day): dark (6 h/day) cycle for 7 days.

3.5 Analytical methods

3.5.1 Optical density measurement

The optical density of *A. halophytica* was determined spectrophotometrically at wavelength of 730 nm (OD_{730}) (Simon, 1977). The measurement was performed in triplicate.

3.5.2 Dry cell weight determination

According to the determination of cell dry weight protocol (Fay, 1976), five mL of cell suspension was filtered through a glass microfiber filter GF/C (1.2 µm). Sterile distilled water was used to wash the cells. Then, cells were collected on the microfiber filter. The filter containing cells was dried in an oven at 70 °C for 24 h. After that, it was put in the desiccator for 1 h before weighing. This method was performed repeatedly until the cell

weight was constant. Dry cell weight was determined as equation 3.1. Each measurement was performed in triplicate.

Dry cell weight (mg) = Weight of filter containing cells (mg) – Weight of filter (mg) (3.1)

3.5.3 Cell concentration measurement by hemocytometer

Measurement of cell concentration by hemocytometer was performed following the protocol of Absher (1973). Ten µL of cell suspension was added into both side of chamber of hemocytometer. When the coverslip is positioned correctly, the thickness between the ruled area and coverslip is precise 0.1 mm (Appendix B) and the volume of liquid over each subgrid is constant of 0.1 mm^3. Cells were counted in each of the corner squares and the middle squares of each side. The sample volume is 10 × 0.1 mm^3 or 1.0 mm^3. The hemocytometer was placed on the stage of a light microscope. Under 100 × magnification, blue-green cells were counted as viable cells. Dilution was performed if cells number exceed 50 cells per subgrid. The calculation of cell count was shown in equation 3.2. Each measurement was performed in triplicate.

Total cell number (cells mL^{-1}) = Average cell count per subgrid × dilution factor × 10^3 (3.2)

3.5.4 Chlorophyll *a* measurement

A. halophytica cells were harvested by centrifugation one mL of cell suspension at 8,000 ×*g* at 4 °C for 10 min. Chlorophyll *a* was extracted from *A. halophytica* cell pellet by adding 1 mL of 90% (v/v) methanol followed by vertexing and incubating at 30 °C for 30 min. The mixture was centrifuged at 12,000 ×*g* for 5 min to separate cell debris. The absorbance of chlorophyll *a* was measured at 665 nm using a spectrophotometer. Chlorophyll *a* concentration was calculated according to MacKinney (1941). Each measurement was performed in triplicate.

3.5.5 H_2 and O_2 production measurement

A. halophytica cells were harvested by centrifugation at 8000 ×*g* at 4 °C for 10 min. Cells were subsequently resuspended in 5 mL of fresh medium. After that, the cell

suspension was transferred into a 12-mL glass vial and sealed with a rubber stopper. The suspension was purged with argon gas for 10 min to enter an anaerobic conditions. Then, cells were shaken at 120 rpm under dark anaerobic incubation for 5 days. The production of H_2 and O_2 in headspace of the vial was measured by GC-TCD with a molecular sieve 5 °A 60/80 mesh packed column (Baebprasert et al., 2010). The gas chromatograph conditions is shown in Table 3.1. H_2 production and H_2 production rate were expressed as μmol H_2 g dry weight^{-1} and μmol H_2 g dry weight^{-1} h^{-1}, respectively. O_2 production rate was expressed as μmol O_2 g dry weight^{-1} h^{-1}. Four percent of H_2 in argon (4%) was used as H_2 standard gas (TIG, Thailand) and O_2 in atmospheric air (20.95%) was used as O_2 standard gas.

Table 3.1 Gas chromatograph conditions used for measurement of H_2 production

Components	Conditions
Detector	Thermal Conductivity Detector
Column	Packed SS Column 2m x 4mm OD x 3 mm ID p/w Molecular sieve 5 °A 60/80 mesh
Temperature Program	Injector Temperature: 100 °C Column Temperature: 50 °C Detector Temperature: 100 °C
Argon Carrier gas	Flow rate 20 ml/min (99.999% purity)

3.5.6 *In vivo* Hydrogenase activity measurement

Bidirectional hydrogenase activity was determined by measuring H_2 evolution in the presence of dithionite-reduced methyl viologen by gas chromatograph (Baebprasert et al., 2010). The reaction mixture consisted of 1 mL of cell suspension and 1 mL of 25 mM sodium phosphate buffer (pH 7.6) consisting of 10 mM methyl viologen dichloride hydrate and 40 mM sodium dithionite. The mixture was incubated under argon atmospheric conditions at 30 °C under darkness for 30 min. H_2 from headspace was subsequently analyzed by gas chromatograph.

3.5.7 Glycogen determination

For glycogen content determination, a protocol for glycogen extraction and hydrolysis was used (Ernst et al., 1984). Cells of *A. halophytica* were harvested by centrifugation at 8,000 ×g at 4°C for 10 min and resuspended in fresh medium with initial chlorophyll *a* concentration of 300 µg chl *a* mL^{-1}. Then, fifty µL of each cell suspension was added to 30% (w/v) KOH. The mixture was incubated at 100 °C in a water bath for 90 min. Cells were lysed by ultrasonication at 20% pulse for 5 min on ice. Absolute ethanol of 600 µL was added into the extract to precipitate glycogen. Each sample was kept on ice for 1 h. After that, glycogen was collected by centrifugation at 12,000 ×g for 5 min at 4 C. Each glycogen pellet was washed twice by absolute ethanol and subsequently dried at 60°C for 10 min. Glycogen was resuspended in a 300 µL of 100 mM acetate buffer (pH 4.75). For each sample, glycogen was broken into glucose by adding amyloglucosidase from *Aspergillus niger* and α-amylase from *Aspergillus oryzae* at final concentrations of 4 and 8 units, respectively. The reaction was incubated at 25°C for 1 h. Insoluble membrane fragments were removed by centrifugation at 12,000 ×g at 4°C for 5 min. Total sugar in each supernatant was determined by phenol sulfuric acid assay (Dubois et al., 1956). Standard glycogen from bovine liver (0–100 µg) was used. The glycogen content was calculated using a standard calibration curve (Appendix C). Each measurement was performed in triplicate.

3.5.8 Phenol sulfuric assay

Phenol sulfuric assay was used to determine total sugar concentration (Dubois et al., 1956). Fifty µL of cell suspension was mixed with 500 µL of 4% (w/v) phenol reagent following by adding 2.5 mL of 96% (v/v) sulfuric acid. The mixture was placed at room temperature for 10 min. Then, it was shaken and placed in a water bath at 30 °C for 10 min. Total sugar in the reaction mixture was measured spectrophotometrically at absorbance of 490 nm. Glycogen content was calculated by using a standard calibration curve of glycogen (Appendix C).

3.5.9 Protein determination by Bradford assay

Protein concentration was measured by Bradford assay (Bradford, 1976). Fifty µL of cell suspension was added 5 mL of Bradford reagent (Appendix D). The reaction mixture was placed at room temperature for 5 min. Protein in the reaction mixture was measured spectrophotometrically at absorbance of 595 nm. Protein concentration was calculated using a standard calibration curve of bovine serum albumin (Appendix D). The protein concentration was expressed as mg mL^{-1}.

3.5.10 Pyruvate kinase activity determination

Pyruvate kinase activity was measured indirectly by determining the oxidation of NADH in the reaction catalyzed by lactate dehydrogenase. The activity of pyruvate kinase was determined by a protocol previously described (Malcovati and Valentini, 1982). To prepare cell-free extract of *A. halophytica*, 100 mL of *A. halophytica* cell culture was harvested by centrifugation at 8,000 ×g at 4°C for 10 min and subsequently resuspended in 1 mL of 10 mM HEPES buffer (pH 7.5). Cells were lysed using 20% pulse of ultrasonication on ice for 5 min. The cell-free extract was obtained after centrifugation at 8,000 ×g at 4°C for 10 min. To examine pyruvate kinase activity, 50 µL of cell-free extract was added into 950 µL of reaction mixture containing 10 mM HEPES buffer, 10 mM $MgCl_2$, 50 mM KCl, 20 mM ADP, 10 mM PEP, 5 mM NADH, and 0.5 U of L-lactate dehydrogenase. The reaction mixture without PEP was used as a negative control. The decrease in NADH was measured spectrophotometrically at a wavelength of 340 nm at 25°C. One unit of pyruvate kinase activity is defined as the amount of enzyme that catalyzes the production of 1.0 µmol pyruvate from the substrate PEP in 1 min according to Malcovati and Valentini (1982). The specific activity of pyruvate kinase was determined as activity per total protein concentration. Protein concentration was determined by Bradford assay (Bradford, 1976).

3.6 Molecular analysis methods

3.6.1 Total RNA isolation

Total RNA was isolated following the protocol of QIAzol®Lysis reagent. *A. halophytica* cells were harvested by centrifugation at 8,000 xg at 4 °C for 10 min. The supernatant was removed and 1 mL of QIAzol®Lysis reagent was added to the cell pellet before mixing gently by pipetting. The mixture was centrifuged at 8,000 xg at 4 °C for 10 min. Then, the supernatant was added with 200 µL of chloroform in the new tube. The sample was incubated on ice for 3 min and centrifuged at 12,000 xg at 4 °C for 10 min. The aqueous phase was collected and added to the new tube. To isolate RNA, 500 µL isopropanol was added to the aqueous phase. The extract was incubated at -20 °C for 30 min followed by centrifugation at 8,000 xg at 4 °C for 10 min. The supernatant was removed. The precipitate was washed by adding 1 mL of 75% ethanol, mixed and centrifuged again. The supernatant was removed from the precipitate and let it dry. The RNA pellet was resuspended in 30 µL of distilled water containing 0.1% (w/v) diethyl pyrocarbonate (DEPC).

3.6.2 Determination of total nucleic acid

3.6.2.1 Quantitative measurement of total nucleic acid concentration by Nanodrop 2000/2000c spectrophotometer

Nanodrop 2000/2000c software was used to determine a quantitative total nucleic acid by measurement of absorbance at 260 and 280 nm of two µL of total RNA samples. The ratio of A_{260} and A_{280} of purified total RNA should be 1.8-2.0 (Sambrook and Russell, 2001).

3.6.2.2 Nucleic acid analysis by agarose gel electrophoresis

For measurement quality of total RNA sample, 1.0 % (w/v) agarose was prepared by dissolving 0.2 g of agarose in 20 mL of 1xTBE buffer containing 89 mM Tris-HCl, 89 mM boric acid, and 2 mM EDTA. The agarose was dissolved completely by heating in a microwave. Gelstar staining solution at the final concentration of 1-fold (from 10,000-fold) was added. An agarose solution was mixed gently. A suitable comb was used to form

the sample slots in the gel. The warm agarose gel was poured into the mold. The gel was placed at room temperature for 30-45 min under darkness. After the gel set solid completely, the gel was transferred to the electrophoresis tank. Then, 1xTBE buffer was filled to cover the gel. Total RNA sample was mixed with tracking dye and loaded into the well. Five-hundred ng of λDNA/*Hin*dIII fragments was used as marker. The electric current with 10 V cm^{-1} was performed to run electrophoresis. After the electrophoresis was finished, the gel was observed using gel documentation under an ultraviolet light.

3.6.3 mRNA sequencing by Illumina HiSeq/Novaseq or MGI2000

The ribosomal RNA (rRNA) was removed from total RNA samples by using a Ribo-Zero rRNA removal Kit (Epicentre, United States) following the manufacturer's instructions. The construction of the next generation sequencing library was conducted by Genewiz (China) according to the standard protocols. The different indices of libraries were multiplexed and loaded on an Illumina HiSeq/Novaseq instrument according to the instructions of the manufacturer (Illumina, United States). RNA sequencing was performed using the 2 × 150 paired end (PE) configuration. Image analysis and base calling were conducted using the HiSeq Control Software (HCS) + OLB + GAPipeline-1.6 (Illumina) on the HiSeq instrument. All RNA sequencing and alignment processes were conducted by Genewiz (China).

3.7 Screening of reducing substance types affecting H_2 production

3.7.1 Screening of reducing sugars

A. halophytica was grown in BG11 supplemented with Turk Island salt solution for 7 days. Cells were subsequently harvested by centrifugation at 8,000 ×g at 4 °C for 10 min before resuspension in 100 mL of nitrogen-free BG11 medium. The resuspended cells were shaken at 120 rpm on a rotary shaker under a white-light fluorescence intensity of 30 µmol photons m^{-2} s^{-1} at 30 °C for 24 h. After that, adapted cells were harvested by centrifugation at 8,000 ×g at 4 °C for 10 min and resuspended in 5 mL of fresh nitrogen-free medium and transferred to a 12-mL glass vial. Various kinds of reducing sugars, glucose, fructose, maltose monohydrate and lactose monohydrate at final concentrations

of 0.189, 1.89, 18.9 and 189 mmol C-atom L^{-1} were added into cell suspension. To allow anaerobic conditions, the vials were sealed with rubber stopper followed by purging with argon gas for 10 min. Cells were incubated on incubator shaker at 120 rpm under dark anaerobic conditions for 24 h. The amount of H_2 in the headspace of the vial was measured by GC-TCD.

3.7.2 Screening of reducing agents

A. halophytica was grown in BG11 supplemented with Turk Island salt solution for 7 days. Cells were subsequently harvested by centrifugation at 8,000 ×g at 4 °C for 10 min before resuspension in 100 mL of nitrogen-free BG11 medium. The resuspended cells were shaken at 120 rpm on a rotary shaker under a white-light fluorescence intensity of 30 µmol photons m^{-2} s^{-1} at 30 °C for 24 h. After that, adapted cells were harvested by centrifugation at 8,000 ×g at 4 °C for 10 min and resuspended in 5 mL of fresh nitrogen-free medium and transferred to a 12-mL glass vial. The reducing agents, L-ascorbic acid, β-mercaptoethanol, DL-dithiothreitol, formic acid, potassium hexacyanoferrate (II) trihydrate, methyl viologen dichloride hydrate, sodium hydrosulfite, sodium sulfide nanohydrate, oxalic acid and L-cysteine, were added to final concentrations of 0.1, 1.0 and 10 mM. To allow anaerobic conditions, the vials were sealed with rubber stopper followed by purging with argon gas for 10 min. Cells were incubated on incubator shaker at 120 rpm under dark anaerobic conditions for 24 h. The amount of H_2 in the headspace of the vial was measured by GC-TCD.

3.7.3 Cell toxicity assay in cells incubated with selective reducing agents

A. halophytica cells were incubated with selective reducing agents at final concentrations of 0.1, 1.0, 10, 20, 50 and 100 mM under dark anaerobic conditions for 24 h. One mL of samples from each culture were withdrawn to measure the cell density by counting total blue-green visible cells under a microscope using a hemocytometer. The number of cells obtained at each concentration, after the exposure period, was expressed as percentage growth reduction with respect to the control (without reducing agent addition). These percentages were used in the calculation of IC_{50} (expressed as reducing agent concentration giving 50% decreasing of cell concentration after 24 h of exposure).

3.7.4 Analysis of redox partners for H_2ase by *in vitro* H_2ase activity measurement

Ferredoxin (Fd) from spinach, reduced β-nicotinamide adenine dinucleotide 2' phosphate (NADPH) and reduced β-nicotinamide adenine dinucleotide (NADH) were chosen for analyzing a redox partner of H_2ase in *A. halophytica*. To prepare cell homogenate of *A. halophytica*, 100 mL of *A. halophytica* cells were harvested by centrifugation at 8,000 ×g at 4 °C for 10 min and resuspended in 0.2 M sodium phosphate buffer (pH 7.0) at a chlorophyll *a* concentration of 300 μg chl *a* mL^{-1}. Then, cells were broken by 20% pulse of ultrasonication on ice for 5 min. The cell-free extract was obtained after centrifugation of the homogenate at 8000 ×*g* at 4 °C for 10 min. One mL of cell-free extract was mixed with 1 mL of reaction mixture containing 10 mM glucose, 40 U glucose oxidase from *Aspergillus niger* and 50 U catalase from *Micrococcus lysodeikticus* to induce anaerobic conditions (Gutekunst et al., 2014). The reaction mixture was treated with various concentrations of ferredoxin, NADH and NADPH was incubated at 30 °C for 15 min before measurement of H_2ase activity of cell-free extract by GC-TCD.

3.8 Cyanobacterial adaptation conditions under nutrient deprivation

H_2 production by *A. halophytica* cultivated with the two-stage system was measured. Firstly, *A. halophytica* was grown in BG11 supplemented with Turk Island salt solution for 7 days for accumulating biomass. Then, cells were harvested by centrifugation at 8,000 ×g at 4 °C for 10 min following by resuspension in 100 mL of various types of single nutrient-deprived media for 24 h.

3.8.1 Screening of nutrient deprivation for H_2 production

A. halophytica cells grown in BG11 supplemented with Turk Island salt solution for 7 days were harvested by centrifugation at 8,000 ×g at 4 °C for 10 min. Cells were resuspended in 100 mL of various types of single nutrient-deprived media: nitrogen-depleted BG11 with Turk Island salt solution ($BG11_0$), phosphorus-depleted BG11 with Turk Island salt solution (BG11-P), potassium-depleted BG11 with Turk Island salt solution (BG11-K), and sulfur-deprived BG11 with Turk Island salt solution (BG11-S). To remove

nitrogen in $BG11_0$, $NaNO_3$ was eliminated from BG11. To remove phosphorus from BG11-P, NaH_2PO_4 was eliminated from BG11. To remove potassium from BG11-K, KCl was eliminated from Turk Island salt solution and K_2HPO_4 was eliminated from BG11 and replaced by Na_2HPO_4. To remove sulfur from BG11-S, $ZnSO_4 \cdot 7H_2O$ and $CuSO_4 \cdot 5H_2O$ were eliminated from BG11 and replaced by $ZnCl_2$ and $CuCl_2$, respectively. In addition, $MgSO_4 \cdot 7H_2O$ was eliminated from both BG11 and Turk Island salt solution and replaced by $MgCl_2$. Then, cells were shaken at 120 rpm on a rotary shaker under a white-light fluorescence intensity of 30 μmol photons m^{-2} s^{-1} at 30 °C for 24 h. After that, adapted cells were harvested by centrifugation at 8,000 ×g at 4 °C for 10 min, resuspended in 5 mL of fresh-nutrient-deprived medium and transferred to a 12-mL glass vial. For setting anaerobic conditions, the vials were sealed with rubber stopper followed by purging with argon gas for 10 min. Cells were incubated on incubator shaker at 120 rpm under dark anaerobic conditions for 120 h. The amount of H_2 in the headspace of the vial was measured by GC-TCD at 2, 8, 16, 24, 48, 72, 96 and 120 h after incubation. The nutrient deprived conditions proving the highest H_2 production is chosen for further experiments.

3.8.2 Effect of limited nutrient concentration on H_2 production under selected nutrient deprivation

The seven-day old cells of *A. halophytica* were harvested and adapted in media containing various concentrations of limited nutrients. For nutrient-limited conditions, the final concentration of $NaNO_3$ was varied from 0, 4.4, 8.8, 13.2 to 17.6 mM, the final concentration of PO_4^{3-} was varied from 0.04, 0.09, 0.13 to 0.175 mM, and the final concentration of K^+ was varied from 2.58, 4.82, 7.05 to 9.28 mM. Cells were transferred to a 12-mL glass vial. For setting anaerobic conditions, the vials were sealed with rubber stopper followed by purging with argon gas for 10 min. Cells were incubated on incubator shaker at 120 rpm under dark anaerobic conditions for 24 h. After that, H_2ase activity, and H_2 production was measured by GC-TCD.

3.8.3 Time course of H_2ase activity, H_2 production, O_2 production, glycogen content and specific activity of pyruvate kinase under selected nutrient deprivation

The seven-day old cells were harvested and adapted under the selected nutrient deprivation for 1, 2, 3, 4 and 5 days under a light exposure of 18 h per day. Then, adapted cells at each time course were harvested by centrifugation at 8,000 ×g at 4 °C for 10 min and resuspended in 5 mL of fresh-nutrient-deprived medium and transferred to a 12-mL glass vial. Cells were incubated on incubator shaker at 120 rpm under dark anaerobic conditions for 24 h. H_2ase activity, H_2 production and O_2 production, glycogen content and specific activity of pyruvate kinase were measured.

3.8.4 mRNA sequencing by Illumina HiSeq/Novaseq or MGI2000 of the selective nutrient deprivation

To study the pathways involved in H_2 production by *A. halophytica*, the deprivation conditions with the selective adaptation time providing the highest H_2 production was chosen to study in RNA-seq based transcriptome analysis compared with that in abundant cells. For total RNA extraction, QIAzol Lysis Reagent was used. After that, total RNA was quantified and qualified using a NanoDrop 2000/2000c spectrophotometer. Ribosomal RNA (rRNA) was removed by using a Ribo-Zero rRNA removal Kit (Epicentre, United States) following the manufacturer's instructions. The construction of the next generation sequencing library was conducted by Genewiz (China) according to the standard protocols. The different indices of libraries were multiplexed and loaded on an Illumina HiSeq/Novaseq instrument according to the instructions of the manufacturer (Illumina, United States). RNA sequencing was performed using the 2 × 150 paired end (PE) configuration. Image analysis and base calling were conducted using the HiSeq Control Software (HCS) + OLB + GAPipeline-1.6 (Illumina) on the HiSeq instrument. All RNA sequencing and alignment processes were conducted by Genewiz (China).

3.9 Statistical Analysis

All experiments were performed in triplicate. All data are shown as the mean ± standard deviation. One-way analysis of variance (ANOVA) was used to analysis with 95% confidence level by IBM SPSS version 19 software.

CHAPTER 4

RESULTS

4.1 Effect of reducing substances on H_2 production by *A. halophytica*

To improve H_2 production in N-deprived cells of *A. halophytica* under dark anaerobic conditions, the effect of type and concentration of reducing substances including reducing sugars and reducing agents on H_2 production was investigated. The reducing sugars include glucose, fructose, maltose, and lactose whereas reducing agents include ascorbic acid, β-mercaptoethanol, dithiothreitol, formic acid, L-cysteine, methyl viologen, oxalic acid, potassium hexacyanoferrate, sodium dithionite and sodium sulfide. H_2 production was measured in headspace gas of vials containing N-free *A. halophytica* cells under dark anaerobic conditions.

4.1.1 Effect of reducing sugars on H_2 production by *A. halophytica*

To investigate the optimal type and concentration of reducing sugars for H_2 production, *A. halophytica* cells were photoautotrophically grown in BG11 supplemented with Turk Island salt solution (pH 7.4) for 7 days. Cells were subsequently harvested by centrifugation and resuspended in fresh $BG11_0$. The reducing sugars, glucose, fructose, maltose, lactose at concentrations of 0, 0.189, 1.89, 18.9 and 189 mmol C-atom L^{-1} was added into the culture. The culture was incubated under dark anaerobic conditions before measurement of H_2 production after 2 and 24 h of incubation. The result showed that the highest H_2 production rate of 55.80 ± 0.50 μmol H_2 g dry $weight^{-1}$ h^{-1} was shown in cells incubated in medium containing 0.189 mmol C-atom L^{-1} glucose (Fig. 4.1). This H_2 production rate was approximately 1.5 folds higher than that of control cells (without any supplementation of reducing sugars) (38.37 ± 0.25 μmol H_2 g dry $weight^{-1}$ h^{-1}). Higher glucose concentrations than 0.189 mmol C-atom L^{-1} obviously decreased H_2 production rate (Fig. 4.1). The addition of other types of sugar to *A. halophytica* cells could not enhance H_2 production rate compared to an addition of glucose at same C-atom concentrations (Fig. 4.1). However, *A. halophytica* cells incubated in medium containing

0.189 and 1.89 mmol C-atom L^{-1} maltose and lactose could also produce higher H_2 production rate than control cells (Fig. 4.1). On the other hand, fructose at all concentrations tested could not enhance H_2 production rate compared to control cells (Fig. 4.1). At 24 h of incubation, accumulation of H_2 production was determined. The highest H_2 accumulation of 336.05 ± 22.53 μmol H_2 g cell dry wt^{-1} was found in N-deprived cells incubated in 1.89 mmol C-atom L^{-1} sodium carbonate (Na_2CO_3) which is usually used in BG11 medium (Table 4.1). Interestingly, glucose at 0.189 mmol C-atom L^{-1} could not provide the maximum H_2 production at 24 h of incubation. *A. halophytica* cells gave the maximum H_2 production of only 211.99 ± 11.37 μmol H_2 g cell dry wt^{-1}. In this study, type, and concentration of reducing sugars seemed not much effect on H_2 production by *A. halophytica* cells.

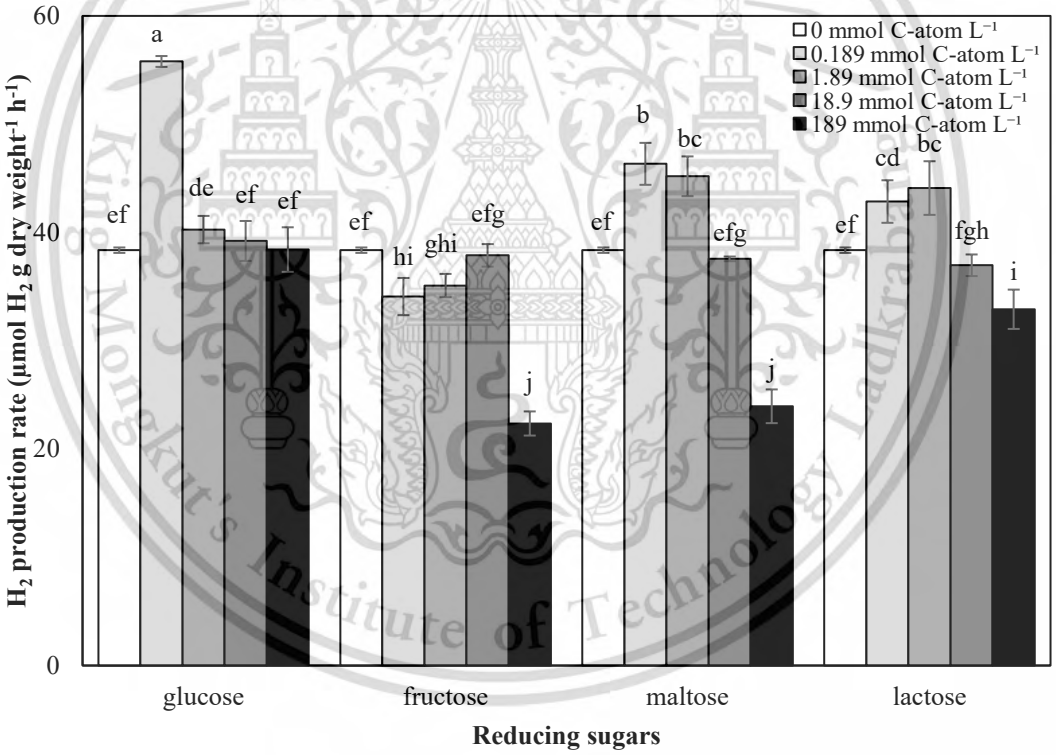

Fig. 4.1 H_2 production rate by *A. halophytica* cells in $BG11_0$ containing various concentrations of 0, 0.189, 1.89, 18.9 and 189 mmol C-atom L^{-1} of glucose, fructose, maltose, and lactose, after 2 h of dark anaerobic conditions. Data represent mean ± SD of triplicate samples with a significant difference level of 95%. Different letters show significant differences between samples.

Table 4.1 H_2 production rate (μmol H_2 g cell dry wt^{-1} h^{-1}) at 2 h and H_2 accumulation (μmol H_2 g cell dry wt^{-1}) at 24 h of *A. halophytica* incubated in $BG11_0$ under dark anaerobic conditions with and without reducing sugars. Data represent mean ± SD of triplicate. Superscripts show significant differences between samples with 95% confidence interval.

Supplements	Conc. of C-atom (mmol C-atom L^{-1})	H_2 production rate (μmol H_2 g cell dry wt^{-1} h^{-1})	H_2 accumulation (μmol H_2 g cell dry wt^{-1})
No supplements (Control)	0	38.37 ± 0.25^{efg}	265.76 ± 7.49^{b}
+Na_2CO_3	189	20.75 ± 0.18^{l}	136.37 ± 2.63^{jk}
	18.9	34.88 ± 0.96^{hij}	237.98 ± 8.30^{cde}
	1.89	35.84 ± 1.47^{ghi}	336.05 ± 22.53^{a}
	0.189	37.54 ± 0.23^{efgh}	264.91 ± 10.09^{b}
+Reducing sugars			
Glucose	189	38.42 ± 2.06^{efg}	253.61 ± 10.91^{bcd}
	18.9	39.22 ± 1.84^{ef}	236.69 ± 10.33^{cde}
	1.89	40.27 ± 1.27^{de}	206.31 ± 0.03^{g}
	0.189	55.80 ± 0.50^{a}	211.99 ± 11.37^{fg}
Fructose	189	22.36 ± 1.11^{kl}	159.66 ± 3.57^{ij}
	18.9	37.88 ± 1.04^{efgh}	179.26 ± 7.69^{hi}
	1.89	35.10 ± 1.08^{hij}	254.03 ± 14.83^{bcd}
	0.189	34.08 ± 1.72^{ij}	218.96 ± 14.24^{efg}
Maltose	189	23.95 ± 1.56^{k}	215.01 ± 13.06^{efg}
	18.9	37.56 ± 0.22^{efgh}	198.53 ± 14.03^{gh}
	1.89	45.19 ± 1.84^{bc}	231.65 ± 5.36^{def}
	0.189	46.34 ± 1.94^{b}	259.36 ± 4.99^{bc}
Lactose	189	32.91 ± 1.82^{j}	108.38 ± 7.10^{l}
	18.9	36.97 ± 1.00^{fghi}	117.69 ± 9.79^{kl}
	1.89	44.10 ± 2.48^{bc}	148.21 ± 13.13^{j}
	0.189	42.86 ± 1.97^{cd}	159.16 ± 5.89^{ij}

4.1.2 Screening of effective reducing agents for H_2 production by *A. halophytica*

To preliminary screening of reducing agents affecting H_2 production by *A. halophytica,* cells were incubated in $BG11_0$ supplemented Turk Island salt solution containing ten different types of reducing agents, ascorbic acid, β-mercaptoethanol, dithiothreitol, formic acid, L-cysteine, methyl viologen, oxalic acid, potassium hexacyanoferrate, sodium dithionite and sodium sulfide, with various concentrations (0, 0.1, 1 and 10 mM) under dark anaerobic conditions. H_2 production rate and H_2 accumulation were measured after incubation cells for 2 h and 24 h, respectively. Moreover, cell concentration and pH of culture after 24 h of incubation were also investigated.

In this study, ten reducing agents showed different effects on H_2 production by *A. halophytica.* These ten reducing agents could be divided into 2 groups. The first reducing agent group contained ascorbic acid, formic acid, methyl viologen, oxalic acid, potassium hexacyanoferrate and sodium dithionite which inhibited H_2 production rate and H_2 accumulation of *A. halophytica* when their concentrations increased (Fig, 4.2, Fig. 4.3). The minimum H_2 production rate and H_2 accumulation was found in cells incubated in medium containing each reducing agents at 10 mM (Fig, 4.2, Fig. 4.3). For ascorbic acid treatment, the highest H_2 production rate with 71.75 ± 3.09 μmol H_2 g dry weight^{-1} h^{-1} was found in cells treated with 0.1 mM, about 2 folds higher than the control cells (cells without any treatments) (Fig. 4.2, Table 4.2). For formic acid treatment, the highest H_2 production rate of 161.12 ± 4.16 μmol H_2 g dry weight^{-1} h^{-1} was shown in cells treated with 0.1 mM. It was about 4.5 folds higher than that of control cells (Fig. 4.2, Table 4.2). But no H_2 production by *A. halophytica* was found in cells treated with 10 mM formic acid (Fig. 4.2, Table 4.2). In terms of methyl viologen treatment, the highest H_2 production rate of 101.84 ± 4.10 μmol H_2 g dry weight^{-1} h^{-1} was obtained in cells treated with 0.1 mM methyl viologen. It was about 3 folds higher than that of control cells (Fig. 4.2, Table 4.2). In oxalic acid treatment, a decrease in H_2 production of N-deprived cells was shown when cells were treated with higher oxalic acid concentrations. no H_2 production was observed in *A. halophytica* treated with 10 mM oxalic acid, similar to what was found with formic acid

treatment (Fig. 4.2, Table 4.2). In case of potassium hexacyanoferrate treatment, N-deprived cells showed the highest H_2 production rate of 87.41 ± 4.98 μmol H_2 g dry weight^{-1} h^{-1} when treated cells with 1 mM potassium hexacyanoferrate. Higher concentrations than 0.1 mM reduced H_2 production by *A. halophytica* (Fig. 4.2, Table 4.2). In sodium dithionite treatment, the highest H_2 production rate of 159.53 ± 11.20 μmol H_2 g dry weight^{-1} h^{-1} was found in N-deprived cells treated with only 0.1 mM. It was about 4 folds higher than control cells (Fig. 4.2, Table 4.2). Among all treatments with these reducing agents, treatment with 0.1 mM formic acid showed the highest H_2 production rate with 161.12 ± 4.16 μmol H_2 g dry weight^{-1} h^{-1}.

The second group of reducing agents contained β-mercaptoethanol, dithiothreitol, L-cysteine and sodium sulfide which promoted H_2 production rate and H_2 accumulation of *A. halophytica* when their concentrations increased (Fig, 4.2, Fig. 4.3). The highest H_2 production rates of 241.80 ± 16.08, 251.87 ± 2.26, 256.53 ± 4.89 and 246.76 ± 11.89 μmol H_2 g dry weight^{-1} h^{-1} were found in cells treated with 10 mM β-mercaptoethanol, dithiothreitol, L-cysteine and sodium sulfide, respectively (Fig. 4.2, Table 4.3). No significant differences in these H_2 production rates were found. They were approximately 7 folds higher than that obtained without reducing agent treatment (36.45 ± 0.99 μmol H_2 g dry weight^{-1} h^{-1}) (Fig. 4.2, Table 4.3).

Considering H_2 accumulation in *A. halophytica*, the highest H_2 accumulations with 1,136.02 ± 41.44, 559.65 ± 23.57, 842.69 ± 53.61 and 1,084.90 ± 71.98 μmol H_2 g dry weight^{-1} were found in *A. halophytica* treated with 10 mM β-mercaptoethanol, dithiothreitol, L-cysteine and sodium sulfide, respectively, under dark anaerobic conditions for 24 h (Fig. 4.3, Table 4.3). Although these four reducing agents provided H_2 production rate with a similar level (about 250 μmol H_2 g dry weight^{-1} h^{-1}), their H_2 accumulations at 24 h were different. Therefore, these four reducing agents were selected as the potential reducing agents for promoting H_2 production by *A. halophytica* to investigate in further experiments.

In this study, H_2 production could not be detected in *A. halophytica* incubated in $BG11_0$ containing 10 mM ascorbic acid, formic acid, and oxalic acid (Table 4.2). These three reducing agents are acidic reductants, causing the low pH level in culture, especially with

high concentrations. The treatment of these agents finally resulted in cell death. The results showed that no H_2 production could be detected in *A. halophytica* cells treated with these reducing agents even only at 2 h of incubation, suggesting that these reducing agents at 10 mM obviously influenced cell physiology. In this study, cell concentration and pH of culture were measured after 24 h of treatment with all reducing agents with 0.1, 1.0 and 10.0 mM. In treatment with most reducing agents, pH of culture was almost stable around 6 and cell concentration was about 2-3 x 10 cells mL^{-1} (Table 4.3). Except treatment with the acid reductants, ascorbic acid, formic acid and oxalic acid, cell concentration was about 0.8 x 10 cells mL^{-1} and pH of culture was about 1.8-3.6 (Table 4.3). These results indicated the toxicity of these acidic reducing agents to *A. halophytica* cells. These agents with high concentration (10 mM) resulted in the low pH of culture, leading to the low cell concentration. This condition is not suitable for H_2 production by cells. Interestingly, the highest pH of culture at 8.94 ± 0.22 was found in cells treated with 10 mM sodium sulfide (Table 4.3).

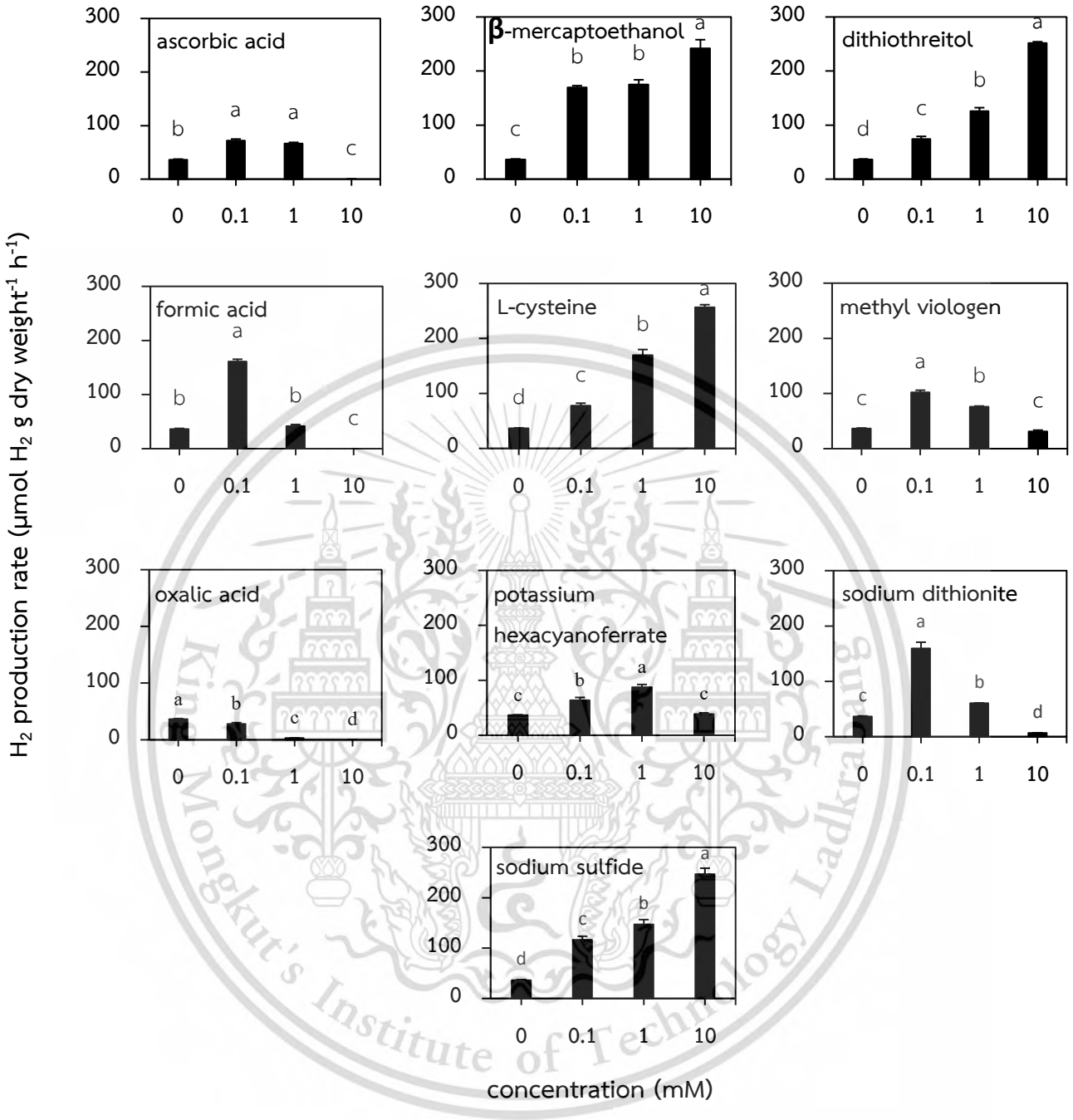

Fig. 4.2 H_2 production rate of *A. halophytica* cells in $BG11_0$ treated with different types of reducing agents at 0, 0.1, 1.0 and 10.0 mM under dark anaerobic conditions for 2 h. Data represent mean ± SD. Superscripts with different letters show significant differences between samples with a significance level of 95%.

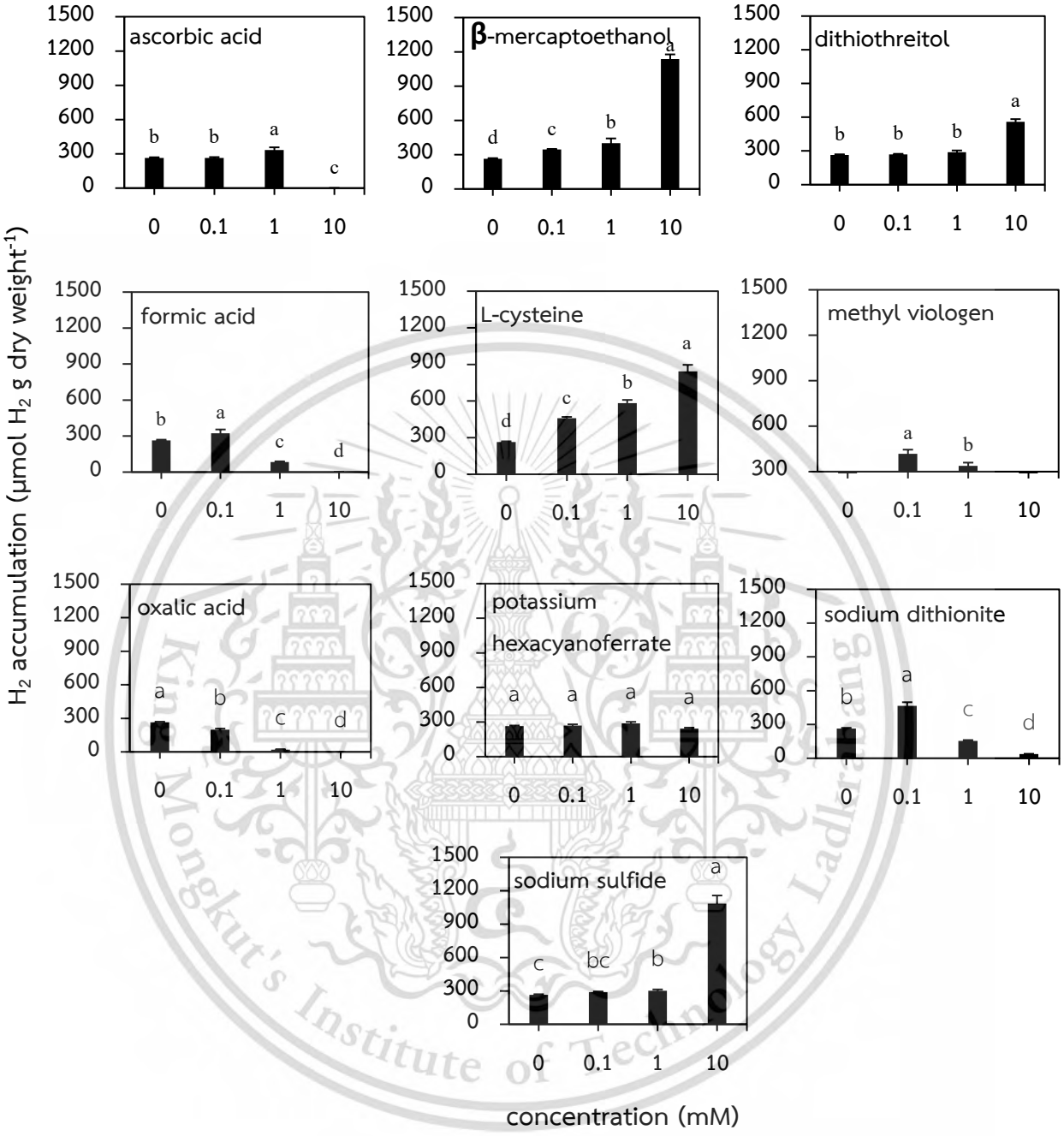

Fig. 4.3 H_2 accumulation of *A. halophytica* cells in $BG11_0$ treated with different types of reducing agents at 0, 0.1, 1.0 and 10.0 mM under dark anaerobic conditions for 24 h. Data represent mean ± SD. Superscripts with different letters show significant differences between samples with a significance level of 95%.

Table 4.2 H_2 production rate and H_2 accumulation of *A. halophytica* cells in $BG11_0$ containing various kinds of reducing agents at concentrations of 0, 0.1, 1.0 and 10.0 mM after dark anaerobic incubation for 2 and 24 h, respectively. Data represent mean ± SD. Superscripts with different letters show differences between samples with a significance level of 95%.

Reducing agents	Conc. (mM)	H_2 production rate (μmol H_2 g dry weight^{-1} h^{-1})	H_2 accumulation (μmol H_2 g dry weight^{-1})
CTRL (No reductants)	0	36.45 ± 0.99^{no}	264.09 ± 5.87^{jk}
ascorbic acid	0.1	71.75 ± 3.09^{jkl}	263.44 ± 8.16^{jk}
	1.0	66.66 ± 2.01^{klm}	334.42 ± 22.46^{hi}
	10.0	ND	ND
β-mercaptoethanol	0.1	169.49 ± 3.36^{cd}	344.71 ± 5.75^{h}
	1.0	175.19 ± 8.54^{c}	401.41 ± 40.93^{g}
	10.0	241.80 ± 16.08^{b}	1,136.02 ± 41.44^{a}
dithiothreitol	0.1	74.10 ± 4.95^{jkl}	268.95 ± 5.45^{jk}
	1.0	125.95 ± 6.28^{f}	289.82 ± 14.52^{ijk}
	10.0	251.87 ± 2.26^{ab}	559.65 ± 23.57^{d}
formic acid	0.1	161.12 ± 4.16^{d}	323.88 ± 31.13^{hi}
	1.0	41.70 ± 2.94^{n}	83.40 ± 5.89^{n}
	10.0	ND	ND
L-cysteine	0.1	77.62 ± 4.70^{j}	458.79 ± 11.21^{ef}
	1.0	169.48 ± 10.44^{cd}	582.32 ± 26.52^{d}
	10.0	256.53 ± 4.89^{a}	842.69 ± 53.61^{c}
methyl viologen	0.1	101.84 ± 4.10^{h}	418.51 ± 26.65^{fg}
	1.0	76.16 ± 1.06^{jk}	337.26 ± 22.27^{h}
	10.0	31.41 ± 2.13^{no}	136.22 ± 4.99^{m}

Table 4.2 (continued) H_2 production rate and H_2 accumulation of *A. halophytica* cells in $BG11_0$ containing various kinds of reducing agents at concentrations of 0, 0.1, 1.0 and 10.0 mM after dark anaerobic incubation for 2 and 24 h, respectively. Data represent mean ± SD. Superscripts with different letters show differences between samples with a significance level of 95%.

Reducing agents	Conc. (mM)	H_2 production rate (μmol H_2 g dry weight^{-1} h^{-1})	H_2 accumulation (μmol H_2 g dry weight^{-1})
oxalic acid	0.1	27.97 ± 2.20^{o}	197.42 ± 10.68^{l}
	1.0	3.06 ± 0.27^{p}	20.64 ± 1.26^{o}
	10.0	ND	ND
potassium	0.1	63.71 ± 5.14^{lm}	268.72 ± 11.47^{jk}
hexacyanoferrate	1.0	87.41 ± 4.98^{i}	288.65 ± 13.08^{ijk}
	10.0	38.56 ± 2.27^{no}	243.01 ± 8.53^{k}
sodium dithionite	0.1	159.53 ± 11.20^{d}	464.95 ± 32.61^{e}
	1.0	60.47 ± 0.23^{m}	155.38 ± 6.25^{m}
	10.0	6.86 ± 0.22^{p}	37.42 ± 2.01^{o}
sodium sulfide	0.1	116.21 ± 7.28^{g}	288.63 ± 5.98^{ijk}
	1.0	147.07 ± 9.52^{e}	301.23 ± 11.74^{hij}
	10.0	246.76 ± 11.89^{ab}	1,084.90 ± 71.98^{b}

Table 4.3 Cell concentration and culture pH of *A. halophytica* cells in $BG11_0$ containing various kinds of reducing agents at 0, 0.1, 1.0 and 10.0 mM after dark anaerobic incubation for 24 h.

Reducing agents	Conc. (mM)	Cell concentration ($\times 10^9$ cells mL^{-1})	Culture pH
CTRL (No reductants)	0	3.63 ± 0.11	6.70 ± 0.03
ascorbic acid	0.1	2.70 ± 0.26	6.20 ± 0.10
	1.0	2.23 ± 0.08	6.09 ± 0.08
	10.0	0.76 ± 0.02	3.68 ± 0.02
β-mercaptoethanol	0.1	3.44 ± 0.09	6.67 ± 0.32
	1.0	3.30 ± 0.07	6.52 ± 0.24
	10.0	3.11 ± 0.18	6.42 ± 0.06
dithiothreitol	0.1	3.15 ± 0.11	6.61 ± 0.21
	1.0	2.54 ± 0.12	6.61 ± 0.13
	10.0	2.39 ± 0.09	6.37 ± 0.06
formic acid	0.1	3.24 ± 0.02	6.63 ± 0.05
	1.0	2.53 ± 0.04	6.07 ± 0.13
	10.0	0.85 ± 0.14	3.18 ± 0.03
L-cysteine	0.1	3.41 ± 0.05	6.67 ± 0.05
	1.0	3.29 ± 0.05	6.72 ± 0.03
	10.0	3.08 ± 0.11	6.57 ± 0.04
methyl viologen	0.1	2.75 ± 0.11	6.25 ± 0.13
	1.0	2.36 ± 0.27	6.20 ± 0.10
	10.0	2.33 ± 0.07	6.01 ± 0.02

Table 4.3 (continued) Cell concentration and culture pH of *A. halophytica* cells in $BG11_0$ containing various kinds of reducing agents at 0, 0.1, 1.0 and 10.0 mM after dark anaerobic incubation for 24 h.

Reducing agents	Conc. (mM)	Cell concentration ($\times 10^9$ cells mL^{-1})	Culture pH
oxalic acid	0.1	2.98 ± 0.21	6.59 ± 0.04
	1.0	2.43 ± 0.25	4.87 ± 0.08
	10.0	0.80 ± 0.03	1.82 ± 0.09
potassium	0.1	3.14 ± 0.05	6.60 ± 0.13
hexacyanoferrate	1.0	2.65 ± 0.07	6.48 ± 0.09
	10.0	2.61 ± 0.16	6.52 ± 0.09
sodium dithionite	0.1	3.14 ± 0.41	6.65 ± 0.31
	1.0	3.51 ± 0.02	6.45 ± 0.25
	10.0	2.65 ± 0.07	5.20 ± 0.11
sodium sulfide	0.1	3.56 ± 0.09	6.52 ± 0.11
	1.0	3.43 ± 0.07	6.94 ± 0.04
	10.0	3.30 ± 0.07	8.94 ± 0.22

4.1.3 Long-term H_2 production by *A. halophytica* treated with reducing agents

After preliminary screening, four reducing agents (β-mercaptoethanol, L-cysteine, dithiothreitol and sodium sulfide) enhancing H_2 production by *A. halophytica* were selected. The final concentrations of these reducing agents were adjusted to 10, 20, 50 and 100 mM (higher than the previous concentrations investigated at 0.1, 1.0 and 10 mM). The N-deprived *A. halophytica* cells were treated with selective reducing agents under dark anaerobic conditions. H_2 production was measured by GC-TCD after 2, 8, 16, 24, 48, 72, 96 and 120 h of incubation. The result showed that H_2 production increased during the first 24 h of incubation in cells treated with all reducing agents (Fig. 4.4). By treatment with β-mercaptoethanol, the highest H_2 production with 1,136 ± 41.44 μmol H_2 g dry wt^{-1} was found in cells treated with 10 mM β-mercaptoethanol at 24 h of incubation (Fig.

4.4). Lower or higher concentration than 10 mM β-mercaptoethanol reduced H_2 production (Fig. 4.4). In the case of dithiothreitol treatment, the highest H_2 production with 3,806.34 ± 50.82 µmol H_2 g dry wt^{-1} was observed in cells treated with 50 mM dithiothreitol at 24 h of incubation (Fig. 4.4). After 24 h of incubation, H_2 accumulation decreased. The treatment with dithiothreitol at all concentrations stimulated H_2 accumulation throughout the incubation time. By L-cysteine treatment, the highest H_2 accumulation of 3,676.29 ± 102.02 µmol H_2 g dry wt^{-1} was obtained in cells treated with 50 mM cysteine at 24 h of incubation (Fig. 4.4). After that, H_2 production was shown significantly decreased until the lowest H_2 production was shown at 120 h of incubation time (Fig. 4.4). By comparison with all reducing agents treated, the highest H_2 production of 4,815.59 ± 194.78 µmol H_2 g dry wt^{-1} was found in cells treated with 50 mM sodium sulfide at 24 h of incubation. It was approximately 18 folds higher than that of control cells without reducing agent treatment (264.10 ± 5.87 µmol H_2 g dry wt^{-1}) (Fig. 4.4).

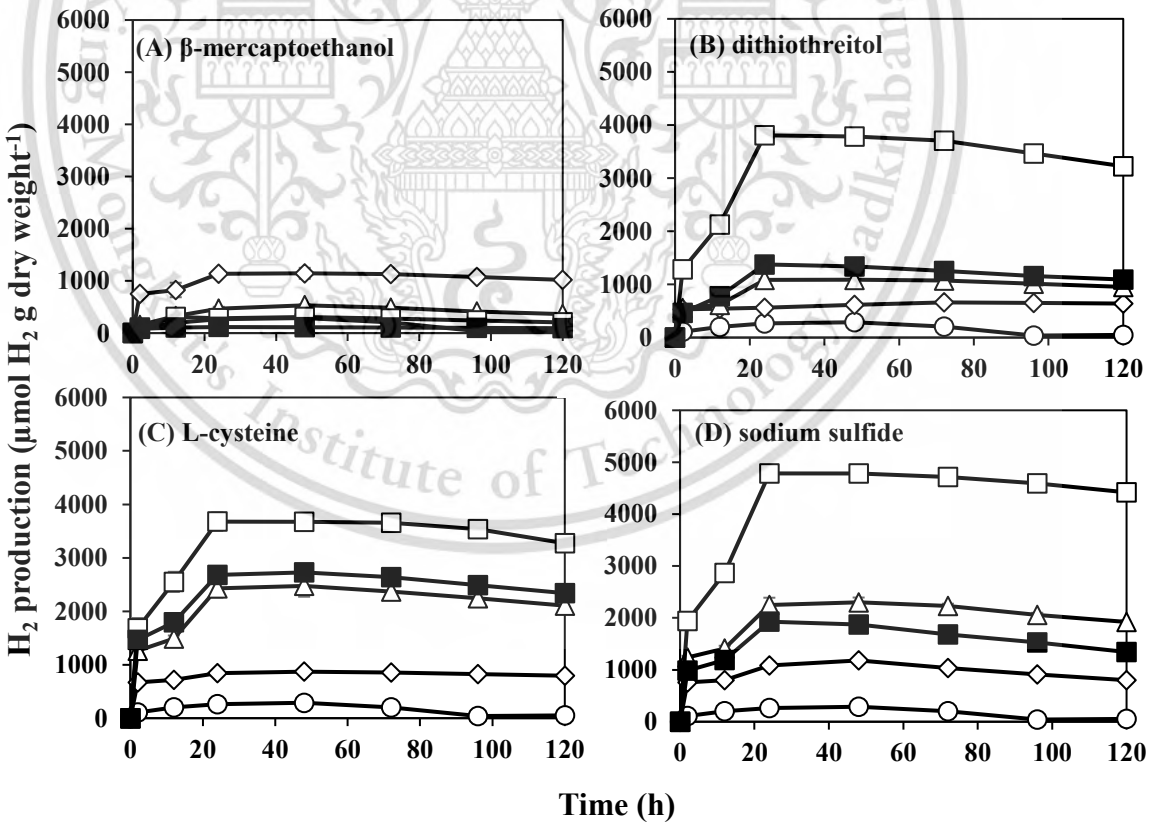

Fig. 4.4 Long-term H_2 production by *A. halophytica* treated with different concentrations of reducing agents (0 MM (O), 10 mM (◊), 20 mM (Δ), 50 mM (□) and 100 mM (■)) under dark anaerobic conditions. Data represent mean ± SD of triplicate with a significance level of 95%.

In summary, the optimal concentration of H_2 production was different depending on the type of reducing agents. The optimal concentrations of β-mercaptoethanol, dithiothreitol, L-cysteine and sodium sulfide for H_2 production by *A. halophytica* were 10, 50, 50 and 50 mM, respectively. To confirm whether H_2 production increased was a result of the enhancement of H_2ase activity due to a decrease in O_2 in system, H_2ase activity and O_2 generation rate was determined in *A. halophytica* cells treated with these reducing agents with optimal concentrations.

Table 4.4 shows that the highest H_2ase activity of 303.45 ± 3.15 μmol H_2 g dry wt^{-1} min^{-1} was found in cells treated with 50 mM sodium sulfide. It was approximately 6 folds higher than that of cells without reducing agent treatment (48.40 ± 2.03 μmol H_2 g dry wt^{-1} min^{-1}). The highest H_2ase activity caused the highest H_2 production of 4,815.59 ± 194.78 μmol H_2 g dry wt^{-1}, which was approximately 18 folds higher than that of cells without reducing agent treatment (264.10 ± 5.87 μmol H_2 g dry wt^{-1}) (Table 4.4). On contrary, the lowest O_2 generation rate of 3.59 ± 0.31 μmol O_2 g dry $weight^{-1}$ h^{-1} was found in cells treated with 50 mM sodium sulfide, which was 10 folds lower than that without any reducing agent treatment (Table 4.4). Our result demonstrates that an increase in H_2 production from reducing agent treatment is due to the enhancement of H_2ase activity, resulting from a decrease in O_2 level in vial.

Table 4.4 H_2 production, *in vivo* H_2ase activity and O_2 generation rate by *A. halophytica* after incubation in $BG11_0$ containing 10 mM β-mercaptoethanol, 50 mM dithiothreitol, 50 mM L-cysteine and 50 mM sodium sulfide under dark anaerobic conditions for 24 h. Data show mean ± SD. Superscripts with different letters show differences between samples with a significant level of 95%.

Reducing agents	H_2 production (μmol H_2 g dry weight^{-1})	H_2ase activity (μmol H_2 g dry weight^{-1} min^{-1})	O_2 generation rate (μmol O_2 g dry weight^{-1} h^{-1})
Control (No reductants)	264.10 ± 5.87^{e}	48.40 ± 2.03^{e}	37.56 ± 1.11^{a}
10 mM β-mercaptoethanol	1,136.02 ± 41.44^{c}	101.88 ± 3.42^{d}	12.77 ± 0.70^{b}
50 mM dithiothreitol	3,806.34 ± 50.82^{b}	251.98 ± 6.99^{c}	12.53 ± 1.29^{b}
50 mM L-cysteine	3,676.29 ± 102.02^{b}	211.31 ± 2.62^{b}	8.17 ± 0.51^{c}
50 mM sodium sulfide	4,815.59 ± 194.78^{a}	303.45 ± 3.15^{a}	3.59 ± 0.31^{d}

4.1.4 Effect of selective reducing agents on cell toxicity

The cell toxicity by IC_{50} and chlorophyll *a* concentration analysis was determined in N-deprived cells of *A. halophytica* incubated in $BG11_0$ supplemented with Turk Island salt solution treated with β-mercaptoethanol, dithiothreitol, L-cysteine and sodium sulfide under dark anaerobic conditions for 24. The concentration of these selective reducing agents was varied at 0.1, 1.0, 10, 20, 50 and 100 mM. IC50 was determined as the concentration of the selective reducing agents that inhibited 50% of cell concentration. The result showed that cell concentration was slightly decreased from 3.63 ± 0.11 × 10^9 cells mL^{-1} to 2.56 ± 0.88 × 10^9 cells mL^{-1} in cells treated with β-mercaptoethanol from 0 to 100 mM (Fig. 4.5a). IC_{50} was calculated as concentration value above 100 mM β-mercaptoethanol. It was shown that chlorophyl concentration was related to cell concentration. Chlorophyll concentration decreased when the concentration of β-mercaptoethanol was higher (Fig. 4.6a). In case of dithiothreitol treatment, cell concentration was exponentially decreased from 3.63 ± 0.11 × 10^9 cells mL^{-1} to 0.19 ± 0.09 × 10^9 cells mL^{-1} in cells treated with dithiothreitol from 0 to 100 mM, which results

in IC_{50} of 18.12 ± 2.07 mM (Fig. 4.5b). The chlorophyll *a* concentration was significantly decreased from 22.39 ± 0.19 μg mL^{-1} to 3.94 ± 0.23 μg mL^{-1} in cells treated with dithiothreitol at 0 to 100 mM (Fig. 4.6b).

By treatment with L-cysteine, cell concentration was decreased significantly from 3.63 ± 0.11 × 10^9 cells mL^{-1} to 1.44 ± 0.08 × 10^9 cells mL^{-1} when concentration of L-cysteine increased from 0 to 100 mM (Fig. 4.5c). The IC_{50} of L-cysteine was 76.94 ± 4.21 mM. Chlorophyll concentration also decreased while the concentration of L-cysteine increased (Fig. 4.6c). In terms of sodium sulfide, cell concentration was slightly decreased from 3.63 ± 0.11 × 10^9 cells mL^{-1} to 2.91 ± 0.11 × 10^9 cells mL^{-1} at the concentration from 0 to 100 mM (Fig. 4.5d), resulting in IC_{50} above 100 mM. Chlorophyll was also decreased from 22.39 ± 0.19 μg mL^{-1} to 9.93 ± 0.29 μg mL^{-1} (Fig. 4.6d). In this study, sodium sulfide at 50 mM shows the most efficient reducing agent for increasing H_2 production by *A. halophytica* since it shows the highest H_2 production, H_2ase activity and lowest O_2 generation rate. In addition, sodium sulfide at 50 mM does not cause toxicity to *A. halophytica* cells due to its IC_{50} above 100 mM.

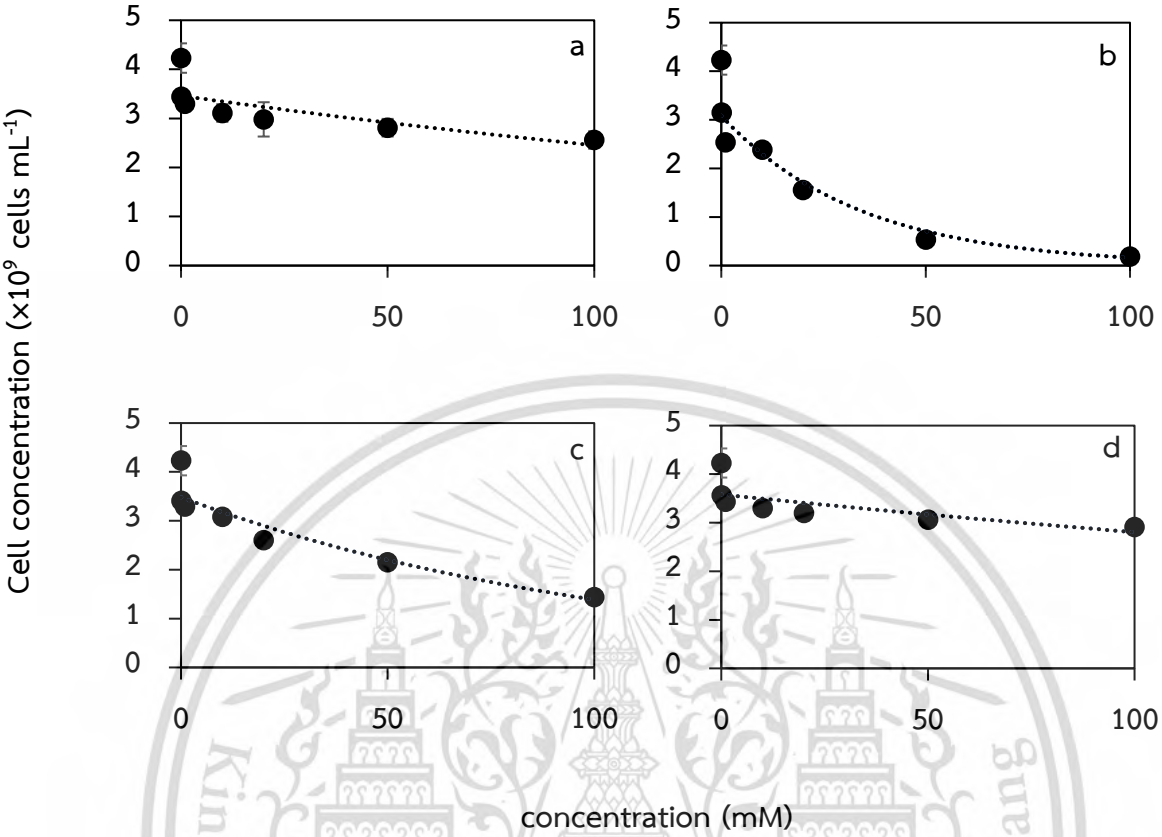

Fig. 4.5 Cell concentration of *A. halophytica* cells after incubation with various concentrations of β-mercaptoethanol (a), dithiothreitol (b), L-cysteine (c), and sodium sulfide (d) under dark anaerobic conditions for 24 h. The initial cell concentration was adjusted at 4.23 ± 0.30 × 10^9 cells mL^{-1}.

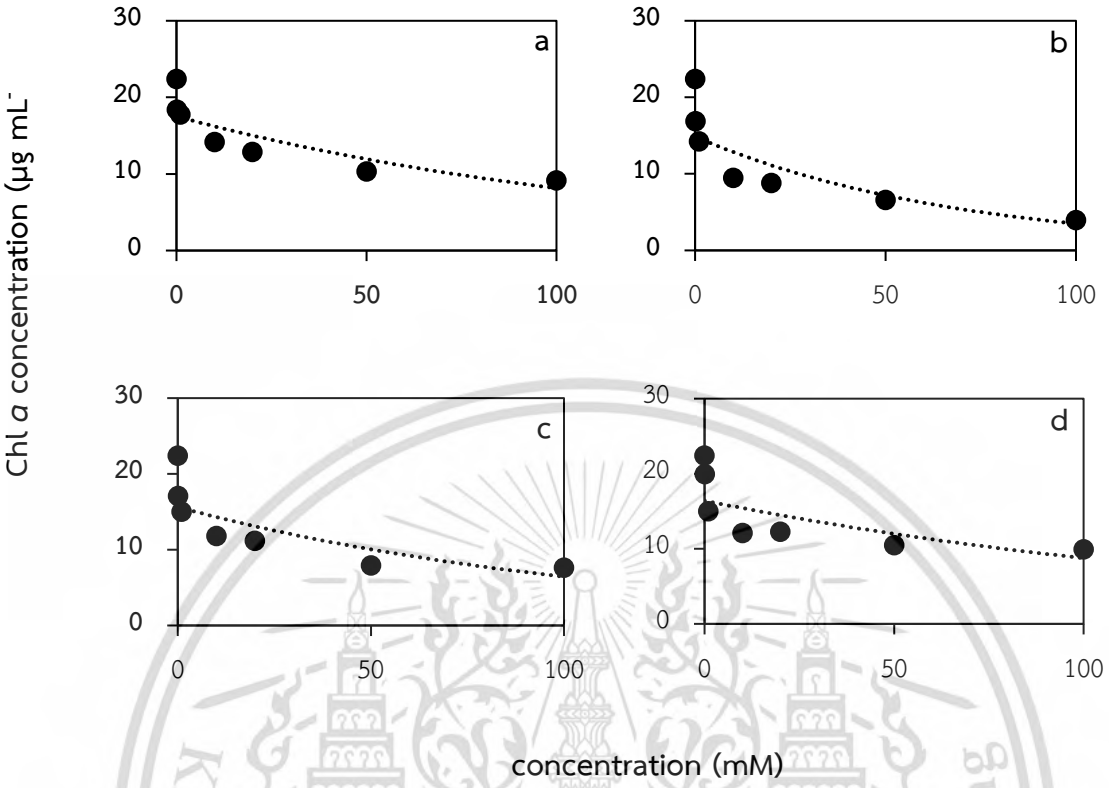

Fig. 4.6 Chlorophyll *a* concentration of *A. halophytica* cells after incubation with various concentrations of β-mercaptoethanol (a), dithiothreitol (b), L-cysteine (c), and sodium sulfide (d) under dark anaerobic conditions for 24 h.

4.2 Effect of ferredoxin, NADH and NADPH on *in vitro* hydrogenase activity

To investigate whether the redox partners, reduced ferredoxin, NADH and NADPH had an ability to provide electrons to H_2ase in *A. halophytica*, the treatment of these redox partners with cell homogenate was performed. The seven days old cells were harvested and resuspended in 0.2 M sodium phosphate buffer (pH 7.0). Then, cell suspension was lysed by ultrasonication. After that, one mL of cell-free extract was mixed with 1 mL of reaction mixture containing 10 mM glucose, 40 U glucose oxidase and 50 U catalase to set anaerobic conditions. Reduced Ferredoxin, NADH, NADPH were added into the reaction mixture to final concentrations of 1.5, 15, 150 µM and 1.5 mM. After incubation at 30 °C under dark anaerobic conditions for 15 min, *in vitro* H_2ase activity was measured by GC-TCD.

The result showed that the highest *in vitro* H_2ase activity of 115.25 ± 3.74 µmol H_2 g dry weight^{-1} min^{-1} was found in reaction mixture containing 2 mM sodium dithionite and 1.5 mM ferredoxin (Table 4.5). In addition, *in vitro* H_2ase activity increased with the higher concentration of ferredoxin, suggesting the role of ferredoxin as a redox partner of H_2ase. However, only sodium dithionite and ferredoxin (even low or high concentrations) could not provide electrons to H_2ase (Table 4.5). It is demonstrated that sodium dithionite is used to reduce ferredoxin only. In the presence of sodium dithionite, reduced ferredoxin at only 1.5 µM could activate *in vitro* H_2ase activity. For NADH and NADPH, *in vitro* H_2ase activity could be detected in the reaction mixture containing 150 µM and 1.5 mM. The highest *in vitro* H_2ase activities of 57.34 ± 2.48 and 51.07 ± 3.04 µmol H_2 g dry weight^{-1} min^{-1} were found in reaction mixture containing 1.5 mM NADH and NADPH, respectively (Table 4.5). This result demonstrates that H_2ase activity of *A. halophytica* prefer reduced ferredoxin to NAD(P)H to be an electron donor.

Table 4.5 *In vitro* H_2ase activity from cell homogenate of *A. halophytica* in the presence of different types of electron donors; sodium dithionite, ferredoxin, NADH and NADPH. To set an anaerobic conditions, cell homogenate in 100 mM phosphate buffer (pH 7.0) was added with glucose, glucose oxidase, and catalase to final concentration of 10 mM, 40 U mL^{-1} and 50 U mL^{-1}, respectively. H_2 was measured by GC-TCD after incubation of cell homogenate and electron donor sources under dark anaerobic conditions for 15 min.

Electron donors	*In vitro* H_2ase activity (μmol H_2 g dry weight^{-1} min^{-1})
No electron donors (CTRL)	ND
2 mM sodium dithionite	ND
1.5 μM ferredoxin	ND
15 μM ferredoxin	ND
150 μM ferredoxin	ND
1.5 mM ferredoxin	ND
2 mM sodium dithionite + 1.5 μM ferredoxin	21.88 ± 1.04^{f}
2 mM sodium dithionite + 15 μM ferredoxin	34.02 ± 0.81^{e}
2 mM sodium dithionite + 150 μM ferredoxin	74.91 ± 3.07^{b}
2 mM sodium dithionite + 1.5 mM ferredoxin	115.25 ± 3.74^{a}
1.5 μM NADH	ND
15 μM NADH	ND
150 μM NADH	9.17 ± 0.19^{g}
1.5 mM NADH	57.34 ± 2.48^{c}
1.5 μM NADPH	ND
15 μM NADPH	ND
150 μM NADPH	5.58 ± 0.33^{g}
1.5 mM NADPH	51.07 ± 3.04^{d}

4.3 Effect of nutrient deprivation on H_2 production and H_2 metabolism of *A. halophytica*

To improve H_2 production by *A. halophytica*, the effect of nutrient deprivation on H_2 production by *A. halophytica* was investigated. Previous studies showed that nitrogen deprivation could induce H_2ase activity and H_2 production by *A. halophytica.* Therefore, in this study the effect of nutrient deprivation such as nitrogen, potassium, phosphorus, and sulfur deprivation on H_2 production was investigated. H_2 metabolism under such nutrient deprivation was also investigated.

4.3.1 Screening of nutrient deprivation on H_2 production

A. halophytica cultivated in BG11 supplemented with Turk Island salt solution (pH 7.4) under a light intensity of 30 μmol photon m^{-2} s^{-1} for 7 days was harvested, resuspended in the BG11, $BG11_0$, BG11-K, BG11-P and BG11-S and incubated under the light for 24 h. Cells were subsequently harvested, resuspended in fresh deprived-medium and incubated under darkness. H_2 was measured by GC-TCD at 2, 8, 16, 24, 48, 72, 96 and 120 h of incubation time. The result showed that H_2 production dramatically increased during the first 24 h of dark incubation in cells incubated in both $BG11_0$ and BG11-K (Fig. 4.7). After that, H_2 production significantly decreased. The highest H_2 production of 332.82 ± 34.02 μmol H_2 g dry cell wt^{-1} was found in cells incubated in BG11-K under darkness for 24 h, which was 33 folds higher than that incubated in BG11 (10.01 ± 5.92 μmol H_2 g dry cell wt^{-1} (Fig. 4.7). In N-deprived cells, the highest H_2 production of 263.75 ± 31.58 μmol H_2 g dry cell wt^{-1} was found, which was 26 folds higher than that incubated in normal BG11 (Fig. 4.7). No significant differences of H_2 production by cells incubated in BG11-P and BG11-S were found compared with that by cells incubated in BG11. Therefore, nitrogen and potassium deprivation were selected to further investigate.

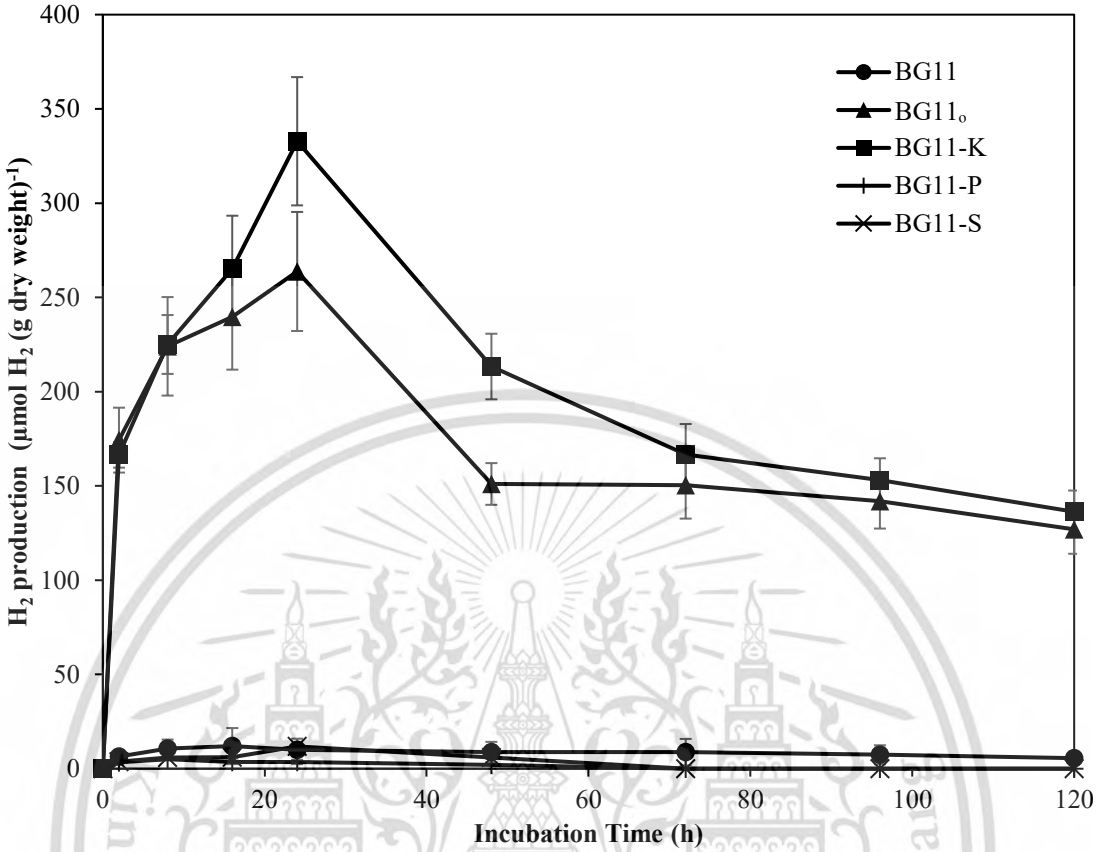

Fig. 4.7 H_2 production by *A. halophytica* cells incubated in BG11 (●), $BG11_0$ (▲), BG11-K (■), BG11-P (+) and BG11-S (✶) under dark anaerobic conditions. Data represent as mean ± SD of triplicate samples.

4.3.2 Effect of nutrient deprivation on H_2 production

4.3.2.1 Effect of nitrogen concentration under potassium deprivation and effect of potassium concentration under nitrogen deprivation on H_2 production and H_2ase activity

H_2 production by the seven-day old cells of *A. halophytica* incubated in K-limited $BG11_0$, N-limited BG11-K and $BG11_0$-K was measured. Under potassium deprivation with various $NaNO_3$ concentrations, the highest H_2 production and H_2ase activity of 449.32 ± 6.08 µmolH_2 g dry weight^{-1} and 81.23 ± 7.03 µmol H_2 g dry weight^{-1} min^{-1}, respectively, was found in cells incubated in BG11-K containing 4.4 mM $NaNO_3$ (Table 4.6). Under

nitrogen deprivation with various potassium concentrations, *A. halophytica* showed the highest H_2 production and H_2ase activity of 388.94 $\pm$ 34.66 μmolH_2 g dry weight^{-1} and 84.70 $\pm$ 6.65 μmol H_2 g dry weight^{-1} min^{-1}, respectively, in cells incubated in $BG11_0$ containing 2.3 mM KCl (Table 4.6). However, the maximum H_2 production and H_2ase activity of 507.51 $\pm$ 13.78 μmol H_2 g dry weight^{-1} and 120.05 $\pm$ 8.98 μmol H_2 g dry weight^{-1} min^{-1}, respectively, was found in cells incubated in both nitrogen- and potassium-deprived BG11 ($BG11_0$-K), (Table 4.6). The results demonstrated that concentration of both potassium and nitrogen in medium played an impact role in H_2ase activity and consequently affecting H_2 production by *A. halophytica*. The less concentration of $NaNO_3$ in BG11-K resulted in the higher both H_2 production and H_2ase activity. Likewise, the less concentration of KCl in $BG11_0$ showed the higher H_2 production and H_2ase activity. Moreover, the highest H_2 production and H_2ase activity was found in *A. halophytica* incubated in nitrogen and potassium deprivation or $BG11_0$-K medium (Table 4.6). Therefore, the effect of nitrogen and potassium deprivation on H_2 production, H_2ase activity, O_2 production, glycogen accumulation and pyruvate kinase activity were investigated in the next experiments.

Table 4.6 H_2 production and H_2ase activity by *A. halophytica* cells incubated in various types of media; BG11, potassium-deprived BG11 containing various concentrations of $NaNO_3$, nitrogen-deprived BG11 containing various concentrations of KCl, potassium- and nitrogen-deprived BG11 for 1 day. Data are means ± SD (n=3). Different letters in columns indicate a significant difference, and the same letter indicates no significant difference according to Duncan's multiple range test at $p < 0.05$.

Type of media	KCl (mM)	$NaNO_3$ (mM)	H_2 production (μmol H_2 g dry weight^{-1})	H_2ase activity (μmol H_2 g dry weight^{-1} min^{-1})
BG11	8.93	17.6	10.55 ± 0.58^{h}	3.20 ± 0.22^{f}
BG11-K	0	17.6	332.58 ± 8.56^{ef}	51.38 ± 1.51^{de}
	0	13.2	354.44 ± 9.15^{de}	60.30 ± 4.68^{cd}
	0	8.8	379.38 ± 17.51^{cd}	62.97 ± 4.78^{c}
	0	4.4	449.32 ± 6.08^{b}	81.23 ± 7.03^{b}
$BG11_0$	8.93	0	260.34 ± 12.24^{g}	46.61 ± 3.30^{e}
	6.70	0	279.10 ± 17.43^{g}	51.83 ± 1.40^{de}
	4.47	0	313.99 ± 21.93^{f}	54.9 ± 3.10^{cde}
	2.23	0	388.94 ± 34.66^{c}	84.70 ± 6.65^{b}
$BG11_0$-K	0	0	507.51 ± 13.78^{a}	120.05 ± 8.98^{a}

4.3.2.2 Effect of adaptation time on H_2 production, H_2ase activity, O_2 production, glycogen accumulation and pyruvate kinase activity

The seven days old cells of *A. halophytica* were adapted in BG11, $BG11_0$, BG11-K and $BG11_0$-K for 1-5 days before measurement of H_2 and O_2 production and H_2ase activity after 24 h of dark anaerobic incubations. The effect of adaptation time on H_2 production was shown in Fig. 4.8. The highest H_2 production of 1,261.96 ± 96.99 μmol H_2 g dry wt^{-1} was found in cells adapted in $BG11_0$-K for 2 days, followed by 1,028.55 ± 22.75 and 764.61 ± 74.19 μmol H_2 g dry wt^{-1} in cells adapted in BG11-K and $BG11_0$, respectively (Fig. 4.8). Interestingly, *A. halophytica* cells adapted in $BG11_0$-K produced the highest H_2 throughout the adaptation time. After 2 days of adaptation time, H_2 production dramatically decreased (Fig. 4.8).

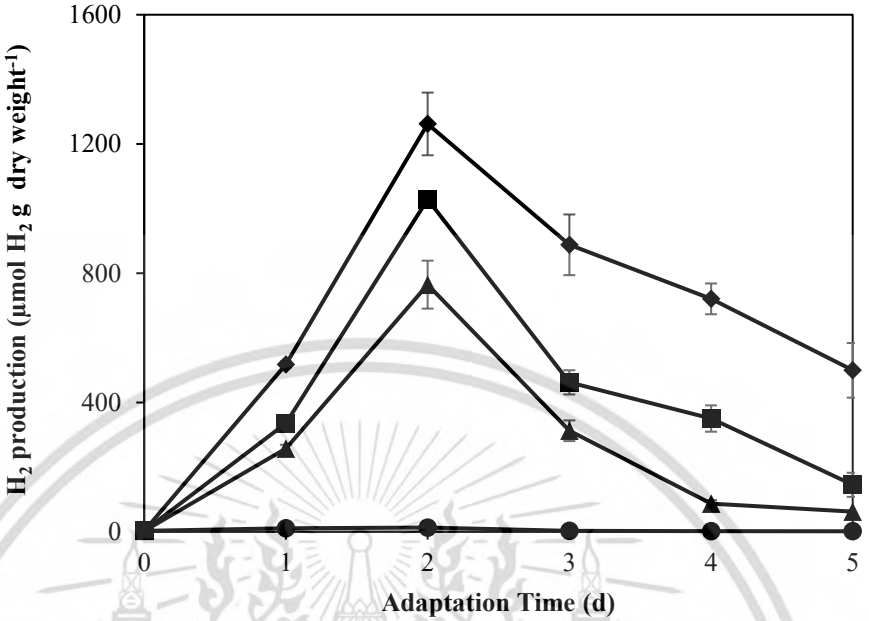

Fig. 4.8 H_2 production by *A. halophytica* cells adapted in BG11 (●), $BG11_0$ (▲), BG11-K (■) and $BG11_0$-K (♦) under light aerobic conditions for 5 days. Data represent mean ± SD of triplicate samples.

Besides measurement of H_2 production, H_2ase activity was also determined. The result showed that H_2ase activity corresponded with H_2 production. The highest H_2ase activity of 179.39 ± 8.19 µmol H_2 g dry wt^{-1} min^{-1} was found in cells adapted in $BG11_0$-K for 2 days (Fig. 4.9). Both nitrogen and potassium deprivation provided the highest H_2ase activity compared with single deprivation of either nitrogen or potassium throughout the adaptation time. Interestingly, H_2 production and H_2ase activity by K-deprived adapted cells were higher than those in N-deprived adapted cells (Fig. 4.8 and Fig. 4.9). *A. halophytica* cells adapted in BG11 provided the lowest H_2 production and H_2ase activity (Fig. 4.8 and Fig. 4.9).

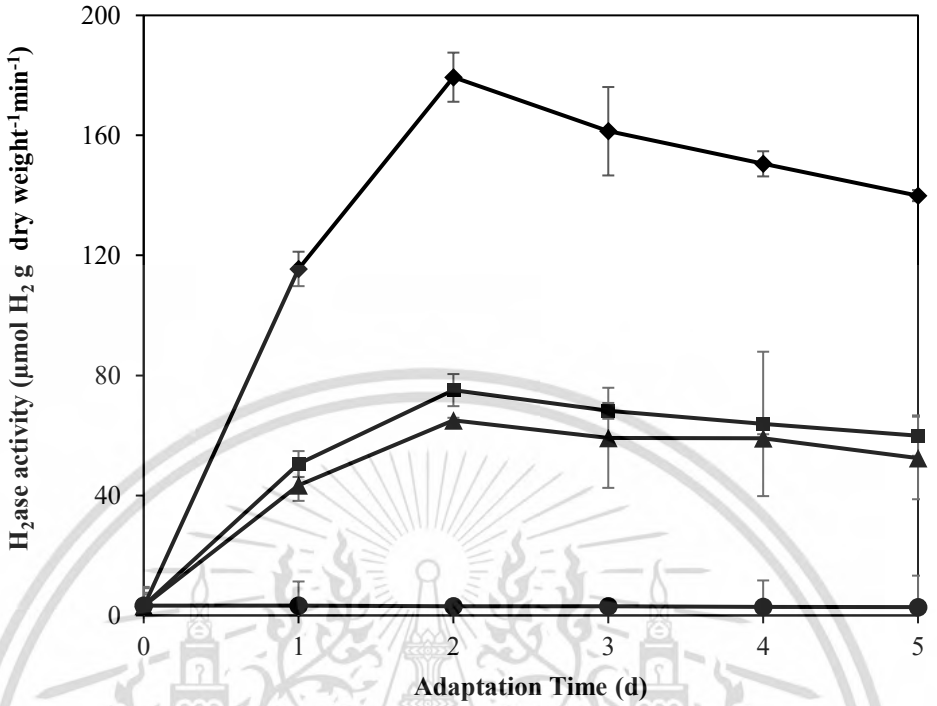

Fig. 4.9 H_2ase activity of *A. halophytica* cells adapted in BG11 (●), $BG11_0$ (▲), BG11-K (■) and $BG11_0$-K (♦) under light aerobic conditions for 5 days. Data represent mean ± SD of triplicate samples.

In the case of O_2 production rate, *A. halophytica* cells adapted under normal condition (in BG11) showed higher O_2 production rate depending on an increase in adaptation time and reached the highest O_2 production rate with 124.98 ± 7.25 µmol O_2 g dry wt^{-1} h^{-1} at 4 days of adaptation time (Fig. 4.10). The lowest O_2 production rate of 8.81 ± 2.94 µmol O_2 g dry wt^{-1} h^{-1} was found in cells adapted in $BG11_0$-K for 5 days (Fig. 4.10). The N-deprived cells provided a higher O_2 production rate than the K-deprived cells at all adaptation times (Fig. 4.10).

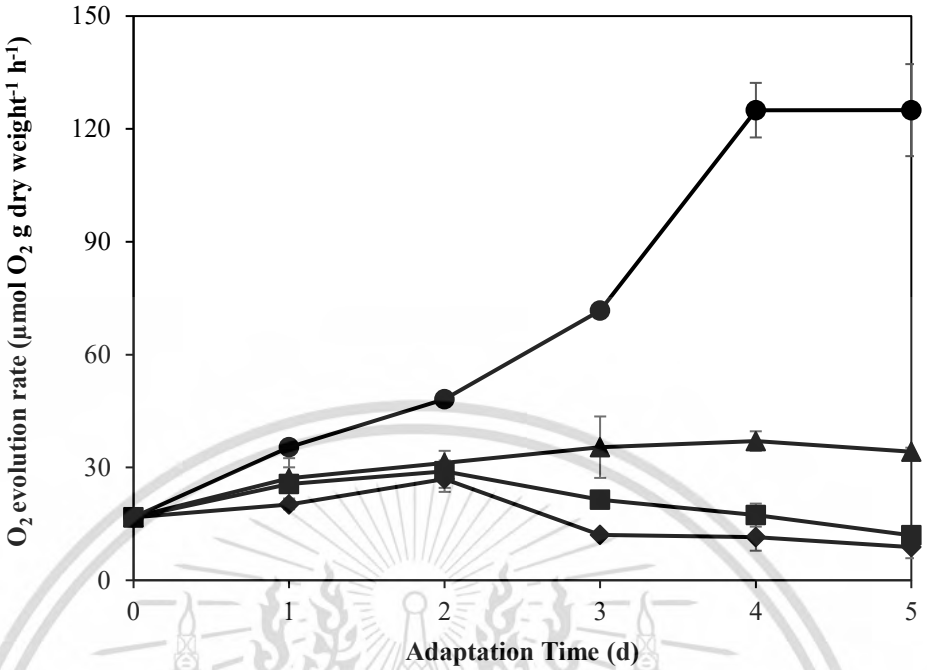

Fig. 4.10 O_2 evolution rate by *A. halophytica* cells adapted in BG11 (●), $BG11_0$ (▲), BG11-K (■) and $BG11_0$-K (♦) under light aerobic conditions for 5 days. Data represent mean ± SD of triplicate samples.

The specific activity of pyruvate kinase was measured in cell-free extract of *A. halophytica* cells adapted in BG11, $BG11_0$, BG11-K and $BG11_0$-K. The result showed that specific activity of pyruvate kinase increased steadily during adaptation time in cells adapted in normal BG11. The highest specific activity of pyruvate kinase of 10.20 ± 0.60 U mg^{-1} protein was found in cells adapted in BG11 for 5 days (Fig. 4.11). On the other hand, under both nitrogen and potassium deprivation (in $BG11_0$-K), the specific activity of pyruvate kinase slightly increased and reached the highest at day 3rd of adaptation time. After that, the specific activity of pyruvate kinase decreased and provided the lowest activity of 0.39 ± 0.01 U mg^{-1} protein after 5 days of adaptation time (Fig. 4.11). In N-deprived cells, the specific activity of pyruvate kinase was higher than that in K-deprived cells throughout the adaptation time (Fig. 4.11).

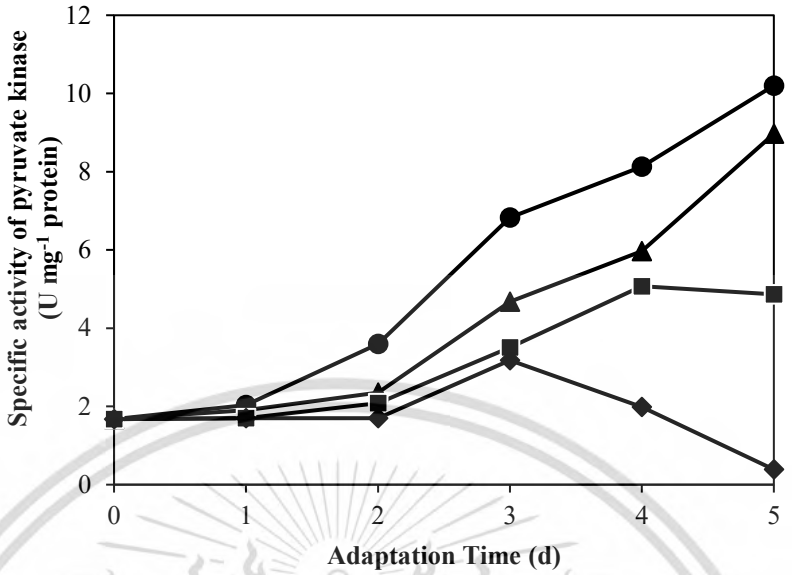

Fig. 4.11 Specific activity of pyruvate kinase of *A. halophytica* cells adapted in BG11 (●), $BG11_0$ (▲), BG11-K (■) and $BG11_0$-K (♦) under light aerobic conditions for 5 days. Data represent mean ± SD of triplicate samples.

Glycogen accumulation in cells was measured after cells were adapted in BG11, $BG11_0$, BG11-K and $BG11_0$-K for 5 days. The highest glycogen accumulation was found in N- and K-deprived adapted cells throughout the adaptation time (Fig. 4.12). At the 3rd day of adaptation, *A. halophytica* cells adapted in N- and K-deprived BG11 showed the highest glycogen of 65.52 ± 0.78 % of cell dry weight, approximately 2.5 folds compared to that in BG11 (24.67 ± 1.97 % of cell dry weight) (Fig. 4.12). Interestingly, glycogen accumulation in K-deprived adapted cells was found higher than that in N-deprived adapted cells throughout the adaptation time (Fig. 4.12).

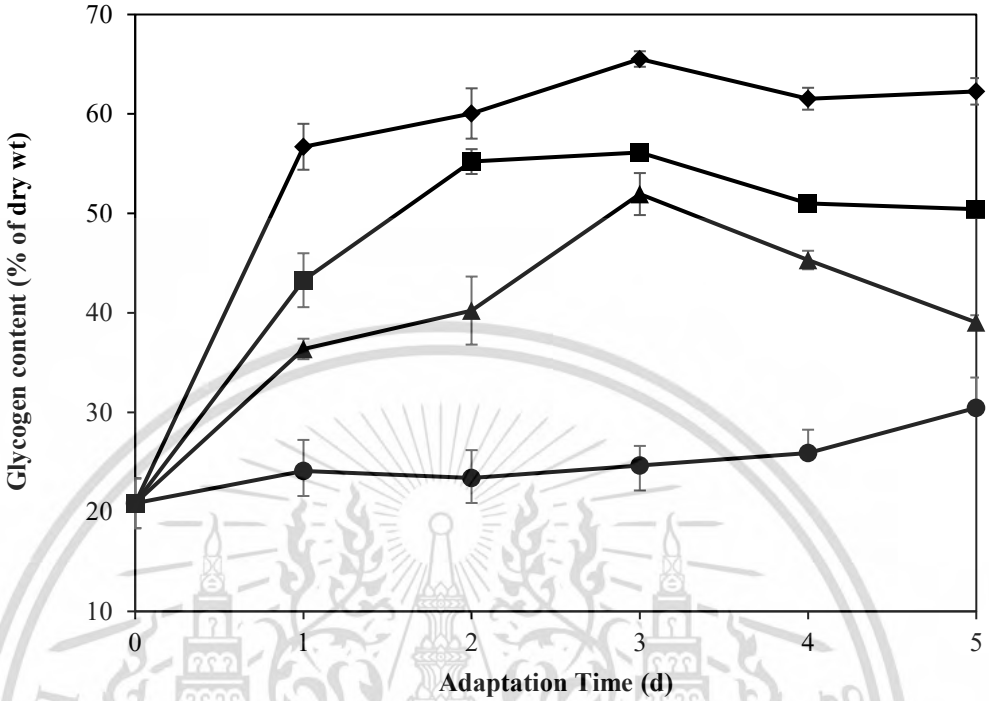

Fig. 4.12 Glycogen accumulation of *A. halophytica* cells adapted in BG11 (●), $BG11_0$ (▲), BG11-K (■) and $BG11_0$-K (♦) under light aerobic conditions for 5 days. Data represent mean ± SD of triplicate samples.

In this study, nitrogen and potassium deprivation promoted H_2 production by stimulating H_2ase activity (Fig. 4.9), resulting from the decrease of O_2 evolution rate (Fig. 4.10). In addition, the substrates for H_2ase were higher due to a decrease in the specific activity of pyruvate kinase (Fig. 4.11), and higher glycogen accumulation during adaptation period (Fig. 4.12). The highest H_2 production and H_2ase activity was found after 2 days of adaptation. *A. halophytica* adapted in BG11, $BG11_0$, BG11-K and $BG11_0$-K for 2 days were selected to analyze transcriptome based on RNA-seq in the next experiment.

4.3.3 RNA-seq based transcriptome analysis of genes involved in H_2 metabolism under N and K deprivation

Since both the highest H_2 production and H_2ase activity were found in cells adapted in all nutrient-deprived media investigated for 2 days (Fig. 4.8 and 4.9), cells adapted in BG11, $BG11_0$ and $BG11_0$-K for 2 days were selected to investigate gene expression in H_2 metabolism by RNA-seq based transcriptome analysis. The gene expression analysis between each treatment was performed. The significant up- or down-regulated gene numbers between groups were shown in Fig. 4.13. For example, the different 331 up-regulated and 331 down-regulated genes were found in cells adapted in BG11 compared to those adapted in BG11-K (Fig. 4.13). However, the lowest up-regulated and down-regulated gene numbers at 80 and 97 genes, respectively, were found in cells adapted in $BG11_0$ compared to $BG11_0$-K (Fig. 4.13). The gene expressions among these conditions were obviously different. Therefore, RNA isolated from cells adapted in $BG11_0$, BG11-K and $BG11_0$-K were selected for transcriptome analysis of gene expression in several pathways, especially pathways involved in H_2 metabolism.

Gene expression involved in H_2 metabolism of cells adapted in $BG11_0$, BG11-K and $BG11_0$-K was analyzed compared with that of control group (cells incubated in normal BG11) and expressed as $\log_2$ fold change. Gene expression in various pathways involved in H_2 metabolism including oxidative phosphorylation (Table 4.7), glycolysis/gluconeogenesis (Table 4.8), pentose phosphate pathway (Table 4.9), nitrogen metabolism (Table. 4.10), photosynthetic pathway (Table 4.11), and carbon dioxide fixation in photosynthetic pathway (Table 4.12) was shown.

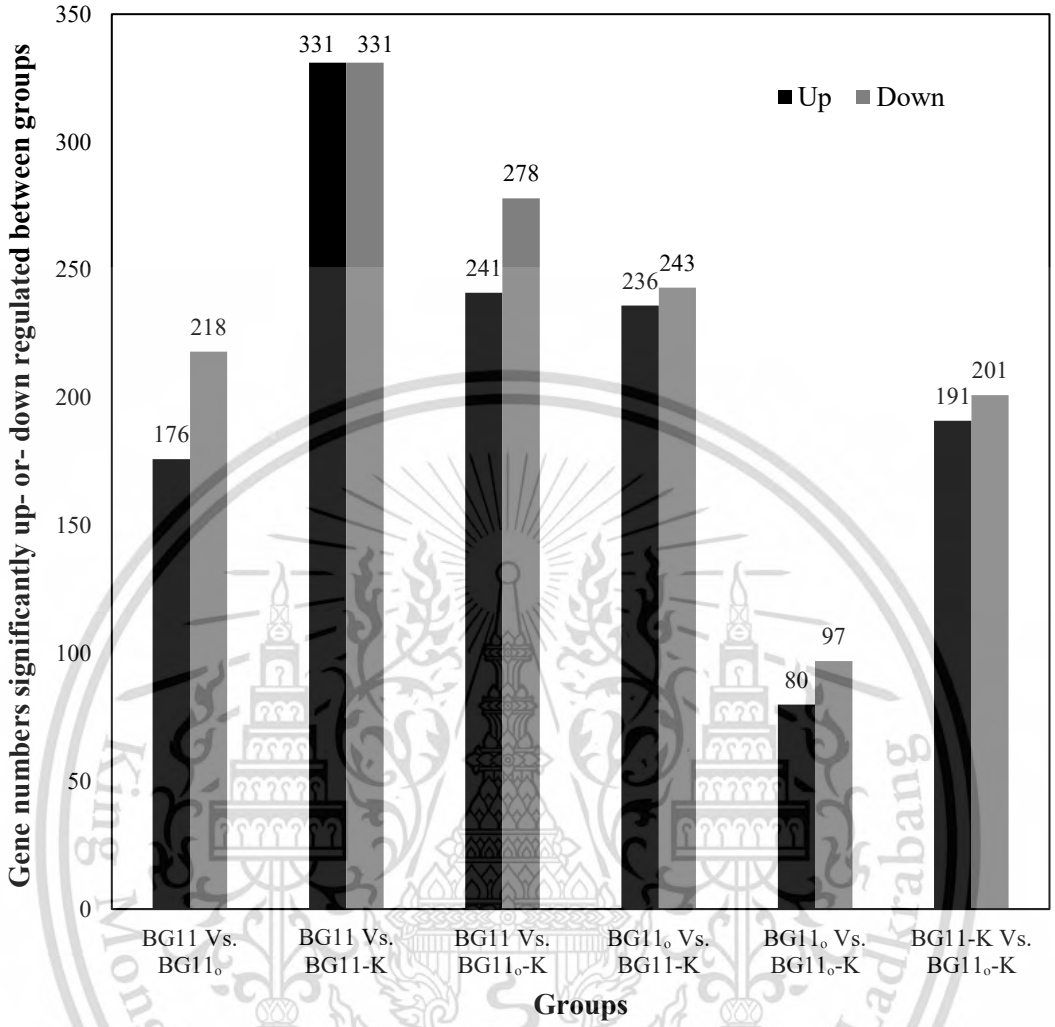

Fig. 4.13 Number of up- and down-regulated genes between treatment samples; *A. halophytica* adapted in BG11, $BG11_0$, BG11-K and $BG11_0$-K ($BG11_0$-K).

Table 4.7 Gene expression as log_2FC in oxidative phosphorylation pathway in cells adapted in $BG11_0$, BG11-K and $BG11_0$-K compared to those in BG11

KO	Gene	Gene Number	Description	Log_2FC		
				$BG11_0$	BG11-K	$BG11_0$-K
K02108	*atpB*	DN32570_c0_g1_i1	F-type H+-transporting ATPase subunit a	-2.03	-1.63	-3.33
K02108	*atpB*	DN21585_c2_g1_i1	F-type H+-transporting ATPase subunit a	2.36	1.06	2.37
K02109	*atpF*	DN29721_c0_g1_i1	F-type H+-transporting ATPase subunit b	-2.01	-1.82	-2.15
K02112	*atpD*	DN20840_c1_g2_i1	F-type H+-transporting ATPase subunit beta	1.24	1.41	0.64
K05572	*ndhA*	DN20948_c0_g1_i1	NAD(P)H-quinone oxidoreductase subunit 1	-1.39	-0.91	-0.38
K01507	*Ppa*	DN20904_c0_g1_i1	inorganic pyrophosphatase	-1.03	0.11	-1.46
K05577	*ndhF*	DN42209_c0_g1_i1	NAD(P)H-quinone oxidoreductase subunit 5	-1.60	-1.12	-0.72
K03885	*Ndh*	DN5046_c4_g2_i1	NADH dehydrogenase	0.60	2.18	1.36
K01507	*Ppa*	DN23654_c29_g1_i1	inorganic pyrophosphatase	0.09	-1.90	-1.72
K05575	*ndhD*	DN23066_c2_g1_i2	NAD(P)H-quinone oxidoreductase subunit 4	-0.54	-3.62	-0.91
K02109	*atpF*	DN4802_c0_g1_i1	F-type H+-transporting ATPase subunit b	-0.46	2.69	1.13
K05577	*ndhF*	DN32959_c1_g1_i1	NAD(P)H-quinone oxidoreductase subunit 5	-0.17	2.74	0.34

Table 4.7 (continued) Gene expression as log_2FC in oxidative phosphorylation pathway *in cells adapted in* $BG11_0$, BG11-K and $BG11_0$-K compared to those in BG11

KO	Gene	Gene Number	Description	Log_2FC		
				$BG11_0$	BG11-K	$BG11_0$-K
K02115	atpG	DN16393_c0_g1_i1	F-type H+-transporting ATPase subunit gamma	-1.02	-1.75	-1.17
K05585	ndhN	DN40850_c2_g1_i1	NAD(P)H-quinone oxidoreductase subunit N	0.67	1.31	1.05
K02274	coxA	DN9346_c1_g1_i1	cytochrome c oxidase subunit 1	-0.85	-0.45	-0.40
K00239	sdhA, frdA	DN23434_c0_g2_i1	succinate dehydrogenase / fumarate reductase, flavoprotein subunit	0.37	0.36	1.06
K00239	sdhA, frdA	DN7067_c0_g1_i1	succinate dehydrogenase / fumarate reductase, flavoprotein subunit	N/A	N/A	2.98
K00240	sdhB, frdB	DN23545_c0_g1_i1	succinate dehydrogenase / fumarate reductase, iron-sulfur subunit	N/A	N/A	2.50
K05587	hoxF	DN23851_c7_g11_i6	bidirectional [NiFe] hydrogenase diaphorase subunit	0.52	0.08	0.07
K02275	coxB, ctaC	DN4214_c0_g1_i1	cytochrome c oxidase subunit II	0.99	0.56	-0.25
K02276	coxC, ctaE	DN5836_c0_g1_i1	cytochrome c oxidase subunit III	-0.64	-2.29	-1.26

Table 4.8 Gene expression as log_2FC in glycolysis and gluconeogenesis pathways in cells adapted in $BG11_0$, BG11-K and $BG11_0$-K compared to those in BG11

KO	Gene	Gene ID	Description	Log2FC		
				$BG11_0$	BG11-K	$BG11_0$-K
K01623	ALDO	DN21032_c0_g1_i2	fructose-bisphosphate aldolase, class I	-3.19	-1.90	-3.02
K11532	*glpX-SEBP*	DN22857_c0_g1_i1	fructose-1,6-bisphosphatase II / sedoheptulose-1,7-bisphosphatase	-2.12	-1.40	-2.38
K01624	*fbaA*	DN37156_c0_g1_i1	fructose-bisphosphate aldolase, class II	-1.97	-2.25	-1.93
K00150	*gap2*	DN18528_c0_g1_i1	glyceraldehyde-3-phosphate dehydrogenase (NAD(P))	-1.33	-0.53	-1.02
K00927	*Pgk*	DN1313_c0_g1_i1	phosphoglycerate kinase	-1.35	-1.83	-1.55
K15634	*gpmB*	DN23959_c0_g1_i1	probable phosphoglycerate mutase	1.63	-0.15	1.03
K00162	*pdhB*	DN23548_c14_g2_i1	pyruvate dehydrogenase E1 component beta subunit	0.48	3.57	0.47
K00873	*Pyk*	DN21042_c0_g1_i1	pyruvate kinase	0.26	-1.77	-0.51
K00121	*adhC*	DN22558_c3_g1_i1	S-(hydroxymethyl)glutathione dehydrogenase / alcohol dehydrogenase	1.29	3.65	1.37

Table 4.9 Gene expression as log_2FC in pentose phosphate pathway in cells adapted in $BG11_0$, BG11-K and $BG11_0$-K compared to those in BG11

KO	Gene	Gene ID	Description	Log_2FC		
				$BG11_0$	BG11-K	$BG11_0$-K
K01623	-	DN21032_c0_g1_i2	fructose-bisphosphate aldolase, class I	-3.19	-1.87	-3.02
K11532	-	DN22857_c0_g1_i1	fructose-1,6-bisphosphatase II / sedoheptulose-1,7-bisphosphatase	-2.12	-1.40	-2.38
K01624	-	DN37156_c0_g1_i1	fructose-bisphosphate aldolase, class II	-1.97	-2.25	-1.93
K01783	-	DN23859_c0_g1_i1	ribulose-phosphate 3-epimerase	-1.90	-1.24	-2.15
K01810	-	DN23654_c25_g1_i1	glucose-6-phosphate isomerase	-0.75	-1.53	-0.90
K00036	*zwf*, G6PD	DN40892_c0_g1_i1	glucose-6-phosphate 1-dehydrogenase	0.01	0.22	0.44
K01057	*pgl*, PGLS	DN634_c2_g1_i1	6-phosphogluconolactonase	-0.31	-0.01	-0.33
K00033	*gnd*, PGD	DN20364_c1_g1_i1	6-phosphogluconate dehydrogenase	0.14	-0.09	-0.19
K01783	*rpe*, RPE	DN40719_c0_g1_i1	ribulose-phosphate 3-epimerase	1.23	0.53	1.57

Table 4.10 Gene expression as log_2FC in nitrogen metabolism in cells adapted in $BG11_0$, BG11-K and $BG11_0$-K compared to those in BG11

KO	Gene	Gene ID	Description	Log_2FC		
				$BG11_0$	BG11-K	$BG11_0$-K
K00266	-	DN32860_c1_g1_i1	glutamate synthase (NADPH/NADH) small chain	-0.10	-1.62	-0.95
K00284	-	DN23759_c15_g1_i1	glutamate synthase (ferredoxin)	0.14	2.50	0.50
K05601	-	DN23701_c6_g1_i1	hydroxylamine reductase	-1.50	0.08	-2.42
K00367	-	DN20240_c0_g2_i1	ferredoxin-nitrate reductase	-0.35	0.80	2.07
K00367	*narB*	DN24333_c0_g1_i1	ferredoxin-nitrate reductase	-0.94	-0.16	-0.90
K00366	*nirA*	DN22025_c0_g1_i1	ferredoxin-nitrite reductase	-1.76	-0.33	-1.77

Table 4.11 Gene expression as log_2FC in photosynthetic pathway in cells adapted in $BG11_0$, BG11-K and $BG11_0$-K compared to those in BG11

KO	Gene	Gene ID	Description		
			$BG11_0$	BG11-K	$BG11_0$-K
DN32745_c0_g1_i1	*psaF*	photosystem I subunit III	-2.59	-1.26	-2.64
DN21036_c0_g1_i1	*psbD*	photosystem II P680 reaction center D2 protein	-2.62	-2.03	-1.94
DN32570_c0_g1_i1	*atpB*	F-type H+-transporting ATPase subunit a	-2.03	-1.63	-3.33
DN21760_c0_g2_i1	*psbC*	photosystem II CP43 chlorophyll apoprotein	-2.29	-2.47	-2.13
DN634_c6_g1_i1	*petD*	cytochrome b6-f complex subunit 4	-1.76	-0.74	-1.31
DN21585_c2_g1_i1	*atpB*	F-type H+-transporting ATPase subunit a	2.36	1.06	2.37
DN23276_c0_g3_i1	*petA*	apocytochrome f	1.81	-0.55	1.09
DN23074_c0_g1_i1	*psaA*	photosystem I P700 chlorophyll *a* apoprotein A1	-1.71	-2.29	-2.29
DN29721_c0_g1_i1	*atpF*	F-type H+-transporting ATPase subunit b	-2.01	-1.82	-3.53
DN20840_c1_g2_i1	*atpD*	F-type H+-transporting ATPase subunit beta	1.24	1.41	0.64
DN28412_c0_g1_i1	*psbE*	photosystem II cytochrome b559 subunit alpha	1.11	0.30	0.91
DN23681_c4_g1_i1	*psbA*	photosystem II P680 reaction center D1 protein	1.48	1.03	0.96
DN23024_c0_g1_i1	*psaD*	photosystem I subunit II	-0.96	-1.40	-2.17
DN22812_c0_g1_i1	*psbB*	photosystem II CP47 chlorophyll apoprotein	-0.88	-1.32	-0.46

Table 4.11 (continued) Gene expression as log_2FC in photosynthetic pathway in cells adapted in $BG11_0$, BG11-K and $BG11_0$-K compared to those in BG11

KO	Gene	Gene ID	Description		
			$BG11_0$	BG11-K	$BG11_0$-K
DN20717_c3_g1_i1	*psbB*	photosystem II CP47 chlorophyll apoprotein	0.85	2.79	1.17
DN20725_c0_g1_i1	*petB*	cytochrome b6	0.70	1.67	0.83
DN4802_c0_g1_i1	*atpF*	F-type H+-transporting ATPase subunit b	-0.46	2.70	1.13
DN23865_c2_g2_i1	*psaF*	photosystem I subunit III	-0.39	1.75	-0.35
DN20717_c6_g1_i1	*psbT*	photosystem II PsbT protein	N/A	3.06	0.56
DN16393_c0_g1_i1	*atpG*	F-type H+-transporting ATPase subunit gamma	-1.02	-1.75	-1.17
DN13991_c1_g1_i1	*petC*	cytochrome b6-f complex iron-sulfur subunit	-0.47	-1.21	-0.65
DN22668_c0_g1_i1	*psaA*	photosystem I P700 chlorophyll *a* apoprotein A1	-0.63	1.42	-0.06
DN171_c0_g1_i1	*psbI*	photosystem II PsbI protein	0.71	1.92	0.63
DN28374_c0_g1_i1	*psb27*	photosystem II Psb27 protein	-0.30	0.54	-1.38
DN20259_c0_g1_i1	*psbM*	photosystem II PsbM protein	-0.11	-0.75	-1.21
DN36953_c1_g1_i1	*cpcB*	phycocyanin beta chain	-2.91	-.098	-3.50
DN38181_c0_g1_i1	*cpcB*	phycocyanin beta chain	-3.41	-1.31	-3.68

Table 4.11 (continued) Gene expression as log_2FC in photosynthetic pathway in cells adapted in $BG11_0$, BG11-K and $BG11_0$-K compared to those in BG11

KO	Gene	Gene ID	Description		
			$BG11_0$	BG11-K	$BG11_0$-K
DN41449_c0_g1_i1	*cpcC*	phycocyanin-associated rod linker protein	-2.27	-1.65	-3.01
DN21264_c0_g1_i1	*cpcG*	phycobilisome rod-core linker protein	-2.56	-1.41	-2.37
DN23086_c1_g2_i1	*apcC*	phycobilisome core linker protein	-2.06	-0.35	-2.00
DN20787_c3_g1_i1	*apcF*	phycobilisome core component	-1.80	-0.44	-2.22
DN20194_c0_g2_i1	*cpcE*	phycocyanobilin lyase subunit alpha	-1.19	-0.89	-1.43
DN36690_c4_g1_i1	*cpcC*	phycocyanin-associated rod linker protein	0.19	1.64	-0.01
DN40669_c0_g1_i1	*apcA*	allophycocyanin alpha subunit	0.50	1.77	0.37
DN23184_c0_g1_i1	*apcE*	phycobilisome core-membrane linker protein	-0.30	-1.48	-1.48
DN22132_c0_g1_i1	*apcE*	phycobilisome core-membrane linker protein	-0.70	-1.65	-3.01

Table 4.12 Gene expression as log_2FC in CO_2 fixation pathway in cells adapted in $BG11_0$, BG11-K and $BG11_0$-K compared to those in BG11

KO	Gene	Gene ID	Description	Log_2FC		
				$BG11_0$	BG11-K	$BG11_0$-K
K01810	*pgi*	DN23654_c25_g1_i1	glucose-6-phosphate isomerase	-0.75	-1.53	-0.90
K01895	*Acs*	DN23810_c26_g1_i1	acetyl-CoA synthetase	-0.07	2.38	1.03
K04072	*adhE*	DN19817_c0_g1_i1	acetaldehyde dehydrogenase / alcohol dehydrogenase	-0.15	1.35	0.22
K00121	*adhC*	DN17107_c0_g1_i1	S-(hydroxymethyl)glutathione dehydrogenase / alcohol dehydrogenase	0.04	3.00	0.25
K00134	*gapA*	DN22881_c0_g2_i1	glyceraldehyde 3-phosphate dehydrogenase	0.04	0.4	0.07
K15634	*gpmB*	DN37532_c0_g1_i1	probable phosphoglycerate mutase	0.38	-1.12	1.02
K01895	*Acs*	DN42961_c0_g1_i1	acetyl-CoA synthetase	-0.37	-0.64	-1.06
K15634	*gpmB*	DN22668_c21_g1_i1	probable phosphoglycerate mutase	-0.13	0.75	1.13
K00382	*pdhD*	DN23834_c40_g1_i1	dihydrolipoamide dehydrogenase	-0.20	-0.24	-1.13

Table 4.12 (continued) Gene expression as log_2FC in CO_2 fixation pathway in cells adapted in $BG11_0$, BG11-K and $BG11_0$-K compared to those in BG11

KO	Gene	Gene ID	Description	Log2foldchange		
				$BG11_0$	BG11-K	$BG11_0$-K
Glycogen Biosynthesis						
K00975	*glgC*	DN19812_c3_g1_i1	glucose-1-phosphate adenylyltransferase	-0.03	1.33	1.24
K00703	*glgA*	DN23494_c3_g1_i1	starch synthase	0.49	0.08	0.66
K00700	*glgB*	DN20737_c1_g2_i1	1,4-alpha-glucan branching enzyme	1.69	4.37	1.29
Glycogen Degradation						
K00688	*glgP*	DN25524_c0_g1_i1	glycogen phosphorylase	3.17	0.62	1.39
K01835	*Pgm*	DN23834_c30_g2_i1	Phosphoglucomutase	-0.12	-0.20	-0.57

In the photosynthetic pathway, most genes encoding allophycocyanin and phycobilisome in N and K deprivation were expressed as $\log_2$FC $\leq$ -0.1; however, ApcA, allophycocyanin alpha subunit encoded by *apcA* (*Halothece* sp. PCC 7418) was upregulated as $\log_2$FC of 0.5 and 1.77 in N and K deprivation, respectively (Table 4.11). Different gene expressions under those deprivations showed the same direction, most of them were upregulated by $\log_2$FC $\leq$ 0.54. However, D1 protein encoded by *psbA* (*Synechococcus* sp. ATCC 27144) was upregulated as $\log_2$FC of 1.48 and 1.03 in N and K deprivation, respectively. Despite, the CP47 and CP43 chlorophyll apoproteins and P680 reaction center D2 protein encoded by *psbB* (*Halothece* sp. PCC 7418), *psbC* (*Halothece* sp. PCC 7418), *psbD* (*Halothece* sp. PCC 7418) were downregulated (Table 4.11).

Under those starved conditions, genes involved in Calvin-Basham-Benson (CBB) cycle were found downregulated. Ribulose-bisphosphate carboxylase encoded by *rbcL* (*Cyanothece* sp. PCC 7424) was significantly downregulated as $\log_2$FC of -2.46 and -1.83 in N and K deprivation, respectively. All genes in this pathway were differently expressed by $\log_2$FC $\leq$ -0.53. Likewise, several genes involved in glycolysis were downregulated under those starved conditions. However, pyruvate kinase encoded by *pyk* (*Halothece* sp. PCC 7418) was expressed differentially between two conditions, as $\log_2$FC of 0.26 and -1.77 in N and K deprivation, respectively (Table 4.8).

Interestingly, the result showed that most genes in glycogen biosynthesis were upregulated. For example, 1,4-alpha-glucan branching enzyme encoded by *glgB* (*Halothece* sp. PCC 7418) was upregulated as $\log_2$FC of 1.69 and 4.37 in N and K deprivation, respectively. In OPP, some genes were upregulated under N and K deprivations, for example, *rpe* (*Halothece* sp. PCC 7418) encoding ribulose-phosphate 3-epimerase was upregulated of 1.23 and 0.52 of $\log_2$FC, respectively. In terms of nitrogen assimilation, as expected, ferredoxin-nitrite reductase encoded by *nirA* (*Halothece* sp. PCC 7418) and *nirB* (*Synechocystis* sp. PCC 6803) were upregulated as $\log_2$FC of -0.94 and -1.76, respectively, under N-deprived condition but no differences of gene expression were found compared with that under K-deprived condition (Table 4.10).

CHAPTER 5

DISCUSSION

5.1 Effect of reducing substances on H_2 production by *A. halophytica*

5.1.1 Effect of reducing sugars on H_2 production

Previous studies showed that *A. halophytica* induced higher H_2 production under nitrogen starvation (Taikhao et al., 2013; 2015). One possible way to enhance H_2 production by *A. halophytica* is an increase in electrons or protons, which are substrates of H_2ase. The reducing substances such as reducing sugars and reducing agents might provide electrons to H_2ase. Our result showed that *A. halophytica* cells incubated in $BG11_0$ containing 0.189 mmol C-atom L^{-1} or 0.032 mM glucose gave the highest H_2 production rate with 55.80 ± 0.50 μmol H_2 g dry $weight^{-1}$ h^{-1} (Fig. 4.1). Other types of reducing sugars, fructose, maltose, and lactose, provided lower H_2 production by *A. halophytica* than glucose. It could be suggested that glucose at 0.189 mmol C-atom L^{-1} or 0.032 mM prefers electron transfer towards H_2ase to generate H_2 in *A. halophytica* than glucose at other concentrations or than other types of reducing sugars. Glucose was also examined as electron donor for H_2ase in other unicellular cyanobacteria such as *Synechocystis* sp. PCC 6803 and *Synechococcus* sp. strain Miami BG 04351 (Baebprasert et al., 2010; Luo and Mitsui, 1994). On the other hand, filamentous cyanobacteria prefer fructose as a favorite sugar source to donor electrons for H_2 production (Taikhao and Phunpruch, 2017; Reddy et al., 1996; Chen et al., 2008). Our study suggested that glucose is easily metabolized in unicellular cyanobacteria including *A. halophytica*. Glucose is metabolized, leading to an increased level of reduced NADH or NADPH. Consequently, electron concentration available for H_2 production increased (Cournac et al., 2004). However, at high glucose concentrations, cyanobacteria may change their metabolism to synthesize glycogen and/or need higher energy to excrete surplus glucose out of cells (Baebprasert et al., 2010; Taikhao et al., 2013).

5.1.2 Effect of reducing agents on H_2 production

From the primary screening of ten reducing agents enhancing H_2 production by the nitrogen-deprived *A. halophytica* cells, four types of reducing agents, β-mercaptoethanol, dithiothreitol, L-cysteine and sodium sulfide, showed a significant increase in H_2 production rate under dark anaerobic conditions (Table 4.2). In addition, an increase in H_2 production depends on the concentration of reducing agents. Among four types of reducing agents, sodium sulfide at 50 mM provided the highest H_2 production by *A. halophytica* (Fig. 4.4). It has been reported that sodium sulfide could reduce O_2 evolution by 30% in *Synechococcus* UTEX 625 (Espie et al., 1989). When O_2 production decreased, H_2ase activity was less inactivated. As a result, H_2 production was higher stimulated. The previous study also indicated that both dithiothreitol and L-cysteine provided higher H_2 production in bacterial cells since they acted as electron donors to plastocyanin and stimulated O_2 absorption (Krasnovsky et al., 1980). Besides, methyl viologen and sodium dithionite at concentration of 0.1 mM enhanced H_2 production rate by N-deprived cells of *A. halophytica* (Table 4.2). Commonly, dithionite-reduced methyl viologen is usually used for an assay of H_2ase activity in cyanobacteria. It has been previously shown that methyl viologen and sodium dithionite could promote H_2 production rate in *A. siamensis* TISTR 8012 incubated in $BG11_0$-S (Taikhao and Phunpruch, 2017).

Our results also examined that H_2 production was strongly inhibited in *A. halophytica* cells treated with 10 mM acidic reducing agents i.e., ascorbic acid, formic acid, and oxalic acid (Fig. 4.1). These acidic reducing agents with high concentrations provided a low medium pH which was between 1.8-3.6 (Table 4.3). The low pH obtained from these acids causes cell toxicity by destroying protein and enzyme function and finally resulting in a cell death. The decreased H_2 production was due to a decrease in biomass concentration and H_2ase activity. However, ascorbic acid and formic acid at low concentration of 0.1 mM could induce H_2 production compared with cells treated without any supplementation. It has been reported that ascorbate could be used as electron donor for *in vitro* H_2 production in cyanobacterium *Thermosynechococcus elongatus* (Iwuchukwu et al., 2010).

To investigate how H_2 production by *A. halophytica* enlarged by selected reducing agents, H_2ase activity coupled with O_2 generation rate was determined in N-deprived cells after dark anoxic incubation for 24 h. As expected, all reducing agents investigated reduced the O_2 generation rate of *A. halophytica*, thus increasing H_2ase activity (Table 4.4). An increase in H_2ase activity caused higher H_2 production (Table 4.4). Interestingly, *A. halophytica* treated with 50 mM sodium sulfide showed the highest H_2ase activity with 303.45 ± 3.15 μmolH_2 g dry wt^{-1} min^{-1} and the lowest O_2 generation rate with 3.59 ± 0.31 μmolO_2 g dry wt^{-1} h^{-1} (Table 4.4). It could be explained that sodium sulfide was suggested to be a favorite reducing agent for providing electrons towards H_2ase in *A. halophytica.* Electrons from sulfide have been suggested to transfer to an electron transport chain via photosystem I in cyanobacterium *Oscillatoria limetica* (Belkin and Padan, 1978). Therefore, the increased electrons were transported to H_2ase for higher H_2 production. In addition, sodium sulfide can react with water and CO_2 and generate H_2S as a product. The reaction is shown as follows: $Na_2S + H_2O + CO_2 \rightarrow Na_2CO_3 + H_2S$. The produced H_2S is considered as an electron source for H_2ase enzyme (Luo and Mitsui, 1996) giving a large amount of electrons in system and can cause an irreversible damage to PSII in most cyanobacteria (Cohen et al., 1986), giving a low level of O_2. Together, sodium sulfide can reduce O_2 evolution and activate H_2ase activity in *A. halophytica*. It has been previously shown that sodium sulfide at high concentration (300 μM) could reduce 30% of O_2 evolution rate and Chl *a* fluorescence yield in *Synechococcus leopoliensis*, owing to the effect of H_2S (Espie et al., 1989). In addition, H_2 production was found increasingly in N-deprived cells of *Synechococcus* sp. Miami BG043511 with 5 mM sodium sulfide (Luo and Mitsui, 1996). Since *A. halophytica* showed an ability to use sulfide as electron donor in CO_2 photoassimilation via photosystem I-driven anoxygenic conditions (Garlick et al., 1977), it could be convinced that *A. halophytica* might use inorganic sulfide to produce H_2 under stress conditions.

Apart from sodium sulfide, dithiothreitol, L-cysteine and β-mercaptoethanol could induce H_2ase activity (Table 4.2). It was probably demonstrated that dithiothreitol can react with O_2 as a following reaction: $2DTT + O_2 \rightarrow 2oxyDTT + 2H_2O$ (Kachur et al., 1997). This reaction causes O_2 consumption and thus reduces the level of O_2 in a system and

finally results in an enhancement of H_2 production. Moreover, the thiol group in β-mercaptoethanol and dithiothreitol structure which is one (thiol) and two (dithiol), respectively, might be the reason why cells incubated in dithiothreitol could provide higher H_2 production compared with that treated with β-mercaptoethanol with at same concentration. The active site of [NiFe]-H_2ase of cyanobacteria contains cysteine in N- and C-terminal conserved motifs (Schmitz and Bothe, 1996; Volbeda et al., 1996). L-cysteine could also be the bioactive agent and mediator for H_2 fermentation in bacteria (Doong and Schink, 2002). β-mercaptoethanol is also a reducing agent and is often used interchangeably with dithiothreitol. In *Synechocystis* sp. PCC6803, β-mercaptoethanol could induce H_2ase activity under sulfur deprivation (Baebprasert et al., 2010). It was suggested that the type of reducing agent stimulating H_2 production was dependent on the cyanobacterial species.

Cell toxicity of *A. halophytica* treated with these reducing agents was determined by IC_{50} measurement. β-mercaptoethanol and sodium sulfide with IC_{50} of above 100 mM seem to provide less toxicity to cells than dithiothreitol and L-cysteine with IC_{50} of 18.12 ± 2.07 and 76.94 ± 4.21 mM, respectively (Fig. 4.5). As a result, it could be suggested that cells treated with higher concentrations of these reductants showed higher cell toxicity than those with lower concentrations. However, cells treated with β-mercaptoethanol and sodium dithionite provided IC_{50} measurement with higher than 100 mM which was the highest concentration in this study. Our results conclude that sodium sulfide is an effective reducing agent for H_2 production by *A. halophytica* since it functions not only increasing in H_2ase activity but also providing low cell toxicity.

5.2 Redox partners for [NiFe]-H_2ase enzyme

In cyanobacteria, NADH and NADPH but not reduced ferredoxin are believed to act as redox partners for [NiFe]-H_2ase (Dutta and Vermaas, 2016). However, it has been previously reported that reduced ferredoxin/flavodoxin and NAD(P)H possibly donor electrons to [NiFe]-H_2ase in *Synechocystis* sp. PCC6803 (Gutekunst et al., 2014). In this study, *in vitro* H_2ase activity was measured in cell-free extract of *A. halophytica.* The result

showed that ferredoxin at all investigated concentrations (1.5 μM-1.5 mM) reduced by 2 mM sodium dithionite could promote *in vitro* H_2ase activity by inducing electrons towards [NiFe]-H_2ase whereas in the presence of only 2 mM dithionite, *in vitro* H_2ase activity could not be detected (Table 4.5). The results indicated that ferredoxin reduced by sodium dithionite is a redox partner for [NiFe]-H_2ase in *A. halophytica.* This result was agreed with previous studies reported that ferredoxin could transfer electrons towards [NiFe]-H_2ase of *Synechocystis* sp. PCC6803 (Gutekunst et al., 2014) and *Methanosarcina barkeri* (Meuer et al., 1999).

Our result also showed that NADH and NADPH with high concentrations (150 μM and 1.5 mM) could increase H_2 production *in vitro* by providing electrons towards [NiFe]-H_2ase in *A. halophytica* (Table 4.5). NADH and NADPH at low concentrations was not enough to transport electrons for activating H_2ase activity (Table 4.5). These results indicated that both NADH and NADPH can also act as electron donors for [NiFe]-H_2ase in *A. halophytica.* NADH and NADPH generated from glycolysis and pentose phosphate pathway, respectively, have been reported to be redox partners for bidirectional hydrogenase in *Synechocystis* sp. PCC6803 (Cournac et al., 2004; Germer et al., 2009; Gutekunst et al., 2014). In conclusion, NAD(P)H and ferredoxin play an important role as electron partners for [NiFe]-H_2ase enzyme for H_2 evolution in *A. halophytica*. However, the preference of electron partners for [NiFe]-H_2ase is suggested to be ferredoxin since ferredoxin at low concentration (only 1.5 μM) could activate [NiFe]-H_2ase.

It was previously reported that nitrogen deprivation induced H_2 production by *A. halophytica* during dark anaerobic conditions (Taikhao et al., 2013; Taikhao et al., 2015). Under nitrogen deprivation, glycogen was accumulated with an increase of 30 % in *A. halophytica* (Taikhao et al., 2015). When cells entered a dark anaerobic conditions, cells degraded accumulated glycogen into glucose, a substrate for electron donor and fermentation of H_2 (Ananyev et al., 2008). Glucose obtained during dark anaerobic conditions provided NADPH via oxidative pentose phosphate pathway and NADH via glycolytic pathway (Kumaraswamy et al., 2013). Therefore, nitrogen deprivation enhances both NADH and NADPH providing electrons to activate [NiFe]-H_2ase activity and finally enhancing H_2 production under dark anaerobic conditions. In this study, NADH, NADPH and

reduced ferredoxin were found as the redox partners of [NiFe]-H_2ase in *A. halophytica*. In *Synechocystis* sp. PCC6803, H_2ase activity of intact cells was stimulated by the addition of NADH and ferredoxin compared with that without addition (Baebprasert et al., 2010). Furthermore, reduced ferredoxin has been previously shown as a redox partner for H_2ase enzyme (Gutekunst et al., 2014).

5.3 Nutrient deprivation on H_2 production and H_2 metabolism in *A. halophytica*

Cyanobacteria are oxygenic microorganisms that can produce H_2 under dark anaerobic conditions, especially when they were incubated in nutrient-deprived medium (Ananyev et al., 2008; Baebprasert et al., 2010; Min and Sherman, 2010). In previous studies, the unicellular halotolerant cyanobacterium *A. halophytica* showed the ability to produce H_2 under nitrogen starvation (Taikhao et al., 2013; Taikhao et al., 2015; Phunpruch et al., 2016). Until now, H_2 production is known to be catalyzed by bidirectional [NiFe]-H_2ase (Phunpruch et al., 2016). This study demonstrated that apart from nitrogen starvation, potassium deprivation could significantly enhance H_2 production by *A. halophytica* under dark anaerobic conditions compared with normal conditions (Fig. 4.7). Under potassium deprivation, a limitation of $NaNO_3$ concentration available in BG11 induced both H_2ase activity and H_2 production (Table 4.6). Similarly, under nitrogen deprivation, a limitation of KCl concentration in BG11 induced both H_2ase activity and H_2 production (Table 4.6). Previous study showed that the presence of potassium in medium reduced H_2ase activity in *Synechocystis* sp. PCC6803 under dark anaerobic conditions. It might be due to the competitive utilization of limited NADPH for H_2 and organic acid production (Ueda et al., 2016). Moreover, there has been suggested that potassium deprivation decreased PSII activity, resulting in a low production of O_2, the inhibitor of H_2ase enzyme. In addition, potassium deprivation increased the degradation of starch in green alga *Scenedesmus obliquus* (Papazi et al., 2014). In N deprivation, H_2ase activity increased in *Anabaena siamensis* TISTR8012 resulting in an increased H_2 production (Taikhao and Phunpruch, 2017). On the other hand, phosphorus and sulfur deprivation could not promote H_2 production by *A. halophytica.* It has been reported that potassium, sulfur and phosphate deprivation might have various important effects on nucleic acids and protein synthesis

and many metabolisms in cells such as photosynthesis, cellular respiration and H_2 metabolism (Warichanan and Phunpruch, 2019). Moreover, starvation combination between nitrogen and sulfur could enhance H_2 production in *Synechocystis* sp. PCC6803 (Baebprasert et al., 2010) and *Arthrospira* sp. PCC8005 (Raksajit et al., 2012).

5.3.1 N- and K- deprivation for H_2 production by *A. halophytica*

It is well known that cyanobacteria could produce H_2 effectively under dark anaerobic conditions, especially under nutrient deprivation (Ananyev et al., 2008; Baebprasert et al., 2010; Min and Sherman, 2010). In *A. halophytica*, H_2 production could be promoted essentially in cells incubated in $BG11_0$ (Taikhao et al., 2013; Pansook et al., 2016; Phunpruch et al., 2016; Pansook et al., 2019). This study showed that apart from nitrogen deprivation, potassium deprivation also enhanced H_2 production by *A. halophytica* under dark anaerobic conditions (Fig. 4.7). An increased H_2 production was due to a higher H_2ase activity (Fig. 4.9), resulting from the reduction of O_2 photoevolution rate (Fig. 4.10), the specific activity of pyruvate kinase (Fig. 4.11) and an increase in glycogen accumulation (Fig. 4.12).

In this study, H_2 production by *A. halophytica* was performed by the two-stage regime. Firstly, cells grown in abundant BG11 medium for 7 days were incubated in nutrient-deprived medium for glycogen accumulation under light: dark (18: 6h) cycle aerobic conditions. Secondly, H_2 production was induced under dark anaerobic conditions, where O_2 was at the lowest level and could not interrupt H_2ase activity. H_2 production was measured by GC-MS in this stage. According to Fig. 4.7, H_2 production rate by *A. halophytica* dramatically increased during the first 8 h of incubation and reached the highest H_2 production at 24 h. The highest H_2 production rate was found in K-deprived cells. The result could be described that potassium deprivation could increase H_2ase activity, glycogen accumulation, and O_2 respiration, which are the relevant effects on H_2 production. In N-free cells, *A. halophytica* produced H_2 highly because of an increase in glycogen accumulation, oxygen evolution, and H_2ase activity, and a decrease in nitrate assimilation (Phunpruch et al., 2016; Taikhao et al., 2013).

In *A. halophytica*, no uptake hydrogenase genes were found, suggesting that H_2 metabolism is involved by only bidirectional [NiFe]-H_2ase (Phunpruch et al., 2016). To find out the association between N- and K-free cells of H_2 production, H_2 production coupling with H_2ase activity was determined under a limitation of K and N concentrations in N- and K-free cells, respectively (Table 4.6). The result showed that no significant differences of H_2 production were found in the N-limited K-deprived cells and only K-deprived cells due to the same level of H_2ase activities. On the other hand, the K-limited L-deprived cells (2.23 mM KCl) could generate higher H_2 than those in N-free cells due to the higher H_2ase activity (Table 4.6). Outstandingly, the highest H_2 production and H_2ase activity was found in both N- and K-deprived cells (Table 4.6). These results suggested the certain role of N and K affecting H_2 production and H_2ase activity of *A. halophytica*.

[NiFe]-H_2ase in cyanobacteria is usually sensitive to O_2 (McIntosh et al., 2011). In this study, the O_2 evolution rate via photoevolution in N-, K- and NK-free cells was less than that in normal cells (Fig. 4.10), suggesting the lower expression of genes encoding phycobilisome, phycocyanin and other photosynthetic genes under N and K deprivation. Under N deprivation, the previous study showed a downregulation of many genes involved in photosynthetic pathways in *Synechococcus elongatus* PCC7942 (Choi et al., 2016). In K deprivation, photosynthetic pigments and activity decreased in *Anabaena torulosa* (Alahari and Apte, 1998) and *Synechocystis* sp. PCC6803 (Nanatani et al., 2015). This study also revealed that several genes encoding cytochrome *c* oxidase and NADH dehydrogenase were upregulated under both N and K starvation (Fig. 5.1). It could be suggested that respiratory mechanism could be increased in *A. halophytica* under N and K starvation. However, expression of genes encoding respiratory electron transport did not show significant differences under N deprivation in *Synechococcus elongatus* PCC7942 (Choi et al., 2016).

As previously described, H_2 production was increased in the two-stage strategy under nutrient-deprived dark anaerobic conditions. The former stage was crucial since cells incubated in deprived media would be expected to accumulate higher glycogen level, the main substrate for H_2ase in *A. halophytica* (Taikhao et al., 2015). Thus, a period of adaptation time is one factor that can increase the performance of H_2 production. H_2

production was found to be rising rapidly in the early 48 h and reached the highest at 48 h in NK-cells (Fig. 4.8). H_2ase activity is related to H_2 production. The highest H_2ase activity was found in cells incubated under N and K deprivation for 48 h as well (Fig. 4.9). Throughout the adaptation time, N- and K-deprived cells showed both higher H_2 production and H_2ase activity than normal cells (Fig. 4.8, Fig. 4.9). To explain the result, glycogen in these cells during various adaptation times was measured. Glycogen content was accumulated increasingly when cells were incubated in nutrient-deprived media compared with that in cells incubated in BG11 (Fig. 4.12). The highest glycogen content was found in NK-free cells during adaptation times and glycogen accumulated in K-free cells was higher than that in N-free cells (Fig. 4.12). Likewise, *glgA* (*Halothece* sp. PCC7418) and *glgB* (*Halothece* sp. PCC7418) encoding starch synthase and 1,4-alpha-glucan branching enzyme, respectively, were upregulated under both N and K deprivation (Table 4.12). The result suggested that a lack of N or/and K in medium could cause an increase in glycogen content. With higher glycogen content, cells could also produce higher H_2 (Taikhao et al., 2015).

Under dark anaerobic conditions, cyanobacteria induce H_2 production via [NiFe] H_2ase reduced by NAD(P)H (Gutekunst et al., 2014) and reduced ferredoxin (Gutekunst et al., 2014; Meuer et al., 1999). The main sources of reductants for H_2 generation under dark anaerobic conditions were NADH and reduced ferredoxin from glycolysis and NADPH from catabolism of accumulated glycogen, provided by oxidative pentose phosphate (OPP) pathway (Kumaraswamy et al., 2013). In glycolytic pathway, as a result, the specific activity of pyruvate kinase of cell incubated under K deprivation was decreased (Fig. 4.11). The specific activity of pyruvate kinase in K- and NK- free cells was less than that in normal and N-free cells throughout the period of adaptation time. Pyruvate kinase was known to be induced by K^+, it would be less activated when K was absent (Oria-Hernández et al., 2005). Therefore, enzyme regulation might control the flux of glycogen catabolism in *A. halophytica*. Furthermore, GAPDH-2 has a major role in CBB cycle using NADPH as preferred electron donor to reduce 1,3-bis-phosphoglycerate to GAP (Koksharova et al., 1998). Under K deprivation, *pyk* (*Halothece* sp. PCC7418) and *gap2* (*Synechocystis* sp. PCC6803) encoding PK and GAPDH-2, respectively, were downregulated (Fig. 5.1).

Consequently, in K-free cells, it could be suggested that upper-glycolytic metabolites could be excess, especially glucose-6-phophate (G6P). G6P is a broken-down molecule of glycogen, and the branching point between glycolysis and OPP pathway. In less activated in both PK and GADPH-2, it could be convinced that G6P preferably flown up to OPP pathway generating more NADPH with using less NADPH in CBB and glycolysis. Therefore, OPP pathway could be favorite for H_2 production in K-deprived cells of *A. halophytica* under dark anaerobic conditions. Previous studies showed that *Escherichia coli* mutant with *pykF* knock out could provide the higher activity of enzymes in OPP but decreased the activity of glycolytic enzymes comparing with those in wild-type cells (Siddiquee et al., 2004). Moreover, low activity of pyruvate kinase could promote the respiration in yeast cells (Grüning et al., 2011).

It has been reported that H_2 could be induced in N-free cells of *Synechocystis* sp. PCC6803 because expression of genes involving glycogen catabolism were increased (Osanai et al., 2006). Moreover, several genes in OPP pathway were extremely upregulated when *Synechocystis* sp. PCC 6803 was incubated in N-free medium (Osanai et al., 2006), which could be described that G6P was likely degraded through OPP pathway. This could be mentioned that glycogen catabolism could prefer to be degraded via OPP pathway producing higher NAD(P)H level compared to that via glycolytic pathway in cells incubated in both N- and K-deprived conditions. Therefore, the effects of both N and K deprivation on H_2 production could have coordinated each other and accelerated the production in *A. halophytica* under dark anaerobic conditions.

The schematic representation of H_2 production by *A. halophytica* incubated in BG11, $BG11_0$, BG11-K and $BG11_0$-K under dark anaerobic conditions is shown in Fig. 5.2 Reductants involved in H_2 production by cyanobacteria, NADH and NADPH, can be generated mainly by the glycolytic and OPP pathways (Kumaraswamy et al., 2013). In the former pathway, one mole of G6P can provide 2 NADH whereas NADPH can be produced of 7 molecules by the same mole of G6P via OPP pathway (Kumaraswamy et al., 2013). One mole NAD(P)H can be oxidized by H_2ase to provide one mole of H_2. Thus, 7 NADPH from OPP pathway could produce higher H_2 compared with that via glycolytic pathway (7 vs. 2 of H_2). In plentiful condition (Fig. 5.2b +NK), normal cells were likely to generate

organic acids compared with K-deprived cells in *Synechocystis* sp. PCC 6803 (Ueda et al., 2016) and NAD(P)H was likely used for nitrate assimilation compared with N-deprived cells in *A. halophytica* (Phunpruch et al., 2016). Therefore, NAD(P)H from normal cells would be used in organic acid production and nitrate assimilation pathway rather than H_2 production. In N-deprived cells, it could be suggested that glycogen catabolism can be occurred via both OPP and glycolytic pathways in *Synechocystis* sp. PCC6803 (Osanai et al., 2006). The activity of pyruvate kinase encoding from *pyk* (*Halothece* sp. PCC7418) in K-free cells was lower than that in normal cells (Fig. 4.11; Fig. 5.1). Consequently, glycogen was mainly degraded via OPP pathway and provided more NADPH for H_2 production. In the combination of both N and K insufficiency in cells, the effects from both deprivations would cooperate with each other to provide higher level of H_2.

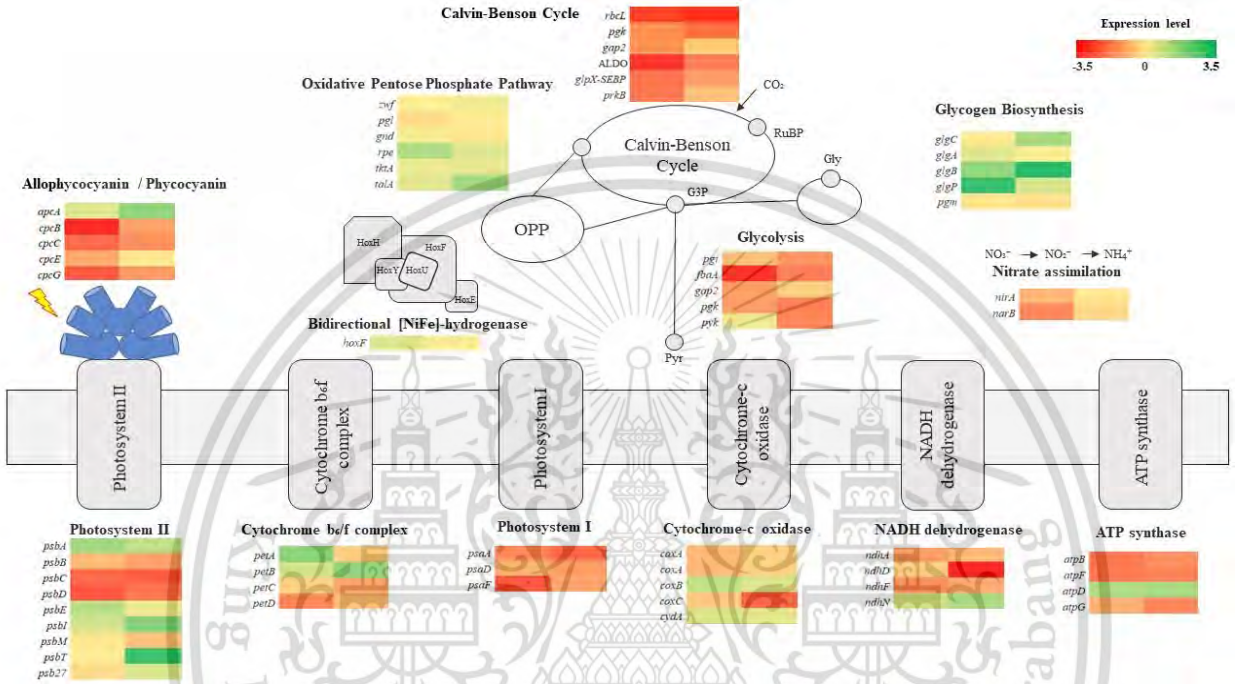

Fig. 5.1 Transcriptional level of genes involving photosynthetic pathway, carbon assimilation such as Calvin-Benson cycle, glycolysis, oxidative pentose phosphate pathway, and nitrate assimilation in *A. halophytica.* The first column shows differences of gene expression between N-deprived adapted cells and normal cells and the second column shows differences of gene expression between K-deprived adapted cells and normal cells. Log_2 FC shows heat maps with gene names, demonstrating different gene expression in many metabolic pathways involving in H_2 production. The metabolic pathways are photosynthesis, oxidative pentose phosphate, glycolytic pathway, glycogen biosynthesis, and nitrate assimilation. Abbreviations: oxidative pentose phosphate pathway, OPP; glucose-3-phosphate, G3P; glycogen, gly; pyruvate, pyr; [NiFe]-bidirectional H_2ase enzyme subunit, HoxEFUY

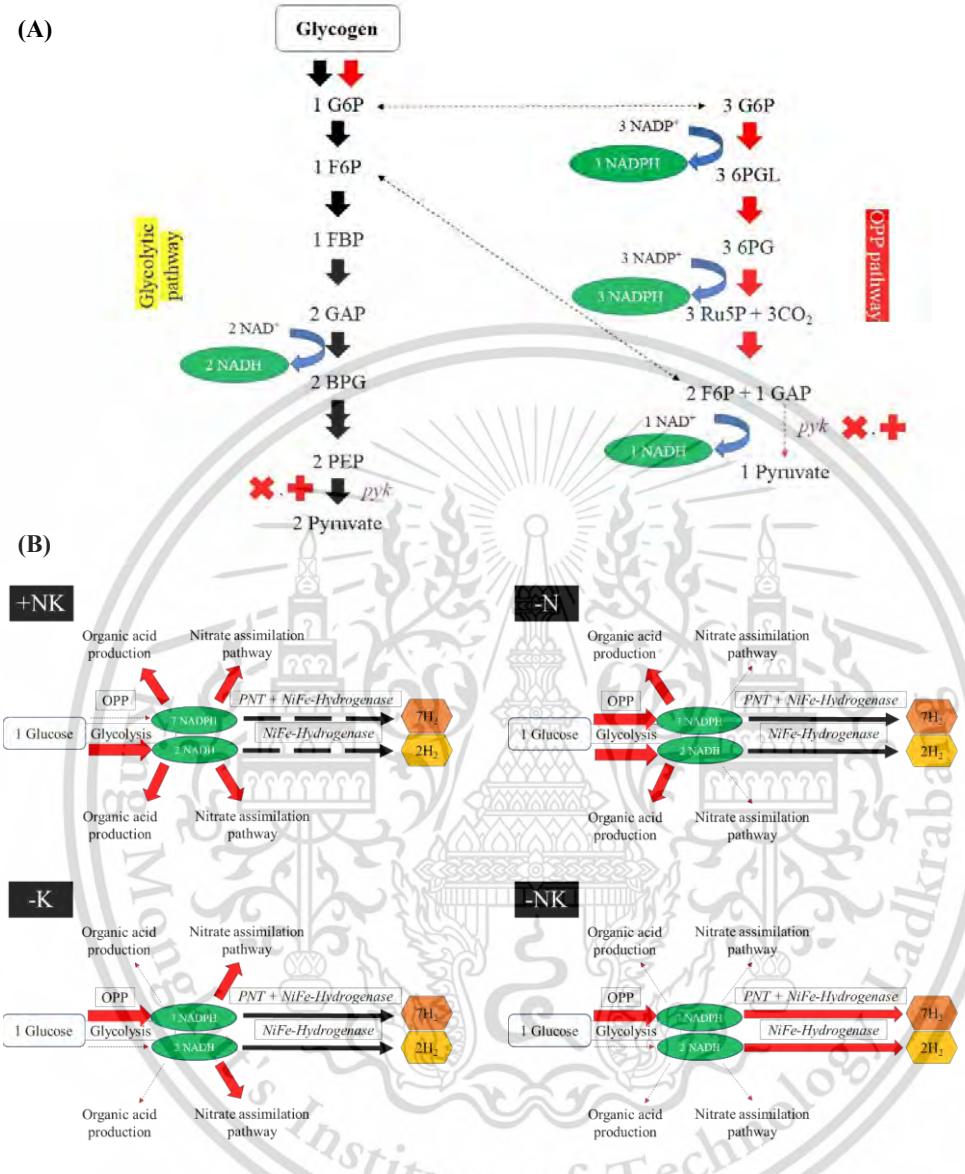

Fig. 5.2 Proposed schematic mechanism of H_2 production by *A. halophytica* based on the RNA-seq after adaptation in nitrogen and/or potassium deprivation for 2 days. Glycolytic and OPP pathway is involved in NAD(P)H generation via glycogen catabolism (A). Proposed H_2 metabolism and involving pathways of *A. halophytica* incubated in BG11 (+NK), $BG11_0$ (-N), BG11-K (-K) and $BG11_0$-K (-NK) under dark anaerobic conditions (B). Arrows show electron transport direction in each pathway.

CHAPTER 6
CONCLUSIONS

In this study, the effects of reducing agents and nutrient deprivation on H_2 production in the unicellular halotolerant cyanobacterium *Aphanothece halophytica* were investigated. This study was divided into 3 parts; (1) Effect of reducing substances on H_2 production by *A. halophytica*, (2) Effect of ferredoxin, NADH and NADPH on *in vitro* hydrogenase activity, and (3) Effect of nutrient deprivation on H_2 production by *A. halophytica*. The nutrient-deprived conditions which provided the highest H_2 production was selected for studying the RNA-seq based transcriptome analysis of genes involved in H_2 metabolism. This study can be summarized as follows:

1. Effect of reducing substances on H_2 production by *A. halophytica*

1.1 The type and concentration of reducing sugar promoted the highest H_2 production by *A. halophytica* was glucose at 0.189 mmol C-atom L^{-1}. The highest H_2 production rate and H_2 accumulation was 55.80 ± 0.50 μmol H_2 g cell dry wt^{-1} h^{-1} and 211.99 ± 11.37 μmol H_2 g cell dry wt^{-1} obtained in cells incubated in $BG11_0$ containing 0.189 mmol C-atom L^{-1} after 2 and 24 h of dark anaerobic conditions, respectively. Other types of reducing sugar showed little effect on H_2 production.

1.2 By primary screening of ten reducing agents affecting H_2 production, four types of potential reducing agents, β-mercaptoethanol, dithiothreitol, L-cysteine and sodium sulfide which enhanced signicantly H_2 production and H_2ase activity in *A. halophytica* were selected. The highest H_2 production of 1,136 ± 41.44 μmol H_2 g dry wt^{-1}, 3,806.34 ± 50.82 μmol H_2 g dry wt^{-1}, 3,676.29 ± 102.02 μmol H_2 g dry wt^{-1} and 4,815.59 ± 194.78 μmol H_2 g dry wt^{-1} was obtained in cells incubated in $BG11_0$ containing 10 mM β-mercaptoethanol, 50 mM dithiothreitol, 50 mM L-cysteine and 50 mM sodium sulfide after 24 h of dark anaerobic conditions.

1.3 Among four selected reducing agents, *A. halophytica* incubated in $BG11_0$ treated with 50 mM sodium sulfide showed the highest H_2 production of 4,815.59 ± 194.78

after 24 h of dark anaerobic conditions, which was approximately 18 folds compared with that without any reducing agent treatment and showed the highest H_2ase activity of 303.45 ± 3.15 after 24 h of dark anaerobic conditions, which was approximately 6 folds compared with that without any reducing agent treatment.

1.4 β-mercaptoethanol and sodium sulfide did not demonstrate the toxicity to *A. halophytica* cells with IC_{50} higher than 100 mM whereas dithiothreitol and L-cysteine provided IC_{50} of 18.12 ± 2.07 mM and 76.94 ± 4.21 mM, respectively.

2. Effect of ferredoxin, NADH and NADPH on *in vitro* hydrogenase activity

The NADPH and reduced ferredoxin can act as electron donors for [NiFe]-H_2ase in *A. halophytica*. The highest *in vitro* hydrogenase activity of 115.25 ± 3.74 μmol H_2 g dry weight^{-1} min^{-1} was found in cell homogenate treated with 2 mM reduced ferredoxin.

3. Effect of nutrient deprivation on H_2 production by *A. halophytica*

3.1 By comparison of H_2 production under nitrogen, potassium, phosphorus, and sulfur deprivation, the highest H_2 production of 332.82 ± 34.02 μmol H_2 g dry cell wt^{-1} was found in *A. halophytica* incubated in BG11-K under dark anaerobic conditions for 24 h, followed by cells incubated in $BG11_0$, which provided H_2 production 263.75 ± 31.58 μmol H_2 g dry cell wt^{-1}.

3.2 The double deprivation of N and K promoted the highest H_2 production of 507.51 ± 13.78 μmol H_2 g dry cell wt^{-1} and H_2ase activity of 120.05 ± 8.98 μmol H_2 g dry cell wt^{-1} under dark anaerobic conditions for 24 h. They were higher than those under the single deprivation.

3.3 In the case of adaptation time effect on H_2 production under both deprivation of N and K, H_2 production and H_2ase activity were found to be the highest in cells adapted in $BG11_0$-K for 2 days. Glycogen was also found highly accumulated in $BG11_0$-K. However, O_2 production and the specific activity of pyruvate kinase were found to be the lowest in cells incubated in $BG11_0$-K. Under N and K deprivation adaptation, glycogen was higher accumulated compared with that of cells incubated in normal BG11. After that, cells incubated in $BG11_0$-K under dark anaerobic conditions produced highly H_2 by using

electron donor, NAD(P)H, from glucose-6-phosphate broken down from accumulated glycogen with high activity of H_2ase enzyme. On the contrary, specific activity of pyruvate kinase was decreased in the absence of potassium. Therefore, glycolytic pathway was suggested as an unfavorable pathway under this condition.

3.4 By transcriptome analysis using RNA-seq of *A. halophytica* cells adapted under both nitrogen and potassium deprivation, several genes involved in glycogen biosynthesis (*glgA*, *glgB* and *glgP*) were upregulated whereas *pyk* and most genes that regulated enzymes in the glycolysis were downregulated. Remarkably, most genes regulated enzymes in the oxidative pentose phosphate pathway (OPP) were upregulated. Consequently, OPP was recommended as a promising pathway for promoting H_2 production in *A. halophytica* cells incubated in both nitrogen and potassium deprivation under dark anaerobic conditions.

3.5 The deprivation of combined nitrogen and potassium in media is a promising strategy for enhancing sustainable H_2 production by *A. halophytica*.

REFERENCES

Absher, M. 1973. “Hemocytometer counting. In: Tissue culture”. **Academic Press**, 395-397.

Aitken, C.E.; Marshall, R.A., Puglisi, J.D. 2008. "An oxygen scavenging system for improvement of dye stability in single-molecule fluorescence experiments". **Biophys J.** 94 (5): 1826–35.

Akhlaghi, N. and Najafpour D.G.A. 2020. “Comprehensive review on biological hydrogen production.” **Int. J. Hydrogen Energy. 2020**, 45: 22492–22512.

Akkerman, I., Janssen, M., Rocha, J. and Wijffels, R.H. 2002. “Photobiological hydrogen production: photochemical efficiency and bioreactor design.” **Int. J. Hydrogen Energy.** 27: 1195–208.

Alahari, A., and Apte, S.K. 1998. “Pleiotropic effects of potassium deficiency in a heterocystous, nitrogen-fixing cyanobacterium, *Anabaena torulosa*.” **Microbiol.** 144(6), 1557-1563.

Alanne, K. and Cao, S. 2019. “An overview of the concept and technology of ubiquitous energy.” **Appl. Energy.** 238: 284-302.

AlNouss, A., McKay, G. and Al-Ansari, T. 2020. “Production of syngas via gasification using optimum blends of biomass.” **J. Clean. Prod.** 242: 118499.

Ananyev, G., Carrieri, D. and Dismukes, G. C. 2008. “Optimization of metabolic capacity and flux through environmental cues to maximize hydrogen production by the cyanobacterium “*Arthrospira* (*Spirulina*) *maxima*”.” **Applied and Environmental Microbiology.** 74(19): 6102-6113.

Ananyev, G. M., Skizim, N. J. and Dismukes, G. C. 2012. “Enhancing biological hydrogen production from cyanobacteria by removal of excreted products. **J. Biotechnol.** 162(1): 97- 104.

Antal, T.K. and Lindblad, P. 2005. “Production of H_2 by sulphur-deprived cells of the unicellular cyanobacteria *Gloeocapsa alpicola* and *Synechocystis* sp. PCC 6803 during dark incubation with membrane or at various extracellular pH.” **J. Appl. Microbiol.** 98 (1), 114–120.

Baebprasert, W., Jantaro, S., Khetkorn, W., Lindblad, P. and Incharoensakdi, A. 2011. "Increased H_2 production in the cyanobacterium *Synechocystis* sp. strain PCC 6803 by redirecting the electron supply *via* genetic engineering of the nitrate assimilation pathway." **Metab. Eng.** 13: 610–6.

Baebprasert, W., Lindblad, P. and Incharoensakdi, A. 2010. "Response of H_2 production and Hox-hydrogenase activity to external factors in the unicellular cyanobacterium *Synechocystis* sp. strain PCC 6803." **Int. J. Hydrog. Energ.** 35(13): 6611-6616.

Baeyens, J., Zhang, H., Nie, J., Appels, L., Dewil, R., Ansart, R. and Deng, Y. 2020. "Reviewing the potential of bio-hydrogen production by fermentation." **Renew. Sust. Energ. Rev.** 131: 110023.

Belkin, S. and Padan, E. 1978. "Hydrogen metabolism in the facultative anoxygenic cyanobacteria (blue-green algae) *Oscillatoria limnetica* and *Aphanothece halophytica*." **Arch. Microbiol.** 116(1): 109-111.

Berland, B., Le-Campion, T. and Campos-Baeta-Neves M.H. 1989. "Interaction de la salinite et de la temperature sur la morphologie, la croissance et la composition cellulaire d'une cyanobacteria halotolerante (*Aphanothece* sp.). **Bot. Mar.** 32: 317- 329.

Blanco, H., Faaij, A.. 2018. "A review at the role of storage in energy systems with a focus on Power to Gas and long-term storage." **Renew Sustain Energy Rev.** 81: 104986.

Blumenthal, G. 2013. "Kuhn and the chemical revolution: a reassessment." **Found. Chem.** 15: 93-101.

Bolatkhan, K., Kossalbayev, B.D., Zayadan, B.K., Tomo, Tatsuya, Veziroglu, T.N. and Allakhverdiev, S.I. 2019. "Hydrogen production from phototrophic microorganisms: reality and perspectives." **Int. J. Hydrogen Energy.** 44: 5799–811.

Boison, G., Steingen, C., Stal, L. and Bothe, H. 2006. "The rice field cyanobacteria *Anabaena azotica* and *Anabaena* sp. CH1 express vanadium-dependent nitrogenase." **Arch. Microbiol.** 186: 367–76.

Boscá, L., Corredor, C. 1984. "Is phosphofructokinase the rate-limiting step of glycolysis?" **Trends Biochem. Sci.**, 9(9), 372-373.

Bothe, H., Schmitz, O., Yates, M.G. and Newton, W.E. 2010. "Nitrogen fixation and hydrogen metabolism in cyanobacteria." **Microbiology and Molecular Biology Reviews.** 74(4): 529-551.

Boudellal, M. 2018. "Power-to-gas : renewable hydrogen economy**. Berlin/Boston, GERMANY: De Gruyter, Inc.**

Bradford, M.M. 1976. "A rapid and sensitive method for the quantitation of microgram quantities of protein utilizing the principle of protein-dye binding". **Analytical biochemistry**, *72*(1), 248-254.

Cao, L., Yu, I.K.M., Xiong, X., Tsang, D.C.W., Zhang, S., Clark, J.H., Hu, C., Ng, Y.H., Shang, J. and Ok, Y.S. 2020. "Biorenewable hydrogen production through biomass gasification: A review and future prospects." **Environ. Res.** 186: 109547.

Carrieri, D., Wawrousek, K., Eckert, C., Yu, I. and Maness, P.J. 2011. "The role of bidirectional hydrogenases in cyanobacteria." **Bioresour. Technol.** 102: 8368–77.

Castello, E., Nunes, F.J.A.D. 2020. "Stability problems in the hydrogen production by dark fermentation: Possible causes and solutions." **Renew. Sust. Energ. Rev.** 119, 109602.

Christopher, F.C., Kumar, P.S., Vo, D.V.N. and Joshiba, G.J. 2021. "A review on critical assessment of advanced bioreactor options for sustainable hydrogen production." **Int. J. Hydrogen Energy.**

Checchetto, V. Segalla A. Allorent G. Rocca N.L. Leanza L. Giacometti G.M. Uozumi N. Finazzi G. Bergantino E. Szabo I. 2012. "Thylakoid potassium channel is required for efficient photosynthesis in cyanobacteria." **Proc. Natl. Acad. Sci.** USA 109, 11043–11048.

Chen, L., Qi, Z., Zhang, S., Su, J. and Somorjai, G.A. 2020. "Catalytic Hydrogen Production from Methane: A Review on Recent Progress and Prospect." **Catalysts.** 10: 858.

Chen, P.C., Fan, S.H., Chiang, C.L., and Lee, C.M. 2008. "Effect of growth conditions on the hydrogen production with cyanobacterium *Anabaena* sp. strain CH3." **Int. J. Hydrog. Energy**, 33(5), 1460-1464.

Chérel, I., Lefoulon, C., Boeglin, M. Sentenac, H. 2014. "Molecular mechanisms involved in plant adaptation to low K+ availability." **J. Exp. Bot.** 65, 833–848.

Choi, S.Y., Park, B., Choi, I.G., Sim, S.J., Lee, S.M., Um, Y., and Woo, H.M. 2016. "Transcriptome landscape of *Synechococcus elongatus* PCC 7942 for nitrogen starvation responses using RNA-seq." **Sci. Rep.** 6(1), 1-10.

Chow, T.J., Tabita, F.R. 1994. "Reciprocal light-dark transcriptional control of *nif* and *rbc* expression and light-dependent posttranslational control of nitrogenase activity in *Synechococcus* sp. strain RF-1." **J. Bacterial.** 176(20): 6281-6285.

Cohen, Y., Jørgensen, B.B., Revsbech, N.P., Poplawski, R. 1986. "Adaptation to hydrogen sulfide of oxygenic and anoxygenic photosynthesis among cyanobacteria." **Appl. Environ. Microbiol.** 51(2), 398-407.

Coleman, M.L., Sullivan, M.B., Martiny, C.A., Steglich, C., Barry, K., DeLong, E. and Chisholm, S.W. 2006. "Genomic islands and the ecology and evolution of Prochlorococcus." **Science.** 311, 1768–1770.

Compaoré, J., Stal, L.J. 2010. "Oxygen and the light–dark cycle of nitrogenase activity in two unicellular cyanobacteria." **Environ. Microbiol.** 12(1): 54-62.

Council, G.R. Bulletin. Ca, USA: GRC; 2018. **ReportFeb 2018.**

Cournac, L., Guedeney, G., Peltier, G., and Vignais, P.M. 2004. "Sustained photoevolution of molecular hydrogen in a mutant of *Synechocystis* sp. strain PCC 6803 deficient in the type I NADPH-dehydrogenase complex." **J. Bacteriol.** *186*(6), 1737-1746.

Dahiya, S., Chatterjee, S., Sarkar, O. and Venkata M.S. 2021. "Renewable hydrogen production by dark-fermentation: Current status, challenges and perspectives." **Biores. Technol.** 321, 124354.

Das, D., editor. 2018 "Microbial fuel cell (microbial fuel cell." **New Delhi, India: Capital Publishing Company, New Delhi, India.**

Dicks, A.L, and Rand, D.A.J. 2018 "Fuel cell systems explained." 3rd ed. **UK: John Wiley & Sons Ltd.**

Doong, R.A., and Schink, B. 2002. "Cysteine-mediated reductive dissolution of poorly crystalline iron (III) oxides by *Geobacter sulfurreducens*." **Environ. Sci. Technol.** 36(13), 2939-2945.

Dor, I., and Homoff. M. 1985. Salinity- temperature relations and morphotypes of a mixed population of coccoid cyanobacteria from a hot, hypersaline pond in Israel." **Mar. Ecol.** 6: 13-25.

Dubois, M., Gilles, K. A., Hamilton, J. K., Rebers, P. T. and Smith, F. 1956. Colorimetric method for determination of sugars and related substances. **Anal. Chem.** 28 (3), 350–356.

Dutta, I., and Vermaas, W.F. 2016. "The electron transfer pathway upon H_2 oxidation by the NiFe bidirectional hydrogenase of *Synechocystis* sp. PCC 6803 in the light shares components with the photosynthetic electron transfer chain in thylakoid membranes. **Int. J. of Hydrog. Energy.** 41(28), 11949-11959.

Dyhrman, S.T. 2016. "Nutrients and their acquisition: Phosphorus physiology in microalgae. In The Physiology of Microalgae." **Springer: Berlin/Heidelberg, Germany,** 155–183.

Epstein, W. 2003. "The roles and regulation of potassium in bacteria." **Prog. Nucl. Acid Res. Mol. Biol.** 75, 293–320.

Ernst, A., Kirschenlohr, H., Diez, J. and Böger, P. 1984. "Glycogen content and nitrogenase activity in *Anabaena variabilis*." **Arch. Microbiol.** 140 (2-3), 120–125.

Espie, G.S., Miller, A.G., and Canvin, D.T. 1989. "Selective and reversible inhibition of active CO_2 transport by hydrogen sulfide in a cyanobacterium." **Plant Physiol.** 91(1), 387-394.

Fang, Z., Chen, W. 2021. "Recent advances in formic acid electro-oxidation: From the fundamental mechanism to electrocatalysts." **Nanoscale Adv.** 3(1), 94-105.

Fay, P. 1976. "Factors influencing dark nitrogen fixation in a blue-green alga." **Appl. Environ. Microbiol.** 31: 376-379.

Ferreira, A.A.E., Cavalcanti, J.H., Vaz, M., Alvarenga, V.L., Adriano, N.N., Araújo, W. 2017. "Cyanobacterial nitrogenases: phylogenetic diversity, regulation and functional predictions." **Genet. Mol. Biol.** 40.

Ferreira, M., Pinto, M. F., Soares, O. S. G. P., Pereira, M. F. R., Órfão, J. J. M., Figueiredo, J. L., Neves I.C., Fonseca A.M., Parpot, P. 2012. "Electrocatalytic oxidation of oxalic

and oxalic acids in aqueous media at carbon nanotube modified electrodes." **Electrochim. Acta**, 60, 278-286.

Flores, E., Frias, J.E., Rubio, L.M., Herrero, A. 2005. "Photosynthetic nitrate assimilation in cyanobacteria." **Photosynth. Res.** 83:117–133.

Fruton, J. S. 1934. "Oxidation-reduction potentials of ascorbic acid." **J. Biol. Chem.** 105, 79-85.

García, D.O., Munoz, R., Rodríguez, E., Rene, E.R., Leon B.E. 2021. "Microbial ecology of a lactate-driven dark fermentation process producing hydrogen under carbohydrate-limiting conditions." **Int. J. Hydrog. Energy.** 110.

Garlick, S., Oren, A. Padan, E. 1977. "Occurrence of facultative anoxygenic photosynthesis among filamentous and unicellular cyanobacteria." **J. Bacteriol.** 129 (2): 623–629.

Germer, F., Zebger, I., Saggu, M., Lendzian, F., Schulz, R., Appel, J. 2009. "Overexpression, isolation, and spectroscopic characterization of the bidirectional [NiFe] hydrogenase from *Synechocystis* sp. PCC 6803." **J. Biol. Chem.** 284(52), 36462-36472.

Ghirardi, M.L. and Mohanty, P. 2010. "Oxygenic hydrogen photoproduction –current status of the technology." **Curr. Sci.** 98: 499–507.

Gielen, D., Boshell, F., Saygin, D., Bazilian, M.D., Wagner, N. Gorini, R. 2019. "The role of renewable energy in the global energy transformation." **Energy Strategy Reviews.** 24: 38-50.

Grasham, O., Dupont, V., Cockerill, T., Alonso C.V.M. Twigg, M.V. 2020. "Hydrogen via reforming aqueous ammonia and biomethane co-products of wastewater treatment: Environmental and economic sustainability." **Sustain. Energy Fuels.** 4, 5835–5850.

Grüning, N.M., Rinnerthaler, M., Bluemlein, K., Mülleder, M., Wamelink, M.M., Lehrach, H., Jakobs, C, Breitenbach, M. Ralser, M. 2011. "Pyruvate kinase triggers a metabolic feedback loop that controls redox metabolism in respiring cells." **Cell Metab.** 14(3), 415-427.

Gupta, P. Parkhey, P. 2017. “Electrohydrogenesis: energy efficient and economical technology for biohydrogen production.” **Advances in Biofeedstocks and Biofuels: Production Technologies for Biofuels.** 2: 201-233.

Gutekunst, K., Chen, X., Schreiber, K., Kaspar, U., Makam, S. Appel, J. 2014. “The bidirectional NiFe-hydrogenase in *Synechocystis* sp. PCC 6803 is reduced by flavodoxin and ferredoxin and is essential under mixotrophic, nitrate-limiting conditions.” **J. Biol. Chem.** 289(4): 1930-1937.

Hallenbeck, P. 2011. “Hydrogen production by cyanobacteria.” **Chapter in book Microbial Technologies in Advanced Biofuels Production.** 15–28.

Happe, T., Schutz, K. Bohme, H. 2000. “Transcriptional and mutational analysis of the uptake hydrogenase of the filamentous cyanobacterium *Anabaena variabilis* ATCC 29413.” **J. Bacteriol.** 182: 1624–31.

Hitam, C.N.C. Jalil, A.A. 2020. “A review on biohydrogen production through photo fermentation of lignocellulosic biomass.” **Biomass Convers. Biorefin.**

Houchins, J.P. 1984. “The physiology and biochemistry of hydrogen metabolism in cyanobacteria.” **Biochem. Biophys. Acta.** 768: 227–55.

Huertas, G.P., Llompart, J.M.D.M. 2017. “Standards, codes and regulations of hydrogen refueling stations and hydrogen fuel cell vehicles.” **Barcelona: ETSEIB, UPC, FINAL DEGREE PROJECT IMSI Department e Fuel cell, UTBM.**

Iwuchukwu, I.J., Vaughn, M., Myers, N., O'neill, H., Frymier, P., Bruce, B.D. 2010. “Self-organized Photosynthetic nanoparticle for cell-free hydrogen production.” **Nat. Nanotechnol.** 5(1) (2010) 73-79.

Iyer, S. S., Accardi, C. J., Ziegler, T. R., Blanco, R. A., Ritzenthaler, J. D., Rojas, M., Roman J., Jones, D. P. 2009. “Cysteine redox potential determines pro-inflammatory IL-1β levels.” **PloS one**, 4(3), 5017.

Kachur, A.V., Held, K.D., Koch, C.J., Biaglow, J.E. 1997. “Mechanism of production of hydroxyl radicals in the copper-catalyzed oxidation of dithiothreitol.” **Radiat. Res.** 147(4), 409-415.

Kao, O.H.W., Berns, D.S. Town, W.R. 1973. “The characterization of C-phycocyanin from an extremely halotolerant ble-green alga, *Coccochloris elabens*.” **Biochem. J.** 131: 39-50.

Kentemich, T., Bahnweg, M., Mayer, F., Bothe, H. 1989. “Localization of the reversible hydrogenase in cyanobacteria.” **Z. Naturforsch. C.** 44(5-6): 384-391.

Kentemich, T., Danneberg, G., Hundeshagen, B., Bothe, H. 1988. **FEMS Microbiol. Lett.** 51: 19–24.

Khetkorn, W., Lindblad, P., Incharoensakdi, A. 2010. “Enhanced biohydrogen production by the N_2-fixing cyanobacterium *Anabaena siamensis* strain TISTR 8012. **Int. J. Hydrog. Energy.** 35 (23), 12767–12776.

Khetkorn, W., Lindblad, P., Incharoensakdi, A. 2020. “Enhanced H_2 production with efficient N_2-fixation by fructose mixotrophically grown *Anabaena* sp. PCC 7120 strain disrupted in uptake hydrogenase”. **Algal Res.** 47, 101823.

Koksharova, O., Schubert, M., Shestakov, S., Cerff, R. 1998. “Genetic and biochemical evidence for distinct key functions of two highly divergent GAPDH genes in catabolic and anabolic carbon flow of the cyanobacterium *Synechocystis* sp. PCC 6803.” **Plant Mol. Biol.** 36(1), 183-194.

Kossalbayev, B.D., Tomo, T., Zayadan, B.K., Sadvakasova, A.K., Bolatkhan, K., Alwasel, S., Allakhverdiev, S.I. 2020. “Determination ofthe potential of cyanobacterial strains for hydrogen production.” **Int. J. Hydrog. Energy.** 45: 2627–2639.

Kotter, E., Schneider, L., Sehnke, F., Ohnmeiss, K., Schroer, R. 2016. “The future electric power system: impact of Power-to-Gas by interacting with other renewable energy components.” **J. Energy Storage.** 5: 113-9.

Krasikov, V., Wobeser, E.A., Yeremenko, N., Ibelings, B.W., Huisman, J., Matthijs, H.C.M. 2010. “Gene expression of the cyanobacterium *Synechocystis* PCC 6803 in response to nitrogen starvation. In: Wobeser EA (ed) Genome-wide expression analysis of environmental stress in the cyanobacterium *Synechocystis* PCC 6803.” **UvADARE, Amsterdam**, pp 55–74.

Krasnovsky, A.A., Van, Ni.C., Nikandrov, V.V., Brin, G.P. 1980. "Efficiency of hydrogen photoproduction by chloroplast-bacterial hydrogenase systems." **Plant Physiol.** 66(5), 925-930.

Kumaraswamy, G.K., Guerra, T., Qian, X., Zhang, S., Bryant, D.A., and Dismukes, G.C. 2013. "Reprogramming the glycolytic pathway for increased hydrogen production in cyanobacteria: metabolic engineering of NAD^+-dependent GAPDH." **Energy Environ. Sci.** 6(12), 3722-3731.

Kumar, R., Kumar, A. and Pal, A. 2020. "An overview of conventional and non conventional hydrogen production methods." **Mater. Today Proc.**

Lambert, G.R. Smith, G.D. 1977. "Hydrogen formation by marine blue-green algae." **FEBS Letters.** 83(1): 159-162.

Lamy, C., Millet, P. 2020. "A critical review on the defnitions used to calculate the energy efficiency coeffcients of water electrolysis cells working under near ambient temperature conditions." **J. Power Sources.** 447: 227350.

Labs, D.N. "Safe use of hydrogen". 30 May. 2019. Available, https://www.energy.gov/eere/fuelcells/safe-use-hydrogen.

Lim, Y., Lee, D.K., Kim, S.M., Park, W., Cho, S.Y. Sim, U. 2020. "Low Dimensional Carbon-Based Catalysts for Efficient Photocatalytic and Photo/Electrochemical Water Splitting Reactions." **Materials.** 13, 114.

Liu, J, Duan, X., Yuan, Z., Liu, Q. Tang, Q. 2017. "Experimental study on the performance, combustion and emission characteristics of a high compression ratio heavy-duty spark-ignition engine fuelled with liquefied methane gas and hydrogen blend." **Appl. Therm. Eng.** 124:585-94.

Luo, Y. H., Mitsui, A. 1994. "Hydrogen production from organic substrates in an aerobic nitrogen-fixing marine unicellular cyanobacterium *Synechococcus* sp. strain Miami BG 043511." **Biotechnol. Bioeng.** 44(10), 1255-1260.

Luo, Y.H. Mitsui, A. 1996. "Sulfide as electron source for H_2-photoproduction in the cyanobacterium *Synechococcus* sp., strain Miami BG 043511, under stress conditions." **J. Photochem. Photobiol. B: Biol.** 35(3): 203-207.

Mackinney, G. 1941. "Absorption of light by chlorophyll solutions." **J. Biol. Chem.** 140 (2), 315–322.

Manis, S. and Banerjee, R. 2008. "Comparison of biohydrogen production processes." **Int. J. Hydrogen Energy.** 33: 279–86.

Malcovati, M., Valentini, G. 1982. "AMP- and Fructose-1, 6, -biphosphateactivated pyruvate kinases from *Escherichia coli*." **Methods Enzym.** 90, 170–179.

Masukawa, H., Kitashima, M., Inoue, K., Sakurai, H. Hausinger, R. 2012. "Genetic engineering of cyanobacteria to enhance biohydrogen production from sunlight and water." **Ambio.** 41: 169–73.

McIntosh, C.L., Germer, F., Schulz, R., Appel, J., Jones, A.K. 2011. "The [NiFe]-hydrogenase of the cyanobacterium *Synechocystis* sp. PCC 6803 works bidirectionally with a bias to H_2 production." **J. Am. Chem. Soc.** 133(29), 11308-11319.

Mehrpooya, M. and Habibi, R. 2020. "A review on hydrogen production thermochemical water-splitting cycles." **J. Clean. Prod.** 275: 123836.

Meuer, J., Bartoschek, S., Koch, J., Künkel, A., Hedderich, R. 1999. "Purification and catalytic properties of *Ech* hydrogenase from *Methanosarcina barkeri*." **Eur. J. Biochem.** 265(1), 325-335.

Min, H., Sherman, L.A. 2010. "Hydrogen production by the unicellular, diazotrophic cyanobacterium *Cyanothece* sp. strain ATCC 51142 under conditions of continuous light. **Appl. Environ. Microbiol.** 76(13), 4293-4301.

Mohr., K.I., Brinkmann, N. Friedl, T. 2011. "Cyanobacteria." In: Reitner, J., Thiel, V. (eds) Encyclopedia of Geobiology." **Encyclopedia of Earth Sciences Series. Springer, Dordrecht.**

Oria-Hernández, J., Cabrera, N., Pérez-Montfort, R. Ramírez-Silva, L. 2005. "Pyruvate kinase revisited: the activating effect of K^+." **J. Biol. Chem.** 280, 37924–37929.

Osanai, T., Imamura, S., Asayama, M., Shirai, M., Suzuki, I., Murata, N., Tanaka, K. 2006. "Nitrogen induction of sugar catabolic gene expression in *Synechocystis* sp. PCC 6803." **DNA Res.** 13:185–195.

Osanai, T. 2016. "Anionic metabolite biosynthesis enhanced by potassium under dark, anaerobic conditions in cyanobacteria." **Sci. Rep.** 6, 32354.

Osazuwa, O.U., Abidin, S.Z., Fan, X., Nosakhare A.A. Azizan, T.M. 2021. "An insight into the effects of synthesis methods on catalysts properties for methane reforming." **J. Environ. Chem. Eng.** 9: 105052.

Page, M. J. Cera, E. D. 2006. "Role of Na^+ and K^+ in enzyme function." **Physiol. Rev.** 86, 1049–1092.

Papazi, A., Gjindali, A.I., Kastanaki, E., Assimakopoulos, K., Stamatakis, K., Kotzabasis, K. 2014. "Potassium deficiency, a "smart" cellular switch for sustained high yield hydrogen production by the green alga *Scenedesmus obliquus*." **Int. J. Hydrog. Energy.** 39(34), 19452-19464.

Perry, J.H. 1963. "Chemical engineers' handbook." **McGraw-Hill, New York, NY, USA.**

Pansook, S., Incharoensakdi, A., Phunpruch, S. 2016. "Hydrogen production by immobilized cells of unicellular halotolerant cyanobacterium *Aphanothece halophytica* in alginate beads". **APST**, 21(2), 248-255.

Pansook, S., Incharoensakdi, A., Phunpruch, S. 2019a. "Enhanced dark fermentative H_2 production by agar-immobilized cyanobacterium *Aphanothece halophytica*." **J. Appl. Phycol.** 31(5): 2869-2879.

Pansook, S., Incharoensakdi, A., Phunpruch, S. 2019b. "Effects of the photosystem II inhibitors CCCP and DCMU on hydrogen production by the unicellular halotolerant cyanobacterium *Aphanothece halophytica*." **Sci. World J.** 1030236.

Pansook, S., Phunpruch, S. Incharoensakdi, A. 2022. "Simazine Enhances Dark Fermentative H_2 Production by Unicellular Halotolerant Cyanobacterium *Aphanothece halophytica*." **Front. Bioeng. Biotechnol.** 1165.

Phunpruch, S., Taikhao, S. Incharoensakdi, A. 2016. "Identification of bidirectional hydrogenase genes and their co-transcription in unicellular halotolerant cyanobacterium *Aphanothece halophytica*." J**. Appl. Phycol.** 28(2): 967-978.

Radcliffe, J.C. 2018. "The water energy nexus in Australia e the outcome of two crises." **Water Energy Nexus.** 1: 66-85.

Raksajit, W., Satchasataporn, K., Lehto, K., Mäenpää, P., Incharoensakdi, A. 2012. "Enhancement of hydrogen production by the filamentous non-heterocystous

cyanobacterium *Arthrospira* sp. PCC 8005." **Inter.l J. hydrog. Energ.** 37(24), 18791-18797.

Rao, N.N. Gómez-García, M.R. Kornberg, 2009. "A Inorganic polyphosphate: Essential for growth and survival." **Annu. Rev. Biochem.** 78, 605–647.

Rashid, N., Song, W., Park, J., Jin, H.F. Lee, K. 2009. "Characteristics of hydrogen production by immobilized cyanobacterium *Microcystis aeruginosa* through cycles of photosynthesis and anaerobic incubation." **J. Ind. Eng. Chem.** 15 (4), 498–503.

Reddy, K.J., Haskell, J.B., Sherman, D.M. Sherman, L.A. 1993. "Unicellular, aerobic nitrogen-fixing cyanobacteria of the genus *Cyanothece*." **J. Bacteriol.** 175(5), 1284-1292.

Reddy, P.M., Spiller, H., Albrecht, S.L., Shanmugam, K.T. 1996. "Photodissimilation of fructose to H (*inf*2) and CO (*inf*2) by a dinitrogen-fixing cyanobacterium, *Anabaena variabilis*." **Appl. Environ. Microbiol**. 62(4), 1220-1226.

Rippka, R., Deruelles, J., Waterbury, J.B., Herdman, M. Stanier, R.Y. 1979. "Generic assignments, strain histories and properties of pure cultures of cyanobacteria." **Microbiol.** 111 (1), 1–61.

Rivkin, R.B.C., Buttner, W. 2015. "Hydrogen technologies safety guide." **USA: National Renewable Energy Laboratory (NREL).**

Rizzo, N. (2011, February 21). "The Definition of Reducing Sugars," livestrong.com.https://www.livestrong.com/article/386795-the-definition-of-reducing-sugars/

Sadvakasova, A.K., Kossalbayev, B.D., Zayadan, B.K., Bolatkhan, K., Alwasel, S., Najafpour, M.M. Allakhverdiev, S.I. 2020. "Bioprocesses of hydrogen production by cyanobacteria cells and possible ways to increase their productivity." **Renew. Sust. Energ. Rev.** 133, 110054.

Sambrook, J. Russell, D. 2001. "Molecular Cloning : a Laboratory Manual." 3rd ed." **New York: Cold Spring Harbor**.

Schopf, J.W. 1993. "Microfossils of the Early Archean Apex Chert – new evidence of the antiquity of life." **Science.** 260, 640–646.

Sankir, M. Sankir, N.D. 2017. "Hydrogen production technologies." **Somerset, United States. Incorporated: John Wiley & Sons.**

Schmitz, O., Boison, G., Salzmann, H., Bothe, H., Schutz, K., Wang, S.H. Happe, T. 2002. HoxE – a subunit specific for the pentameric bidirectional hydrogenase complex (HoxEFUYH) of cyanobacteria. **Biochim Biophys Acta.** 1554: 66–74.

Serebryakova, L.T., Sheremetieva, M.E. Tsygankov, A.A. 1998. "Reversible hydrogenase activity of *Gloeocapsa alpicola* in continuous culture." **FEMS Microbiol. Lett.** 166(1): 89-94.

Serebryakova, L.T., Sheremetieva, M.E. 2006. "Characterization of catalytic properties of hydrogenase isolated from the unicellular cyanobacterium *Gloeocapsa alpicola* CALU 743". **Biochemistry (Mosc)**, 71, 1370-1376.

Shen, Q., Jiang, Y., Xia, F., Wang, B., Lv, X., Ye, W. Yang, G. 2020. "Hydrogen production by Co-based bimetallic nano-catalysts and their performance in methane steam reforming." **Pet. Sci. Technol.** 38: 618–625.

Siddiquee, K.A.Z., Arauzo-Bravo, M.J., Shimizu, K. 2004. "Effect of a pyruvate kinase (*pykF*-gene) knockout mutation on the control of gene expression and metabolic fluxes in *Escherichia coli*." **FEMS Microbiol. Lett.** 235(1), 25-33.

Silveira, J.L., editor. 2017. "Sustainable hydrogen production processes (green energy and technology." **Switzerland Springer International Publishing Switzerland.**

Simon, R.D. 1977. "Sporulation in the filamentous cyanobacterium *Anabaena cylindrica*. The course of spore formation." **Arch. Microbiol.** 111: 283-288.

Singh, S.S., Zhang, Q., Sun, C., Thakur, S., Kumar, G.V. Kumar, T.V. 2020. "Energy production from steam gasification processes and parameters that contemplate in biomass gasifier—A review." **Bioresour. Technol.** 297: 122481.

Sjoholm. J., Oliveira, P., Lindblad, P. 2007. "Transcription and regulation of the bidirectional hydrogenase in the cyanobacterium *Nostoc* sp. strain PCC 7120." **Appl. Environ. Microbiol.** 73(17): 5435-5446.

Smith, G.D., Ewart, G.D. Tucker, W. 1992. "Hydrogen production by cyanobacteria." **Int. J. Hydrogen Energy.** 1992;17:695–8.

Srirangan, K., Pyne, M. E., Chou, C. P. 2011. "Biochemical and genetic engineering strategies to enhance hydrogen production in photosynthetic algae and cyanobacteria." **Bioresource Technology.** 102(18): 8589-8604.

Sukrachan, T., Incharoensakdi, A. 2020. “Enhanced hydrogen production by Nostoc sp. CU2561 immobilized in a novel agar bead”. **J. Appl. Phycol.** *32*, 1103-1115.

Suzuki, I., Horie, N., Sugiyama, T., Omata, T. 1995. “Identification and characterization of two nitrogen-regulated genes of the cyanobacterium *Synechococcus* sp. Strain PCC7942 required for maximum efficiency of nitrogen assimilation.” **J. Bacteriol.** 177: 290–6.

Tabkhi, F., Azzaropantel, C., Pibouleau, L., Domenech, S. 2008. “A mathematical framework for modelling and evaluating natural gas pipeline networks under hydrogen injection.” **Int. J. Hydrog. Energy.** 33: 6222-31.

Taikhao, S., Phunpruch, S. 2017. “Increasing hydrogen production efficiency of N_2-fixing cyanobacterium *Anabaena siamensis* TISTR 8012 by cell immobilization.” **Energy Procedia.** 138: 366-371.

Taikhao, S., Incharoensakdi, A., Phunpruch, S. 2015. “Dark fermentative hydrogen production by the unicellular halotolerant cyanobacterium *Aphanothece halophytica* grown in seawater.” **J. Appl. Phycol.** 27(1), 187-196.

Taikhao, S., Junyapoon, S., Incharoensakdi, A. Phunpruch, S. 2013. “Factors affecting biohydrogen production by unicellular halotolerant cyanobacterium *Aphanothece halophytica*.” **Journal of Applied Phycology.** 25(2): 575-585.

Takabe, T., Incharoensakdi, A., Arakawa, K., Yokota, S. 1988. “CO_2 fixation rate and RuBisCO content increase in the halotolerant cyanobacterium *Aphanothece halophytica* grown in high salinities. “**Plant Physiol.** 88: 1120-1124.

Tamagnini, P., Axelsson, R., Lindberg, P., Oxelfelt, F., Wunschiers, R., Lindblad, P. 2002. Hydrogenases and hydrogen metabolism of cyanobacteria. **Microbiol. Mol. Biol.** 66: 1–20.

Tatsuhiko, Y., Higuchi, Y. 2013 “Studies on hydrogenase. In: Proceedings of the Japan academy.” **Series B, Physical and Biological Sciences.** 89: 16–33.

Thiel, T., Lyons, E.M., Erker, J.C. 1997. “Characterization of genes for a second Modependent nitrogenase in the cyano-bacterium *Anabaena variabilis*.” **J. Bacteriol.** 179: 5222–5.

Tian, Y. 2018 “Grid-connected energy storage systems: benefits, planning and operation.” **Ann. Arbor.: Michigan State University.** 13423254 Ph.D.

Tindall, D.R., Yopp, J.H., Miller D.M., Schmid, W.E. 1978. “Physico-chemical parameters governing the growth of *Aphanothece halophytica* (Chroococcales) in hypersaline media.” **Phycologia.** 17: 179-185.

Tsygankov, A.A. 2007. “Azotfiksiruyushchiye tsianobakterii – produtsenty vodovoda (Obzor).” **Prikl Biokhim Mikrobiol.** 43: 279–88.

Ueda, S., Kawamura, Y., Iijima, H., Nakajima, M., Shirai, T., Okamoto, M., Kondo, A., Hirai M.Y. Osanai T. 2016. “Anionic metabolite biosynthesis enhanced by potassium under dark, anaerobic conditions in cyanobacteria.” **Sci. Rep.** 6, 32354.

Vignais, P. 2008 “Hydrogenases and H^+ reduction in primary energy conservation.” **Results Probl. Cell Differ.** 45: 223–52.

Vincent, I., Bessarabov, D. 2018. “Low cost hydrogen production by anion exchange membrane electrolysis: a review.” **Renew. Sustain Energy Rev.** 1690-704.

Warichanan, K., Phunpruch, S. 2019. “Effect of cell density and nutrient deprivation on hydrogen production by unicellular green alga *Scenedesmus* sp. KMITL-OVG1.” **Asia-Pacific J. Sci. Technol.** 24(2).

Weare, N.M. Benemann, J.R. 1973. “Nitrogen fixation by *Anabaena cylindrica*. Nitrogenase activity during induction and aging of batch cultures.” **Arch. Mikrobiol.** 93: 101–12.

Whitton, B. 1992. “Diversity, ecology and taxonomy of the cyanobacteria.” In: Mann, H., Carr, N. (eds.) “Photosynthetic prokaryotes.” **Plenum Press, New York.** pp. 1–51.

Wykoff, D.D, Davies, J.P., Melis, A., Grossman A.R. 1998. The regulation of photosynthetic electron transport during nutrient deprivation in *Chlamydomonas reinhardtii*. **Plant Physiol.** 117:129-39.

Yopp, J.H., Tindall, D.R., Miller, D.M. Schmid, W.E. 1978. “Isolation, purification and evidence of the obligate halophilic nature of the blue-green alga *Aphanothece halophytica* Fremy (Chroococcales).” **Phycol.** 17: 172-177.

Yuan, H. 2017. “Electrocatalytic water splitting to produce fuel hydrogen.” **Ann. Arbor: Michigan State University.** 10262133 Ph.D.

Zhang, J. 2018. “Techno-economic analysis and optimization of distributed energy systems.” **Ann. Arbor: Mississippi State University** 10842440 Ph.D.

APPENDIX A

BG11 medium

Composition of 1000x Trace metal mix

H_3BO_3	46.30	mM
$MnCl_2•4H_2O$	4.15	mM
$ZnSO_4•7H_2O$	0.77	mM
$NaMoO_4•2H_2O$	1.61	mM
$CuSO_4•5H_2O$	0.32	mM
$Co(NO_3)•6H_2O$	0.17	mM

Composition of 100x BG11

$NaNO_3$	17.6	M
$MgSO_4•7H_2O$	30.40	mM
$CaCl_2•2H_2O$	24.50	mM
Citric Acid	3.12	mM
Na_2EDTA	279	mM
1000X Trace metal mix	100	mL
Adjust volume	1000	mL

Composition of BG11 medium

100x BG11	10	mL
Na_2CO_3 (2g/100 mL)	1	mL
K_2HPO_4 (3.05 g/100 mL)	1	mL
$FeNH_4$•Citrate (0.60 g/100 mL)	1	mL
1 M TES	10	mL

Adjust the volume to 1 L with deionized water. The pH was adjusted to 7.4 by adding 2N NaOH before autoclaving at 121 °C, 15 psi for 15 min.

APPENDIX B

BG11 medium supplemented with Turk Island Salt Solution

Composition of BG11 medium supplemented with Turk Island salt solution

100x BG11 (Appendix A)	10	mL
*Stock A solution	100	mL
**Stock B solution	100	mL
Na_2CO_3 (2 g/100mL)	1	mL
K_2HPO_4 (3.05 g/100 mL)	1	mL
$FeNH_4$•Citrate (0.60 g/100 mL)	1	mL
NaCl	28.16	g

Adjust volume to 1 L with deionized water. Adjust the pH of the medium to 7.4 by slowly adding 2 N NaOH

*Stock A solution

Composition per liter

KCl	6.6	g
$MgCl_2$•$6H_2O$	55	g
$CaCl_2$•$2H_2O$	14.66	g

**Stock B solution

Composition per liter

$MgSo_4$•$7H_2O$	74.48	g

APPENDIX C

Hemocytometer

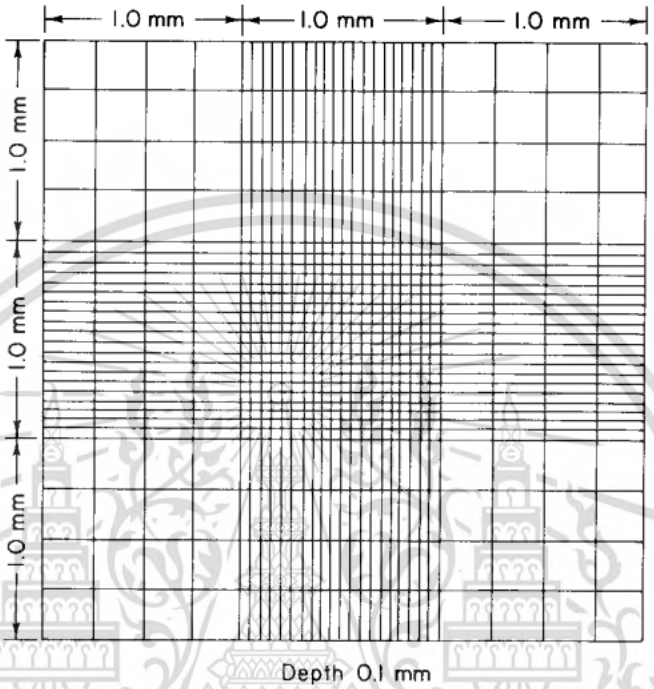

Fig. A Line drawing of ruling of Neubauer type hemocytometer chamber. Chamber units are 1 mm with a depth of 0.1 mm. (Absher, 1973)

APPENDIX D

Glycogen standard curve

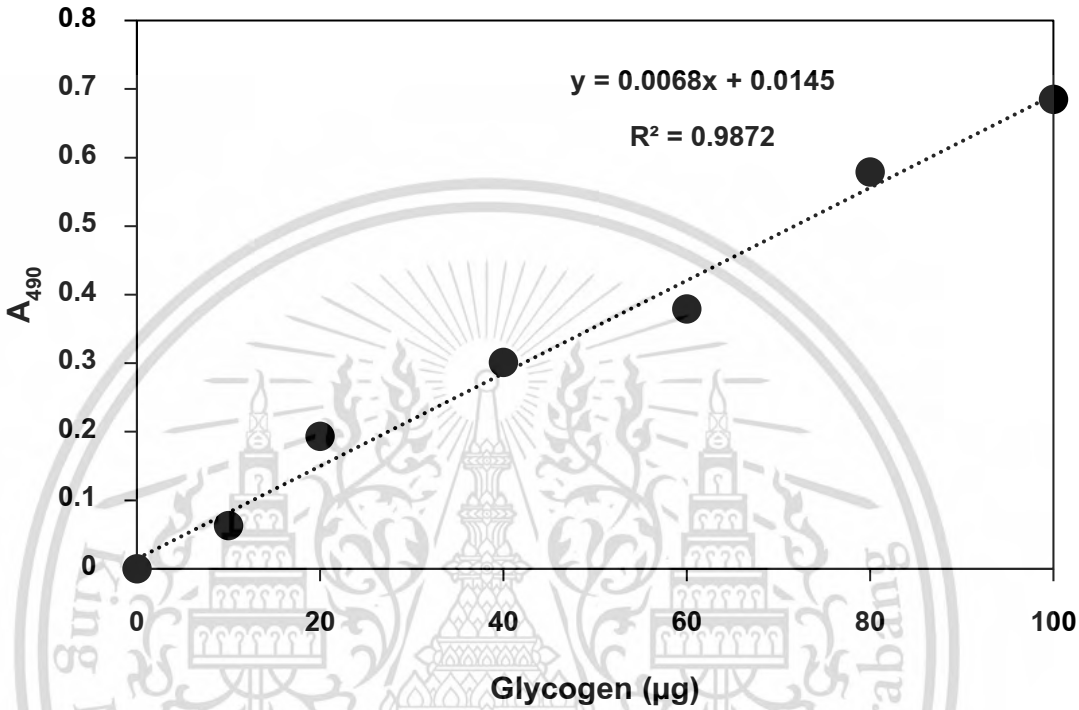

Fig. B Standard calibration curve of glycogen

APPENDIX E

Protein standard graph and Bradford reagent

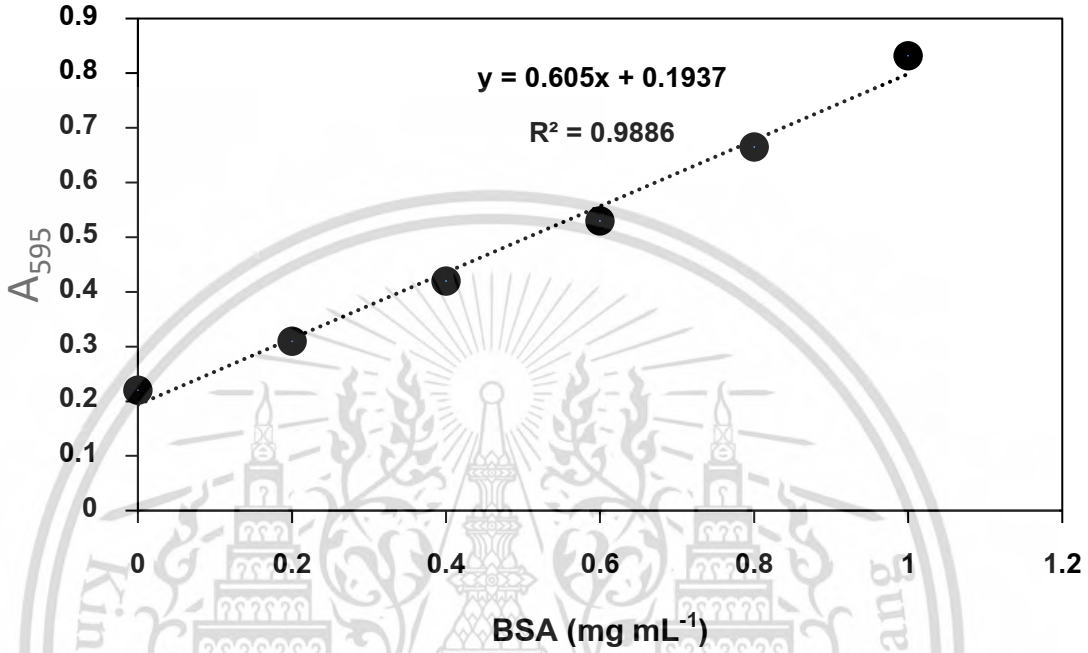

Fig. C Standard calibration curve of bovine serum albumin

Table A Bradford reagent

Composition	Volume
Coomassie Blue G250	100 mg
95% ethanol	50 mL
85% phosphoric acid	100 mL
Add distilled Water until total volume	1,000 mL

AUTHOR'S BIOGRAPHY

Mr. Nattanon Chinchusak was born on September 6th, 1993, in Uthai Thani, Thailand. He graduated with a Bachelor of Science degree in Biotechnology, School of Science, King Mongkut's Institute of Technology Ladkrabang in 2016. After graduating bachelor's degree of science, he has continuously been studying for Doctor of Philosophy (Ph.D.) degree in Program of Biotechnology, School of Science, King Mongkut's Institute of Technology Ladkrabang since 2016.

Publications

1. Chinchusak, N., Incharoensakdi, A., Phunpruch, S. 2022. "Enhancement of dark fermentative hydrogen production in nitrogen-deprived halotolerant unicellular cyanobacterium *Aphanothece halophytica* by treatment with reducing agents." **Biomass Bioenerg.**, 167, 106624.
2. Chinchusak, N., Incharoensakdi, A., Phunpruch, S. 2023. "Dark fermentative hydrogen production and transcriptional analysis of genes involved in the unicellular halotolerant cyanobacterium *Aphanothece halophytica* under nitrogen and potassium deprivation." **Front. Bioeng. Biotechnol** *10*, 1028151.

Biomass and Bioenergy 167 (2022) 106624

Contents lists available at ScienceDirect

Biomass and Bioenergy

journal homepage: www.elsevier.com/locate/biombioe

Enhancement of dark fermentative hydrogen production in nitrogen-deprived halotolerant unicellular cyanobacterium *Aphanothece halophytica* by treatment with reducing agents

Nattanon Chinchusak [a], Aran Incharoensakdi [b,c], Saranya Phunpruch [a,d,*]

[a] Department of Biology, School of Science, King Mongkut's Institute of Technology Ladkrabang, Bangkok, 10520, Thailand
[b] Laboratory of Cyanobacterial Biotechnology, Department of Biochemistry, Faculty of Science, Chulalongkorn University, Bangkok, 10330, Thailand
[c] Academy of Science, Royal Society of Thailand, Bangkok, 10330, Thailand
[d] Bioenergy Research Unit, School of Science, King Mongkut's Institute of Technology Ladkrabang, Bangkok, 10520, Thailand

ARTICLE INFO

Keywords:
Enhanced hydrogen production
Aphanothece halophytica
Reducing agents
Redox partner

ABSTRACT

To enhance H_2 production by the halotolerant unicellular cyanobacterium *Aphanothece halophytica*, effect of various kinds of reducing sugar and reducing agent on H_2 production was investigated. The highest H_2 production rate of 55.80 ± 0.50 μmol H_2 g dry weight^{-1} h^{-1} was obtained when the cells were incubated in $BG11_0$ medium containing 0.189 mmol C-atom L^{-1} glucose under dark anaerobic condition. This rate was 1.5 folds higher than that without glucose. Among ten reducing agents tested, β-mercaptoethanol, dithiothreitol, L-cysteine and sodium sulfide had high potential as an effective reducing agent to increase H_2 production by *A. halophytica*. Cells treated with 50 mM sodium sulfide showed the highest H_2 accumulation with 4815.59 ± 194.78 μmol H_2 g dry weight^{-1} after 24 h of dark anaerobic incubation. An increase in H_2 production was ascribed to an increase of hydrogenase activity and a decrease of O_2 production rate. This H_2 production yield was approximately 20 folds higher than that without reducing agent. Furthermore, 50 mM sodium sulfide appeared to be non-toxic to *A. halophytica* cells, since the IC_{50} of sodium sulfide was higher than 100 mM. The reduced ferredoxin at 1.5 μM-1.5 mM, NADH and NADPH at 0.15–1.5 mM could support *in vitro* [NiFe]-H_2ase activity, demonstrating the ability of these compounds to provide electrons towards [NiFe]-H_2ase in *A. halophytica*.

1. Introduction

Nowadays, energy is essential for human life. The primary but finite energy source, fossil fuel, is going to run out in the near future due to an increase in human population, industrial growth and economic expansion. Combustion of fossil fuel results in an emission of various kinds of greenhouse gases leading to global warming. One of promising sustainable alternative energy sources is hydrogen gas (H_2) which shows a lot of advantages compared to other energy sources. H_2 combustion provides a high heating value with 141.6 MJ kg^{-1} [1] and does not generate any greenhouse gases. H_2 can be produced by chemical and biological processes. For biohydrogen production, microorganisms such as bacteria, photosynthetic bacteria, green algae, and cyanobacteria have high potential as H_2 producers.

Cyanobacteria are photosynthetic prokaryotes whose characteristics are varied depending on morphology, physiological conditions, and evolutionary diversity. In cyanobacteria, three enzymes are involved in H_2 metabolism. Nitrogenase catalyzes nitrogen fixation to produce ammonia as a main product and this reaction simultaneously produces H_2 as a by-product. Nitrogenase is usually found in heterocyst cells of N_2-fixing cyanobacteria; however, it can also be found in non-heterocystous unicellular cyanobacteria such as *Gloeothece* sp., *Synechococcus* sp. and *Cyanothece* sp. [2–4]. Uptake or unidirectional hydrogenase occurs in N_2-fixing species. It can oxidize H_2 produced by nitrogenase activity. The last enzyme, reversible or bidirectional hydrogenase, can both oxidize and generate H_2. It can be found in all types of cyanobacteria including heterocystous, filamentous and unicellular species [5–9]. All enzymes involving H_2 metabolism are highly sensitive

* Corresponding author. Department of Biology, School of Science, King Mongkut's Institute of Technology Ladkrabang, Chalongkrung road, Bangkok, 10520, Thailand.
E-mail address: saranya.ph@kmitl.ac.th (S. Phunpruch).

https://doi.org/10.1016/j.biombioe.2022.106624
Received 17 May 2022; Received in revised form 30 September 2022; Accepted 9 October 2022
Available online 29 October 2022

to O_2, a main product of water photolysis in photosystem II [10].

The unicellular halotolerant cyanobacterium *Aphanothece halophytica* is one of potential cyanobacteria for H_2 production [5,11]. *A. halophytica* can use H_2 as an electron donor in the photosystem I-driven reaction for CO_2 assimilation [12]. Only *hox* operon encoding bidirectional [NiFe]-hydrogenase has been identified in *A. halophytica* and it shows the highest identity to that of *Halothece* sp. PCC 7418 [13]. However, in genome sequences of *Halothece* sp. PCC 7418 launched in GenBank under accession number CP00945.1, *nif* operon encoding nitrogenase has also been reported. Previously, *Aphanothece* sp. could grow in nitrogen free medium and showed capable of N_2 fixation under light aerobic condition. However, under dark condition its N_2 fixation was not found [14]. Under dark anaerobic condition, bidirectional hydrogenase catalyzes H_2 production by using electrons obtained from a glycogen degradation of carbohydrate catabolism [11]. Factors affecting H_2 production such as nutrient deprivation, concentrations of NaCl and carbon sources, pH, light intensity and temperature have been previously reported in *A. halophytica* [5,11]. Nitrogen deprivation significantly enhances H_2 production in two-stage culture [11]. In addition, H_2 production by *A. halophytica* is enhanced by cell immobilization [15] and by treatment with photosystem II inhibitors CCCP (Carbonyl cyanide 3-chlorophenylhydrazone) and DCMU (3-(3,4-dichlorophenyl)-1, 1-dimethylurea) [16]. Recently, the herbicide simazine was found to be a potential inhibitor for H_2 production by *A. halophytica* under both light and dark conditions [17].

Reducing agent is one of external factors as excessive electron sources that could possibly increase H_2 production by cyanobacteria [18]. Reducing agent can provide electrons to bidirectional [NiFe] H_2ase for balancing redox reactions, thus generating H_2 [7]. Previously, some reducing agents were shown to stimulate H_2 production in various cyanobacteria; however, the results showed not much increase in H_2 yield [19–21] which might be due to the toxic effect of the reducing agents used on the cells.

In this study, effect of reducing sugars and reducing agents on dark fermentative H_2 production by N-deprived *A. halophytica* was investigated. Apart from reducing agents, an investigation of redox partners, NADH, NAD(P)H and ferredoxin, as electron donors for bidirectional [NiFe]-H_2ase was also performed to understand H_2 metabolism in *A. halophytica*.

2. Materials and methods

2.1. Growth and adaptation condition

The halotolerant cyanobacterium *A. halophytica* originally isolated from Solar Lake, Israel was obtained from Dr. Tetsuko Takabe (Nagoya University). It was cultivated in a 250-mL of Erlenmeyer flask containing 100 mL of BG11 medium (pH 7.4) [22] supplemented with Turk Island salt solution [23] on incubator shaker with a speed of 120 rpm at 30 °C under a light intensity of 30 μmol photons m^{-2} s^{-1} with a light-dark cycle (16 h: 8 h) for 7 days. Cell density was initially adjusted with an optical density at 730 nm (OD_{730}) of 0.1. After 7 days of cultivation, cells were harvested by centrifugation at 8000×*g* at 4 °C for 10 min, subsequently washed twice and resuspended in 100 mL of fresh N-deprived BG11 ($BG11_0$) supplemented with Turk Island salt solution. Cells were adapted in N-deprived medium for 24 h before subjecting to H_2 production experiments under various conditions.

2.2. Chlorophyll *a* measurement

A. halophytica cells were harvested by centrifugation of 1 mL of cell suspension at 8000×*g* at 4 °C for 10 min. Chlorophyll *a* was extracted from *A. halophytica* cell pellet by adding 1 mL of 90% (v/v) methanol followed by vortexing and incubating at 30 °C for 30 min. The extract was centrifuged for 5 min. The absorbance of chlorophyll *a* was measured at 665 nm using a spectrophotometer and chlorophyll *a* concentration was calculated according to MacKinney [24].

2.3. Cell dry weight and cell concentration measurement

Five mL of cell suspension was filtered through a glass microfiber filter GF/C (Whatman, UK). The cells collected on the filter were washed twice with sterile distilled water and dried in an oven at 70 °C until constant weight was achieved. For cell concentration measurement, cells were counted by hemocytometer and expressed as a number of cells mL^{-1}.

2.4. H_2 and O_2 production measurement

The measurement of H_2 and O_2 was performed on 7 days old cells of *A. halophytica* adapted in a 250-mL Erlenmeyer flask containing 100 mL of N-deprived BG11 medium supplemented with Turk Island salt solution for 24 h. Cells were harvested by centrifugation and resuspended in 5 mL of fresh N-deprived medium before transferring into a 12-mL glass vial and sealed with a rubber stopper. To set an anaerobic condition, the suspension was purged with argon gas for 10 min. Cells were then shaken at 120 rpm under dark anaerobic incubation for 120 h. The amount of H_2 and O_2 in headspace of the vial was measured by GC-TCD with a molecular sieve 5°A 60/80 mesh packed column [20] H_2 production and H_2 production rate were expressed as μmol H_2 g dry $weight^{-1}$ and μmol H_2 g dry $weight^{-1}$ h^{-1}, respectively. The O_2 production rate was expressed as μmol O_2 g dry $weight^{-1}$ h^{-1}.

2.5. *In vivo* bidirectional H_2ase activity measurement

In vivo bidirectional H_2ase activity was measured from an analysis of H_2 production of cells mediated by dithionite-reduced methyl viologen [5]. One mL of cyanobacterial cell suspension was mixed with 1 mL of 25 mM sodium phosphate buffer (pH 7.6) containing 20 mM dithionite and 5 mM methyl viologen. The reaction was performed in a vial and incubated under dark anaerobic condition for 30 min before H_2 measurement by GC-TCD.

2.6. Screening of reducing substances enabling increased H_2 production

Seven days old cells of *A. halophytica* grown in BG11 supplemented with Turk Island salt solution were harvested by centrifugation, resuspended, and incubated in N-free medium under conditions mentioned above for 24 h. Cells were then harvested by centrifugation, resuspended in 5 mL of fresh medium and transferred to a 12-mL glass vial. Various kinds of reducing sugars, glucose (Carlo Erba, Italy), fructose (Carlo Erba, Italy), maltose monohydrate (Merck, Germany) and lactose monohydrate (Sigma, USA) at final concentrations of 0.189, 1.89, 18.9 and 189 mmol C-atom L^{-1} were added into cell suspension. The reducing agents, L-ascorbic acid (Vetec, China), β-mercaptoethanol (Plusone, Sweden), DL-dithiothreitol (Sigma, Canada), formic acid (Carlo Erba, Italy), potassium hexacyanoferrate (II) trihydrate (Sigma, Japan), methyl viologen dichloride hydrate (Sigma, Germany), sodium hydrosulfite (Sigma, Germany), sodium sulfide nanohydrate (Carlo Erba, Italy), oxalic acid (Sigma, USA) and L-cysteine (Sigma, China) were added to final concentrations of 0.1, 1.0 and 10 mM. Vials were sealed with rubber stopper before purging with argon gas for 10 min. Cells were incubated on incubator shaker at 120 rpm under dark anaerobic condition for 24 h. The amount of H_2 in headspace of the vial was measured by GC-TCD as mentioned above.

2.7. Cell toxicity assay

A. halophytica cell cultures containing $3.63 \pm 0.11 \times 10^9$ cells mL^{-1} were incubated with selective reducing agents at final concentration of 0.1, 1.0, 10, 20, 50 and 100 mM under dark anaerobic condition for 24 h. Samples (1 mL) from each culture were withdrawn to determine the

cell density, by counting total blue-green visible cells under a microscope using a hemocytometer. The number of cells obtained at each concentration, after the exposure period, was expressed as percentage growth reduction with respect to the control (without reducing agent addition). These percentages were used in the calculation of IC_{50} (expressed as reducing agent concentration giving 50% decreasing of cell concentration after 24 h exposure).

2.8. Analysis of redox partners for H_2ase by in vitro H_2ase activity measurement

Ferredoxin (Fd) from spinach (Sigma, USA), reduced β-nicotinamide adenine dinucleotide 2' phosphate (NADPH) (Sigma, USA) and reduced β-nicotinamide adenine dinucleotide (NADH) (Sigma, USA) were analyzed for a redox partner of H_2ase in *A. halophytica*. To prepare cell homogenate of *A. halophytica*, 100 mL of 7 days old cells were harvested by centrifugation and resuspended in 0.2 M sodium phosphate buffer (pH 7.0) at a chlorophyll *a* concentration of 300 μg chl a mL^{-1}. Cells were broken by 20% pulse of ultrasonication on ice for 5 min. The cell-free extract was obtained after centrifugation of the homogenate at 8000×*g* at 4 °C for 10 min. One mL of cell-free extract was mixed with 1 mL of reaction mixture containing 10 mM glucose, 40 U glucose oxidase from *Aspergillus niger* (Sigma, UK) and 50 U catalase from *Micrococcus lysodeikticus* (Sigma, Japan) to induce anaerobic condition [7]. The reaction mixture treated with various concentrations of ferredoxin, NADH and NADPH was incubated at 30 °C for 15 min before measurement of H_2ase activity of cell-free extract by GC-TCD.

2.9. Statistical analysis

All experiments were performed in triplicate. All data are expressed as the mean ± standard deviation. The statistical analysis of differences was performed using one-way analysis of variance (ANOVA) with 95% confidence level by a software of IBM SPSS version 19.

3. Results and discussion

3.1. Effect of reducing sugars on H_2 production rate by A. halophytica

The effect of four reducing sugars; glucose, fructose, maltose and lactose, at 0.189, 1.89, 18.9 and 189 mmol C-atom L^{-1} on H_2 production by *A. halophytica* was investigated under nitrogen deprivation and dark anaerobic condition. The highest H_2 production rate of 55.80 ± 0.50 μmol H_2 g dry weight^{-1} h^{-1} was observed in cells incubated in medium containing 0.189 mmol C-atom L^{-1} glucose for 2 h of incubation time (Fig. 1). This rate was approximately 1.5 folds higher than that of control cells (without any supplementation of reducing sugars) (38.37 ± 0.25 μmol H_2 g dry weight^{-1} h^{-1}). Higher glucose concentrations than 0.189 mmol C-atom L^{-1} obviously decreased H_2 production rate (Fig. 1). The other two reducing sugars, maltose and lactose, at low concentration could also enhance H_2 production, whereas fructose showed no increase in H_2 production (Fig. 1).

In this study, glucose at 0.189 mmol C-atom L^{-1} could better provide electrons towards H_2ase to generate H_2 in *A. halophytica* than glucose at other concentrations or than other types of reducing sugars. Glucose was also found as electron donor for H_2ase in other unicellular cyanobacteria such as *Synechocystis* sp. PCC 6803 and *Synechococcus* sp. strain Miami BG 04351 [20,25]. On the other hand, filamentous cyanobacteria rather use fructose as a favorite sugar source to donate electrons for H_2 production [26–28]. The results suggested that glucose is preferably metabolized compared to other sugar sources in unicellular cyanobacterial cells including *A. halophytica*. It could be explained that under darkness glucose might not provide electrons directly to bidirectional [NiFe]-H_2ase for H_2 production but it is preferably catabolized in glycolytic, tricarboxylic acid cycle and oxidative pentose phosphate pathways. As the tricarboxylic acid cycle in cyanobacteria is incomplete, excess NADPH is produced [29]. Previous study showed that *Synechocystis* sp. PCC 6803 enhanced dark respiration when incubated cells in BG11 supplemented with 0.120 mmol C-atom L^{-1} glucose under dark condition, suggesting that glucose addition corresponded in an increase in electrons via oxidative pentose phosphate pathway, thus NADPH

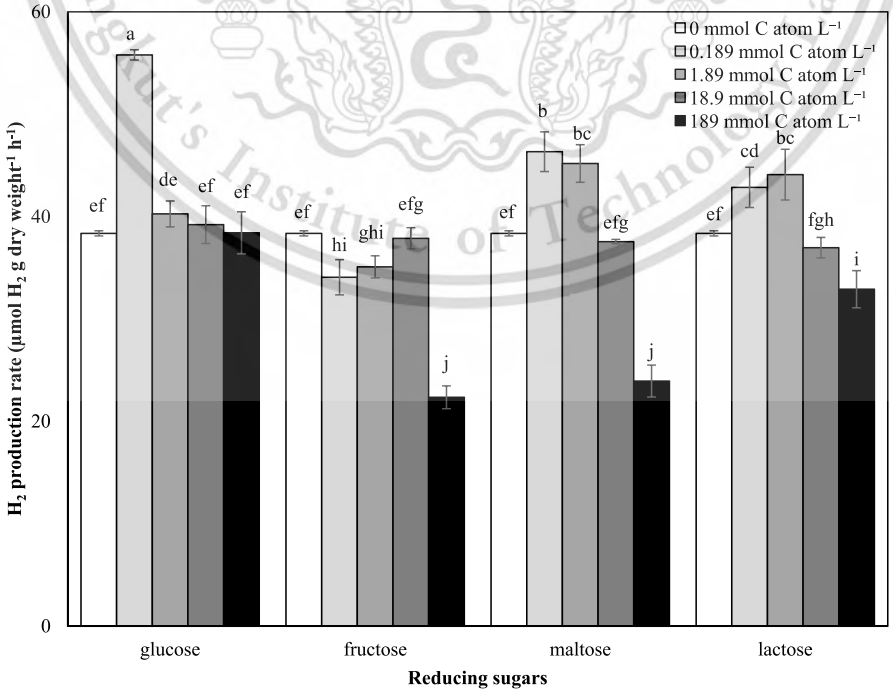

Fig. 1. H_2 production rate by *A. halophytica* after incubation in $BG11_0$ containing various concentrations of reducing sugars under dark anaerobic condition for 2 h. Data represents as mean ± SD of triplicate samples with a significance level of 95%. Superscripts show significant differences between samples.

production was increased [30]. To protect cell from overreduction, these excess NADPH could provide electrons towards bidirectional [NiFe]--H_2ase to produce H_2, especially under dark anaerobic condition where bidirectional [NiFe]-H_2ase is constitutively active. However, at high glucose concentrations, cyanobacterial cells might change their metabolism to synthesize glycogen and/or need higher energy to excrete surplus glucose out of cells, thus decreasing a level of NADPH and finally reducing H_2 production [5,20].

Table 1
H_2 production rate, H_2 production, cell concentration and pH of *A. halophytica* cell culture after dark anaerobic incubation for 24 h in $BG11_0$ containing various kinds of reducing agent at 0, 0.1, 1.0 and 10.0 mM. Data represent mean ± SD. Superscripts with different letters show significant differences between samples with a significance level of 95%. For H_2 production rate, it was determined after 2 h incubation where the linear increase was detected.

Reducing agent	Conc. (mM)	H_2 production rate (μmol H_2 g dry weight^{-1} h^{-1})	H_2 production (μmol H_2 g dry weight^{-1})	Cell concentration (× 10^9 cells mL^{-1})	pH
CTRL (No reductants)	0	36.45 ± 0.99^{no}	264.09 ± 5.87^{jk}	3.63 ± 0.11	6.70 ± 0.03
ascorbic acid	0.1	71.75 ± 3.09^{jkl}	263.44 ± 8.16^{jk}	2.70 ± 0.26	6.20 ± 0.10
	1.0	66.66 ± 2.01^{klm}	334.42 ± 22.46^{hi}	2.23 ± 0.08	6.09 ± 0.08
	10.0	ND	ND	0.76 ± 0.02	3.68 ± 0.02
β-mercaptoethanol	0.1	169.49 ± 3.36^{cd}	344.71 ± 5.75^{h}	3.44 ± 0.09	6.67 ± 0.32
	1.0	175.19 ± 8.54^{c}	401.41 ± 40.93^{g}	3.30 ± 0.07	6.52 ± 0.24
	10.0	241.80 ± 16.08^{b}	1136.02 ± 41.44^{a}	3.11 ± 0.18	6.42 ± 0.06
dithiothreitol	0.1	74.10 ± 4.95^{jkl}	268.95 ± 5.45^{jk}	3.15 ± 0.11	6.61 ± 0.21
	1.0	125.95 ± 6.28^{f}	289.82 ± 14.52^{ijk}	2.54 ± 0.12	6.61 ± 0.13
	10.0	251.87 ± 2.26^{ab}	559.65 ± 23.57^{d}	2.39 ± 0.09	6.37 ± 0.06
formic acid	0.1	161.12 ± 4.16^{d}	323.88 ± 31.13^{hi}	3.24 ± 0.02	6.63 ± 0.05
	1.0	41.70 ± 2.94^{n}	83.40 ± 5.89^{n}	2.53 ± 0.04	6.07 ± 0.13
	10.0	ND	ND	0.85 ± 0.14	3.18 ± 0.03
L-cysteine	0.1	77.62 ± 4.70^{j}	458.79 ± 11.21^{ef}	3.41 ± 0.05	6.67 ± 0.05
	1.0	169.48 ± 10.44^{cd}	582.32 ± 26.52^{d}	3.29 ± 0.05	6.72 ± 0.03
	10.0	256.53 ± 4.89^{a}	842.69 ± 53.61^{c}	3.08 ± 0.11	6.57 ± 0.04
methyl viologen	0.1	101.84 ± 4.10^{h}	418.51 ± 26.65^{fg}	2.75 ± 0.11	6.25 ± 0.13
	1.0	76.16 ± 1.06^{jk}	337.26 ± 22.27^{h}	2.36 ± 0.27	6.20 ± 0.10
	10.0	31.41 ± 2.13^{no}	136.22 ± 4.99^{m}	2.33 ± 0.07	6.01 ± 0.02
oxalic acid	0.1	27.97 ± 2.20^{o}	197.42 ± 10.68^{l}	2.98 ± 0.21	6.59 ± 0.04
	1.0	3.06 ± 0.27^{p}	20.64 ± 1.26^{o}	2.43 ± 0.25	4.87 ± 0.08
	10.0	ND	ND	0.80 ± 0.03	1.82 ± 0.09
potassium hexacyanoferrate	0.1	63.71 ± 5.14^{lm}	268.72 ± 11.47^{jk}	3.14 ± 0.05	6.60 ± 0.13
	1.0	87.41 ± 4.98^{i}	288.65 ± 13.08^{ijk}	2.65 ± 0.07	6.48 ± 0.09
	10.0	38.56 ± 2.27^{no}	243.01 ± 8.53^{k}	2.61 ± 0.16	6.52 ± 0.09
sodium dithionite	0.1	159.53 ± 11.20^{d}	464.95 ± 32.61^{e}	3.14 ± 0.41	6.65 ± 0.31
	1.0	60.47 ± 0.23^{m}	155.38 ± 6.25^{m}	3.51 ± 0.02	6.45 ± 0.25
	10.0	6.86 ± 0.22^{p}	37.42 ± 2.01^{o}	2.65 ± 0.07	5.20 ± 0.11
sodium sulfide	0.1	116.21 ± 7.28^{g}	288.63 ± 5.98^{ijk}	3.56 ± 0.09	6.52 ± 0.11
	1.0	147.07 ± 9.52^{e}	301.23 ± 11.74^{hij}	3.43 ± 0.07	6.94 ± 0.04
	10.0	246.76 ± 11.89^{ab}	1084.90 ± 71.98^{b}	3.30 ± 0.07	8.94 ± 0.22

ND = non-detected.

3.2. Screening of efficient reducing agents for H_2 production by *A. halophytica*

H_2 production by *A. halophytica* cells incubated under dark anaerobic condition in N-deprived medium containing ten different types of reducing agents at final concentrations of 0.1, 1 and 10 mM was investigated. Maximum H_2 production rate of 256.53 ± 4.89, 251.87 ± 2.26, 246.76 ± 11.89 and 241.80 ± 16.08 μmol H_2 g dry weight^{-1} h^{-1} was found in N-deprived cells treated with 10 mM L-cysteine, dithiothreitol, sodium sulfide and β-mercaptoethanol, respectively, after 2 h incubation (Table 1). Interestingly, the highest yield of H_2 reached 1136.02 ± 41.44 μmol H_2 g dry weight^{-1} after treatment cells with 10 mM β-mercaptoethanol under dark anaerobic condition for 24 h (Table 1). It was approximately four folds higher than that of cells without any treatments. L-cysteine and sodium sulfide could also significantly enhance H_2 production by *A. halophytica* whereas dithiothreitol slightly increased H_2 production (Table 1).

In *A. halophytica*, H_2 production was dependent on types and concentrations of reducing agent (Table 1). The increased H_2 production by a treatment with sodium sulfide was probably due to a decrease in a level of O_2, an inhibitor of H_2ase. The previous study showed that in *Synechococcus* sp. UTEX 625, sodium sulfide at 150 μM could not affect O_2 evolution but sodium sulfide at 300 μM could reduce O_2 evolution by 30% [31]. As a result, H_2ase could be activated and finally the level of H_2 was highly produced. For L-cysteine, L-cysteine at 0.1 and 10 mM could enhance H_2 production by *A. halophytica* (Table 1). L-cysteine might function as a reducing agent by directly donating electrons towards H_2ase to produce H_2. Moreover, cysteine is known as one of the constituent molecules for cyanobacterial [NiFe]-H_2ase [32,33]. In [NiFe]--H_2ase, at active site Ni is coordinated by four cysteine-S ligands, two of which are bridging to the $Fe(CO)(CN)_2$ fragment [34]. In photo-fermentative bacterium *Rhodopseudomonas faecalis* RLD-53, L-cysteine could improve H_2 production by promoting the production of extracellular polymeric substances, especially secretion of protein containing more disulfide bonds, and help for enhancement stability of floc [35]. Similarly, L-cysteine at 0.1–1 mM increased H_2 production in bacterium *Clostridium butyricum* under dark anaerobic condition [36]. For dithiothreitol, it has been reported that dithiothreitol at 0.1 mM could also slightly stimulate H_2 production in nitrogen- and sulfur-deprived cells of *Synechocystis* sp. strain PCC 6803 under dark anaerobic condition [20]. Besides, the presence of methyl viologen and sodium dithionite at 0.1 mM could also gave the highest H_2 production rate by *A. halophytica* (Table 1). Dithionite-reduced methyl viologen is often used for an assay of H_2ase activity in cyanobacteria [37]. Previously, methyl viologen was shown to stimulate H_2 production in immobilized cells of *A. siamensis* TISTR 8012 incubated in sulfur- and nitrogen-deprived BG11 [18].

The lowest H_2 production rate of 3.06 ± 0.27 μmol H_2 g dry weight^{-1} h^{-1} was observed in cells treated with 1 mM oxalic acid (Table 1). Moreover, H_2 production could not be detected in cells treated with 10 mM ascorbic acid, formic acid and oxalic acid (Table 1). These acidic reducing agents with high concentration provided a low medium pH between 1.8 and 3.6 (Table 1). Proteins can be normally more positive or negative charge by earning or losing protons due to pH value. These acidic reducing agents might cause an isoelectric point of proteins and turn protein's charge into positive charge, resulting in protein structure loss from its natural structure or loss ability to bind metal ions at active site. Thus, H_2ase might probably be denatured in this acidic environment. The previous study showed that *A. halophytica* incubated in optimal seawater showed lower dark anaerobic H_2 production at low pH (pH 4.0) than that at neutral pH [11]. However, ascorbic acid and formic acid at low concentration (0.1 mM) could induce H_2 production compared with control cells without any supplementation. Similarly, ascorbate has been used as electron donor for *in vitro* H_2 production in cyanobacterium *Thermosynechococcus elongatus* [38]. Moreover, a decreased O_2 production and an increased H_2 production was obtained in *Chlamydomonas reinhardtii* CC124 cells incubated in reaction containing 1 mM ascorbate, 2 mM glucose and 0.2 mg mL^{-1} glucose oxidase under dark anaerobic condition [39].

Besides H_2 production measurement, effect of these reducing agents on cell concentration and pH of cell culture after treatment for 24 h was also investigated. The results revealed that some acidic reducing agents, for example, ascorbic acid, formic acid and oxalic acid, obviously decreased pH and cell concentrations. After treatment with 10 mM ascorbic acid, formic acid and oxalic acid, pH of cell culture was decreased to 3.68 ± 0.02, 3.18 ± 0.03 and 1.82 ± 0.09, respectively (Table 1). These reducing agents provide acidity, giving rise to a low pH which could cause a loss of enzyme activity and a toxicity to cells. As a result, these acidic reducing agents decreased chlorophyll and cell concentrations. As shown in Table 1, cell concentration was decreased from 3.63 × 10^9 cells mL^{-1} to 0.85 × 10^9 cells mL^{-1} or lower after treatment with 10 mM of these acidic reducing agents. Increasing the concentrations of these reducing agents resulted in a decrease of pH, i.e., an increase in H^+. This increased H^+ will tend to gain electrons, thus reducing the available electrons flowing to the hydrogenase, causing the decreased H_2 production. On the other hand, it is noted that pH of cell culture was high at 8.94 ± 0.22 when treated with 10 mM of an alkali reductant sodium sulfide yielding high H_2 production of 1084.90 ± 71.98 μmol H_2 g dry weight^{-1} (Table 1). From these results, β-mercaptoethanol, dithiothreitol, L-cysteine and sodium sulfide were chosen to study further due to the high yield of H_2 production and low impact on cell density.

3.3. Long-term H_2 production under various concentrations of reducing agents

In this study, H_2 production by N-deprived *A. halophytica* cells treated with various concentrations (0–100 μM) of the selected reducing agents, β-mercaptoethanol, dithiothreitol, L-cysteine, and sodium sulfide, under dark anaerobic condition up to 120 h was investigated. H_2 production of cells treated with all reducing agents tested was obviously increased within 24 h of incubation (Fig. 2). It was found that concentrations of reducing agents affected specifically H_2 production by *A. halophytica*. Among the four reducing agents, 50 mM sodium sulfide had the highest H_2 production of 4815.59 ± 194.78 μmol H_2 g dry weight^{-1} after 24 h of dark anaerobic incubation (Fig. 2D). In addition, 50 mM dithiothreitol and 50 mM L-cysteine could also provide high H_2 production of 3806.34 ± 50.82 and 3676.29 ± 102.02 μmol H_2 g dry weight^{-1}, respectively (Fig. 2B and C). Higher concentrations than 50 mM of these chemicals decreased H_2 production (Fig. 2A,B,C,D). A treatment with β-mercaptoethanol obviously resulted in lowest H_2 production (Fig. 2A).

H_2 accumulation in N-deprived *A. halophytica* cells was slightly declined after 24 h of incubation (Fig. 2). Normally, H_2 gas is hardly soluble in water. However, H_2 can be highly dissolved in liquid phase when there is high partial pressure of H_2 in the gas phase occurring in the sealed container. [40]. We suggested that a slight decrease in H_2 level might result from the headspace leak during needle injection and withdrawn of the container. Similar observation was found in agar-immobilized cells of *A. halophytica* [15] and in free cells of other cyanobacterial strains such as *Ficherella muscicola* TISTR 8215 [41] and *Lyngbya perelegans* [42].

O_2 production rate and H_2ase activity of cells treated with optimal concentrations of each reducing agent was determined. O_2 production rate was decreased in cells treated with all investigated reducing agents (Table 2). The lowest O_2 production rate of 3.59 ± 0.31 μmol O_2 g dry weight^{-1} h^{-1} was found in cells treated with 50 mM sodium sulfide (Table 2). Lower O_2 production rate led to higher H_2 production and H_2ase activity in *A. halophytica* depending on type of reducing agents. The maximum H_2 production of 4815.59 ± 194.78 μmol H_2 g dry weight^{-1} and H_2ase activity of 303.45 ± 3.15 μmol H_2 g dry weight^{-1} min^{-1} were found in cells treated with 50 mM sodium sulfide (Table 2). This

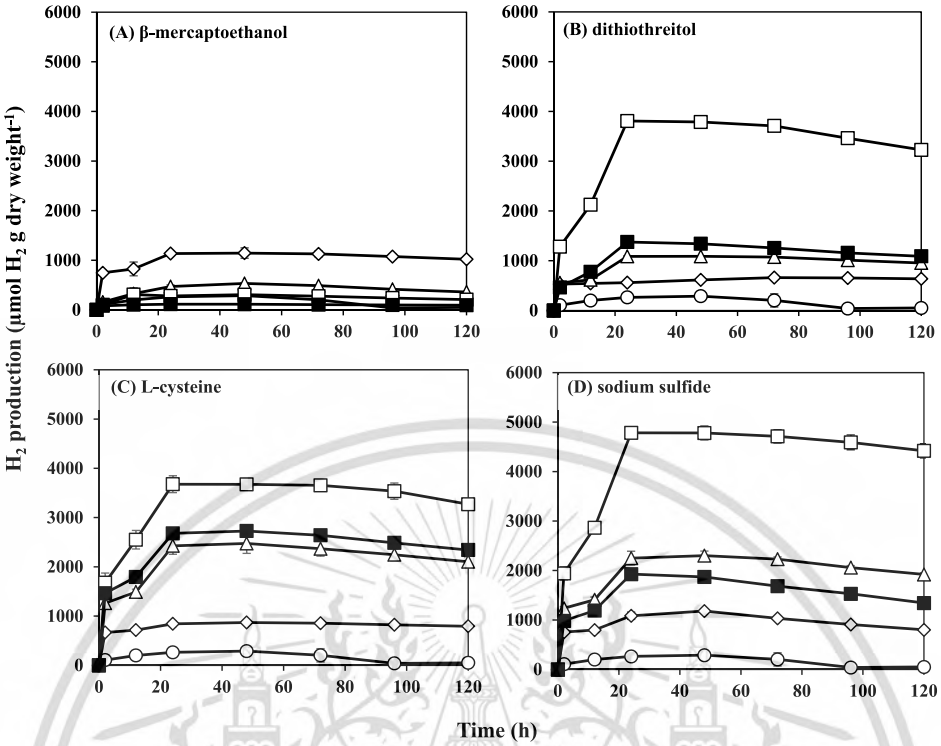

Fig. 2. Long-term H2 production by A. halophytica treated with different concentrations (0 mM ( ), 10 mM ( ), 20mM ( ), 50mM ( ) and 100 mM ( )) of β-mercaptoethanol (A), dithiothreitol (B), L-cysteine (C) and sodium sulfide (D) for various times under dark anaerobic condition. Data represents as mean ± SD of triplicate samples with a significance level of 95%.

Table 2
H_2 production, *in vivo* H_2ase activity and O_2 generation rate by *A. halophytica* after incubation in $BG11_0$ containing 10 mM β-mercaptoethanol, 50 mM dithiothreitol, 50 mM L-cysteine and 50 mM sodium sulfide under dark anaerobic condition for 24 h. H_2ase activity was measured after mixing cyanobacterial cell suspension with a reaction mixture for 30 min. Data represent mean ± SD. Superscripts with different letters show significant differences between samples with a significance level of 95%.

Reducing agents	H_2 production (μmol H_2 g dry weight^{-1})	H_2ase activity (μmol H_2 g dry weight^{-1} min^{-1})	O_2 generation rate (μmol O_2 g dry weight^{-1} h^{-1})
Control (No reductants)	264.10 ± 5.87^{e}	48.40 ± 2.03^{e}	37.56 ± 1.11^{a}
10 mM β-mercaptoethanol	1136.02 ± 41.44^{c}	101.88 ± 3.42^{d}	12.77 ± 0.70^{b}
50 mM dithiothreitol	3806.34 ± 50.82^{b}	251.98 ± 6.99^{c}	12.53 ± 1.29^{b}
50 mM L-cysteine	3676.29 ± 102.02^{b}	211.31 ± 2.62^{b}	8.17 ± 0.51^{c}
50 mM sodium sulfide	4815.59 ± 194.78^{a}	303.45 ± 3.15^{a}	3.59 ± 0.31^{d}

maximum H_2ase activity was six folds higher than that found in control cells without reducing agent treatment.

Sodium sulfide was suggested to be a favorite reducing agent to provide electrons towards H_2ase for higher H_2 production in *A. halophytica.* As selective reducing agents in this study, it could be suggested that sodium sulfide was favorable reducing agent for H_2 production under nitrogen-deprived and dark anaerobic condition by *A. halophytica* (Fig. 2). As previously shown in cyanobacterium *Oscillatoria limetica*, electrons from sulfide were transferred to an electron transport chain via photosystem I [43]. In addition, sodium sulfide can react with water and CO_2 to generate H_2S as a product. Under nitrogen- and sulfur-free medium, sulfide (5 μM) could be used as electron donor for H_2 photoproduction in *Synechococcus* sp. strain Miami BG043511 [21]. It provides a large number of electrons in the system. H_2S is suggested to cause an irreversible damage to PSII in most cyanobacteria, thus giving a low level of O_2 [44]. It could be suggested that sodium sulfide can reduce O_2 evolution and can also activate H_2ase activity in *A. halophytica* (Table 2). It has been previously shown that sodium sulfide at high concentration (300 μM) could reduce 30% O_2 evolution rate and Chl *a* fluorescence yield in *Synechococcus leopoliensis*, owing to the effect of H_2S [31].

Apart from sodium sulfide, dithiothreitol, L-cysteine and β-mercaptoethanol could induce H_2ase activity (Table 2). Dithiothreitol can react with O_2 producing 2-oxydithiothreitol [45]. This reaction causes an O_2 consumption, thus reducing a level of O_2 in a system and finally resulting in an enhancement of H_2 production. Cysteine is a constituent

molecule at active site of cyanobacterial [NiFe]-H_2ase [32,33]. Moreover, L-cysteine was shown to be bioactive agent for enhancing H_2 production in bacteria [36]. β-mercaptoethanol is also a reducing agent and is often used interchangeably with dithiothreitol. In *Synechocystis* sp. PCC 6803, β-mercaptoethanol could induce H_2ase activity under sulfur deprivation [20]. It is suggested that the type of reducing agent for stimulating H_2 production can vary depending on the cyanobacterial species.

3.4. Effect of reducing agents on cell toxicity

Cell toxicity and chlorophyll concentrations after treatment with various concentrations of reducing agents for 24 h were determined. IC_{50} of each reducing agent in N-deprived cells was also determined. The results showed that cell density and chlorophyll concentrations were decreased after treatment with high concentrations of reducing agents (Table 3). Dithiothreitol caused highest toxicity to cells with IC_{50} of 18.12 ± 2.07 mM followed by L-cysteine with IC_{50} of 60.96 ± 4.05 mM (Table 3). On the other hand, treatment with β-mercaptoethanol and sodium sulfide had little effect on cell and chlorophyll concentrations, as evidenced by high IC_{50} over 100 mM (Table 3). It was previously reported that 3 mM dithiothreitol decreased the specific growth rate of *Escherichia coli* MC4100 under anaerobic condition [46] and 10 mM L-cysteine could reduce the growth of *Anabaena cylindrica* PCC 7122 [47]. In autotrophic bacteria, toxicity of amino acids has been attributed to an imbalance of amino acid metabolism [48]. Cell toxicity by these reducing agents might be dependent on species of cyanobacteria. Since sodium sulfide was reported to be an electron donor of CO_2 photoassimilation in cyanobacteria [23], it is possible that *A. halophytica* might metabolize sulfide and could tolerate high concentrations of sodium sulfide. However, too high concentrations of sodium sulfide inhibited the growth of *A. halophytica*. The overall results indicate that sodium sulfide was an effective reducing agent for H_2 production by *A. halophytica* since it not only induced high H_2ase activity, but also showed a low cell toxicity.

Table 3
Cell concentration and chlorophyll *a* concentration of *A. halophytica* cells after incubation with various concentrations of selected reducing agents under dark anaerobic condition for 24 h. Data represent mean ± SD. Superscripts with different letters show significant differences between samples with a significance level of 95%. IC_{50} was determined as the concentration of reducing agent that inhibited cell concentration by 50%.

Reducing agents	Conc. (mM)	Cell concentration ($\times 10^9$ cells mL^{-1})	Chl a concentration (μg mL^{-1})	IC_{50} (mM)
CTRL	–	3.63 ± 0.11^{a}	22.39 ± 0.19^{a}	–
β-mercaptoethanol	0.1	3.44 ± 0.09^{abc}	18.37 ± 0.15^{c}	>100
	1.0	3.30 ± 0.07^{cd}	17.77 ± 0.25^{c}	
	10	3.11 ± 0.18^{def}	14.18 ± 0.19^{f}	
	20	2.98 ± 0.35^{fgh}	12.87 ± 0.32^{g}	
	50	2.81 ± 0.88^{h}	10.33 ± 0.15^{j}	
	100	2.56 ± 0.88^{ij}	9.14 ± 0.13^{lm}	
Dithiothreitol	0.1	3.15 ± 0.11^{def}	16.86 ± 0.34^{d}	18.12
	1.0	2.54 ± 0.12^{ij}	14.23 ± 0.27^{f}	± 2.07
	10	2.39 ± 0.09^{j}	9.47 ± 0.64^{kl}	
	20	1.56 ± 0.09^{l}	8.79 ± 0.49^{m}	
	50	0.54 ± 0.05^{m}	6.59 ± 0.65^{o}	
	100	0.19 ± 0.09^{n}	3.94 ± 0.23^{p}	
L-cysteine	0.1	3.41 ± 0.05^{bc}	17.09 ± 0.56^{d}	60.96
	1.0	3.29 ± 0.05^{cd}	15.03 ± 0.45^{e}	± 4.05
	10	3.08 ± 0.11^{efg}	11.82 ± 0.34^{h}	
	20	2.60 ± 0.14^{i}	11.17 ± 0.24^{i}	
	50	2.15 ± 0.14^{k}	7.93 ± 0.71^{n}	
	100	1.44 ± 0.08^{l}	7.63 ± 0.27^{n}	
Sodium sulfide	0.1	3.56 ± 0.09^{ab}	19.94 ± 0.33^{b}	>100
	1.0	3.43 ± 0.07^{bc}	14.99 ± 0.38^{e}	
	10	3.30 ± 0.07^{cd}	12.08 ± 0.25^{h}	
	20	3.20 ± 0.07^{de}	12.25 ± 0.22^{h}	
	50	3.06 ± 0.09^{efg}	10.49 ± 0.32^{j}	
	100	2.91 ± 0.05^{gh}	9.93 ± 0.29^{jk}	

3.5. Effect of ferredoxin, NADH and NADPH on in vitro H_2ase activity

The *in vitro* H_2ase activity from cell-free extract of *A. halophytica* treated with sodium dithionite-reduced ferredoxin, NADH and NADPH at different concentrations under anaerobic condition was determined. The results showed that *in vitro* H_2ase activity could not be detected in reactions containing 2 mM sodium dithionite and all concentrations of ferredoxin (1.5, 15, 150 μM and 1.5 mM) (Table 4). Neither was the activity detected in reactions containing low concentrations of NADH and NADPH (1.5 and 15 μM). On the contrary, *in vitro* H_2ase activity was shown in reactions containing dithionite-reduced ferredoxin, and high concentrations of NADH and NADPH (150 μM and 1.5 mM) (Table 4). The highest H_2ase activity with 115.25 ± 3.74 μmol H_2 g dry wt^{-1} min^{1} was found in cell-free extract treated with 1.5 mM ferredoxin plus 2 mM sodium dithionite (Table 4), which was about two folds higher activity than those treated with 1.5 mM NADH and NADPH (Table 4). The failure of activating H_2ase at low concentration of NAD(P)H was also observed in cell-free extract of *Synechocystis* sp. PCC 6803. It was suggested that NAD(P)H might activate H_2ase under high ratios of intracellular NAD(P)H/NAD(P) [7]. In this study, cell-free extract of *A. halophytica* was induced to enter anaerobic condition by using glucose, glucose oxidase and catalase before H_2ase activity measurement. The purified H_2ase should be used instead of the cell-free extract. However, due to the O_2 sensitivity of H_2ase the purification procedure was problematic in our laboratory. In fact, the cell-free extract which contains many kinds of proteins and enzymes provides a small amount of H_2ase, resulting in the lower H_2ase activity than the purified enzyme does.

In cyanobacteria, NADH and NADPH were suggested to act as a redox partner for [NiFe]-H_2ase [49,50]. Reduced ferredoxin/flavodoxin and NAD(P)H were shown to be an electron donor for [NiFe]-H_2ase in *Synechocystis* sp. PCC 6803 [7]. Our result indicated that ferredoxin reduced by sodium dithionite is a redox partner for [NiFe]-H_2ase in *A. halophytica*. This result agreed with previous studies showing the transfer of electron by ferredoxin towards [NiFe]-H_2ase of *Synechocystis*

Table 4
In vitro H_2ase activity from cell homogenate of *A. halophytica* in the presence of different types of electron donors; sodium dithionite, ferredoxin, NADH and NADPH. Cell homogenate in 100 mM phosphate buffer (pH 7.0) was added with glucose, glucose oxidase, and catalase to final concentration of 10 mM, 40 U mL^{-1} and 50 U mL^{-1}, respectively to enter an anaerobic condition. H_2 was measured by GC-TCD after incubation of cell homogenate and electron donor sources under dark anaerobic condition for 15 min. Data represent mean ± SD. Superscripts with different letters show significant differences between samples with a significance level of 95%.

Electron donors	*In vitro* H_2ase activity (μmol H_2 g dry $weight^{-1}$ min^{-1})
No electron donors (CTRL)	ND
2 mM sodium dithionite	ND
1.5 μM ferredoxin	ND
15 μM ferredoxin	ND
150 μM ferredoxin	ND
1.5 mM ferredoxin	ND
2 mM sodium dithionite + 1.5 μM ferredoxin	21.88 ± 1.04^{f}
2 mM sodium dithionite + 15 μM ferredoxin	34.02 ± 0.81^{e}
2 mM sodium dithionite + 150 μM ferredoxin	74.91 ± 3.07^{b}
2 mM sodium dithionite + 1.5 mM ferredoxin	115.25 ± 3.74^{a}
1.5 μM NADH	ND
15 μM NADH	ND
150 μM NADH	9.17 ± 0.19^{g}
1.5 mM NADH	57.34 ± 2.48^{c}
1.5 μM NADPH	ND
15 μM NADPH	ND
150 μM NADPH	5.58 ± 0.33^{g}
1.5 mM NADPH	51.07 ± 3.04^{d}

ND = non-detected.

sp. PCC 6803 [7]. In addition, NADH and NADPH at high concentrations (150 μM and 1.5 mM) also increased H_2 production *in vitro* by providing electrons towards [NiFe]-H_2ase in *A. halophytica* (Table 4). It is noted that NADH and NADPH at low concentrations were not able to efficiently transport electrons to H_2ase (Table 4). These results indicated that both NADH and NADPH could act as an electron donor for [NiFe]-H_2ase in *A. halophytica.* Under nitrogen deprivation, glycogen was accumulated with an increase of 30% in *A. halophytica* [11]. When cells were grown under dark anaerobic condition, cells degraded the accumulated glycogen into glucose, a substrate used for donating electron and fermentation of H_2 [29]. Glucose obtained during dark anaerobic condition provided NADPH via oxidative pentose phosphate (OPP) pathway and NADH via glycolytic pathway [51]. Therefore, nitrogen deprivation enhances both NADH and NADPH, providing electron transfer to activate [NiFe]-H_2ase activity and finally enhancing H_2 production under dark anaerobic condition. In this study, NADH, NADPH and reduced ferredoxin were checked as the redox partners of [NiFe]-H_2ase in *A. halophytica*. In *Synechocystis* sp. PCC 6803, H_2ase activity of intact cells was stimulated by the addition of NADH and ferredoxin compared with that without addition [20]. Furthermore, reduced ferredoxin has been previously shown as a redox partner for H_2ase enzyme in *Synechocystis* sp. PCC 6803 [7]. NADH and NADPH generated from glycolysis and pentose phosphate pathway, respectively, have been reported to be redox partners for bidirectional hydrogenase in *Synechocystis* sp. PCC 6803 [7,49,52]. In conclusion, NAD(P)H and ferredoxin play an important role as an electron partner for [NiFe]--H_2ase enzyme for H_2 evoluton in *A. halophytica*. However, the preference of electron partners for [NiFe]-H_2ase is suggested to be ferredoxin since ferredoxin at low concentration (only 1.5 μM) could better activate [NiFe]-H_2ase.

4. Conclusion

A. halophytica showed 1.5 folds increase of H_2 production in the presence of glucose as a reducing sugar under dark anaerobic and nitrogen-deprived condition. Four types of reducing agents, β-mercaptoethanol, dithiothreitol, L-cysteine and sodium sulfide, could enhance H_2 production in *A. halophytica*. However, the optimal concentration for H_2 production was dependent on the type of reducing agents. Sodium sulfide at 50 mM stimulated the highest H_2 production, resulting from the highest *in vivo* H_2ase activity and lowest O_2 generation rate. Moreover, sodium sulfide and β-mercaptoethanol showed less cell toxicity than other two reducing compounds. In this study, reduced ferredoxin, NADH and NADPH could produce H_2 by providing electrons towards bidirectional [NiFe]-H_2ase in *A. halophytica*. H_2 production by *A. halophytica* incubated in nitrogen-deprived medium under dark anaerobic condition was suggested to be catalyzed by only bidirectional [NiFe]-H_2ase. Whether H_2 is produced by nitrogenase activity in such condition, further study is needed to clarify.

Data availability

No data was used for the research described in the article.

Acknowledgements

This study was financially supported by research grant from Faculty of Science, King Mongkut's Institute of Technology Ladkrabang (KMITL) Thailand (2563-02-05-33). Nattanon Chinchusak would like to thank School of Science, KMITL for a Ph.D. scholarship.

References

[1] J.H. Perry, Chemical Engineers' Handbook, McGraw-Hill, New York, 1963.
[2] K.J. Reddy, J.B. Haskell, D.M. Sherman, L.A. Sherman, Unicellular, aerobic nitrogen-fixing cyanobacteria of the genus *Cyanothece*, J. Bacteriol. 175 (5) (1993) 1284–1292.
[3] T.J. Chow, F.R. Tabita, Reciprocal light-dark transcriptional control of *nif* and *rbc* expression and light-dependent posttranslational control of nitrogenase activity in *Synechococcus* sp. strain RF-1, J. Bacterial. 176 (20) (1994) 6281–6285.
[4] J. Compaoré, L.J. Stal, Oxygen and the light–dark cycle of nitrogenase activity in two unicellular cyanobacteria, Environ. Microbiol. 12 (1) (2010) 54–62.
[5] S. Taikhao, S. Junyapoon, A. Incharoensakdi, S. Phunpruch, Factors affecting biohydrogen production by unicellular halotolerant cyanobacterium *Aphanothece halophytica*, J. Appl. Phycol. 25 (2) (2013) 575–585.
[6] J. Sjoholm, P. Oliveira, P. Lindblad, Transcription and regulation of the bidirectional hydrogenase in the cyanobacterium *Nostoc* sp. strain PCC 7120, Appl. Environ. Microbiol. 73 (17) (2007) 5435–5446.
[7] K. Gutekunst, X. Chen, K. Schreiber, U. Kaspar, S. Makam, J. Appel, The bidirectional NiFe-hydrogenase in *Synechocystis* sp. PCC 6803 is reduced by flavodoxin and ferredoxin and is essential under mixotrophic, nitrate-limiting conditions, J. Biol. Chem. 289 (4) (2014) 1930–1937.
[8] T. Kentemich, M. Bahnweg, F. Mayer, H. Bothe, Localization of the reversible hydrogenase in cyanobacteria, Z. Naturforsch. C. 44 (5–6) (1989) 384–391.
[9] L.T. Serebryakova, M.E. Sheremetieva, A.A. Tsygankov, Reversible hydrogenase activity of *Gloeocapsa alpicola* in continuous culture, FEMS Microbiol. Lett. 166 (1) (1998) 89–94.
[10] P. Tamagnini, E. Leitão, P. Oliveira, D. Ferreira, F. Pinto, D.J. Harris, P. Lindblad, Cyanobacterial hydrogenases: diversity, regulation and applications, FEMS Microbiol. Rev. 31 (6) (2007) 692–720.
[11] S. Taikhao, A. Incharoensakdi, S. Phunpruch, Dark fermentative hydrogen production by the unicellular halotolerant cyanobacterium *Aphanothece halophytica* grown in seawater, J. Appl. Phycol. 27 (1) (2015) 187–196.
[12] S. Belkin, E. Padan, Hydrogen metabolism in the facultative anoxygenic cyanobacteria (blue-green algae) *Oscillatoria limnetica* and *Aphanothece halophytica*, Arch. Microbiol. 116 (1) (1978) 109–111.
[13] S. Phunpruch, S. Taikhao, A. Incharoensakdi, Identification of bidirectional hydrogenase genes and their co-transcription in unicellular halotolerant cyanobacterium *Aphanothece halophytica*, J. Appl. Phycol. 28 (2) (2016) 967–978.
[14] P.K. Singh, Nitrogen fixation by the unicellular blue-green alga *Aphanothece*, Arch. Microbiol. 92 (1) (1973) 59–62.
[15] S. Pansook, A. Incharoensakdi, S. Phunpruch, Enhanced dark fermentative H_2 production by agar-immobilized cyanobacterium *Aphanothece halophytica*, J. Appl. Phycol. 31 (5) (2019) 2869–2879.
[16] S. Pansook, A. Incharoensakdi, S. Phunpruch, Effects of the photosystem II inhibitors CCCP and DCMU on hydrogen production by the unicellular halotolerant cyanobacterium *Aphanothece halophytica*, Sci. World J. (2019), 1030236.
[17] S. Pansook, A. Incharoensakdi, S. Phunpruch, Simazine enhances dark fermentative H_2 production by unicellular halotolerant cyanobacterium *Aphanothece halophytica*, Front. Bioeng. Biotechnol. 10 (2022), 904101.
[18] A.K. Sadvakasova, B.D. Kossalbayev, B.K. Zayadan, K. Bolatkhan, S. Alwasel, M. M. Najafpour, S.I. Allakhverdiev, Bioprocesses of hydrogen production by cyanobacteria cells and possible ways to increase their productivity, Renew. Sustain. Energy Rev. 133 (2020), 110054.
[19] S. Taikhao, S. Phunpruch, Increasing hydrogen production efficiency of N_2-fixing cyanobacterium *Anabaena siamensis* TISTR 8012 by cell immobilization, Energy Proc. 138 (2017) 366–371.
[20] W. Baebprasert, P. Lindblad, A. Incharoensakdi, Response of H_2 production and Hox-hydrogenase activity to external factors in the unicellular cyanobacterium *Synechocystis* sp. strain PCC 6803, Int. J. Hydrogen Energy 35 (13) (2010) 6611–6616.
[21] Y.H. Luo, A. Mitsui, Sulfide as electron source for H_2-photoproduction in the cyanobacterium *Synechococcus* sp., strain Miami BG 043511, under stress conditions, J. Photochem. Photobiol. B Biol. 35 (3) (1996) 203–207.
[22] R. Rippka, J. Deruelles, J.B. Waterbury, M. Herdman, R.Y. Stanier, Generic assignments, strain histories and properties of pure cultures of cyanobacteria, Microbiol. 111 (1) (1979) 1–61.
[23] S. Garlick, A. Oren, E. Padan, Occurrence of facultative anoxygenic photosynthesis among filamentous and unicellular cyanobacteria, J. Bacteriol. 129 (2) (1977) 623–629.
[24] G. Mackinney, Absorption of light by chlorophyll solutions, J. Biol. Chem. 140 (2) (1941) 315–322.
[25] Y.H. Luo, A. Mitsui, Hydrogen production from organic substrates in an aerobic nitrogen-fixing marine unicellular cyanobacterium *Synechococcus* sp. strain Miami BG 043511, Biotechnol. Bioeng. 44 (10) (1994) 1255–1260.
[26] W. Khetkorn, P. Lindblad, P.A. Incharoensakdi, Enhanced H_2 production with efficient N_2-fixation by fructose mixotrophically grown *Anabaena* sp. PCC 7120 strain disrupted in uptake hydrogenase, Algal Res. 47 (2020), 101823.
[27] P.C. Chen, S.H. Fan, C.L. Chiang, C.M. Lee, Effect of growth conditions on the hydrogen production with cyanobacterium *Anabaena* sp. strain CH3, Int. J. Hydrogen Energy 33 (5) (2008) 1460–1464.
[28] P.M. Reddy, H. Spiller, S.L. Albrecht, K.T. Shanmugam, Photodissimilation of fructose to H_2 and CO_2 by a dinitrogen-fixing cyanobacterium, *Anabaena variabilis*, Appl. Environ. Microbiol. 62 (4) (1996) 1220–1226.
[29] L.J. Stal, R. Moezelaar, Fermentation in cyanobacteria, FEMS Microbiol. Rev. 21 (2) (1997) 179–211.
[30] J. Appel, S. Craig, M. Theune, V. Hüren, S. Künzel, B. Forberich, S. Bryan, K. Gutekunst, Evidence for electron transfer from the bidirectional hydrogenase to the photosynthetic complex I (NDH-1) in the cyanobacterium *Synechocystis* sp. PCC 6803, Microorganisms 10 (8) (2022) 1617.
[31] G.S. Espie, A.G. Miller, D.T. Canvin, Selective and reversible inhibition of active CO_2 transport by hydrogen sulfide in a cyanobacterium, Plant Physiol. 91 (1) (1989) 387–394.

[32] O. Schmitz, H. Bothe, The diaphorase subunit HoxU of the bidirectional hydrogenase as electron transferring protein in cyanobacterial respiration? Naturwissenschaften 83 (11) (1996) 525–527.
[33] A. Volbeda, M.H. Charon, C. Piras, E.C. Hatchikian, M. Frey, J.C. Fontecilla-Camps, Crystal structure of the nickel–iron hydrogenase from *Desulfovibrio gigas*, Nature 373 (6515) (1995) 580–587.
[34] Z. Li, Y. Ohki, K. Tatsumi, Dithiolato-bridged dinuclear iron-nickel complexes [Fe $(CO)_2$ $(CN)_2$ (μ-$SCH_2CH_2CH_2S$) Ni (S_2CNR_2)]-Modeling the active site of [NiFe] hydrogenase, J. Am. Chem. Soc. 127 (25) (2005) 8950–8951.
[35] G.J. Xie, B.F. Liu, D.F. Xing, J. Nan, J. Ding, N.Q. Ren, Photo-fermentative bacteria aggregation triggered by L-cysteine during hydrogen production, Biotechnol, Biofuels 6 (1) (2013) 1–14.
[36] Z. Yuan, H. Yang, X. Zhi, J. Shen, Enhancement effect of L-cysteine on dark fermentative hydrogen production, Int. J. Hydrogen Energy 33 (22) (2008) 6535–6540.
[37] A. Daday, G.R. Lambert, G.D. Smith, Measurement in vivo of hydrogenase-catalysed hydrogen evolution in the presence of nitrogenase enzyme in cyanobacteria, Biochem. J. 177 (1) (1979) 139–144.
[38] I.J. Iwuchukwu, M. Vaughn, N. Myers, H. O'neill, P. Frymier, B.D. Bruce, Self-organized photosynthetic nanoparticle for cell-free hydrogen production, Nat. Nanotechnol. 5 (1) (2010) 73–79.
[39] V. Nagy, A. Podmaniczki, A. Vidal-Meireles, R. Tengölics, L. Kovács, G. Rákhely, A. Scoma, S.Z. Tóth, Water-splitting-based, sustainable and efficient H_2 production in green algae as achieved by substrate limitation of the Calvin-Benson-Bassham cycle, Biotechnol. Biofuels 11 (1) (2018) 69.
[40] Y. Zhao, T. Zhou, Y. Zhao, T. Zhou (Eds.), Anaerobic Fermentation Process for Biohydrogen Production from Food Waste, Biohydrogen Production and Hybrid Process Development, Elsevier, 2021, pp. 1–24.
[41] P. Wutthithien, P. Lindblad, A. Incharoensakdi, Improvement of photobiological hydrogen production by suspended and immobilized cells of the N_2-fixing cyanobacterium *Fischerella muscicola* TISTR 8215, J. Appl. Phycol. 31 (6) (2019) 3527–3536.
[42] K. Anjana, A. Kaushik, A. Enhanced hydrogen production by immobilized cyanobacterium *Lyngbya perelegans* under varying anaerobic conditions, Biomass Bioenergy 63 (2014) 54–57.
[43] S. Belkin, E. Padan, Sulfide-dependent hydrogen evolution in the cyanobacterium *Oscillatoria limnetica*, FEBS Lett. 94 (2) (1978) 291–294.
[44] Y. Cohen, B.B. Jørgensen, N.P. Revsbech, R. Poplawski, Adaptation to hydrogen sulfide of oxygenic and anoxygenic photosynthesis among cyanobacteria, Appl. Environ. Microbiol. 51 (2) (1986) 398–407.
[45] A.V. Kachur, K.D. Held, C.J. Koch, J.E. Biaglow, Mechanism of production of hydroxyl radicals in the copper-catalyzed oxidation of dithiothreitol, Radiat. Res. 147 (4) (1997) 409–415.
[46] G. Kirakosyan, K. Bagramyan, A. Trchounian, Redox sensing by *Escherichia coli*: effects of dithiothreitol, a redox reagent reducing disulphides, on bacterial growth, Biochem. Biophys. Res. Commun. 325 (3) (2004) 803–806.
[47] D.M. Rawson, The effects of exogenous amino acids on growth and nitrogenase activity in the cyanobacterium *Anabaena cylindrica* PCC 7122, Microbiol. 131 (10) (1985) 2549–2554.
[48] M. Eccleston, D.P. Kelly, Assimilation and toxicity of exogenous acids amino in the methane-oxidizing bacterium *Methylococcus capsulatus*, Microbiol. 71 (3) (1972) 541–554.
[49] L. Cournac, G. Guedeney, G. Peltier, P.M. Vignais, Sustained photoevolution of molecular hydrogen in a mutant of *Synechocystis* sp. strain PCC 6803 deficient in the type I NADPH-dehydrogenase complex, J. Bacteriol. 186 (6) (2004) 1737–1746.
[50] L.T. Serebryakova, M.E. Sheremetieva, Characterization of catalytic properties of hydrogenase isolated from the unicellular cyanobacterium *Gloeocapsa alpicola* CALU 743, Biochem. (Mosc.) 71 (12) (2006) 1370–1376.
[51] G.K. Kumaraswamy, T. Guerra, X. Qian, S. Zhang, D.A. Bryant, G.C. Dismukes, Reprogramming the glycolytic pathway for increased hydrogen production in cyanobacteria: metabolic engineering of NAD^+-dependent GAPDH, Energy Environ. Sci. 6 (12) (2013) 3722–3731.
[52] F. Germer, I. Zebger, M. Saggu, F. Lendzian, R. Schulz, J. Appel, Overexpression, isolation, and spectroscopic characterization of the bidirectional [NiFe] hydrogenase from *Synechocystis* sp. PCC 6803, J. Biol. Chem. 284 (52) (2009) 36462–36472.

frontiers | Frontiers in Bioengineering and Biotechnology

TYPE Original Research
PUBLISHED 06 January 2023
DOI 10.3389/fbioe.2022.1028151

OPEN ACCESS

EDITED BY
Suyun Xu,
University of Shanghai for Science and Technology, China

REVIEWED BY
Amit Srivastava,
University of Jyväskylä, Finland
Binghua Yan,
Hunan Agricultural University, China
Jun Zhou,
Nanjing Tech University, China

*CORRESPONDENCE
Saranya Phunpruch,
saranya.ph@kmitl.ac.th

SPECIALTY SECTION
This article was submitted to Industrial Biotechnology, a section of the journal Frontiers in Bioengineering and Biotechnology

RECEIVED 25 August 2022
ACCEPTED 19 December 2022
PUBLISHED 06 January 2023

CITATION
Chinchusak N, Incharoensakdi A and Phunpruch S (2023), Dark fermentative hydrogen production and transcriptional analysis of genes involved in the unicelllular halotolerant cyanobacterium *Aphanothece halophytica* under nitrogen and potassium deprivation. *Front. Bioeng. Biotechnol.* 10:1028151. doi: 10.3389/fbioe.2022.1028151

Dark fermentative hydrogen production and transcriptional analysis of genes involved in the unicellular halotolerant cyanobacterium *Aphanothece halophytica* under nitrogen and potassium deprivation

Nattanon Chinchusak[1], Aran Incharoensakdi[2,3] and Saranya Phunpruch[1,4]*

[1]Department of Biology, School of Science, King Mongkut's Institute of Technology Ladkrabang, Bangkok, Thailand, [2]Laboratory of Cyanobacterial Biotechnology, Department of Biochemistry, Faculty of Science, Chulalongkorn University, Bangkok, Thailand, [3]Academy of Science, Royal Society of Thailand, Bangkok, Thailand, [4]Bioenergy Research Unit, School of Science, King Mongkut's Institute of Technology Ladkrabang, Bangkok, Thailand

The unicellular halotolerant cyanobacterium *Aphanothece halophytica* is known as a potential hydrogen (H_2) producer. This study aimed to investigate the enhancement of H_2 production under nutrient deprivation. The results showed that nitrogen and potassium deprivation induced dark fermentative H_2 production by *A. halophytica*, while no differences in H_2 production were found under sulfur and phosphorus deprivation. In addition, deprivation of nitrogen and potassium resulted in the highest H_2 production in *A. halophytica* due to the stimulation of hydrogenase activity. The effect of adaptation time under nitrogen and potassium deprivation on H_2 production was investigated. The results showed that the highest H_2 accumulation of 1,261.96 ± 96.99 μmol H_2 g dry wt^{-1} and maximum hydrogenase activity of 179.39 ± 8.18 μmol H_2 g dry wt^{-1} min^{-1} were obtained from *A. halophytica* cells adapted in the nitrogen- and potassium-deprived BG11 medium supplemented with Turk Island salt solution ($BG11_0$-K) for 48 h. An increase in hydrogenase activity was attributed to the decreased O_2 concentration in the system, due to a reduction of photosynthetic O_2 evolution rate and a promotion of dark respiration rate. Moreover, nitrogen and potassium deprivation stimulated glycogen accumulation and decreased specific activity of pyruvate kinase. Transcriptional analysis of genes involved in H_2 metabolism using RNA-seq confirmed the above results. Several genes involved in glycogen biosynthesis (*glgA*, *glgB*, and *glgP*) were upregulated under both nitrogen and potassium deprivation, but genes regulating enzymes in the glycolytic pathway were downregulated, especially *pyk* encoding pyruvate kinase. Interestingly, genes involved in the oxidative pentose phosphate pathway (OPP) were upregulated. Thus, OPP became the favored pathway for glycogen catabolism and the generation of reduced nicotinamide adenine dinucleotide phosphate (NADPH), which resulted in an increase in H_2 production under dark anaerobic condition in both nitrogen- and potassium-deprived cells.

KEYWORDS

***Aphanothece halophytica*, hydrogen production, gene expression, potassium deprivation, nitrogen deprivation**

1 Introduction

Huge amounts of energy are used by humans in households, in industry, and in agriculture. Fossil fuel is the main energy source worldwide, but it is non-renewable and limited in supply. Due to annual increases in energy consumption, there is a high demand for fossil fuel. As a result, greenhouse gases produced from the combustion of fossil fuels have increased. This has led to environmental problems, including global warming. In addition, the amount of fossil fuel will not be sufficient for human energy consumption in the future. Hydrogen (H_2) is an alternative energy carrier that can be used instead of the limited fossil fuel resources since its combustion releases a high heating value of 141.6 MJ kg^{-1} (Perry 1963). This combustion of H_2 is an environmentally friendly process that does not produce greenhouse gases as by-products (Gupta and Parkhey 2017). H_2 can be produced by various types of microorganisms, such as purple bacteria, green sulfur bacteria, green algae, and cyanobacteria.

Cyanobacteria or blue-green algae are prokaryotic and photoautotrophic microorganisms that have oxygenic photosynthetic activity (Bothe et al., 2010). Cyanobacteria can convert abundant raw materials for photosynthesis such as water, sunlight, and CO_2 into carbohydrate and O_2. Cyanobacteria can produce H_2 through many processes, depending on the cyanobacterial type and metabolism. Three enzymes are involved in H_2 metabolism in cyanobacteria, namely, bidirectional hydrogenase, uptake hydrogenase, and nitrogenase (Khetkorn et al., 2013). Despite the fact that cyanobacteria are capable of photobiological H_2 production, all enzymes involved are sensitive to O_2. To sustain and increase the yield of H_2 production and prevent enzyme inactivity from O_2, a two-stage H_2 production scheme was proposed (Ananyev et al., 2012). In the first stage, cyanobacteria are grown in complete media to accumulate biomass. Then, cells enter the second stage by incubating under stress conditions and produce H_2 when anaerobic conditions are established.

The deliberate depletion of nutrients in media is a technique used to induce H_2 production and is an effective way to maintain sustainable H_2 production in cyanobacteria (Srirangan et al., 2011). Under nitrogen deprivation, *A. halophytica* shows high H_2 production in dark anaerobic conditions (Taikhao et al., 2013; Taikhao et al., 2015). Moreover, nitrogen deprivation also induces H_2 evolution in *Oscillatoria brevis*, *Calothrix membranacea* (Lambert and Smith 1977), and Anabaena siamensis TISIR 8012 (Khetkorn et al., 2010; Taikhao and Phunpruch 2017). Under nitrogen deprivation, the accumulation of glycogen is carried out *via* photoautotrophic processes. The accumulated glycogen is degraded into glucose-6-phosphate with the generation of reduced nicotinamide adenine dinucleotide phosphate (NADPH), the electron donor of [NiFe]-H_2ase, and hydrogen is generated thereafter under dark anaerobic conditions (Ananyev et al., 2008). Previous research showed that under nitrogen deprivation, the bidirectional H_2ase activity of *A. halophytica* was obviously induced during dark anaerobic incubation and the expression of *narB* encoding ferredoxin-nitrate reductase was downregulated (Phunpruch et al., 2016). Consequently, reduced nicotinamide adenine dinucleotide (NADH) was enhanced and subsequently H_2 was increasingly generated (Phunpruch et al., 2016). In addition, sulfur deprivation enhanced H_2 production in *Gloeocapsa alpicola* (Antal and Lindblad 2005) and Microcystis aeruginosa (Rashid et al., 2009). Potassium deficiency increased H_2 production by *Synechocystis* sp. PCC 6803 (Ueda et al., 2016).

The unicellular halotolerant cyanobacterium *Aphanothece halophytica*, originally isolated from Solar Lake (Israel), has the ability to grow at high salinity at concentrations of NaCl up to 3 M (Takabe et al., 1988). Since it is an obligately halophilic strain that is unable to grow under NaCl-deprived conditions, it is a model microorganism for studying the halotolerance mechanism in cyanobacteria. *A. halophytica* is well able to produce dark fermentative H_2 under nitrogen depletion in enriched medium (Taikhao et al., 2013). It has advantages of growing and producing H_2 when cells were incubated in natural seawater without any supplementation of $NaNO_3$ (Taikhao et al., 2015). The bidirectional [NiFe]-H_2ase was identified in *A. halophytica* (Phunpruch et al., 2016). Moreover, H_2 production by *A. halophytica* was enhanced by cell immobilization using alginate and agar (Pansook et al., 2016; Pansook et al., 2019a). In addition, *A. halophytica* treated with photosystem II inhibitors clearly increased H_2 production (Pansook et al., 2019b). Recently, simazine, an herbicide of the triazine class, was shown to significantly enhance H_2 production by *A. halophytica* under dark anaerobic condition (Pansook et al., 2022). In addition, sodium sulfide was an effective reducing agent for enhancing H_2 production by *A. halophytica* due to the reduced O_2 concentration in the system, thus increasing hydrogenase activity (Chinchusak et al., 2022).

In this study, we focused on H_2 production by *A. halophytica* under nutrient-deprived conditions and investigated H_2 metabolism under these conditions. Photosynthesis and carbon and nitrogen assimilation pathways in N- and K-deprived cells were studied by RNA-seq based transcriptome analysis. H_2ase activity, glycogen content, and pyruvate kinase activity were also determined. The patterns of the transcriptome and experimental evidence were mutually supportive.

2 Materials and methods

2.1 Cyanobacterial cultivation

Aphanothece halophytica was grown photoautotrophically in a 250-ml Erlenmeyer flask containing 100 ml of BG11 medium (pH 7.4) (Rippka et al., 1979) supplemented with Turk Island salt solution (Garlick et al., 1977). The BG11 medium consisted of 17.6 mM $NaNO_3$ as a nitrogen source. The Turk Island salt solution contained high concentrations of minerals, including 0.5 M NaCl, 49 mM $MgCl_2 \bullet 6H_2O$, 30 mM $MgSO_4 \bullet 7H_2O$, and 8.9 mM KCl as main components. Cells were initially adjusted to a density of OD_{730} at approximately 0.1 and subsequently shaken at 120 rpm on a rotary shaker at 30°C under a white-light fluorescence intensity of 30 μmol photons m^{-2} s^{-1} with a light (18 h/day): dark (6 h/day) cycle for 7 days.

2.2 Cyanobacterial adaptation condition under nutrient deprivation

H_2 production by A. halophytica was measured as part of its two-stage cultivation. Firstly, A. halophytica was grown in BG11 with Turk Island salt solution for 7 days to accumulate biomass. The seven-day-

old cells were harvested by centrifugation at 8,000 × g at 4 C for 10 min before resuspension in various types of single nutrient-depleted media: nitrogen-deprived BG11 supplemented with Turk Island salt solution ($BG11_0$), phosphorus-deprived BG11 supplemented with Turk Island salt solution (BG11-P), potassium-deprived BG11 supplemented with Turk Island salt solution (BG11-K), and sulfur-deprived BG11 supplemented with Turk Island salt solution (BG11-S). To remove nitrogen in $BG11_0$, $NaNO_3$ was omitted from BG11. In BG11-P, NaH_2PO_4 was omitted from BG11. To remove potassium from BG11-K, KCl was omitted from Turk Island salt solution. In addition, K_2HPO_4 was also omitted from BG11 and replaced by the addition of Na_2HPO_4. In BG11-S, $ZnSO_4{\bullet}7H_2O$ and $CuSO_4{\bullet}5H_2O$ were omitted from BG11 and replaced by $ZnCl_2$ and $CuCl_2$, respectively. In addition, $MgSO_4{\bullet}7H_2O$ was omitted from both BG11 and Turk Island salt solution and replaced by the addition of $MgCl_2$. Thereafter, the cell suspensions were incubated for 24 h before H_2 was measured, under anaerobic conditions.

2.3 H_2 measurement

Aphanothece halophytica adapted in each single nutrient-deprived media for 24 h was harvested by centrifugation and resuspended in a fresh medium. Five ml of cell suspension was transferred to a 10-ml glass vial. The vial was sealed with a rubber stopper and the cyanobacterial cells were made to enter anaerobic conditions by purging with argon gas for 10 min. Each cell suspension was then incubated at 30°C under darkness for 2 h before H_2 measurement was undertaken. H_2 measurement was performed using a Gas Chromatograph (Hewlett-Packard HP5890A, Japan) with a molecular sieve 5 °A 60/80 mesh packed column and a thermal conductivity detector using argon as the carrier gas (Baebprasert et al., 2010). H_2 production was expressed as μmol H_2 evolved per milligram dry cell weight. All experiments were done in triplicate.

2.4 Hydrogenase activity measurement

Bidirectional hydrogenase activity was determined by measuring H_2 evolution in the presence of dithionite-reduced methyl viologen. The reaction mixture comprised 1 ml of cell suspension and 1 ml of 25 mM sodium phosphate buffer (pH 7.6) containing 10 mM methyl viologen dichloride hydrate (Roche, Germany) and 40 mM sodium dithionite (Sigma, Germany). The mixture was incubated under argon atmospheric conditions at 30°C under darkness for 30 min. H_2 from headspace was subsequently analyzed by a gas chromatograph.

2.5 Dry cell weight and glycogen content determination

For each dry cell weight determination, 5 ml of cyanobacterial cell suspension was filtered through a glass microfiber filter GF/C (Whatman, United Kingdom). Sterile distilled water was used to wash the cells collected on the microfiber filter. Then, the filter containing cells was dried in an oven at 70°C until weight was constant. The dry cell weight was calculated. For glycogen content determination, glycogen extraction and hydrolysis were performed following the previous studied procedure (Ernst et al., 1984). *A. halophytica* cells that had been adapted in various media were harvested by centrifugation at 8,000 × g at 4°C for 10 min and resuspended in fresh medium that contained chlorophyll *a* at a concentration of 300 μg chl *a* mL^{-1}. Fifty μL of each cell suspension was added to 200 μL of 30% (w/v) KOH. The mixture was then incubated at 100 °C in a water bath for 90 min. Cells were lysed by ultrasonication at 20% pulse for 5 min on ice. To precipitate glycogen, 600 μL of absolute ethanol was added into the extract. Each sample was kept on ice for 1 h. Glycogen was collected by centrifugation at 12,000 × g for 5 min at 4 C. Then, each glycogen pellet was washed twice by absolute ethanol and subsequently dried at 60°C for 10 min. Glycogen was resuspended in 300 μL of 100 mM acetate buffer (pH 4.75). For each sample, glycogen was digested into glucose by adding amyloglucosidase from *Aspergillus niger* (Sigma, United States) and α-amylase from *Aspergillus oryzae* (Sigma, Switzerland) at final concentrations of 4 and 8 units, respectively. The reaction was incubated at 25°C for 1 h. Insoluble membrane fragments were removed by centrifugation at 12,000 × g at 4°C for 5 min. Total sugar in each supernatant was determined by phenol-sulfuric acid assay (Dubois et al., 1956). Standard glycogen from bovine liver (Sigma, United States) (0–100 μg) was used. The glycogen content was calculated using a standard calibration curve. Each experiment was performed in triplicate.

2.6 Pyruvate kinase activity determination

Pyruvate kinase activity was determined indirectly by measuring the oxidation of NADH in the reaction catalyzed by lactate hydrogenase. The activity of pyruvate kinase was determined by a protocol previously described (Malcovati and Valentini, 1982). To prepare cell-free extract of *A. halophytica*, 100 ml of *A. halophytica* cell culture was harvested by centrifugation at 8,000 × g at 4°C for 10 min and subsequently resuspended in 1 ml of 10 mM (2-[4-(2-hydroxyethyl) piperazine-1-yl] ethanesulfonic acid (HEPES) buffer (pH 7.5). Cells were lysed using 20% pulse of ultrasonication on ice for 5 min. The cell-free extract was obtained after centrifugation at 8,000 × g at 4°C for 10 min. To assay pyruvate kinase activity, 50 μL of cell-free extract was added into 950 μL of reaction mixture containing 10 mM HEPES buffer, 10 mM $MgCl_2$, 50 mM KCl, 20 mM ADP (Adenosine 5′-diphosphate sodium salt) (Sigma, United States), 10 mM PEP (Phosphoenolpyruvic acid monopotassium salt) (Sigma, Switzerland), 5 mM NADH (β-nicotinamide adenine dinucleotide, reduced disodium salt hydrate) (Sigma, United States), and 0.5 U of L-lactate dehydrogenase (Roche, Germany). The reaction mixture without PEP was used as a negative control. The decrease of NADH was measured spectrophotometrically at a wavelength of 340 nm at 25°C. One unit of pyruvate kinase activity is defined as the amount of enzyme that catalyzes the production of 1.0 μmol pyruvate from the substrate PEP in 1 min. The specific activity of pyruvate kinase was measured as activity per total protein concentration. Protein concentration was determined by Bradford assay (Bradford 1976).

2.7 mRNA sequencing by Illumina HiSeq/ Novaseq or MGI2000

Seven-day old *A. halophytica* cells adapted in $BG11_0$, BG11-K, and $BG11_0K$ for 2 days were harvested by centrifugation at 12,000 × g at 4 C for 10 min. The total RNA of each sample was extracted using

10.3389/fbioe.2022.1028151

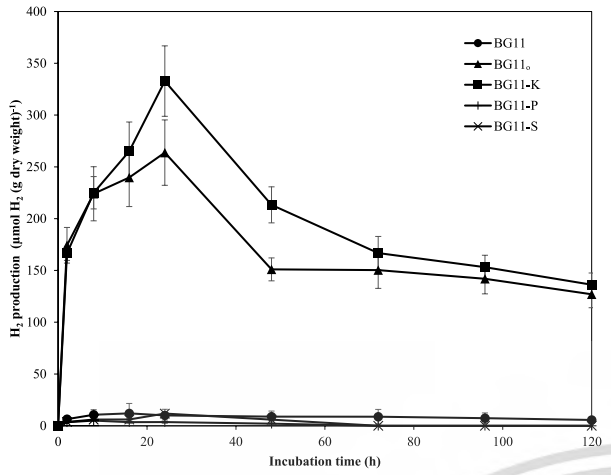

FIGURE 1
H_2 production (µmol H_2 g dry wt^{-1}) by *A. halophytica* incubated for various times in BG11 (●), BG11$_0$ (▲), BG11-K (■), BG11-P (+), and BG11-S (*) medium under dark anaerobic condition. Data are means ± SD (n = 3).

QIAzol Lysis Reagent (Qiagen, United States). Then, total RNA was qualified and quantified using a NanoDrop 2000/2000c spectrophotometer (Thermo Fisher Scientific, United States). Ribosomal RNA (rRNA) was removed by using a Ribo-Zero rRNA removal Kit (Epicentre, United States) following the manufacturer's instructions. The construction of the next generation sequencing library was conducted by Genewiz (China) according to the standard protocols. The different indices of libraries were multiplexed and loaded on an Illumina HiSeq/Novaseq instrument according to the instructions of the manufacturer (Illumina, United States). RNA sequencing was performed using the 2 × 150 paired end (PE) configuration. Image analysis and base calling were conducted using the HiSeq Control Software (HCS) + OLB + GAPipeline-1.6 (Illumina) on the HiSeq instrument. All RNA sequencing and alignment processes were conducted by Genewiz (China).

2.8 Statistical analysis

All experiments were performed in triplicate. All data are shown as the mean ± standard deviation. One-way analysis of variance (ANOVA) was used for analysis to the 95% confidence level with IBM SPSS version 19 software.

3 Results

3.1 H_2 production in deprived and limited media

The result showed that *A. halophytica* cells incubated in BG11$_0$ and BG11-K showed clearly higher H_2 production than those in BG11, BG11-P, and BG11-S (Figure 1). The highest H_2 accumulation of 332.82 ± 34.02 µmol H_2 g dry cell wt^{-1} was shown by cells incubated in BG11-K for 24 h. It was 33-fold higher than that of cells cultivated in normal BG11 medium (10.01 ± 5.92 µmol H_2 g dry cell wt^{-1}) (Figure 1). In addition, cells incubated in BG11$_0$ accumulated maximum H_2 of 263.75 ± 31.58 µmol H_2 g dry cell wt^{-1}, or 26-fold higher than that of cells incubated in normal BG11 medium (Figure 1). This study demonstrated the activation of H_2 production by *A. halophytica* under nitrogen and potassium deprivation.

In this study, the effects of various concentrations of nitrogen and potassium on H_2 production and H_2ase activity by *A. halophytica* with focus on potassium and nitrogen deprivation was investigated. The results showed that during potassium deprivation, a decrease in nitrogen concentration resulted in higher H_2ase activity and H_2 production by *A. halophytica* (Table 1). Similarly, during nitrogen deprivation, lower potassium concentration resulted in significantly higher H_2 production and H_2ase activity by *A. halophytica* (Table 1). The highest H_2ase activity with 120.05 ± 8.98 µmol H_2 g dry wt^{-1} min^{-1} and maximum H_2 accumulation with 507.51 ± 13.78 µmol H_2 g dry wt^{-1} was shown in cells incubated under a combined K- and N-deprived conditions (Table 1). This H_2ase activity and H_2 production was approximately 40 and 50-fold higher than those under normal conditions (incubated in BG11), respectively. The deprivation of both nitrogen and potassium together promoted H_2ase activity, and thus resulted in higher H_2 production.

3.2 Time course of H_2ase activity, H_2 production, and O_2 production under nitrogen and potassium deprivation

In this study, *A. halophytica* cells were adapted in BG11, BG11$_0$, BG11-K, and BG11$_0$-K media under photoautotrophic conditions with light exposure (18 h/day) for 1, 2, 3, 4, and 5 days. The hydrogenase activity, H_2 production, and O_2 production of adapted cells were measured after incubation under dark anaerobic condition for 24 h. The result showed that under nitrogen and/or potassium deprivation, *A. halophytica* cells gave higher H_2 production and hydrogenase activity than cells under normal condition (Figures 2A, B). On the other hand, O_2 production was highest in cells adapted in normal BG11 medium (Figure 2C). The combined deprivation of nitrogen and potassium promoted higher H_2ase activity and H_2 production in *A. halophytica* than did single nutrient deprivation. *A. halophytica* incubated under nitrogen and potassium deprivation showed maximum H_2 production rate of 40.87 ± 1.07 µmol H_2 g dry wt^{-1} h^{-1}. The highest H_2 production of 1,261.96 ± 96.99 µmol H_2 g dry wt^{-1} was obtained in cells adapted in BG11$_0$-K for 2 days (Figure 2A). The lowest O_2 evolution rate of 8.81 ± 2.93 nmol O_2 g dry wt^{-1} h^{-1} was obtained in cells adapted in BG11$_0$-K after 3 days (Figure 2C). It was found that H_2 production was related to H_2ase activity (Figures 2A, B). H_2ase activity increased dramatically at the first 48 h of adaptation incubation and the highest H_2ase activity with 179.39 ± 8.18 µmol H_2 g dry wt^{-1} min^{-1} was found in cells adapted in BG11$_0$-K for 2 days (Figure 2B).

3.3 Glycogen accumulation under nitrogen and potassium deprivation

The glycogen content of *A. halophytica* cells adapted in BG11, BG11$_0$, BG11-K, and BG11$_0$-K media for 1, 2, 3, 4, and 5 days was

10.3389/fbioe.2022.1028151

TABLE 1 H_2 production and H_2ase activity by *A. halophytica* cells incubated in various types of media: BG11 supplemented with Turk Island salt solution (BG11), potassium-deprived BG11 supplemented with Turk Island salt solution (BG11-K) containing various concentrations of $NaNO_3$, nitrogen-deprived BG11 supplemented with Turk Island salt solution ($BG11_0$) containing various concentrations of KCl, and potassium- and nitrogen-deprived BG11 supplemented with Turk Island salt solution ($BG11_0$-K) for 24 h. Data are means ± SD (n = 3). Different letters in columns indicate a significant difference, and the same letter indicates no significant difference according to Duncan's multiple range test at $p < 0.05$.

Type of media	KCl (mM)	$NaNO_3$ (mM)	H_2 production (μmol H_2 g dry weight^{-1})	H_2ase activity (μmol H_2 g dry weight^{-1} min^{-1})
BG11	8.93	17.6	10.55 ± 0.58^{h}	3.20 ± 0.22^{f}
BG11-K	0	17.6	332.58 ± 8.56^{ef}	51.38 ± 1.51^{de}
	0	13.2	354.44 ± 9.15^{de}	60.30 ± 4.68^{cd}
	0	8.8	379.38 ± 17.51^{cd}	62.97 ± 4.78^{c}
	0	4.4	449.32 ± 6.08^{b}	81.23 ± 7.03^{b}
$BG11_0$	8.93	0	260.34 ± 12.24^{g}	46.61 ± 3.30^{e}
	6.70	0	279.10 ± 17.43^{g}	51.83 ± 1.40^{de}
	4.47	0	313.99 ± 21.93^{f}	54.9 ± 3.10^{cde}
	2.23	0	388.94 ± 34.66^{c}	84.70 ± 6.65^{b}
$BG11_0$-K	0	0	507.51 ± 13.78^{a}	120.05 ± 8.98^{a}

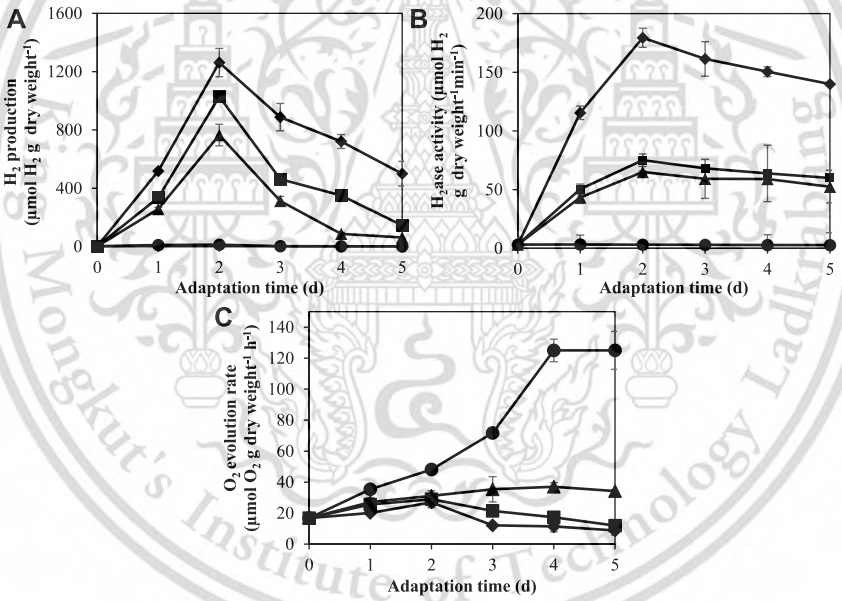

FIGURE 2
Effect of adaptation time on H_2 production **(A)**, H_2ase activity **(B)**, and O_2 evolution rate **(C)** by *A. halophytica* cells. *A. halophytica* was adapted in various kinds of media for various times, BG11 (●), $BG11_0$ (▲), BG11-K (■), and $BG11_0$-K (□) for 1–5 days before harvesting and resuspending in a fresh medium. H_2 production was measured in incubated cells under dark anaerobic condition for 24 h. Data are means ± SD (n = 3).

measured. The results revealed that under nitrogen and/or potassium deprivation, *A. halophytica* clearly produced and accumulated higher intracellular glycogen than under normal conditions. The glycogen content of cells adapted in $BG11_0$, BG11-K, and $BG11_0$-K clearly increased during the first 3 days of adaptation, whereas in the case of BG11 adapted cells, it was almost constant over the period of adaptation (Figure 3A). The highest glycogen content at 65.53 ± 0.78% of cell dry wt was obtained in cells adapted in $BG11_0$-K for 3 days (Figure 3A). It was approximately three times higher than glycogen content of cells adapted in BG11 (24.66 ± 1.97% of cell dry wt) (Figure 3A). In the case of only single-nutrient deprivation, glycogen accumulated under potassium deprivation was higher than that under nitrogen deprivation. Under K-deprivation, cells accumulated the maximum glycogen content of 56.13 ± 0.66% of cell dry wt whereas under N-deprivation, cells accumulated the maximum glycogen content at 51.95 ± 2.11% of cell dry wt after 3 days of adaptation.

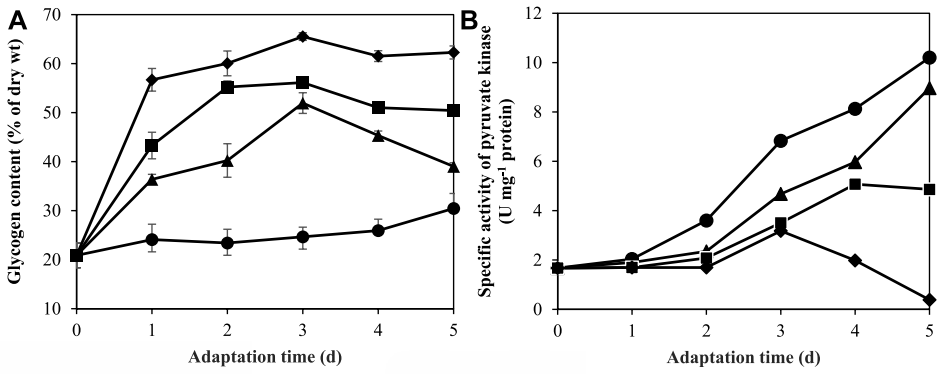

FIGURE 3
Effect of adaptation time on glycogen content **(A)** and specific activity of pyruvate kinase **(B)** by *A. halophytica* cells. *A. halophytica* was adapted in various kinds of media for various times, BG11 (●), $BG11_0$ (▲), BG11-K (■), and $BG11_0$-K (□) for 1–5 days before harvesting and resuspending in a fresh medium. H_2 production was measured in incubated cells under dark anaerobic condition for 24 h. Data are means ± SD (n = 3).

3.4 Specific activity of pyruvate kinase under nitrogen and potassium deprivation

Pyruvate kinase (PK) is known to be activated by K^+ (Oria-Hernández et al., 2005). It has an important role in regulating the glycolytic pathway in carbohydrate metabolism. The measurement of pyruvate kinase (PK) activity was performed in *A. halophytica* cells adapted in BG11, $BG11_0$, BG11-K, and $BG11_0$-K for 1, 2, 3, 4, and 5 days. The results showed that specific activity of PK was highest with 10.20 ± 0.60 U mg^{-1} protein in *A. halophytica* adapted in BG11 for 5 days (Figure 3B). The deprivation of either nitrogen or potassium reduced specific activity of PK significantly compared with normal conditions (Figure 3B). Similarly, combined deprivation of both nitrogen and potassium had significant effects on PK activity. It was especially notable that after 5 days of adaptation time, cells clearly showed very low PK specific activity at 0.39 ± 0.01 U mg^{-1} protein (Figure 3B).

3.5 Photosynthetic oxygen evolution rate and respiration rate under nitrogen and potassium deprivation

Since O_2 is a strong inhibitor of H_2ase, the presence of O_2 in systems plays an important role in H_2 production. In cyanobacteria, O_2 is generated *via* oxygenic photosynthesis and the produced O_2 is consumed in cellular respiration *via* the electron transport chain. To investigate how O_2 evolution decreased under nitrogen and potassium deprivation, the photosynthetic O_2 evolution rate and respiration rate of *A. halophytica* cells adapted in BG11, $BG11_0$, BG11-K, and $BG11_0$-K for 2 days was measured. The results showed that the highest photosynthetic O_2 evolution rate of 16.94 ± 0.64 nmol O_2 mg dry wt^{-1} min^{-1} was found in cells adapted in BG11. Under single or combined nitrogen and potassium deprivation, its photosynthetic O_2 evolution rate decreased (Table 2). The combined deprivation of both nitrogen and potassium resulted in the lowest photosynthetic O_2 evolution rate of 2.78 ± 0.09 nmol O_2 mg dry wt^{-1} min^{-1} (Table 2). On the contrary, O_2 consumption by respiration increased under nitrogen and/or potassium deprivation (Table 2). The ratio of photosynthetic O_2 evolution rate and respiratory rate was calculated and evaluated. This ratio implies the quantity of O_2 in a vial container. The highest ratio between photosynthetic O_2 evolution rate and respiratory rate of 22.49 ± 0.81 was found in cells adapted in BG11 for 24 h whereas the lowest ratio of 2.57 ± 0.04 was shown in cells adapted in $BG11_0$-K for 24 h (Table 2).

3.6 RNA-seq based transcriptome analysis of genes involved in photosynthetic, carbon, and nitrogen assimilation pathways under nitrogen and potassium deprivation

Gene expression based on the RNA-seq of *A. halophytica* under nitrogen and potassium deprivation was compared with that under normal conditions. The results are shown in Figure 4. Transcripts of genes involved in photosynthetic, carbon, and nitrogen assimilation pathways were analyzed. In this study, log_2FoldChange (log_2FC) was used to indicate the differences between transcript expression in the experimental and control groups. The results showed that genes encoding allophycocyanin and phycobilisome under N and K deprivation were expressed as $log_2FC \leq -0.1$. However, ApcA, the allophycocyanin alpha subunit encoded by *apcA*, was upregulated by 0.5 and 1.77 of log_2FC under N and K deprivation, respectively. In addition, the expression of different genes involved in photosynthesis showed harmonic direction under N and K deprivation. Most of these genes were upregulated by $log_2FC \leq 0.54$. Especially, D1 protein encoded by *psbA* was upregulated by log_2FC of 1.48 and 1.03 under N and K deprivation, respectively. However, the CP47, CP43 chlorophyll apoproteins, and P_{680} reaction center D2 protein encoded by *psbB*, *psbC*, and *psbD* respectively were downregulated.

Under N and K deprivation, genes involved in the Calvin-Basham-Benson (CBB) cycle were downregulated (Figure 4). Ribulose-1,5-bisphosphate carboxylase/oxygenase large subunit encoded by *rbcL* was significantly down-regulated by log_2FC of −2.46 and −1.83 under N and K deprivation, respectively. All genes in this pathway were differently expressed by $log_2FC \leq -0.53$. Likewise, several genes involved in glycolysis were downregulated under these starvation conditions. However, pyruvate kinase encoded by *pyk* was expressed differentially, as log_2FC of 0.26 and −1.77 under N and K deprivation, respectively. Interestingly, most genes involved in

TABLE 2 Photosynthetic O_2 evolution rate, dark respiration rate, and ratio of photosynthetic O_2 evolution rate and respiratory rate in A. halophytica cells incubated in BG11, BG110, BG11-K, and BG110-K under dark anaerobic condition for 24 h before measuring. Data are means ± SD (n = 3). Different letters in columns indicate a significant difference, and the same letter indicates no significant difference according to Duncan's multiple range test at $p < 0.05$.

Type of media	Photosynthetic O_2 evolution rate (nmol O_2 mg dry wt^{-1} h^{-1})	Dark respiration rate (nmol O_2 mg dry wt^{-1} h^{-1})	Ratio of photosynthetic O_2 evolution rate and dark respiration rate
BG11	16.94 ± 0.64^a	0.75 ± 0.03^c	22.49 ± 0.81^a
$BG11_0$	5.39 ± 0.87^b	1.12 ± 0.01^b	4.79 ± 0.73^b
BG11-K	5.47 ± 0.59^b	1.31 ± 0.04^a	4.17 ± 0.57^b
$BG11_0$-K	2.78 ± 0.09^c	1.08 ± 0.02^b	2.57 ± 0.04^c

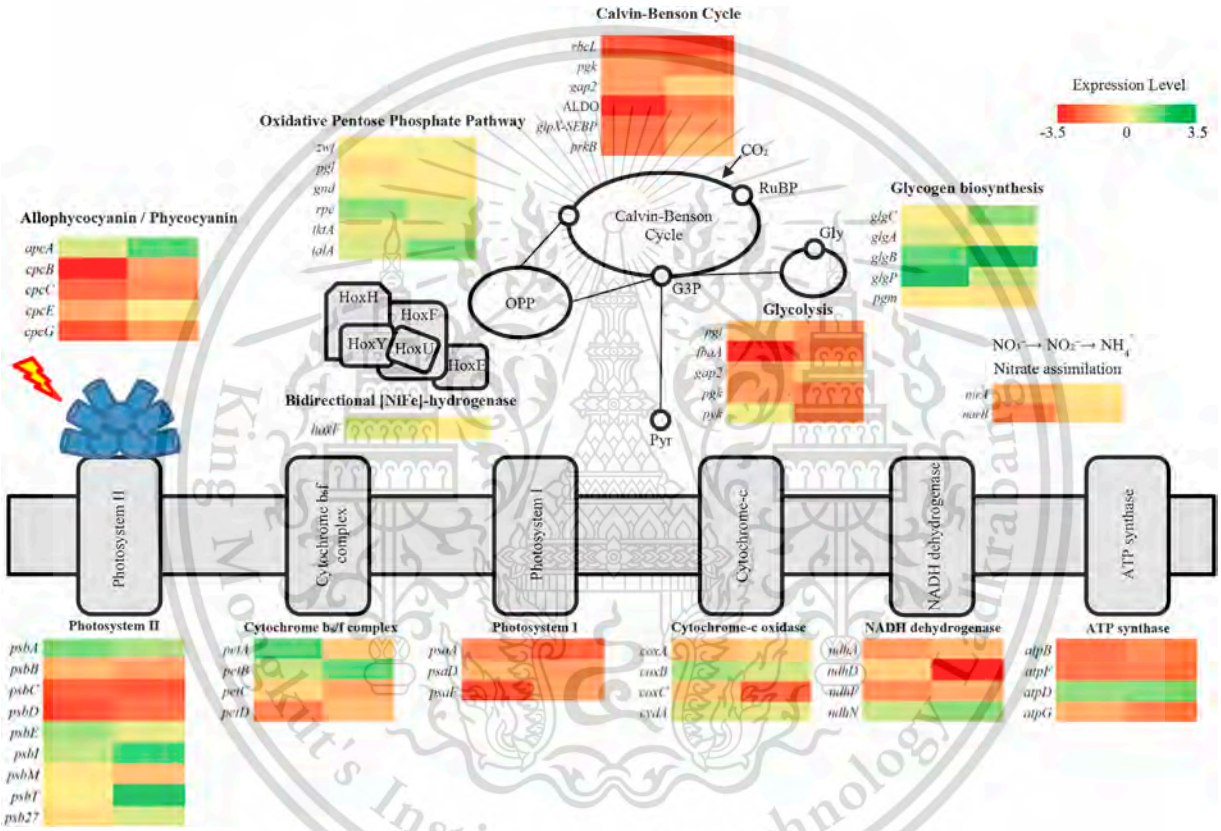

FIGURE 4
Transcriptional level of genes involved in photosynthetic pathway, carbon assimilation such as Calvin-Benson cycle, glycolysis, oxidative pentose phosphate pathway, and nitrate assimilation in *A. halophytica*. The first column shows differences of gene expression between N-deprived adapted cells and normal cells and the second column shows differences of gene expression between K-deprived adapted cells and normal cells. Expression levels are shown as heat maps with gene names, demonstrating different gene expression in many metabolic pathways involved in H_2 production. The metabolic pathways are photosynthesis, oxidative pentose phosphate, glycolytic pathway, glycogen biosynthesis, and nitrate assimilation. Abbreviations: oxidative pentose phosphate pathway, OPP; glucose-3-phosphate, G3P; glycogen, gly; pyruvate, pyr; [NiFe]-bidirectional H_2ase enzyme subunits, HoxEFUYH.

glycogen biosynthesis were upregulated. For example, 1,4-alpha-glucan branching enzyme encoded by *glgB* was upregulated as log_2FC of 1.69 and 4.37 under N and K deprivation, respectively. In the oxidative pentose phosphate pathway (OPP), some genes were upregulated under N and K deprivation. For example, *rpe* encoding ribulose phosphate 3-epimerase was upregulated by 1.23 and 0.52 of log_2FC, respectively. In terms of nitrogen assimilation, as expected, ferredoxin-nitrite reductase encoded by *nirA* and *nirB* was downregulated as log_2FC of −0.94 and −1.76, respectively, under N-deprived conditions. On the contrary, no differences of expression of these genes were found under K-deprived conditions.

4 Discussion

Cyanobacteria are oxygenic microorganisms that can produce H_2 under dark anaerobic conditions, especially when they are incubated in nutrient-deprived media (Ananyev et al., 2008; Baebprasert et al.,

TABLE 3 Maximum dark fermentative H_2 production rate by *A. halophytica* incubated under various conditions.

Condition	Maximum H_2 production rate	References
Free cells incubated in $BG11_0$-K, dark, 120 rpm, pH 7.4, 30°C	40.87 ± 1.07 μmol H_2 g dry wt^{-1} h^{-1}	This study
Free cells incubated in $BG11_0$ with 0.4 μM Fe^{3+}, dark, 120 rpm, pH 7.4, 30°C	13.80 ± 0.373 μmol H_2 mg^{-1} chl a h^{-1}	Taikhao et al. (2013)
Free cells incubated in optimal seawater, dark, 120 rpm, pH 6.0, 35°C	82.79 ± 3.47 μmol H_2 g dry wt^{-1} h^{-1}	Taikhao et al. (2015)
Alginate-immobilized cells incubated in $BG11_0$, 120 rpm, pH 7.4, 30°C	0.532 μmol H_2 mg chl a^{-1} h^{-1}	Pansook et al. (2016)
Free cells incubated in $BG11_0$ with 0.5 μM CCCP, dark, 120 rpm, pH 7.4, 30°C	39.50 ± 2.13 μmol H_2 g dry wt^{-1} h^{-1}	Pansook et al. (2019a)
Agar-immobilized cells incubated in $BG11_0$, dark, 120 rpm, pH 7.4, 40°C	135.54 ± 1.92 μmol H_2 g dry wt^{-1} h^{-1}	Pansook et al. (2019b)
Free cells incubated in $BG11_0$ with 25 μM simazine, dark, 120 rpm, pH 7.4, 30°C	58.88 ± 0.22 μmol H_2 g dry wt^{-1} h^{-1}	Pansook et al. (2022)
Free cells incubated in $BG11_0$ with 50 mM sodium sulfide, dark, 120 rpm, pH 7.4, 30°C	542.45 ± 35.99 μmol H_2 g dry wt^{-1} h^{-1}	Chinchusak et al. (2022)

2010; Min and Sherman 2010). In a previous study, the unicellular halotolerant cyanobacterium *A. halophytica* showed the ability to produce H_2 under nitrogen starvation (Taikhao et al., 2013; Taikhao et al., 2015; Phunpruch et al., 2016). Previously, H_2 production was shown to be catalyzed by bidirectional [NiFe]-H_2ase (Phunpruch et al., 2016). The results in this study demonstrated that, apart from nitrogen starvation, potassium deprivation could also significantly enhance H_2 production by *A. halophytica* under dark anaerobic conditions compared with normal conditions (Figure 1). Potassium and nitrogen deprivation could induce glycogen catabolism with subsequent generation of increased electrons and hydrogenase activity was simultaneously induced after entering anaerobic conditions. After 24 h of incubation, H_2 production was decreased, as a result of the decreased number of electrons and the lower hydrogenase activity. Under potassium and nitrogen deprivation, biomass was not much changed due to the low level of nutrient concentration for cell division. However, *A. halophytica* incubated in seawater with the supplementation of 378 mmol C L^{-1} glucose, 0.25 M NaCl, and 0.4 μM Fe^{3+} at 35°C, pH six gave the highest H_2 production at day 8 of dark incubation under anoxic condition, and the high yield of H_2 was sustained at least up to 14 days (Taikhao et al., 2015).

Under potassium deprivations, a limitation of the $NaNO_3$ concentration available in BG11 medium induced both H_2ase activity and H_2 production (Table 1). Similarly, under nitrogen deprivations, a limited KCl concentration in BG11 medium induced both H_2ase activity and H_2 production (Table 1). In a previous study, it was shown that the presence of potassium reduced H_2ase activity in *Synechocystis* 6,803, under dark anaerobic conditions, which might have been due to competitive utilization of limited NADPH for H_2 and organic acid production (Ueda et al., 2016). Moreover, it has been suggested that potassium deprivation decreased PSII activity, lowering the production of O_2, which is an inhibitor of H_2ase enzyme. Furthermore, potassium deprivation increased the degradation of starch in green alga *Scenedesmus obliquus* (Papazi et al., 2014) and in *Tetraspora* sp. CU2551 (Pewnual et al., 2022). With nitrogen deprivation, H_2ase activity increased in *Anabaena siamensis* TISTR8012, resulting in enhanced H_2 production (Taikhao and Phunpruch 2017). On the other hand, phosphorus and sulfur deprivation did not promote H_2 production by *A. halophytica*. In addition, potassium, sulfur, and phosphate deprivation was observed to likely have important effects on nucleic acids, protein synthesis, and other metabolic pathways in cells, such as photosynthesis, cellular respiration, and H_2 metabolism (Warichanan and Phunpruch 2019). Moreover, a combination of nitrogen and sulfur depletion enhanced H_2 production in *Synechocystis* sp. strain PCC 6803 (Baebprasert et al., 2010) and in *Arthrospira* sp. PCC 8005 (Raksajit et al., 2012). Table 3 shows the comparison of maximum H_2 production rate by *A. halophytica* under various conditions. It was shown that deprivation of potassium together with nitrogen promoted higher H_2 production by *A. halophytica* than only nitrogen deprivation. However, H_2 production rate by free cells of *A. halophytica* in this study was lower than that of agar-immobilized cells (Pansook et al., 2019b) and free cells incubated in $BG11_0$ treated with 25 μM simazine (Pansook et al., 2022) and 50 mM sodium sulfide (Chinchusak et al., 2022).

H_2ase, including the [NiFe]-H_2ase enzyme in cyanobacteria, is usually sensitive to the presence of O_2 (McIntosh et al., 2011). The fundamental pathways involved in O_2 generation and consumption in cyanobacteria are photosynthesis and dark respiration, respectively. Our result showed that a combined deprivation of both nitrogen and potassium promoted H_2 production by reducing O_2 concentration in the vial (Figure 2). A decrease in O_2 concentration induced H_2ase activity, resulting in a higher H_2 production (Figure 2). The balance of O_2 concentration in a system therefore plays a decisive role in H_2 production. In cyanobacteria, O_2 in the system is normally generated by photosynthetic activity of PSII. However, a measurement of H_2 production in this study was performed under darkness when photosynthetic activity should have been less than under light conditions. The deprivation of either nitrogen or potassium reduced the photosynthetic O_2 evolution rate by 3-fold, whereas combined deprivation of both nitrogen and potassium reduced the photosynthetic O_2 evolution rate by 6-fold (Table 2). A decrease in photosynthetic O_2 evolution rate caused the reduction of O_2 in the system. This in turn induced H_2ase activity, resulting in higher H_2 production. In the case of nitrogen deprivation, the result was in agreement with a previous study showing the reduction of photosynthetic activities in *Synechococcus elongatus* PCC 7942 under nitrogen starvation (Choi et al., 2016). Potassium deprivation decreased photosynthetic pigments and activity in *Synechocystis* sp. strain PCC 6803 (Nanatani et al., 2015) and in *Anabaena torulosa* (Alahari and Apte 1998).

In addition, the produced O_2 can be consumed by dark intracellular respiration. An increased respiration rate for *A. halophytica* was observed in cells deprived of nitrogen or

10.3389/fbioe.2022.1028151

potassium or both (Table 2). As a result, a decreased level of O_2 in the vial containing cells incubated under nitrogen and potassium deprivation was obtained. The ratio of photosynthetic O_2 evolution rate and dark respiration rate was used to monitor the level of O_2 concentration in the system (Table 2). A higher ratio indicated higher activity of photosynthetic O_2 evolution activity over respiration activity, suggesting the presence of high O_2 concentration in the vial, and thus lower H_2ase activity and lower H_2 production. A low ratio of photosynthetic O_2 evolution rate to dark respiration rate was found in nitrogen- and potassium-free adapted cells (Table 2). This probably involved a combined effect of nitrogen and potassium deprivation suppressing related genes. In terms of photosynthetic O_2 evolution: respiratory rate ratio (Table 2), the results implied that the lower the ratio, the lower the O_2 concentration. Cells incubated in deprived media showed lower photosynthetic O_2 evolution rate and dark respiration rate than did normal cells. Several genes encoding cytochrome *c* oxidase and NADH dehydrogenase were upregulated in cells under both nitrogen and potassium starvation (Figure 4). The results suggested that *A. halophytica* increased dark respiration under nitrogen and potassium starvation. However, no significant differences of expression of genes encoding respiratory electron transport system were reported in *Synechococcus elongatus* PCC 7942 under nitrogen deprivation (Choi et al., 2016).

H_2 production by *A. halophytica* was established by the two-stage regime: cyanobacterial growth followed by adaptation in nutrient deprivation condition to induce an increase of H_2 production. Firstly, cells were grown in rich BG11 medium for 7 days to accumulate biomass. Then, the cells were made to enter the adaptation period, or the second stage, by incubation in nutrient-deprived media to accumulate glycogen under illumination and aerobic conditions. Subsequently, cells were transferred into a glass vial and H_2 production was induced under dark anaerobic condition. The adaptation period during nutrient deficiency was very crucial since cells incubated in deprived media needed to accumulate a high content of glycogen, or other chemical compounds, in order to provide electrons for H_2ase to produce H_2. Individually and combined nitrogen and potassium deprivation were chosen for this study. The result showed that H_2ase activity and H_2 production was highest in cells adapted in nitrogen- and potassium-deprived media for 48 h (Figures 2A, B), suggesting a high accumulation of glycogen in adapted cells. Glycogen in the adapted cells was extracted and determined. Glycogen was seen to have accumulated more in cells incubated in nitrogen- and potassium-deprived media compared to that of cells incubated in BG11 (Figure 3B). The highest glycogen was found in combined nitrogen- and potassium-free cells during the adaptation period (Figure 3B). This result was confirmed with transcriptional analysis. Transcriptional analysis by RNA-seq showed that the *glgA* and *glgB* genes encoding the starch synthase and 1,4-alpha-glucan branching enzymes, respectively, were upregulated under both nitrogen and potassium deprivation (Figure 4). The results suggested that a lack of nitrogen and/or potassium causes an increase in glycogen content, giving rise to higher H_2 production (Taikhao et al., 2015).

Under dark anaerobic condition, cyanobacterial H_2 can be produced *via* [NiFe] H_2ase reduced by NAD(P)H (Gutekunst

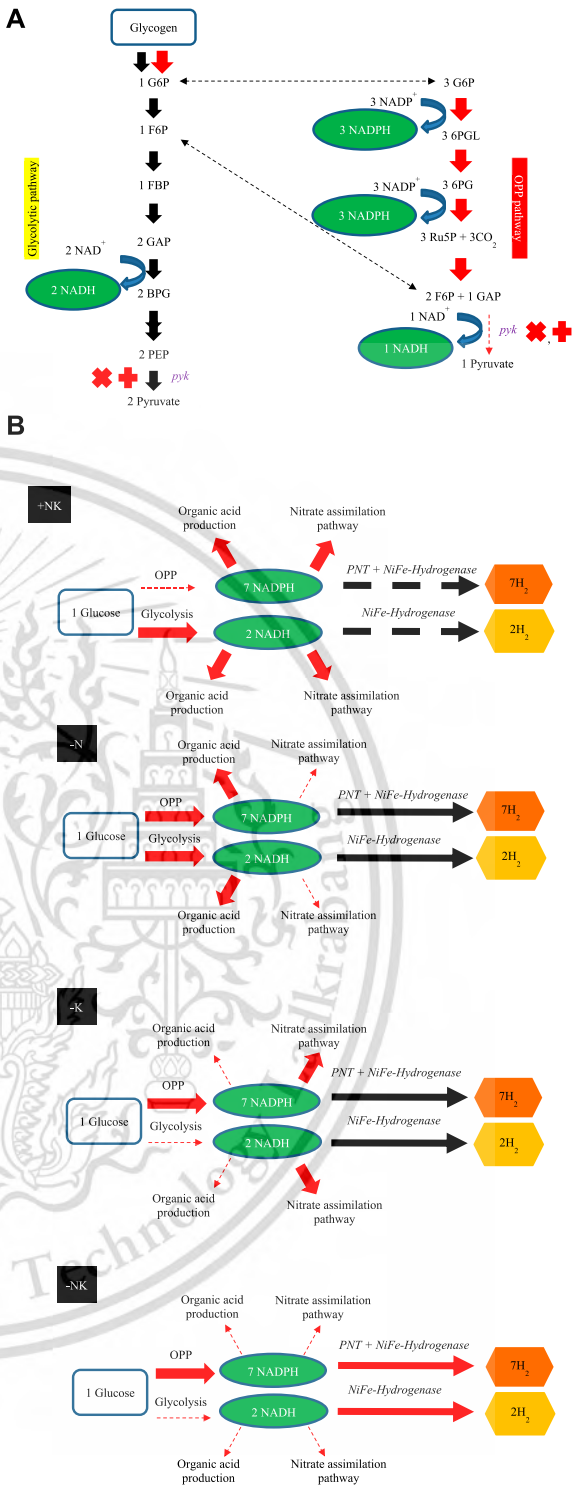

FIGURE 5
Proposed schematic mechanism of H_2 production by *A. halophytica* based on the RNA-seq after adaptation in nitrogen and/or potassium deprivation for 2 days. Glycolytic and OPP pathways are involved in NAD(P)H generation *via* glycogen catabolism **(A)**. Proposed H_2 metabolism and involved pathways of *A. halophytica* incubated in BG11 (+NK), $BG11_0$ (-N), BG11-K (-K), and $BG11_0$-K (-NK) under dark anaerobic conditions **(B)**. Arrows show electron transport direction in each pathway.

et al., 2014) and reduced ferredoxin (Meuer et al., 1999; Gutekunst et al., 2014). The main sources of reductants for H_2 generation under dark anaerobic condition are NADH and reduced ferredoxin from glycolysis and NADPH from catabolism of accumulated glycogen, provided by oxidative pentose phosphate (OPP) pathway (Kumaraswamy et al., 2013). In this study, the specific activity of PK in glycolytic pathway decreased in *A. halophytica* under K deprivation (Figure 3A). The specific activity of PK in K- and NK- free adapted cells was less than that in abundant and N-free adapted cells throughout the period of adaptation time. PK is known to be induced by K^+ and it is less activated when K is absent in a system (Oria-Hernández et al., 2005). Therefore, this associated enzyme regulation might have controlled the flux of glycogen catabolism in *A. halophytica*. Furthermore, GAPDH-2 has a major role in the CBB cycle, using NADPH as a preferred electron donor to reduce 1,3-bis-phosphoglycerate to GAP (Koksharova et al., 1998). Under potassium deprivation, transcriptional analysis revealed that *pyk* and *gap2* encoding PK and GAPDH-2, respectively, were downregulated (Figure 4). Consequently, in potassium-free adapted cells, it could be suggested that upper-glycolytic metabolites could be in excess, especially glucose-6-phophate (G6P). G6P is a broken-down molecule of glycogen, and the branching point between glycolysis and OPP pathway. For a reduced activity of both PK and GADPH-2, it could be the case that G6P preferentially enters the OPP pathway, generating more NADPH and using less NADPH in CBB and glycolysis. Therefore, OPP pathway may well be the favored pathway for H_2 production in potassium-deprived adapted cells of *A. halophytica* under dark anaerobic conditions. In a previous study, the *pykF* knocking out *Escherichia coli* mutant provided higher activity of enzymes in OPP, but the activities of glycolytic enzymes decreased compared with those in wild-type cells (Siddiquee et al., 2004). Moreover, low activity of pyruvate kinase was shown to promote respiration in yeast (Grüning et al., 2011). Prior to this study, H_2 production was induced in nitrogen-free cells because the expression of genes involved in glycogen catabolism had increased (Osanai et al., 2006). Moreover, several genes in the OPP pathway were extremely upregulated in *Synechocystis* sp. PCC 6803 incubated in nitrogen-free medium (Osanai et al., 2006). This was probably due to G6P being degraded through the OPP pathway. It seems that glycogen catabolism might preferentially take place *via* the OPP pathway, producing more NAD(P)H compared to that *via* the glycolytic pathway in cells incubated in both nitrogen- and potassium-deprived conditions. Therefore, the described effects of both nitrogen and potassium deprivation on H_2 production may have been synergistic, and accelerated H_2 production in *A. halophytica* under dark anaerobic conditions.

The schematic H_2 production by *A. halophytica* during deprivation of individual nitrogen and potassium, and combined nitrogen and potassium, under dark anaerobic conditions is shown in Figure 5. The reductants involved in H_2 metabolism by cyanobacteria, NADH, and NADPH are generated mainly by the glycolytic and OPP pathways (Kumaraswamy et al., 2013). In the former, one molecule of G6P can provide two molecules of NADH whereas seven molecules of reduced pyridine nucleotides can be produced from the same molecule of G6P (6 NADPH per glucose and one NADH per glucose) *via* the OPP pathway (Kumaraswamy et al., 2013). One molecule of NAD(P)H can be oxidized by H_2ase to provide one molecule of H_2. Therefore, the reduced pyridine nucleotides from the OPP pathway can produce more H_2 compared with that from the glycolytic pathway (seven molecules vs. two molecules of H_2). In plentiful conditions or in the case of the BG11 (Figure 5B (+NK)), cells were more likely to generate organic acid compounds than potassium-deprived adapted cells were. This corresponded with a previous study of *Synechocystis* sp. PCC 6803 that suggested that, under dark anaerobic conditions, where NADPH was limited, there was a competing demand to consume NADPH for H_2 and organic acid production. In the presence of potassium, cells preferred to utilize NADPH for production of organic acids (Ueda et al., 2016). Therefore, NAD(P)H is normally used for organic acid production and the nitrate assimilation pathway rather than H_2 production. In nitrogen-deprived cells, it may be that glycogen catabolism occurs *via* both the OPP and glycolytic pathway, as shown in *Synechocystis* sp. PCC 6803 (Osanai et al., 2006). In potassium-free cells, PK activity (Figure 3) and the gene expression of *pyk* encoding PK was lower than that found in normal cells (Figure 4). Consequently, glycogen was mainly degraded *via* the OPP pathway and provided more NADPH for H_2 production.

5 Conclusion

Under dark anaerobic conditions, the maximum H_2 production of 1,261.96 ± 96.99 μmol H_2 g dry wt^{-1} and the maximum hydrogenase activity of 179.39 ± 8.18 μmol H_2 g dry wt^{-1} min^{-1} was found in *A. halophytica* cells incubated in the nitrogen- and potassium-deprived BG11 medium supplemented with Turk Island salt solution for 48 h. The increased hydrogenase activity was due to a reduction of O_2 in the system, resulting from the lower photosynthetic O_2 evolution and higher dark respiration. Under nitrogen and potassium deprivation, *A. halophytica* cells promoted the production and accumulation of glycogen and reduced pyruvate kinase activity. Transcriptional analysis by RNA-seq helped to understand the effect of nitrogen and potassium deprivation on H_2 production by *A. halophytica*. Several genes involved in glycogen biosynthesis (*glgA*, *glgB*, and *glgP*) were upregulated in both nitrogen- and potassium-deprived cells. However, *pyk* and most genes that regulated enzymes in the glycolytic pathway were down-regulated in both nitrogen- and potassium-deprived cells. Interestingly, most genes that regulated enzymes in the oxidative pentose phosphate pathway (OPP) were upregulated. Accordingly, the OPP was suggested as a promising pathway for enhancing H_2 production under dark anaerobic conditions in both nitrogen- and potassium-deprived *A. halophytica* cells. This study indicated that combined nitrogen and potassium deprivation in media is a promising strategy to promote sustainable H_2 production by the halotolerant cyanobacterium *A. halophytica*.

Data availability statement

The original contributions presented in the study are included in the article/SupplementaryMaterial; further inquiries can be directed to the corresponding author.

Author contributions

SP contributed to conception and design of the study. SP received the research grant. NC performed the experiments and statistical analysis. NC wrote the first draft of the manuscript. SP and NC wrote sections of the manuscript. All authors contributed to manuscript revision, and read and approved the submitted version.

Funding

This work was financially supported by King Mongkut's Institute of Technology Ladkrabang (2563-02-05-33). NC would like to thank School of Science, King Mongkut's Institute of Technology Ladkrabang for a Ph.D. scholarship.

Conflict of interest

The authors declare that the research was conducted in the absence of any commercial or financial relationships that could be construed as a potential conflict of interest.

Publisher's note

All claims expressed in this article are solely those of the authors and do not necessarily represent those of their affiliated organizations, or those of the publisher, the editors and the reviewers. Any product that may be evaluated in this article, or claim that may be made by its manufacturer, is not guaranteed or endorsed by the publisher.

References

Alahari, A., and Apte, S. K. (1998). Pleiotropic effects of potassium deficiency in a heterocystous, nitrogen-fixing cyanobacterium, *Anabaena torulosa*. *Microbiology* 144 (6), 1557–1563. doi:10.1099/00221287-144-6-1557

Ananyev, G., Carrieri, D., and Dismukes, G. C. (2008). Optimization of metabolic capacity and flux through environmental cues to maximize hydrogen production by the cyanobacterium "*Arthrospira (Spirulina) maxima*". *Appl. Environ. Microbiol.* 74 (19), 6102–6113. doi:10.1128/AEM.01078-08

Ananyev, G. M., Skizim, N. J., and Dismukes, G. C. (2012). Enhancing biological hydrogen production from cyanobacteria by removal of excreted products. *J. Biotechnol.* 162 (1), 97–104. doi:10.1016/j.jbiotec.2012.03.026

Antal, T. K., and Lindblad, P. (2005). Production of H_2 by sulphur-deprived cells of the unicellular cyanobacteria *Gloeocapsa alpicola* and *Synechocystis* sp. PCC 6803 during dark incubation with membrane or at various extracellular pH. *J. Appl. Microbiol.* 98 (1), 114–120. doi:10.1111/j.1365-2672.2004.02431.x

Baebprasert, W., Lindblad, P., and Incharoensakdi, A. (2010). Response of H_2 production and Hox-hydrogenase activity to external factors in the unicellular cyanobacterium *Synechocystis* sp. Strain PCC 6803. *Int. J. Hydrog. Energy* 35 (13), 6611–6616. doi:10.1016/j.ijhydene.2010.04.047

Bothe, H., Schmitz, O., Yates, M. G., and Newton, W. E. (2010). Nitrogen fixation and hydrogen metabolism in cyanobacteria. *Microbiol. Mol. Biol. Rev.* 74 (4), 529–551. doi:10.1128/mmbr.00033-10

Bradford, M. M. (1976). A rapid and sensitive method for the quantitation of microgram quantities of protein utilizing the principle of protein-dye binding. *Anal. Biochem.* 72 (1), 248–254. doi:10.1016/0003-2697(76)90527-3

Chinchusak, N., Incharoensakdi, A., and Phunpruch, S. (2022). Enhancement of dark fermentative hydrogen production in nitrogen-deprived halotolerant unicellular cyanobacterium *Aphanothece halophytica* by treatment with reducing agents. *Biomass Bioenergy* 167, 106624. doi:10.1016/j.biombioe.2022.106624

Choi, S. Y., Park, B., Choi, I. G., Sim, S. J., Lee, S. M., Um, Y., et al. (2016). Transcriptome landscape of *Synechococcus elongatus* PCC 7942 for nitrogen starvation responses using RNA-seq. *Sci. Rep.* 6 (1), 30584. doi:10.1038/srep30584

Dubois, M., Gilles, K. A., Hamilton, J. K., Rebers, P. T., and Smith, F. (1956). Colorimetric method for determination of sugars and related substances. *Anal. Chem.* 28 (3), 350–356. doi:10.1021/ac60111a017

Ernst, A., Kirschenlohr, H., Diez, J., and Böger, P. (1984). Glycogen content and nitrogenase activity in *Anabaena variabilis*. *Arch. Microbiol.* 140 (2-3), 120–125. doi:10.1007/bf00454913

Garlick, S., Oren, A., and Padan, E. (1977). Occurrence of facultative anoxygenic photosynthesis among filamentous and unicellular cyanobacteria. *J. Bacteriol.* 129 (2), 623–629. doi:10.1128/jb.129.2.623-629.1977

Grüning, N. M., Rinnerthaler, M., Bluemlein, K., Mülleder, M., Wamelink, M. M., Lehrach, H., et al. (2011). Pyruvate kinase triggers a metabolic feedback loop that controls redox metabolism in respiring cells. *Cell Metab.* 14 (3), 415–427. doi:10.1016/j.cmet.2011.06.017

Gupta, P., and Parkhey, P. (2017). Electrohydrogenesis: Energy efficient and economical technology for biohydrogen production. *Adv. Biofeedstocks Biofuels Prod. Technol. Biofuels* 2, 201–233. doi:10.1002/9781119117551.ch8

Gutekunst, K., Chen, X., Schreiber, K., Kaspar, U., Makam, S., and Appel, J. (2014). The bidirectional NiFe-hydrogenase in *Synechocystis* sp. PCC 6803 is reduced by flavodoxin and ferredoxin and is essential under mixotrophic, nitrate-limiting conditions. *J. Biol. Chem.* 289 (4), 1930–1937. doi:10.1074/jbc.m113.526376

Khetkorn, W., Lindblad, P., and Incharoensakdi, A. (2010). Enhanced biohydrogen production by the N_2-fixing cyanobacterium *Anabaena siamensis* strain TISTR 8012. *Int. J. Hydrog. Energy* 35 (23), 12767–12776. doi:10.1016/j.ijhydene.2010.08.135

Khetkorn, W., Khanna, N., Incharoensakdi, A., and Lindblad, P. (2013). Metabolic and genetic engineering of cyanobacteria for enhanced hydrogen production. *Biofuels* 4 (5), 535–561. doi:10.4155/bfs.13.41

Koksharova, O., Schubert, M., Shestakov, S., and Cerff, R. (1998). Genetic and biochemical evidence for distinct key functions of two highly divergent GAPDH genes in catabolic and anabolic carbon flow of the cyanobacterium *Synechocystis* sp. PCC 6803. *Plant Mol. Biol.* 36 (1), 183–194. doi:10.1023/a:1005925732743

Kumaraswamy, G. K., Guerra, T., Qian, X., Zhang, S., Bryant, D. A., and Dismukes, G. C. (2013). Reprogramming the glycolytic pathway for increased hydrogen production in cyanobacteria: Metabolic engineering of NAD^+-dependent GAPDH. *Energy & Environ. Sci.* 6 (12), 3722–3731. doi:10.1039/c3ee42206b

Lambert, G. R., and Smith, G. D. (1977). Hydrogen formation by marine blue-green algae. *FEBS Lett.* 83 (1), 159–162. doi:10.1016/0014-5793(77)80664-9

Malcovati, M., and Valentini, G. (1982). AMP- and Fructose-1, 6, -biphosphate-activated pyruvate kinases from *Escherichia coli*. *Methods Enzym.* 90, 170–179. doi:10.1016/s0076-6879(82)90123-9

McIntosh, C. L., Germer, F., Schulz, R., Appel, J., and Jones, A. K. (2011). The [NiFe]-hydrogenase of the cyanobacterium *Synechocystis* sp. PCC 6803 works bidirectionally with a bias to H_2 production. *J. Am. Chem. Soc.* 133 (29), 11308–11319. doi:10.1021/ja203376y

Meuer, J., Bartoschek, S., Koch, J., Künkel, A., and Hedderich, R. (1999). Purification and catalytic properties of *Ech* hydrogenase from *Methanosarcina barkeri*. *Eur. J. Biochem.* 265 (1), 325–335. doi:10.1046/j.1432-1327.1999.00738.x

Min, H., and Sherman, L. A. (2010). Hydrogen production by the unicellular, diazotrophic cyanobacterium *Cyanothece* sp. strain ATCC 51142 under conditions of continuous light. *Appl. Environ. Microbiol.* 76 (13), 4293–4301. doi:10.1128/aem.00146-10

Nanatani, K., Shijuku, T., Takano, Y., Zulkifli, L., Yamazaki, T., Tominaga, A., et al. (2015). Comparative analysis of *kdp* and *ktr* mutants reveals distinct roles of the potassium transporters in the model cyanobacterium *Synechocystis* sp. strain PCC 6803. *J. Bacteriol.* 197 (4), 676–687. doi:10.1128/jb.02276-14

Oria-Hernández, J., Cabrera, N., Pérez-Montfort, R., and Ramírez-Silva, L. (2005). Pyruvate kinase revisited the activating effect of K^+. *J. Biol. Chem.* 280 (45), 37924–37929. doi:10.1074/jbc.m508490200

Osanai, T., Imamura, S., Asayama, M., Shirai, M., Suzuki, I., Murata, N., et al. (2006). Nitrogen induction of sugar catabolic gene expression in *Synechocystis* sp. PCC 6803. *DNA Res.* 13 (5), 185–195. doi:10.1093/dnares/dsl010

Pansook, S., Incharoensakdi, A., and Phunpruch, S. (2016). Hydrogen production by immobilized cells of unicellular halotolerant cyanobacterium *Aphanothece halophytica* in alginate beads. *Asia Pac. J. Sci. Technol.* 21 (2), 248–255. doi:10.14456/kkurj.2016.34

Pansook, S., Incharoensakdi, A., and Phunpruch, S. (2019a). Effects of the photosystem II inhibitors CCCP and DCMU on hydrogen production by the unicellular halotolerant cyanobacterium *Aphanothece halophytica*. *Sci. World J.* 2019, 1030236. doi:10.1155/2019/1030236

Pansook, S., Incharoensakdi, A., and Phunpruch, S. (2019b). Enhanced dark fermentative H_2 production by agar-immobilized cyanobacterium *Aphanothece halophytica*. *J. Appl. Phycol.* 31 (5), 2869–2879. doi:10.1007/s10811-019-01822-9

Pansook, S., Incharoensakdi, A., and Phunpruch, S. (2022). Simazine enhances dark fermentative H_2 production by unicellular halotolerant cyanobacterium *Aphanothece halophytica*. *Front. Bioeng. Biotechnol.* 10, 904101. doi:10.3389/fbioe.2022.904101

Papazi, A., Gjindali, A. I., Kastanaki, E., Assimakopoulos, K., Stamatakis, K., and Kotzabasis, K. (2014). Potassium deficiency, a "smart" cellular switch for sustained high yield hydrogen production by the green alga *Scenedesmus obliquus*. *Int. J. Hydrog. Energy* 39 (34), 19452–19464. doi:10.1016/j.ijhydene.2014.09.096

Perry, J. H. (1963). *Chemical engineers' handbook*. New York, NY, USA: McGraw-Hill.

Pewnual, T., Jampapetch, N., Saladtook, S., Raksajit, W., Klinsalee, R., and Maneeruttanarungroj, C. (2022). Response of green alga *Tetraspora* sp. CU2551 under potassium deprivation: A new promising strategy for hydrogen production. *J. Appl. Phycol.* 34 (2), 811–819. doi:10.1007/s10811-021-02672-0

Phunpruch, S., Taikhao, S., and Incharoensakdi, A. (2016). Identification of bidirectional hydrogenase genes and their co-transcription in unicellular halotolerant cyanobacterium *Aphanothece halophytica*. *J. Appl. Phycol.* 28 (2), 967–978. doi:10.1007/s10811-015-0664-8

Raksajit, W., Satchasataporn, K., Lehto, K., Mäenpää, P., and Incharoensakdi, A. (2012). Enhancement of hydrogen production by the filamentous non-heterocystous cyanobacterium. *Arthrospira* sp. PCC 8005. *Int. J. Hydrog. Energy* 37 (24), 18791–18797. doi:10.1016/j.ijhydene.2012.10.011

Rashid, N., Song, W., Park, J., Jin, H. F., and Lee, K. (2009). Characteristics of hydrogen production by immobilized cyanobacterium *Microcystis aeruginosa* through cycles of photosynthesis and anaerobic incubation. *J. Ind. Eng. Chem.* 15 (4), 498–503. doi:10.1016/j.jiec.2008.12.013

Rippka, R., Deruelles, J., Waterbury, J. B., Herdman, M., and Stanier, R. Y. (1979). Generic assignments, strain histories and properties of pure cultures of cyanobacteria. *Microbiology* 111 (1), 1–61. doi:10.1099/00221287-111-1-1

Siddiquee, K. A. Z., Arauzo-Bravo, M. J., and Shimizu, K. (2004). Effect of a pyruvate kinase (*pykF*-gene) knockout mutation on the control of gene expression and metabolic fluxes in *Escherichia coli*. *FEMS Microbiol. Lett.* 235 (1), 25–33. doi:10.1111/j.1574-6968.2004.tb09563.x

Srirangan, K., Pyne, M. E., and Chou, C. P. (2011). Biochemical and genetic engineering strategies to enhance hydrogen production in photosynthetic algae and cyanobacteria. *Bioresour. Technol.* 102 (18), 8589–8604. doi:10.1016/j.biortech.2011.03.087

Taikhao, S., Junyapoon, S., Incharoensakdi, A., and Phunpruch, S. (2013). Factors affecting biohydrogen production by unicellular halotolerant cyanobacterium *Aphanothece halophytica*. *J. Appl. Phycol.* 25 (2), 575–585. doi:10.1007/s10811-012-9892-3

Taikhao, S., Incharoensakdi, A., and Phunpruch, S. (2015). Dark fermentative hydrogen production by the unicellular halotolerant cyanobacterium *Aphanothece halophytica* grown in seawater. *J. Appl. Phycol.* 27 (1), 187–196. doi:10.1007/s10811-014-0292-8

Taikhao, S., and Phunpruch, S. (2017). Effect of metal cofactors of key enzymes on biohydrogen production by nitrogen fixing cyanobacterium *Anabaena siamensis* TISIR 8012. *Energy Procedia* 138, 360–365. doi:10.1016/j.egypro.2017.10.166

Takabe, T., Incharoensakdi, A., Arakawa, K., and Yokota, S. (1988). CO_2 fixation rate and RuBisCO content increase in the halotolerant cyanobacterium, *Aphanothece halophytica*, grown in high salinities. *Plant Physiol.* 88 (4), 1120–1124. doi:10.1104/pp.88.4.1120

Ueda, S., Kawamura, Y., Iijima, H., Nakajima, M., Shirai, T., Okamoto, M., et al. (2016). Anionic metabolite biosynthesis enhanced by potassium under dark, anaerobic conditions in cyanobacteria. *Sci. Rep.* 6, 32354. doi:10.1038/srep32354

Warichanan, K., and Phunpruch, S. (2019). Effect of cell density and nutrient depriyation on hydrogen production by unicellular green alga *Scenedesmus* sp. KMITL-OVG1. *Asia Pac. J. Sci. Technol.* 24 (2). APST-24-02-05. doi:10.14456/apst.2019.12